



Department
Of
Mechanical
Engineering

Thesis

Investigation into Tribological Performance of Vegetable Oils as Biolubricants at Severe Contact Conditions

Author: Adli Bahari

Supervisors: Dr. Tom Slatter

Prof. Roger Lewis

Date: October 2017

Thesis submitted to the University of Sheffield in partial fulfilment of the requirements for the degree of Doctor of Philosophy

Abstract

The concern about the pollution created by the use of mineral oil based lubricants and the depletion stock of petroleum has inspired research on alternative lubricants known as biolubricants. The tribological performance of vegetable oils (palm oil and soybean oil) as biolubricants and their blends with mineral oil and anti-wear additives was evaluated in order to assess their potential use in automotive engines. The tests were performed using a reciprocating ball-on-flat test-rig at severe contact conditions with grey cast iron specimens. The performance was compared with a commercial mineral engine oil for benchmarking purposes.

At severe contact conditions, the friction and wear results of vegetable oil lubricants were found to be greatly influenced by the wide hardness range of the grey cast iron specimens. The measurement of hardness on the intended wear scar region prior to testing was used in order to provide more robust tribological data. In a pure oil state, the palm oil performance was found to be competitive in friction coefficient with mineral engine oil. However, the mineral oil is far superior in wear protection over vegetable oils due to the additive package it contains its superior oxidative stability

For a vegetable oil-mineral oil blend in equal ratio, the reduction of friction and wear was not significant. However, the addition of 2% zinc dialkyl dithiophosphate in vegetable oils gave significant improvement on the friction and wear. The friction coefficient of palm oil with this additive was very close to the commercial mineral engine oil. The zinc dialkyl dithiophosphate in vegetable oil was found to perform three functions; as an anti-wear agent, anti-oxidant and friction modifier. The blend of vegetable oils with

boron nitride, however, did not give better results. This could be mainly due to the selection of particles size which was not suitable with the surface roughness.

When putting all the results together, the downside of pure vegetable oils is found to be greater in terms of wear resistance and oxidative stability compared to friction. This effect was prominent when they were blended with mineral oils where their tribological performance dominated. However, with the commercial anti-wear additive, specifically the zinc dialkyl dithiophosphate, the vegetable oils showed positive signs as a potential candidate to be used as an alternative lubricant in automotive engine systems even though there is still much room for improvement.

Acknowledgements

First and foremost, I would like to express my sincere appreciation to my supervisors, Dr. Tom Slatter and Prof. Roger Lewis for their guidance, advice and support throughout this research.

Secondly, I would like to acknowledge the valuable support from Malaysian government agency, *Majlis Amanah Rakyat (MARA)*. This work would not materialise without the financial support from them.

I would also like to thank my fellow doctoral students, especially from Tribology group, Nopparat Seemuang, Julius Abere, Julia Carrell, Lawal Abdulqadir, Kei Ishizaka and Rob Thornton for their help, feedback, cooperation and of course friendship. In addition, I would like to express my gratitude to all technicians of Mechanical Engineering Department especially Mr. Dave Butcher and Mr. Karl Rotchell.

Finally, the author wishes to express special thanks to dad and mom. Most importantly to my wife, Fadzlina and kids; Nani, Dira and Luqman for all kind support during this hard time. I would not have made it this far without you.

Abbreviations

AISI	American Iron and Steel Institute
AN	Acid number
ANOVA	Analysis of variance
ASTM	American Society for Testing and Materials
COF	Coefficient of friction
EDX	Electron dispersive analysis of X-rays
GCI	Grey cast iron
hBN	Hexagonal boron nitride
MO	Mineral oil
MO:PO	Blend of mineral oil and palm oil
MO:SBO	Blend of mineral oil and soybean oil
ppm	Part per million
PO	Palm oil
PO:SBO	Blend of palm oil and soybean oil
RPVOT	Rotary pressure vessel oxidation test
SAE	Society of Automotive Engineers
SEM	Scanning electron microscopy
SBO	Soybean oil
ZDDP	Zinc dialkyl dithiophosphate

Nomenclature

a	Radius of circular region	m
A	Nominal contact area	m^2
A'	cross sectional area of ploughing track	m^2
A_r	Real contact area	m^2
d	Track width of wear scar	m
E'	Effective elastic modulus	Pa
F	Friction force	N
F_s	Shearing force	N
F_p	Ploughing force	N
G	Dimensionless material parameter	m
h_{min}	Minimum film thickness	m
H	Indentation hardness	N/m^2
H_{min}	Dimensionless minimum film thickness	-
k	Thermal conductivity	W/mK
k	Elipticity parameter	-
K	Thermal diffusivity	m^2/s
K	Wear coefficient	-
L	Wear scar length	m
l_b	Effective diffusion length	m
N	Normal load	N
p, P	Contact pressure	N/m^2
P_e	Peclet number	-
Q	volume removed per unit sliding distance	m^3/m
q	Heat generated per unit area	W/m^2

r	Radius of curvature	m
r	Ball radius	m
R_a	Average surface roughness	m
R_q	R.m.s of surface roughness	m
R_x, R_y	Effective radius in x and y direction	m
S	Shearing strength	N/m ²
T_b	Total contact temperature	°C
T_c	Bulk material temperature	°C
ΔT_{nom}	Nominal contact temperature	°C
ΔT_f	Flash temperature rise	°C
U	Dimensionless speed	-
V	Velocity	m/s
V_w	Total wear volume	m ³
w	Wear scar width	m
w	Applied load	N
W	Dimensionless load	-
μ	Coefficient of friction	-
η_o	Absolute viscosity at atmosphere pressure	Pa.s
ν	Poisson ratio	-
λ	Lambda factor	-
σ^*	R.m.s of surface roughness of two surfaces	m

Table of Contents

Abstract	i
Acknowledgements	iii
Abbreviations	iv
Nomenclature	v
Table of Contents.....	vii
Chapter 1: Introduction.....	1
1.1 Motivation for research project	1
1.2 Problem statement	4
1.3 Aim, objectives and scope of research	5
1.3.1 Aim.....	5
1.3.2 Objectives.....	6
1.3.3 Scopes of research.....	6
1.4 Outline of the thesis.....	7
1.5 Novelties of the project	8
Chapter 2: Literature review	11
2.1 Friction	11
2.1.1 Tribometer and friction force measurement.....	14
2.1.2 Friction behaviour during running-in of sliding contact.....	15
2.1.3 Frictional heating and contact temperature rise	18
2.2 Wear	19
2.2.1 Wear measurement methods	21
2.2.2 Wear mechanisms	23
2.2.2.1 Adhesive wear	23
2.2.2.2 Abrasive wear.....	25
2.2.2.3 Fatigue wear	27
2.2.2.4 Chemical Wear.....	29
2.3 Lubrication	30
2.3.1 Lubrication Regimes	30
2.3.2 Mineral oil based lubricants	33
2.3.3 Lubricant Additives.....	36

2.3.3.1	Friction Modifiers	36
2.3.3.2	Anti-wear and Extreme-pressure Additives	40
2.3.3.3	Anti-oxidants	43
2.4	Vegetable oils	44
2.4.1	Palm oil	50
2.4.2	Soybean oil.....	52
2.4.3	Oxidation of oils.....	53
2.4.3.1	Mechanism of vegetable oil autoxidation	54
2.4.3.2	Oil oxidation impact on lubrication	55
2.5	Tribological performance of vegetable oil lubricants	57
2.5.1	Performance of pure vegetable oil lubricants	58
2.5.1.1	Tribological performance of palm oil and soybean oil	64
2.5.2	Performance of vegetable oil-mineral oil blends	67
2.5.3	Performance of vegetable oil with anti-wear additives.....	68
2.6	Grey cast iron	72
2.6.1	Tribological performances of grey cast iron	73
2.6.2	Influence of hardness on tribological performance of grey cast iron	75
2.7	Piston Ring and Cylinder Liner Materials.....	78
2.7.1	Piston rings.....	78
2.7.2	Piston ring materials.....	80
2.7.3	Cylinder liner	81
2.7.4	Cylinder liner materials.....	82
2.8	Summary	84
Chapter 3:	Experimental methodologies.....	86
3.1	Introduction	86
3.2	Experimental Equipment.....	86
3.2.1	Friction and wear test	86
3.2.1.1	Justification of Test Method.....	88
3.2.1.2	Limitation of the friction and wear test.....	92
3.2.2	Hardness Test	93
3.3	Materials.....	95
3.3.1	Specimens	95

3.3.2	Lubricants.....	96
3.3.2.1	Biolubricants	96
3.3.2.2	Mineral oil	97
3.3.2.3	Blended lubricants.....	97
3.3.2.3.1	Vegetable oil-mineral oil blend	98
3.3.2.3.2	Vegetable oil-additive blend.....	99
3.4	Material Analysis	100
3.4.1	Surface morphology evaluation	100
3.4.2	Surface topography evaluation.....	101
3.5	Lubricant Analysis Methods	104
3.5.1	Oxidation test	104
3.5.2	Oil viscosity test.....	105
3.5.3	Acid number test	105
3.5.4	Spectrochemical test	106
3.5.5	Gas chromatography test.....	106
3.5.6	Lubrication regime determination.....	107
3.6	Statistical analysis	110
3.7	Summary of test method	110

Chapter 4: Hardness characterisation of grey cast iron and its tribological performance in a contact lubricated with soybean oil113

4.1	Introduction	113
4.2	Hardness properties of grey cast iron.....	114
4.3	Friction analysis	117
4.4	Wear analysis	120
4.5	Wear scar appearance.....	123
4.6	Surface waviness analysis	131
4.7	Surface morphology	132
4.8	Elemental analysis.....	136
4.9	Conclusions and Summary.....	137

Chapter 5: Investigation into the tribological performance of palm oil and soybean oil in a reciprocating sliding contact at severe contact conditions139

5.1	Introduction	139
-----	--------------------	-----

5.2	Friction analysis	140
5.3	Wear analysis	144
5.4	Surface topography and waviness analysis	150
5.5	Surface roughness analysis.....	152
5.6	Surface morphology and elemental analysis.....	153
5.7	Acid number analysis	157
5.8	Oil viscosity analysis.....	158
5.9	Oxidative stability analysis	160
5.10	Conclusions and Summary.....	161

Chapter 6: Friction and Wear Performance of Vegetable Oil-Mineral Oil Blend in a Severe Reciprocating Sliding Contact163

6.1	Introduction	163
6.2	Friction Analysis	164
6.3	Wear Analysis	168
6.4	Surface Topography Analysis	173
6.5	Surface Morphology Analysis.....	176
6.6	Oxidative Stability Analysis	179
6.7	Acid Number Analysis	180
6.8	Oil Viscosity Analysis.....	181
6.9	Conclusions and Summary.....	182

Chapter 7: Improving the friction and wear performance of vegetable oils at severe contact condition through the use of additives.....184

7.1	Introduction	184
7.2	Friction Analysis	186
7.3	Wear Analysis	190
7.4	Surface Topography Analysis	195
7.5	Surface Morphology Analysis.....	198
7.6	Elemental Analysis of Worn Specimens.....	201
7.7	Oil Viscosity Analysis.....	203
7.8	Oxidative Stability Analysis	205
7.9	Acid Number Analysis	206
7.10	Conclusions and Summary.....	208

Chapter 8: Discussion of the tribological performance of vegetable oils	211
8.1 Responses of grey cast iron specimens' hardness on friction and wear of vegetable oil	211
8.2 Tribological performance of pure vegetable oils	215
8.3 Tribological Performance of vegetable oil-mineral oil blend	222
8.4 Tribological Performance of vegetable oil-anti-wear additive blend.....	228
8.5 Summary	234
Chapter 9: Conclusions and suggestions	237
9.1 Achievement on Objective 1	237
9.2 Achievement on Objective 2	238
9.3 Achievement on Objective 3	238
9.4 Achievement on Objective 4	239
9.5 Achievement on Project Aim	240
9.6 Contribution to scientific knowledge and industrial field.....	240
9.7 Recommendations for future work.....	241
9.8 Publications arising from this work	244
References.....	246
Appendices	I
Appendix 1	I
Measurement datasheet for hardness on intended wear scar of GCI specimens.....	I
Appendix 2	IV
Main lubricants used in this study: (a) Palm oil (b) Soybean oil (c) Mineral oil	IV
Appendix 3	V
Product information sheet for ZDDP	V
Appendix 4	VI
Product information sheet for hBN.....	VI
Appendix 5	VII
Example of calculation sheet for estimating the film thickness (Mineral Oil).....	VII
Appendix 6	VIII
Calculation sheet for estimating the lambda value	VIII

Appendix 7	IX
Calculation sheet for ANOVA analysis of COF for Mineral Oil, Palm Oil, Soybean Oil lubricated specimens	IX
Appendix 8	X
Elements spectrum of low, medium and high hardness specimens	X
Appendix 9	XI
Surface temperature calculation sheet	XI

Chapter 1: Introduction

1.1 Motivation for research project

Friction develops during relative motion of contacting surfaces. It is a force that resists the motion which then leads to heat and increases surface temperature. In machinery applications, friction is needed in the case of vehicle braking systems, clutches, belts and pulleys. However, in other situations like bearing support systems and the piston ring interface, friction is undesirable and needs to be reduced as much as possible. An increase of friction in an engine causes mechanical energy loss and consequently more fuel to be used in order to perform the same work. In addition, the engine quickly overheats and its working parts may wear or seize due to excessive friction.

Wear is associated with the interaction between two surfaces and more specifically the removal and deformation of the surface due to the rubbing action of the surfaces. In most cases wear occurs through surface interaction at asperities. Components in an automotive engine may experience failure and need to be substituted after relatively little material has been removed or if the surface is roughened due to excessive wear.

A lubricant is normally applied to the contacting surfaces in order to minimise the friction and wear. In an automotive engine, the piston ring and the cylinder liner are lubricated by oil to ensure optimum engine performance and wear protection. Lubricants smooth the movement and facilitate the transfer of heat and thus, cool the engine parts. It also cleans the internal engine components by flushing out the small particles of metal and

dirt. Proper design of lubricant systems may contribute to quieter engine operation and an increase in engine life.

Commercial lubricants used currently in automotive engines are mainly based on mineral oil (MO) due to its availability, performance and cost. However, these factors could not be maintained in the future as the base stock of petroleum is non-renewable and concerns over environmental pollution of mineral oil have increased [1, 2]. Several studies have predicted the timing where the peak of conventional oil production would reach [3-5]. For example, Wood [3] has foreseen 12 peaks (Figure 1.1) based on annual production growth rates (0 to 3%) of world oil and the United States Geological Survey (USGS) at 5%, 95% probability and mean (expected value) of recoverable oil resources volumes. Wood shows that the minimum and maximum peaks were estimated at year 2021 and 2112, a range of 91 years. Once the conventional oil hits its production peaks, all Wood's scenarios suggest that a catastrophically rapid depletion of oil will occur.

The pollution of the environment caused by mineral oil is one of the concerns and could not be taken too lightly. The oil spillage into the land and water may happen mainly due to human negligence which may be caused by the spillage of used engine oil or petroleum crude oil. In the ocean, the oil spill may come from the oil tankers and offshore oil platforms. It was reported that the total volume of oil lost to the environment from 2010 until 2015 was about 33,000 tonnes in which the total number of spillages involving oil more than 700 tonnes was 11 cases (Table 1.1) [6]. An oil spill can cause problems for plant, animal and human life. Floating oil on water prevents sunlight from passing through it making it difficult for plants and sea animals to survive.

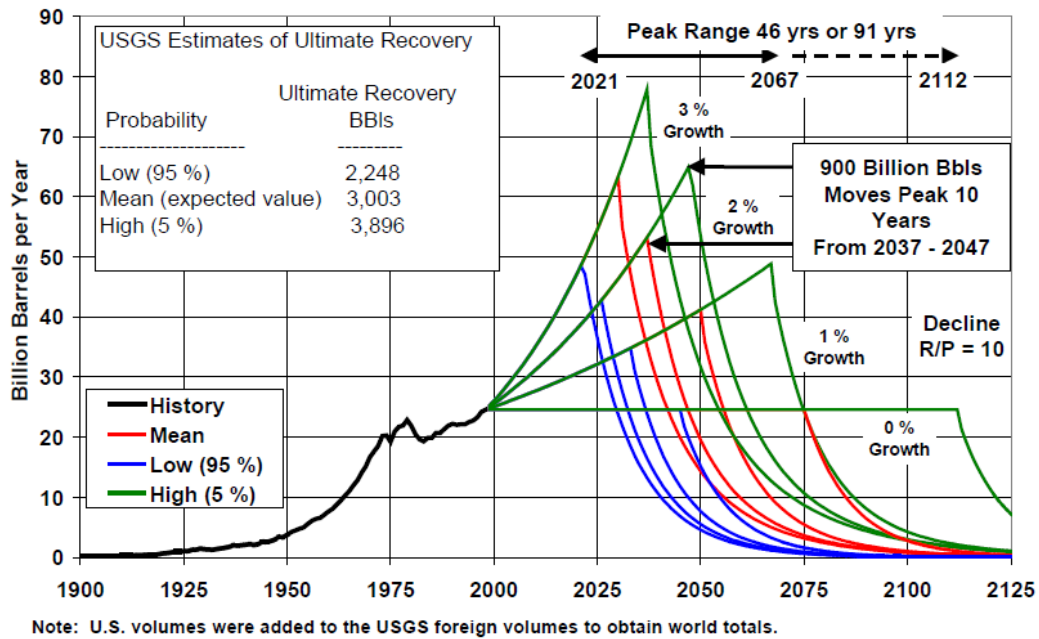


Figure 1.1: Prediction of world conventional oil production scenarios [3]

Table 1.1: Annual number of oil spills from 2010 to 2015 [6]

Year	7-700 tonnes	>700 tonnes
2010	5	4
2011	4	1
2012	7	0
2013	5	3
2014	4	1
2015	6	2
Total	31	11

With this in mind, the research on biolubricants as an alternative lubricant to mineral oil has received increasing attention. Biolubricants are formulated from renewable base stocks such as vegetable oils or esters derived from them. Unlike mineral oil, biolubricants are absolutely biodegradable and less toxic which means they are more environmentally friendly [7, 8]. However, there are some shortcomings of the vegetable

oils lubricants such as poor oxidative stability that could affect to their tribological performance. In view of this, a tribological investigation needs to be implemented of the vegetable oils lubrication in order to investigate their possible use as biolubricants in automotive engine systems.

1.2 Problem statement

A great deal of research has been conducted on investigating the tribological performance of vegetable oils as biolubricants. Typically, vegetable oils have been tested in various forms including their pure state [9-19]; blended with other oils [20-23]; formulated with additives [12, 16, 24-34] and with modification through chemical synthesis [18, 28, 30, 35-39]. Their results can be found in many literatures, some of which have claimed that the vegetable oil base lubricants gave better friction reduction and wear resistance compared to the commercial lubricants [9, 12, 15, 18-22, 25, 27, 29, 31, 35, 37].

Although extensive research has been carried out on the performance of vegetable oils on friction and wear, most are limited to unidirectional sliding test rigs (four-ball-tester [9, 11-13, 15, 20, 24-26, 28-31, 36-39] and pin-on-disc [10, 16, 18, 19, 21-23, 25, 32-34]) with steel and aluminium alloys as counterface materials. In addition, many of the tribological tests reported were run at a lubricant temperature less than 100 °C [9-15, 17-22, 25, 26, 28-30, 32, 34-39] which is inappropriate for higher temperature lubricant applications such as oil in a sump of an internal combustion engine [40].

In investigating the potential use of vegetable oils in an automotive engine, setting up a tribological test that replicates the motion of piston ring in an internal combustion engine is one of the crucial matters. In view of this, the combination of a sliding reciprocating test rig with grey cast iron, tested at a temperature close to engine oil sump temperature is more suitable. A higher contact pressure is also preferred in order to evaluate the lubricants performance at a more extreme environment which beyond the typical contact pressure of a piston ring ($10^4 \sim 10^5$ Pa) [41]. Expansion of engine components might be possible during the failure of a cooling system. This would promote a higher contact pressure, lead to excessive wear and consequent failure of machine parts.

Therefore, in this work, the friction and wear performance of the vegetable oils were evaluated at a lubricant temperature 100 °C by a reciprocating test rig. A point contact with an initial contact pressure > 1 GPa was applied, leading to a severe contact condition. Careful attention has also been emphasised on the use of grey cast iron specimens as the wide hardness range that inherently exists in its properties might cause inconsistency of friction and wear data.

1.3 Aim, objectives and scope of research

1.3.1 Aim

The aim of this project was to investigate the tribological performance of vegetable oils as biolubricants in order to assess their potential application in automotive engines.

1.3.2 Objectives

To achieve the aim above, four main objectives of this research were identified:

- i. To investigate the tribological response of grey cast iron specimens to vegetable oil lubrication;
- ii. To benchmark the tribological performance of pure vegetable oils with commercial mineral engine oil;
- iii. To investigate the tribological performance of vegetable oils blends with mineral oil at equal ratio;
- iv. To improve the tribological performance of vegetable oils through the use of additives.

1.3.3 Scopes of research

To ensure the research was feasible within the time available, the following scope was defined:

- i. The vegetable oils used were limited to palm oil and soybean oil only
- ii. The tribological tests were conducted by a reciprocating sliding point contact test rig
- iii. The test parameters were fixed at one test condition only
- iv. The tribological investigation was performed on flat specimens of grey cast iron
- v. The additives used were limited to commercial antiwear additives

1.4 Outline of the thesis

This thesis has been divided into eight chapters. Chapter 1 introduces the motivation of this research project in general. The problem statement is then defined in order to specifically identify the research gaps that have been left by the previous researchers which need to be undertaken in this study. The project's aim, main objectives and the scope of work are also stated.

Chapter 2 describes the literature survey related to biolubricants work that have been published so far. It begins from the general background of knowledge on vegetable oils and then followed by the tribological results found in the previous work. Some of the tools that have been used in analysing the test results like theoretical calculation and statistical analysis are also explained.

Chapter 3 is a detailed explanation of materials and experimental methods that are related to this research. This includes the specimens and lubricants used, the test rigs involved as well as the measurement or inspection techniques for the lubricants and worn specimens.

The analysis and discussions of the test results begin in Chapter 4. In this chapter, the response of wide hardness range of grey cast iron on lubrication performance is investigated. A measurement method of specimens' hardness prior to test is also proposed in order to produce more robust friction and wear results.

In Chapter 5, the benchmarking of oil performance between the pure vegetable oils with commercial engine oil is presented which includes the friction, wear and lubricant properties. This is to provide baseline data for further improvement of the vegetable oils.

In Chapter 6, the analysis of the effect of vegetable oil-commercial mineral engine oil blends on friction and wear is reported.

Chapter 7 describes attempts to improve on how the vegetable oils are formulated with commercial anti-wear additives. The significant improvement in terms of friction and wear is discussed.

Chapter 8 highlights the major tribology outcomes found in Results and Discussions chapters (Chapters 4-7). They are linked together to establish the relationship of each chapter to the overall aim of the study.

Finally, Chapter 9 summarises all findings from the test results found in Chapter 4, 5, 6, 7 and 8. It also suggests some of the future work that might be performed for further improvement. In line with this, the list of publications papers from this work are also presented.

1.5 Novelties of the project

As stated in the Problem statement (Section 1.2), many of previous experimental works on biolubricants studies were carried out on unidirectional test rigs (either four-ball-

tester or pin-on-disc) and the lubricant temperature was set at a low temperature (less than 100 °C). In order to assess the potential use of vegetable oils in automotive engines, more appropriate test conditions which are closer to its system are required.

Thus, the novelties of this study are distinguishable through the combinations of the methodologies and material which are presented simultaneously. They can be highlighted as several points below:

- (i) Due to wide hardness distribution of the grey cast iron, the hardness of the specimens used in this study was measured directly on the intended wear scar region prior to friction and wear tests. This was to minimise the error or inconsistency of friction and wear results. Most of the previous studies used a bulk hardness value to represent the specimens' hardness.
- (ii) The use of a reciprocating test rig (bidirectional) in this study is more appropriate for replicating the motion of a piston ring in an internal combustion engine compared to previously performed by the four-ball tester or pin-on-disc machine.
- (iii) The lubricant temperature was set to a higher temperature (100 °C) which is the typical lubricant temperature in a sump of car engine. Running a test with a lubricant temperature close to room temperature is not suitable for automotive engine applications as performed previously.
- (iv) The contact pressure used in the tests is higher than that typically found in the piston ring system contact. The higher pressure is important in preparing the environment for the lubricants to serve at more severe contact conditions.

Severe contact conditions replicate the worst case scenario that possibly to occur during the failure of engine cooling system.

Based on the above combinations, the use of palm oil and soybean oil with the mineral oil blends and commercial antiwear additives have narrowed down the novelties into very specific area of study.

Chapter 2: Literature review

In this chapter, the previous research works related to this project are presented. It begins with general background knowledge of tribology (friction, wear and lubrication) and basic chemistry aspects of vegetable oils and oxidation process. This is followed by a literature survey related to the objectives of this study. The previous work regarding grey cast iron hardness and its tribological performance are also reviewed.

2.1 Friction

Friction is a resistance force to tangential motion between two surfaces in a contact. The laws of friction were published by Guillaume Amontons (1663-1705) which stated that the friction force is proportional to the normal load applied and independent of the apparent area of contact [42]. The friction force, F can be stated by the basic equation:

$$F = \mu N \quad (\text{Equation 2.1})$$

where μ is called the coefficient of friction (COF) and N is the normal load.

Thereafter, Bowden and Tabor developed a more detailed model of metallic friction. They described the friction force as a summation of two components; the adhesive force, F_s and ploughing force, F_p [43] in which:

$$F = F_s + F_p \quad (\text{Equation 2.2})$$

During the relative motion of two contacting bodies, the adhesion force is required to shear the contacting junctions where the adhesion occurs, while the ploughing force is needed to plough the asperities of the harder surface through the softer surface. Bowden and Tabor [43] suggested that the contact occurred only at the surface asperities. This contact area is known as the real contact area, which is very small, and independent of the apparent area of contact. This real contact area is also proportional to the applied load where the asperities could deform. These come to a formula stating that:

$$F = A_r \cdot S + A'p \quad (\text{Equation 2.3})$$

where A_r is the real contact area, S is the shearing strength of metallic junctions, A' is the cross sectional area of the ploughing track and p is the pressure to cause plastic flow of the softer metal (close to the indentation hardness value [44]). When the load is applied, the asperities of the softer material deform at the contact region until the real area of contact is sufficient enough to support the load. In this situation $N=pA_r$. Equation 2.4 then can be written as:

$$F = \frac{NS}{p} + A'p \quad (\text{Equation 2.4})$$

Finally, the coefficient of friction is given by:

$$\mu = \frac{F}{N} = \frac{S}{p} + \frac{A'p}{N} \quad (\text{Equation 2.5})$$

Bowden and Tabor [43] showed that the ploughing force for ball-on-flat contact is also dependent on the ploughing track width, d and radius of curvature, r of the contact and can be derived as:

$$F_p = \frac{d^3 p}{12r} \quad (\text{Equation 2.6})$$

and this theoretical result agreed with test data (Figure 2.1).

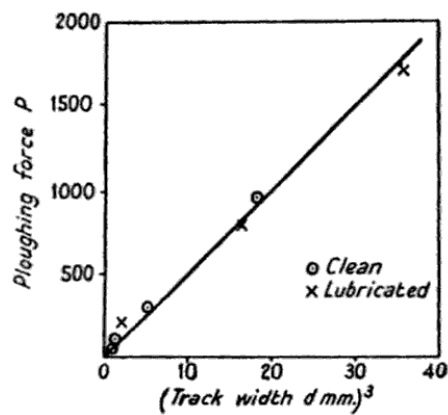


Figure 2.1: Effect of track width on the ploughing force of indium with a flat steel for dry and lubricated surfaces [45]. The line is the predicted value.

2.1.1 Tribometer and friction force measurement

Prior to performing a tribological research, it is very important for a researcher to understand the system of a test rig or tribometer. Most of the tribometers used for experimental work in tribology are commercially available and designed in a small scale in order to replicate the application in the real system. They include four-ball-tribometers, pin-on-disk-tribometers and linear reciprocating friction testers. A close application for the four-ball-tribotester could be a ball bearing system while the pin-on-disk could duplicate the disc brake system. A sliding motion in a linear reciprocating friction tester could replicate the piston ring motion in an internal combustion engine. Typical configurations of commercial tribometers with the direction of normal load applied are shown in Figure 2.2.

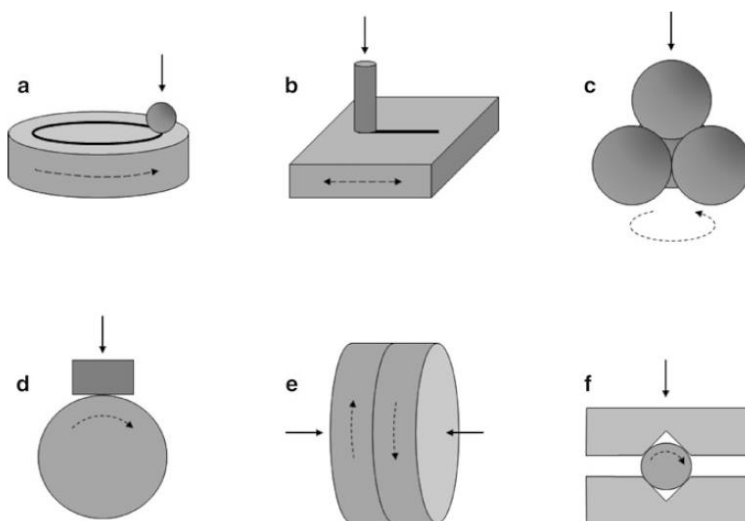


Figure 2.2: Typical configuration of commercial tribometer where normal load is indicated by arrows; (a) ball-on-disc, (b) reciprocating pin-on-flat, (c) four-ball, (d) block-on-wheel, (e) flat-on-flat and (f) pin and vee-block [46].

The basic set-up in friction force measurement for a tribometer is by applying a normal load between two contacting bodies that have a relative motion (one body is moving while the other partner is static). The normal force then should be adjustable so that it could be increased gradually until a measurable tangential force is detected by a force measurement device. For evaluating the friction force, F in the linear reciprocating test rig, a spring balance is sometimes used in order to produce an adjustable normal load, N that applied to the contacting bodies. A calibrated load cell is normally attached to the static body as a friction force measurement device. The coefficient of friction is then calculated by dividing the friction force, F by the value of normal load, N .

2.1.2 Friction behaviour during running-in of sliding contact

Running-in is a process of changes in friction and/or wear in tribosystem prior to steady state when two contacting surfaces are in contact under a normal load and relative motion. The running-in process is an effective way of matching two contacting components and gives important clues to system designer for identification of various contributions to overall friction performance of machines. In order to achieve long-term service life, some machines (for example a new engine) are exposed to certain running-in procedure after assembly. There are eight common shapes of running-in behaviour (friction-time curves) in metal sliding contact that were categorised by Blau [47] based on his literature survey of the tribology tests conducted in the early 1980s (Figure 2.3) [48]. Table 2.1 indicates some of the possible causes for each type of curve. From the outcome of his research, Blau [47] concluded that there was no evidence that these eight curves were representative of specific contact conditions [48].

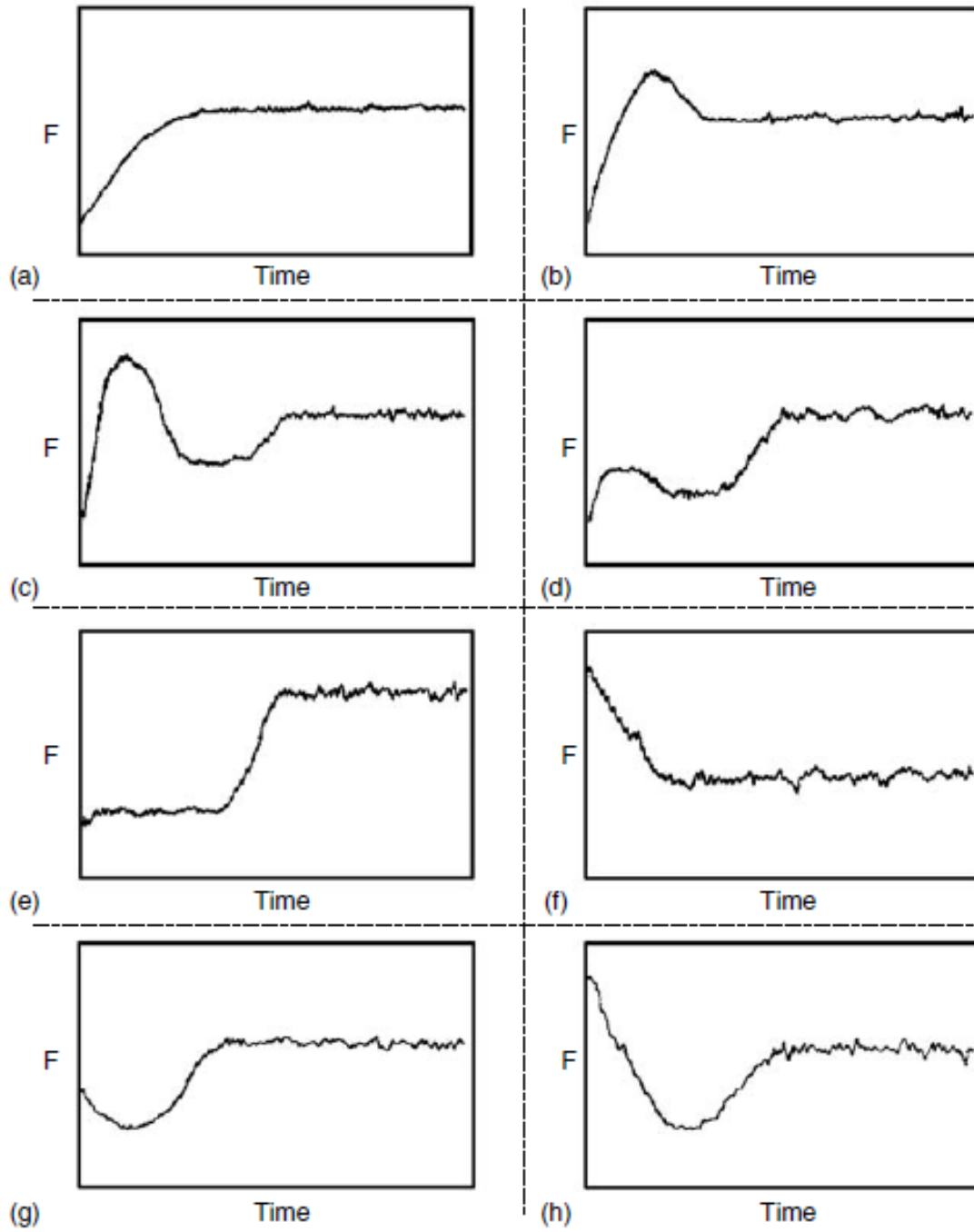


Figure 2.3: Eight typical forms of initial friction behaviour during running-in process [48].

Table 2.1: Possible causes of friction running-in behaviour as shown in Figure 2.3 (adapted from [48]).

Type	Occurrence	Possible Cause(s)
a	Contaminant surfaces	(i) A thin film of lubricious contaminant is worn off the sliding surface [48]. (ii) Effects of component temperature rises due to sliding friction [49]. (iii) Mechanical disruption of surface oxide films with increasing metallic contact [50]. (iv) contact geometry changes [51].
b	Boundary-lubricated metals	Surfaces wear-in; initial wear rate high until the sharpest asperities are worn off and surface becomes smoother [52].
c	Unlubricated oxidised metals, often observed in ferrous or ferrous/nonferrous pairs	Wear-in, as in type (b), but with the subsequent development of a debris layer (debris accumulation) or excessive transfer of material [52].
d	Same as type (c)	Similar to type (c), but the initial oxide film maybe more tenacious and protective [52].
e	Coated systems; also, systems in which wear is controlled by subsurface fatigue processes.	Wear-through of a coating; or subsurface fatigue cracks grow until debris is first produced. The debris then creates third bodies, which induce a rapid transition in friction. Sometimes a few initial spikes in friction signal the onset of this transition [53].
f	Clean, pure metals.	Crystallographic reorientation of regions in near surface layers reduces their shear strength and lowers their friction [54]. Alternatively, the initial roughness of the surface is worn off, leaving smoother surfaces [48].
g	Graphite on graphite; metal on graphite.	Creation of a thin film during running-in; debris or transfer produces a subsequent rise in friction [48].
h	Hard coatings on ceramics.	Roughness changes, then a fine-grained debris layer forms [55].

2.1.3 Frictional heating and contact temperature rise

Part of the mechanical energy used to slide a material in frictional contacts dissipates as heat energy. This energy dissipation is known as frictional heating which may contribute to an increase in the temperature of the two sliding bodies. Frictional heating and temperature rise in sliding contacts could affect on the tribological behaviour and failure of the sliding components. Increase in surface temperature sometimes is sufficient to cause melting of material, surface oxidation and possible changes of the structure and material properties at the contacting areas [56]. The surface temperature on the sliding bodies could be measured experimentally or estimated by calculation. The total contact temperature (T_c) at a given point can be estimated based on the summation of three components [56]:

$$T_c = T_b + \Delta T_{nom} + \Delta T_f \quad (\text{Equation 2.5})$$

where T_b is the bulk material temperature, ΔT_{nom} is the nominal (or mean) contact temperature and ΔT_f is the short duration flash temperature rise at the various asperity contact.

In the case of a stationary heat source on moving body (with circular region of radius, a), the maximum flash temperature rise can be approximated as [56]:

$$\Delta T_{f_{max}} = \frac{2qa}{k\sqrt{\pi(1.273 + P_e)}} \quad (\text{Equation 2.6})$$

where $q = \mu PU$ is the rate of heat generated per unit area (W/m^2), μ is the coefficient of friction, P is the contact pressure (N/m^2), a is the radius of circular region (m), k is the thermal conductivity (W/mK), P_e is the Peclet number $= \frac{Va}{2K}$, V is the velocity (m/s) and $K = \frac{k}{\rho c}$ is the thermal diffusivity (m^2/s).

The nominal surface temperature rise is an additional surface temperature due to a heat source that passes repeatedly over the same point on the surface. The nominal surface temperature rise for the moving body is determined by [56]:

$$\Delta T_{nom} = q_{nom} \frac{l_b}{k} \quad (\text{Equation 2.7})$$

where $q_{nom} = q \frac{A_r}{A}$, A_r is the real contact area (m^2), $A = \pi a^2$ is the nominal contact area (m^2), $l_b = \frac{a}{\pi^{1/2}} \tan^{-1} \left[\frac{2\pi K}{aV} \right]^{\frac{1}{2}}$ is the effective diffusion length (m).

2.2 Wear

Wear can be defined as progressive loss of substance from the operating surface of a body occurring as a result of relative motion at the surface [57]. The basic mathematical model of the relationship between wear rate and normal load is given by the formula (Archard wear equation):

$$Q = \frac{KN}{H} \quad (\text{Equation 2.8})$$

where Q is the volume removed from the surface per unit sliding distance (m^3/m), N is the normal load applied to the surface (N) and H is the indentation hardness of the wearing surface (N/m^2) and $K =$ wear coefficient. Archard equation is limited to a linear relationship between the normal load, sliding distance, material hardness and wear volume. Provided that the K , N and H are remain constant during wear test, the volume of material lost from the surface is directly proportional to the relative sliding distance or experiment time [57].

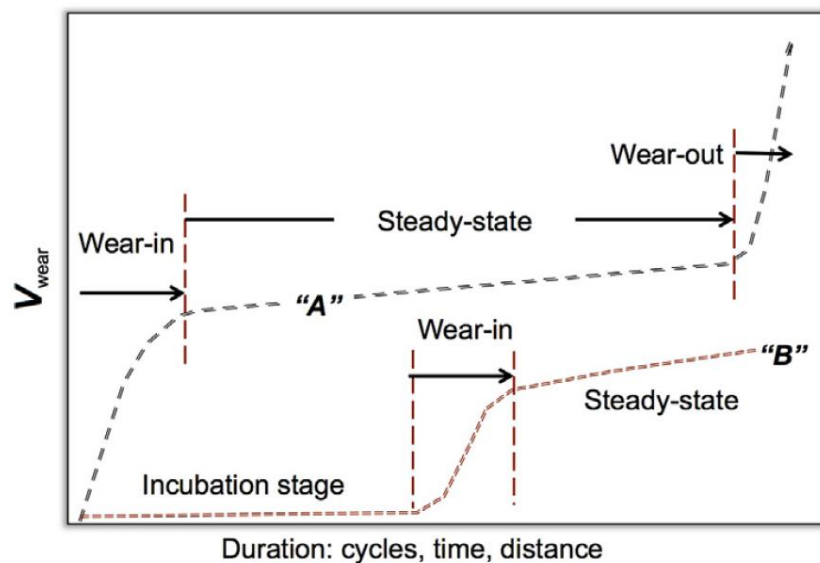


Figure 2.4: Common curves of non-linear sliding wear behaviour [58].

Typical wear behaviours of sliding contact for non-induced wear transition is shown in Figure 2.4 in which they can be influenced by the material selection in a

tribosystem [58]. It shows that the wear progress (Curve “A” in Figure 2.4) can be taking place at different stages; wear increases quickly through wear-in process, development of a period of stable wear (steady-state) and wear increases again during wear-out stage. In the case of mild wear at the beginning of the sliding process (Curve “B”), at a lower normal load, the initial wear transition is likely to stay longer (incubation stage) prior to the onset of wear-in process.

The study of wear transitions requires an accurate method for in situ wear measurement. In some cases where the continuous wear measurement is impractical (due to the limitation of test rigs), some researcher chooses to stop the test rig periodically in order to measure the wear [59]. However, this method is susceptible to a possibility of inducing an alignment error in contact region when reassembling the specimens for the second time. Thus, the development of a device for in situ wear measurement without disturbing the running conditions is still becoming an important area in wear research.

2.2.1 Wear measurement methods

Wear is involving progressive loss of material and thus, mass loss is frequently used as a measure of wear. This is performed by measuring the mass of a specimen before and after the test. Other than mass loss measurement, calculation of wear volume could also be performed based on geometry of the wear scar of a worn specimen (length and width) which can be measured by a profilometer. For example, a typical top view of wear scar on flat specimen in the case of ball-on-flat linearly reciprocating sliding wear test is

shown in Figure 2.5. The total wear volume, V_w is then calculated based on the formula given by [60]:

$$V_w = L \left\{ r^2 \sin^{-1} \left(\frac{w}{2r} \right) - \frac{w}{2} \sqrt{r^2 - \frac{w^2}{4}} \right\} + \frac{\pi}{3} \left\{ 2r^3 - 2r^2 \sqrt{r^2 - \frac{w^2}{4}} - \frac{w^2}{4} \sqrt{r^2 - \frac{w^2}{4}} \right\}$$

(Equation 2.9)

where w is the wear scar width (m), L is the wear scar length (m) and r is the ball radius (m).

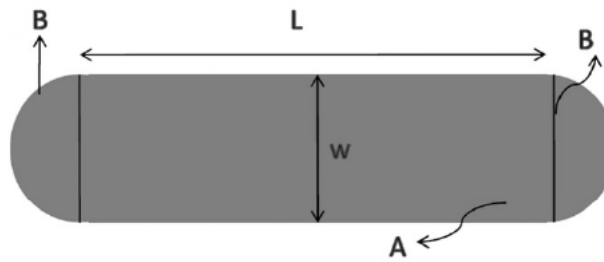


Figure 2.5: Top view of typical wear scar produced on flat specimen by ball-on-flat linearly reciprocating wear test. The calculation of wear volume is based on divided region of wear scar, A and B [60].

The use of other equipment with the aid of software could also facilitate the measurement of wear scar geometry. For example, Sharma et al. [60] proposed a method for calculating the wear volume for a ball-on-flat reciprocating sliding wear test by an optical microscopic technique. In this technique, the geometry at different positions of the worn section were measured by focusing and defocusing on the flat surface of the sample.

Although there are several methods in measuring wear, the accuracy of wear volume calculation is limited to wear scars of ‘uniform’ shape. In the case of non-uniform shape of wear scar produced on the surface, the mass loss measurement method is a better choice.

2.2.2 Wear mechanisms

Wear initiates when there is insufficient protection between two contacting surfaces. The process by which wear occurs on the surfaces is commonly known as the wear mechanism. It is very important to understand and identify the mechanisms of wear before a step can be taken in order to control wear. There are four main classes of wear mechanisms namely: adhesive wear, abrasive wear, surface fatigue wear and chemical wear.

2.2.2.1 Adhesive wear

In the adhesive wear mechanism, material is removed through a sliding process when surface asperities come into contact under a normal load. The material transfer (typically from softer to harder material) is initiated by a micro-welding process occurring at two contacting asperities when sufficient heat is generated and followed by a material shearing process (Figure 2.6). In order for the adhesive wear to take place, fracture must occur in the subsurface of one of the materials (Figure 2.7). The formation of transfer films is a characteristic feature of adhesive wear where material is transferred from one surface to another before being released as a wear particle (Figure 2.8).

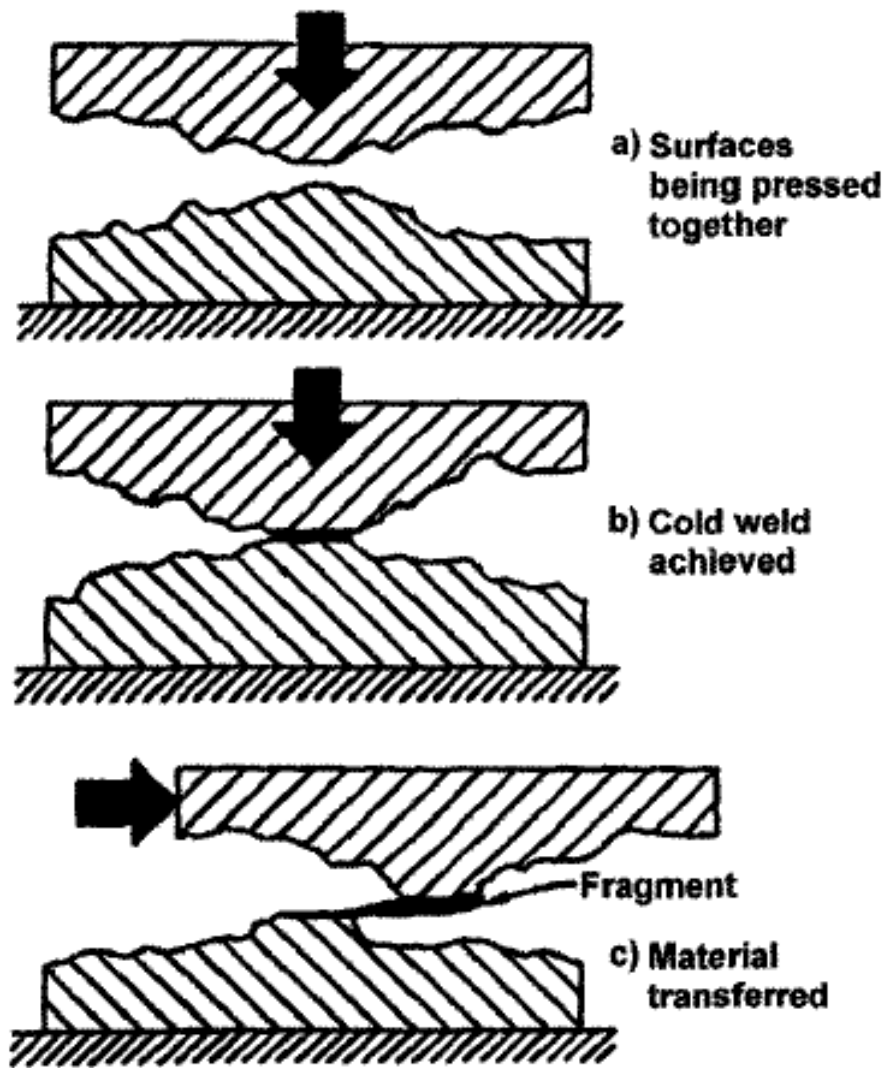


Figure 2.6: Mechanism of adhesive wear [61].

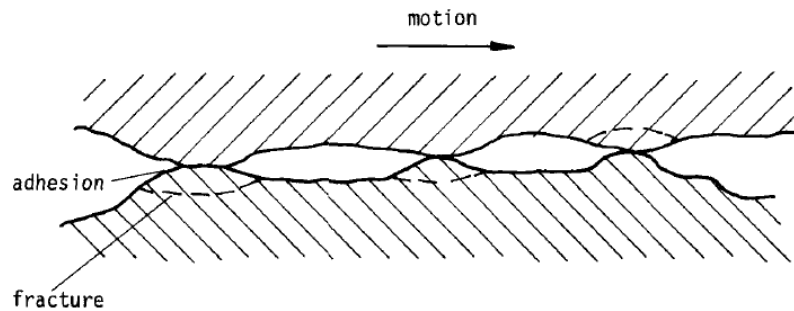


Figure 2.7: Formation of fracture in the subsurface of materials due to adhesive wear [62].

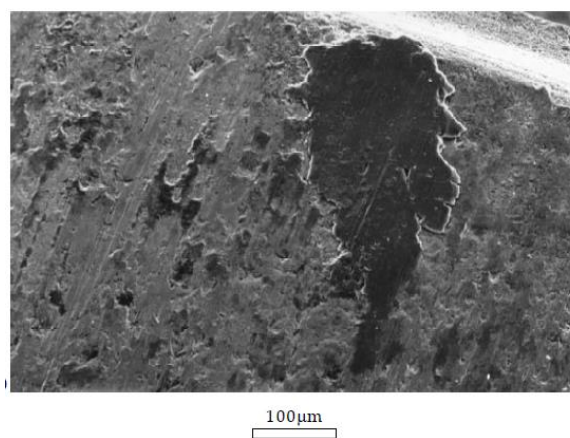


Figure 2.8: Example of adhesive wear appearance (Al-Si alloy transfer film onto a piston ring) [44].

2.2.2.2 Abrasive wear

Abrasive wear occurs when hard particles (wear debris) or hard protuberances (asperities) are forced to slide on the contacting surfaces. When abrasive wear is produced by the hard particles, it is called three-body abrasive, while two-body abrasive is caused by a harder asperities penetrating into a softer material (Figure 2.9). In abrasive wear, material is removed by a ploughing or microcutting process which is influenced by factors such as

particle size, shape and material hardness. A typical appearance on a worn surface caused by abrasive wear is shown in Figure 2.10.

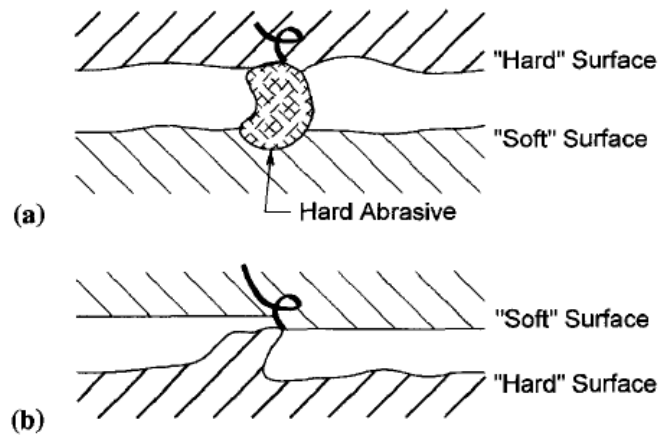


Figure 2.9: Schematic of three-body and two-body abrasive wear model [61].

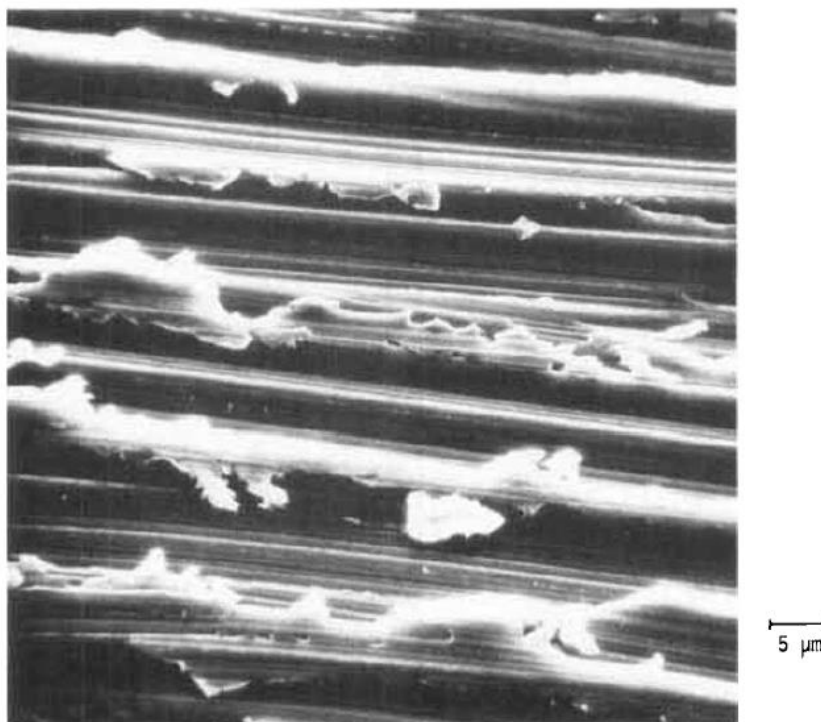


Figure 2.10: Example of abrasive wear appearance [62].

2.2.2.3 Fatigue wear

The fatigue wear occurs on the surfaces when repeated stress cycling in a rolling or sliding contact occurs. Cracks or fracture can be developed after a sufficient number of fluctuating stresses and strains as shown in Figure 2.11. Fatigue wear can be visualised microscopically by surface pitting and spalling (Figure 2.12) which are caused by subsurface shear stresses that exceed the material shear strength.

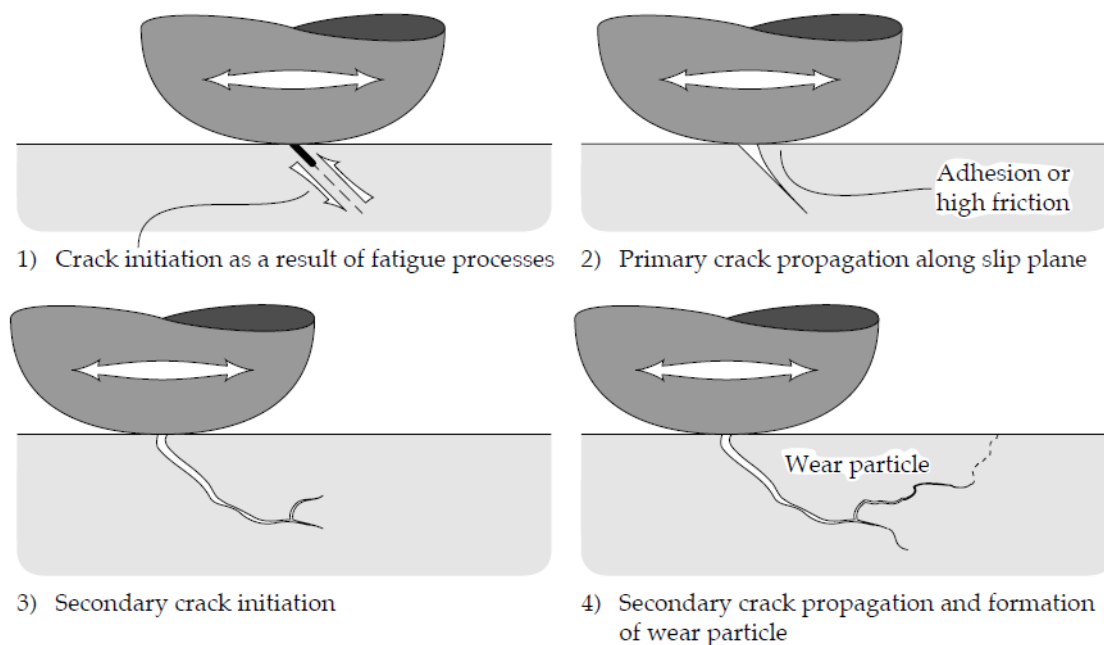


Figure 2.11: The process of surface crack initiation and propagation [44].

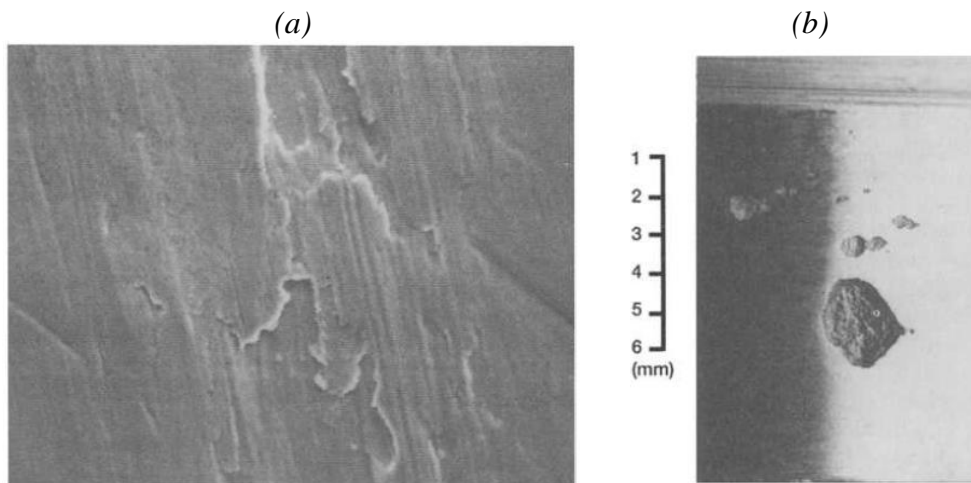


Figure 2.12: Examples wear scar appearances due to fatigue wear mechanism. (a) Spalling wear and (b) Pitting wear [61].

Another type of wear which can be categorised as a subset of fatigue wear is delamination wear as a result of subsurface cracks. In delamination theory, which was proposed by Suh [63] (Figure 2.13), dislocations are generated at sub-surface due to continuous loading. Pile-ups of dislocations then occur and lead to the formation of voids due to the inclusions (hard particles) that are contained in most engineering material. The voids will coalesce leading to cracks parallel to the surface. This ends up with the removal of a thin layer of material in the form of sheet-like laminar particle. A typical appearance on a worn surface caused by delamination wear is shown in Figure 2.14[52].

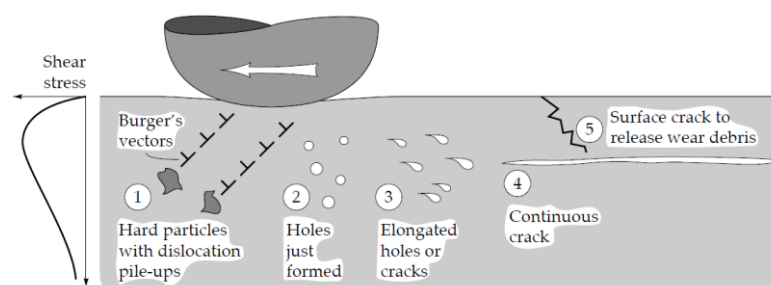


Figure 2.13: Crack formation at subsurface by growth and link up of voids [44].

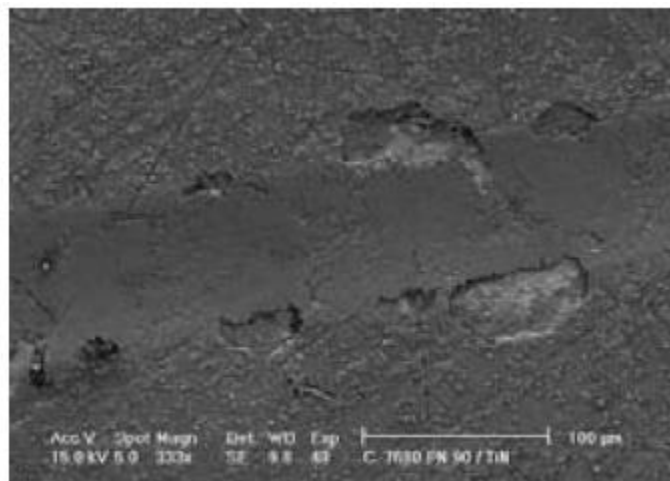


Figure 2.14: Example of delamination wear appearance [52].

2.2.2.4 Chemical Wear

Chemical wear (corrosive wear) occurs when a sliding process take place in a corrosive environment. Corrosion can occur as a result of a chemical or an electrochemical reaction on the metal surfaces from the lubricant or corrosive contaminants such as salts, water and acids. The mechanism of corrosive wear is shown in Figure 2.15 in which pitting is normally produced on the worn surface. Chemical wear in air is generally called oxidative wear since the most dominant corrosive medium is oxygen. Chemical wear can be controlled by the use of appropriate inhibiting additives. An example of a worn surface due to chemical wear is shown in Figure 2.16.

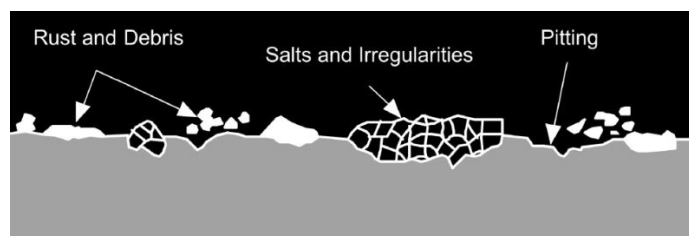


Figure 2.15: Mechanism of corrosive wear [64].

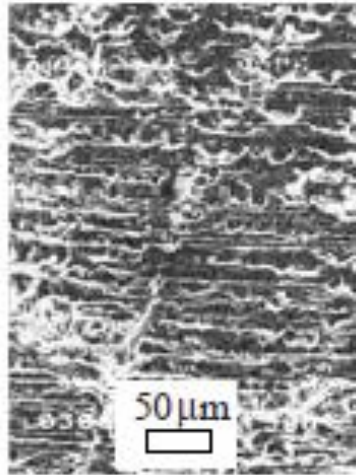


Figure 2.16: Example of chemical wear of cast iron due to sulphuric acid [44].

2.3 Lubrication

In order to reduce friction and minimise wear between two contacting materials, a lubricant is applied to the contacting surfaces. A lubricant reduces the friction by providing a low shear strength layer between both surfaces which is less than the material shear strength [44]. A good lubricant may also play other important roles such as heat transfer, removal of contaminants and reducing corrosion. Two forms of lubricants are available; solid lubricants and liquid lubricants. Solid lubricants are in the form of powder lubricants such as molybdenum disulphide and graphite. Liquid lubricants are typically those derived from base oil with the addition of additives in order to improve the performance.

2.3.1 Lubrication Regimes

As described in Section 2.3, a lubricant's primary function is to provide a protective layer that reduces friction and minimises wear between two surfaces. However,

the magnitude of the normal load between the contacting surfaces gives different level of lubrication conditions, which may be classified into different lubrication regimes. Lubricants operate under three common lubricating regimes that comprise of hydrodynamic, mixed and boundary lubrications. A summary of lubrication regimes can be explained by the Stribeck curve (Figure 2.17) which is a plot of a fluid-lubricated bearing system that presents the coefficient of friction versus $\eta N/P$, where η is the lubricant viscosity, N is the rotational speed and P is the load per unit projected bearing area.

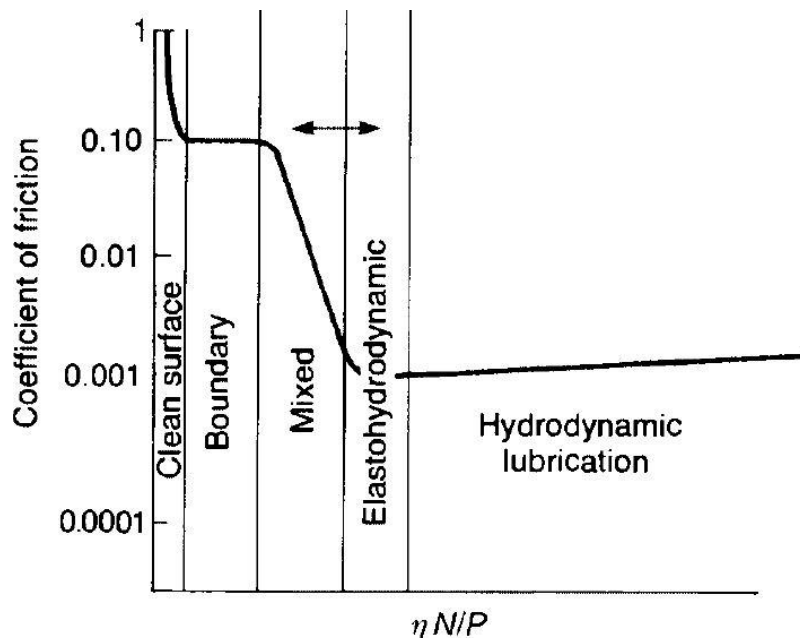


Figure 2.17: Stribeck curve showing different lubrication regimes which related to coefficient of friction, speed and lubricant viscosity [56].

Hydrodynamic, also known as full film lubrication is the condition when the contact load between the sliding surfaces is fully supported by a relatively thick film between them ($> 0.25 \mu\text{m}$ [56]). Metal-to-metal contact is avoided under this lubrication regime, making the friction coefficient solely depended on the lubricant viscosity (at a

constant load and speed). Elastohydrodynamic is a subset of hydrodynamic lubrication in which the contact load is sufficiently enough for the surfaces to elastically deform during the hydrodynamic action. The lubricating film is normally very thin (typically 0.025-5 μm thick) [56] compared to the film thickness formed in hydrodynamic lubrication.

The mixed lubrication regime deals with either; lower speed, higher load or higher temperature that significantly reduces lubricant viscosity. Under this condition, the asperities of the contacting surfaces at some areas will occasionally come in to contact.

In boundary lubrication, the lubricant film thickness is thinner (1-3 nm [56]) than the height of some of the asperities and there is considerable asperity contact. This occurs when the speed is reduced or the load is increased. Boundary lubrication represents a more severe contact condition compared to other lubrication regime. It is found in engine contacts (i.e., between the piston ring and cylinder liner) during the first half of the power stroke when crank angle is 0° to 90° (Figure 2.18) [65]. Under this lubrication condition, the physical and chemical properties of thin surface films are significant.

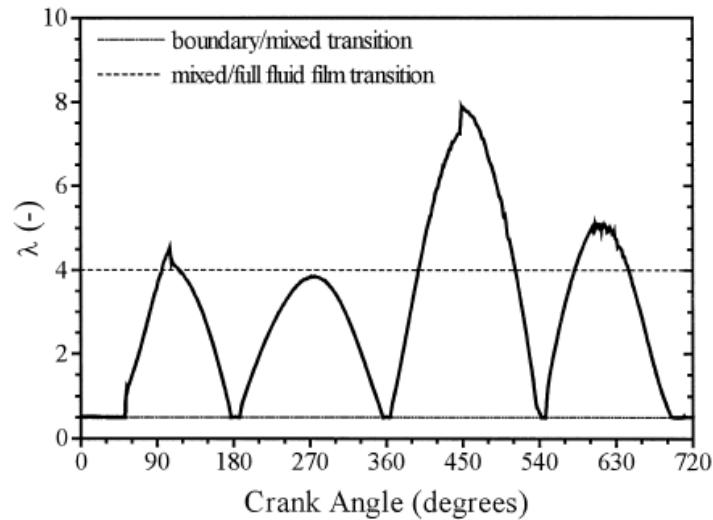


Figure 2.18: Cyclic variation of specific film thickness, λ between a top compression ring and the cylinder wall showing the lubrication regime [65].

2.3.2 Mineral oil based lubricants

Mineral oils produced by the refining process of crude oil are the most common lubricants used in industry. Typical applications of mineral oils are in engines and turbines. Mineral oils can be classified into three types based on the chemical structure which comprise of paraffinic (straight and branched hydrocarbons), naphthenic (cyclic carbon molecules) and aromatic (benzene type compounds) (Figure 2.19). The existence of different molecule structure in the mineral oils may influence to the physical properties of the lubricants. For example, the viscosity-temperature characteristics between paraffinic and naphthenic oils are significantly different [44].

Commercial mineral engine oils are those mineral oils blended with additives. Additives are synthetic chemicals which serve to improve existing properties or introduce

new properties in the base oil. Additives may represent about 1 to 25% of a lubricant [64].

The main types of additives in lubricating oil are listed in Table 2.2.

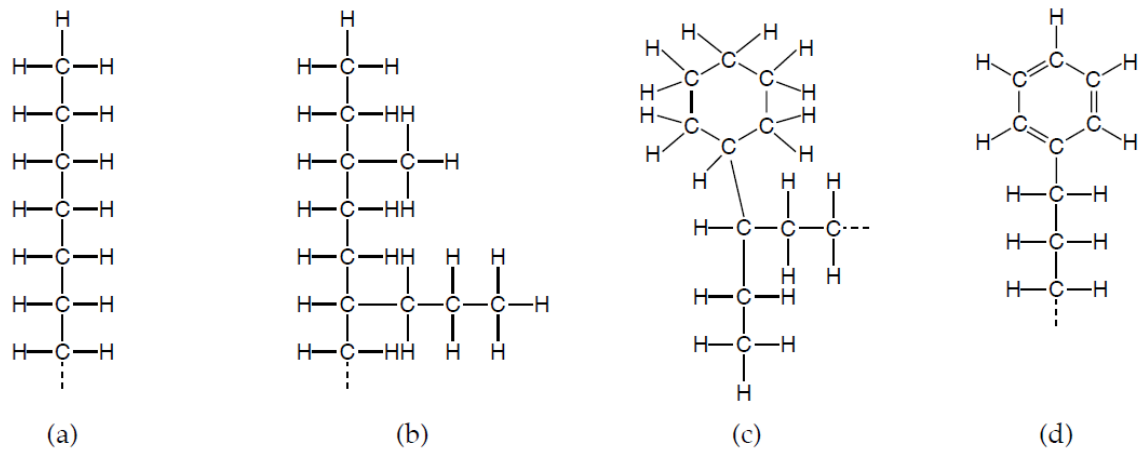


Figure 2.19: Types of mineral oils which include (a) straight paraffin, (b) branched paraffin, (c) naphthene and (d) aromatic [44].

Table 2.2: Types of additives used in lubricating oil (adapted from [108]).

Types of additive	Purpose	Example
Anti-oxidants	to delay the oil ageing process	zinc dialkyl dithiophosphates
Viscosity Modifiers	to give a desired viscosity index	olefin copolymers, polyalkylmethacrylates
Detergents and Dispersants	to keep oil-insoluble combustion by-products in suspension and prevent the agglomeration of the oxidation products into solid particles	calcium phenates, polyisobutene succinimide
Anti-foam Agents	to prevent foaming of lubricants	polydimethylsiloxanes
Anti-wear and Extreme Pressure Additives	to reduce wear	zinc dialkyldithiophosphates
Friction Modifiers	to reduce friction coefficient	Molybdenum disulfide
Corrosion Inhibitors	to protect the metal surface from the attack of oxygen and moisture	petroleum sulfonates
Pour-point Depressants	to enable a lubricant to flow at low temperatures	polymethacrylates

2.3.3 Lubricant Additives

Lubricant additives are chemicals added to base oils to provide certain characteristics to the finished oil. The limits of the properties that exist in the base oils have caused them to be unable to meet the demands of a high performance lubricant. Additives work in a variety of ways such as to improve the properties of the existing base oil, suppress unwanted properties and introduce new features to the base oil. Proper formulation of the lubricant additives and the base oils are capable of enhancing the tribological performance of oil especially in the application of the boundary lubrication. For this purpose, additives are usually blended with a base oil in order to minimise friction, improve wear resistance, increase viscosity, improve viscosity index, control corrosion, improve oxidation stability, increase the life span and reduce contamination. The general classification of lubricant additives includes: friction modifiers, anti-wear and extreme pressure additive, anti-oxidants, corrosion control additives, contamination control additives, viscosity improvers, pour point depressants and foam inhibitors. In line with the scope of this research, only the first three of the additives above (friction modifiers, anti-wear and extreme pressure additives and anti-oxidants) will be discussed in this section.

2.3.3.1 Friction Modifiers

Friction modifiers are an important additive type in boundary lubrication, which act under the mechanism of adsorption (physical or chemical adsorption) to form a “carpet” of molecules on the substrate surface (Figure 2.20) and are used to reduce surface friction and prevent stick-slip phenomena [44]. Typically, they are polar chemical compounds with a

high affinity for metal surfaces and possessing long alkyl chains. Friction modifiers for base oils can be divided into three groups: organic friction modifiers, organo-molybdenum compounds, and nanoparticles [66].

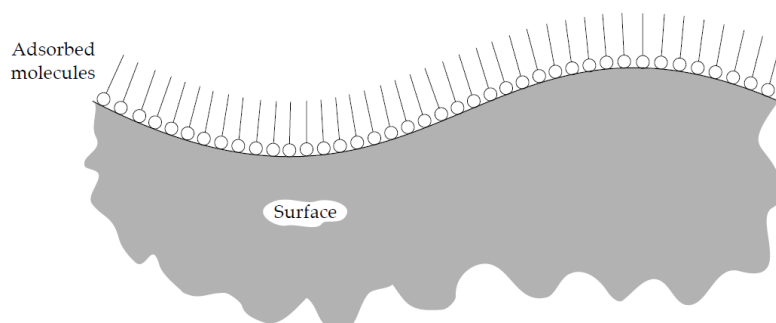


Figure 2.20: Adsorption lubrication mechanism by boundary additives (adapted from [44]).

The organic friction modifiers which were discovered almost a century ago [67], are generally long chain hydrocarbon with polar end groups. They include carboxylic acids [68, 69], esters [70], alcohols [71], amines [72], polymers [66, 73] etc. Their polar end groups are attached to the metal surface by either physical adsorption or chemical reaction, while the hydrocarbon chains extend into the lubricants. Fatty acids are typical additives used in the group of carboxylic acid. Their friction behaviour in hexadecane solution using a ball-on-disc tribometer were found to be influenced by their acid types, where a saturated fatty acid (stearic acid) gave a lower friction coefficient compared to its unsaturated counterpart (oleic acid) (Figure 2.21) [74]. The behaviour of the saturated fatty acid as a linear configuration was suggested to promoted a more closely-packed monolayer to be formed on the surface [68] which contributed to the lower friction result [74]. However, application of carboxylic acids as an additive in an engine oil or transmission fluid is currently reduced because they were found to be corrosive to the engine bearings [75].

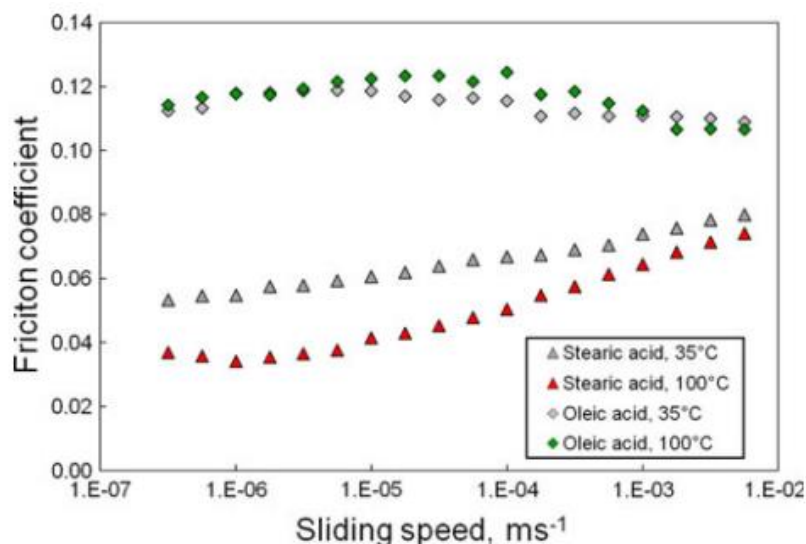


Figure 2.21: Friction versus sliding speed for 0.01 M fatty acids in hexadecane solution at 35 °C and 100 °C [74].

The organo-molybdenum compounds which were recognised in the 1980s [67] are efficient additives as they can reduce friction and wear in the boundary lubrication regime [76-78]. They can be divided into three groups (Figure 2.22): sulphur containing and phosphorus-free compounds, i.e., molybdenum dithiocarbamates (MoDTC); sulphur and phosphorus-containing compounds, i.e., molybdenum dialkyldithiophosphates (MoDTP); and sulphur and phosphorus-free compounds, such as molybdate [79]. It is suggested that the friction reduction on the rubbing surface was related to the formation of tiny nano-sheets of molybdenum disulphide (MoS_2) with a special lamellar-type structure [67] and that produce a low shear strength material [66, 80]. For example, it was reported that the MoS_2 was formed together with the molybdenum oxides from the degradation of MoDTC on the contact surfaces by the tribochemical reaction [81]. Another interesting property of the organo-molybdenum compounds is that instead of working as a friction modifier, they could also perform as anti-wear additives as both MoDTC and MoDTP were found to

reduce friction and wear [82]. In addition, it was reported that the MoDTP has good anti-wear properties in a mineral oil [83] while the molybdate and MoDTC exhibit better anti-wear synergisms with zinc dialkyldithiophosphates (ZDDP) [78, 79].

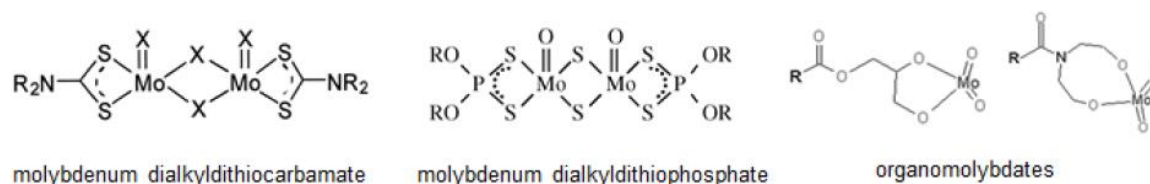


Figure 2.22: Three types of organo-molybdenum friction modifiers [67].

Recent research and development activities in the field of chemistry and nanotechnology have provided the possibility of producing a friction modifier based on nanoparticles [84]. Nanoparticles are particles in the size range of 2-120 nm [66] that variously consist of metals (e.g. copper, Cu), metallic oxides (e.g. copper oxide, CuO and titanium dioxide, TiO₂), borates and phosphates, fullerenes, inorganic fullerenes, or oxides and nitrides of boron [67]. They are added into lubrication oils as friction modifiers to reduce friction and wear [84-86]. It was reported that their tribological performance as a friction modifier is influenced by factors such as the structure of the nanoparticles, size, shape and concentration [87]. There are three mechanisms by which the nanoparticles may reduce the friction which are pressure dependent, as proposed by Joly et al. (Figure 2.23) [88]. Particle rolling can occur at low pressure which is subject to the particles' shape and hardness. At moderate pressure the particles remain intact, but slide against the bounding surfaces. At higher pressures the particles are crushed to form a low shear strength layer-lattice film and thus, give a lower friction coefficient [88].

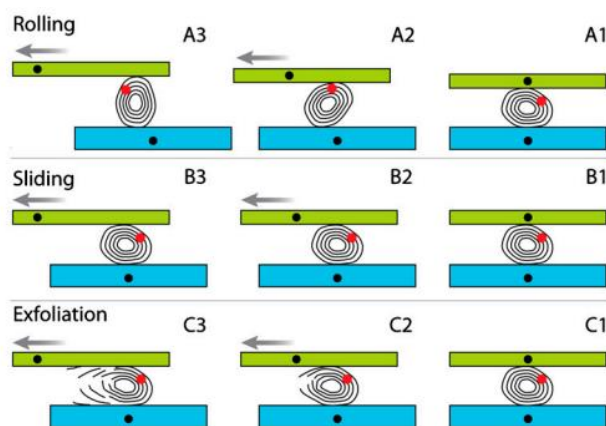


Figure 2.23: The three main mechanisms of friction: rolling (A), sliding (B) and exfoliation (C). The lower substrate is fixed while the upper substrate is slit to the left. The red mark is a reference point of a nanoparticle [88].

2.3.3.2 Anti-wear and Extreme-pressure Additives

Anti-wear and extreme-pressure (EP) additives protect rubbing surfaces from metal-to-metal contact and thus minimise wear and prevent seizure under a boundary lubrication condition. Anti-wear additives serve to form surface films in minimising the wear rate, whereas EP additives are expected to react rapidly with a surface under severe distress (higher load) to prevent more catastrophic damage such as scuffing, galling, and seizure [89]. Some EP additives tend to be very reactive and may influence the oil oxidative stability [90], and others are corrosive to metals [91, 92] and can reduce the life span of machine components [93]. EP additives are not typically used in motor oil. They should only be used when the lubricant is subjected to severe distress conditions such as in a gear tooth contact. A wide variety of anti-wear and EP additives are available and include phosphate esters, sulfurized olefins (EP additives), borates, phosphites, metal dithiophosphates and metal dithiocarbamates [94]. Of the additives classification listed

above, the zinc dialkyldithiophosphates (ZDDP) are still widely used in engine oil even though it was first developed in the 1940s [95].

ZDDP is synthesised by the reaction of alcohols with phosphorus pentasulfide (P_2S_5) to produce dialkyldithiophosphoric acid. It is then neutralised by the zinc oxide to give the product as is shown in Figure 2.24 [96]. A large volume of research has been conducted to comprehend the lubrication mechanism performed by the ZDDP [95, 97, 98]. The mechanism starts with the formation of the layer which consists of the organic iron compound and ZDDP decomposition compound (OIC) and metal oxides mixed with the metallic substrate (OMM) on the metal surface (Figure 2.25) [99]. During sliding, the ZDDP is decomposed to produce a glassy zinc and iron polyphosphate which mixes with the OMM layer and provides the wear resistant behaviour. Next, the organic ZDDP compound can generate the simultaneous formation of OMM and OIC layers at elevated temperature and loading. Anti-wear pads of iron phosphates and a durable anti-wear film containing higher concentrations of S, Zn, and P is then formed (known as OIC-Zn film). As sliding continues, the OMM layers could wear out, but the OIC-Zn films form a strong protection layer from wear. In addition, the OIC-Zn films can induce a film formation of iron oxide, metallic iron, and iron carbide. These ZDDP induced films have much higher loading capacity and serve as an anti-wear and anti-scuffing film to protect steel substrates [99].

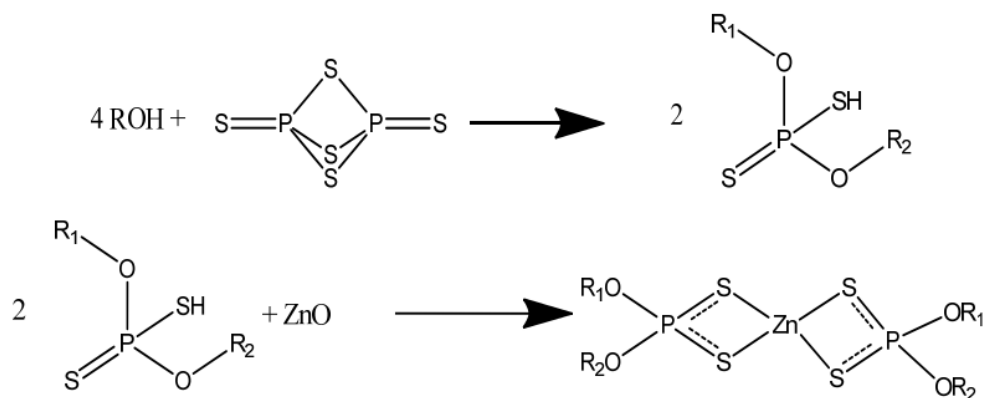


Figure 2.24: Method for the preparation of zinc dialkyldithio-phosphate (ZDDP) [96].

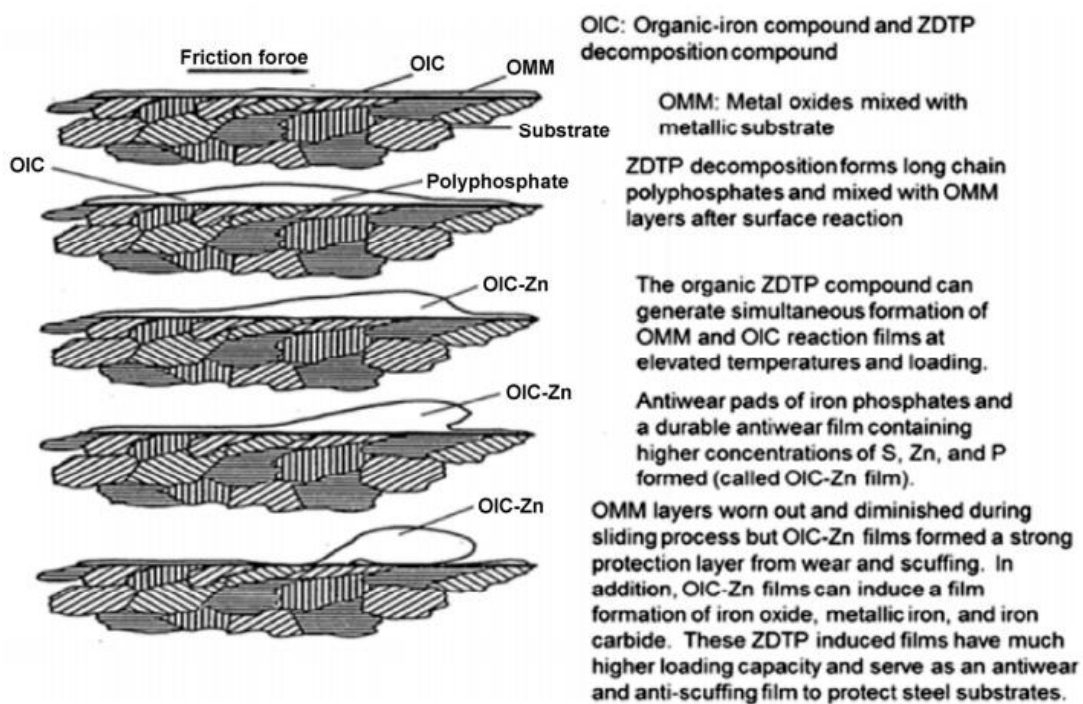


Figure 2.25: Antiwear film formation mechanism by ZDDP [99].

2.3.3.3 Anti-oxidants

Oxidation stability is an important aspect in the field of lubrication and should be properly controlled. Engine oil is more susceptible to undergo a process of oxidation compared to other lubricants due to the condition of the internal combustion engine. For example, the presence of oxygen during the combustion process, the production of heat and the presence of metallic materials on engine components such as copper and iron can act as an effective catalyst for oxidation. Oxidation of a lubricating oil generally increases its viscosity and results in the formation of the acidic compounds and hydroperoxides, which may promote corrosion, particularly of hard alloy bearings [100]. Therefore, it is very important for the oxidation stability of an engine oil to be maximised. Antioxidants are additives that protect the oxidative degradation of lubricating oil, allowing them to meet the demanding requirements for use in engines and industrial applications.

There are three steps as the oxidation process takes place; initiation, propagation and termination [44]. During the initial stage, a free radical is generated by breaking a bond with a hydrogen atom from a hydrocarbon molecule. The free radical is a very reactive chemical that can react with oxygen to form a peroxy radical. A peroxy radical then may react with another hydrocarbon molecule to form hydroperoxides during the propagation stage. Finally, two radical species can react with each other to form a stable compound. This is known as the termination stage because it removes free radicals from the system.

The existence of antioxidant may disrupt the oil degradation process by destructing the free radicals and peroxy radicals. This can be performed through the use of radical scavengers and peroxide decomposers. The radical scavengers are known as primary antioxidants inhibits oxidation by reacting with free radicals, interrupting the radical chain mechanism of the auto-oxidation process to form stable molecules [101]. Hindered phenolics and aromatic amines are the two chemical classes of primary antioxidants for lubricants [100]. The peroxide decomposers are known as secondary antioxidants act by specifically decomposing the peroxy radicals. Sulphur and phosphorus compounds may reduce the alkyl hydroperoxides in the radical chain to alcohols while being oxidised. The ZDDP, phosphites, and thio-ethers are examples of different chemical classes of secondary antioxidants.

Several effective antioxidants classes have been developed over the years and have seen use in engine oils, automatic transmission fluids, gear oils and metal-working fluids. The main classes of oil-soluble organic and organo-metallic antioxidants include the following types: sulphur compounds[102], phosphorus compounds [103], sulfur-phosphorus compounds [100], amine compounds [104], hindered phenolic compounds [105], organo-zinc compounds, organo-copper compounds and organo-molybdenum compounds [100].

2.4 Vegetable oils

Vegetable oils are those oils extracted from plant seeds like palm oil, soybean oil and rapeseed oil. They are essential elements in food preparation because they act as

medium for cooking or frying. While most of the vegetable oils are suitable for cooking (known as edible oils), there are several types of vegetable oils that are unsuitable for human consumption due to the presence of toxic components in the oil [106]. These oils are categorised as non-edible oils which include karanja oil, jojoba oil and jatropha oil. There are nine major vegetable oils produced by several countries around the world [107]. Palm oil and soybean oil are two types of vegetable oils that have the largest production volume (Figure 2.26).

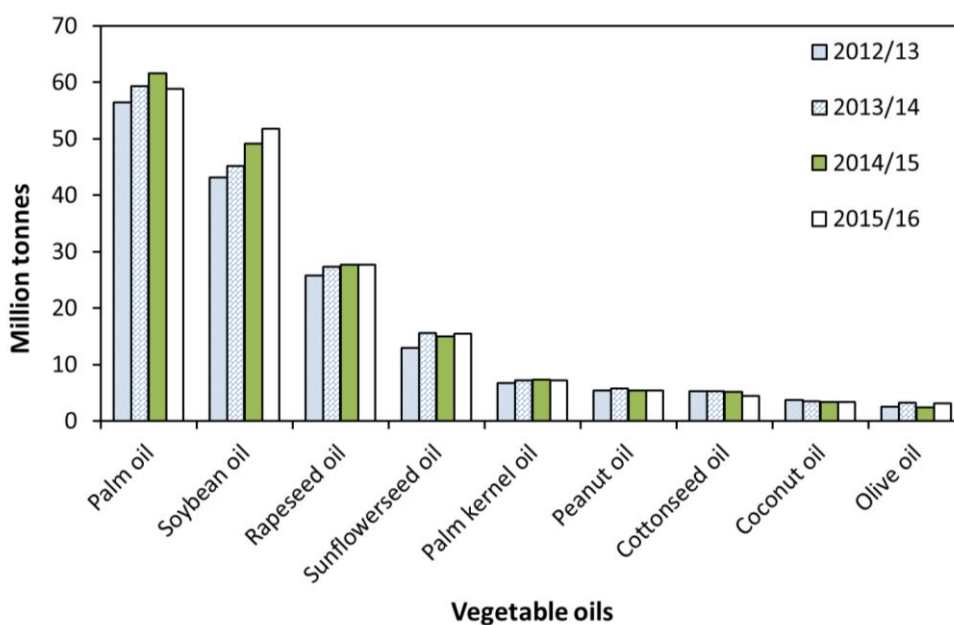


Figure 2.26: Production in million tonnes of nine major vegetable oils from 2012/13 to 2015/16 (adapted from [107]). Production data are often reported in harvest years such as 2012/13.

The chemical structure of vegetable oil is constructed from glycerol and fatty acids known as triglycerides. Triglycerides are an ester derived from one molecule of glycerol (an organic alcohol) bonding chemically with three fatty acids (an organic acid) as shown in Figure 2.27. Apart from the existence of triglycerides in vegetable oils, it is also a type

of fat (lipid) that can be found in human blood whose function is to store excessive calories and convert them into energy.

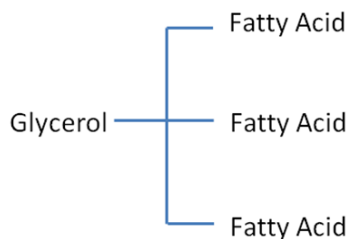


Figure 2.27: Structure of triglycerides

Fatty acids can be classified into two main categories; saturated and unsaturated, based on the number of double bonds existing in their carbon chain. Stearic acid and palmitic acid, for example, have no double bonds in their carbon to carbon chain and are grouped as saturated acids. Unsaturated acids are those constructed with double bonds in their carbon chain and comprise of ‘mono’ and ‘poly’ unsaturated groups. Monounsaturated fatty acids are those with one double bonds in their carbon chain such as oleic acid. If the fatty acid consists of two or more double bonds, they are classified as polyunsaturated acids. Linoleic and linolenic acid are examples of polyunsaturated fatty acid. The molecular structure of the fatty acid groups is depicted in Table 2.3 [109]. While a saturated fatty acid is a linear molecule, the double bonds in an unsaturated fatty acid cause the structure to bend.

Table 2.3: Classification of Fatty Acids (adapted from [109])

Fatty acids group	Number of double bonds in hydrocarbon chain	Example	Molecular structure
Saturated	0	Stearic acid	<chem>CCCCCCCCCCCCCCCC(=O)O</chem>
Monounsaturated	1	Oleic acid	<chem>CCCC=CCCCCCCC(=O)O</chem>
Polyunsaturated	2	Linoleic acid	<chem>CCCC=CC=CCCC(=O)O</chem>

A fatty acid is an organic polar molecule which contains a carboxyl group (COOH) in its chain. The polarity of the fatty acid causes one end of its molecule (carboxyl group, -COOH) to be attracted to the metal surface, while the other end (alkyl group, -CH₃) is repelled from the surface. This process is known as physical adsorption (physisorption) which involves intermolecular forces like van de Waals and is able to provide a monomolecular layer which serves to minimise friction on the surface (Figure 2.28a) [110]. Another adsorption mechanism of fatty acids on a metal surface is called chemical adsorption (chemisorption). This involves some degree of chemical bonding between carboxyl groups and a metal surface (substrate) via electron exchange with substrate atoms (Figure 2.28b) [110]. An example of this is stearic acid molecules that adhere on an iron oxide surface (Figure 2.28c) to form iron carboxylate [111].

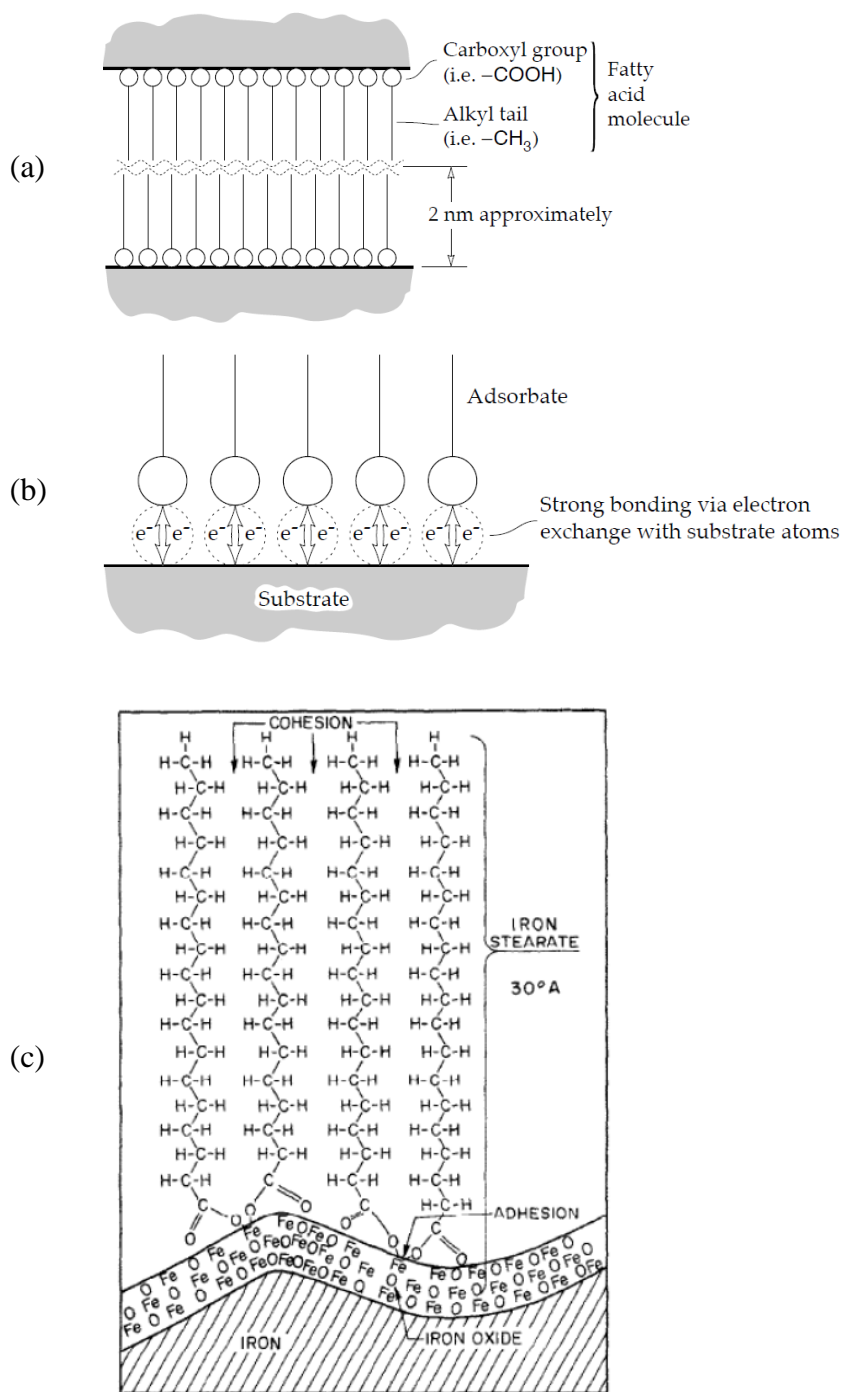


Figure 2.28: (a) Mechanism of physisorption of fatty acid molecule [110], (b) Model of chemisorption of fatty acid molecule on metal surfaces [110] and (c) chemisorption of stearic acid on iron oxide surface [111].

2.4.1 Palm oil

Palm oil is an edible vegetable oil extracted from the fruit of palm trees and grown mainly across the region of the equator. Production and exports of this oil are dominated by two South East Asian countries; Indonesia and Malaysia. It was reported that in 2015/16 Indonesia was producing 32 million tonnes, which is 54 % of global palm oil production; for Malaysia these figures were 17.7 million tonnes and 30% respectively [107].

At room temperature, palm oil is a semi-solid and thus, requires a treatment process to make it viable as a liquid at room temperature. Palm oil can be fractionated into fluid part (palm olein) and solid part (palm stearin) through further process such as refining, bleaching and deodorising. However, the palm olein contains higher levels of oleic acid (46%) and linoleic acid (11%) compared to palm oil (Table 2.5) making it more unsaturated which means more susceptible to oxidation. Some of the properties of palm olein are listed in Table 2.4 as a comparison to commercial mineral engine oil (15W40) properties [112].

Table 2.4: Properties of palm olein and soybean oil (adapted from [112-115])

		Palm Olein	Soybean Oil	Mineral Engine Oil (15W40)
Density (mg/ml)		0.8975	0.9075	0.873
Viscosity (cSt)	@ 40 °C	45.9	30.52	110
	@ 100 °C	9.4	7.42	15.0
Viscosity index		195	224	142
Acid number (mgKOH/g)		-	0.10	2.8
Pour point (°C)		5	-9	-30
Flash point (°C)		320	314	204

Table 2.5: Fatty acid composition of major vegetable oils (adapted from [114])

Oil	Unsaturated/ Saturated Ratio	Saturated					Mono- unsaturated	Poly- unsaturated	Alpha Linolenic acid C18:3
		Capric acid C10:0	Lauric acid C12:0	Myristic acid C14:0	Palmitic acid C16:0	Stearic acid C18:0	Oleic acid C18:1	Linoleic acid C18:2	
Coconut Oil	0.1	6	47	18	9	3	6	2	-
Palm Kernel Oil	0.2	4	48	16	8	3	15	2	-
Palm Oil	1	-	-	1	45	4	40	10	-
Palm Olein	1.3	-	-	1	37	4	46	11	-
Cottonseed Oil	2.8	-	-	1	22	3	19	54	1
Peanut Oil	4	-	-	-	11	2	48	32	-
Olive Oil	4.6	-	-	-	13	3	71	10	1
Soybean Oil	5.7	-	-	-	11	4	24	54	7
Sunflower Oil	7.3	-	-	-	7	5	19	68	1
Rapeseed Oil	15.7	-	-	-	4	2	62	22	10

 Degree of unsaturated increases

2.4.2 Soybean oil

Soybean oil has the second largest production volume of vegetable oils (Figure 2.26) around the world. China and the United States are two major producers of soybean oil, followed by Brazil and Argentina [107]. It was reported that in 2015/16 production term, China was producing 14.6 million tonnes of soybean oil which is equivalent to 28 % of total production globally, while the United States was in second place with 9.9 million tonnes production (19 % of total production) [107].

Crude soybean oil (also known as unrefined oil) can be produced by using a hydraulic press without the use of chemicals. However, this process is not widely used because of cost constraints and gives lower output. Refined soybean oil can be produced from soybeans through processes such as cleaning and cracking before they are rolled into flakes. The extraction process is performed in which a solution of hexane is used to extract oil from the flakes. This oil will then go through the process called degumming and refining before the refined soybean oil is produced [116]. The composition of free fatty acids and concentrations of minor constituents are reduced in refined soybean oil compared to unrefined oil (Table 2.6) [117].

Soybean oil is relatively more unsaturated compared to palm oil due to a higher content of linoleic and linolenic acid (Table 2.5). These fatty acids are essential for human nutrition, but they have the disadvantage of providing oxidative instability to the oil. Some alteration has been made to the soybean oil through a hydrogenation process [118] and genetic modification [119] in order to modify fatty acid composition for oxidative stability improvement.

Table 2.6: Composition for crude and refined soybean oil [117]

Components	Crude oil	Refined oil
Triacylglycerols (%)	95–97	>99
Phospholipids (%)	1.5–2.5	0.003–0.045
Unsaponifiable matter (%)	1.6	0.3
Phytosterols	0.33	0.13
Tocopherols	0.15–0.21	0.11–0.18
Hydrocarbons	0.014	0.01
Free fatty acids (%)	0.3–0.7	<0.05
Trace metals (ppm)		
Iron	1–3	0.1–0.3
Copper	0.03–0.05	0.02–0.06

2.4.3 Oxidation of oils

Most materials will react when exposed to oxygen, but it depends on the degree of reaction of that particular material with oxygen. For example, when exposed to heat, air and moisture during a frying process, vegetable oils could oxidise rapidly. Normally, the initiation of vegetable oil oxidation can be identified by the smell of oil rancidity. Other clues that show oxidation occurs in a lubricating oil (mineral oil) include an increase in oil viscosity and acid number (Figure 2.29) [44, 120] which indicate that acids are produced during the oxidation process. Changes in oil viscosity indicate that the oil has undergone a thickening process in which changes in the molecular structure occur resulting in the start of the polymerization process [114]. There was a sharp increase in the oil viscosity after 120 hours of oxidation time and at 150 hours the viscosity was about 8 fold (Figure 2.29). A similar trend can also be seen with oil acidity, expressed as Acid Number. An oil that is severely oxidised needs to be replaced because it causes loss of power due to increased viscous drag and corrosion in an engine components [44].

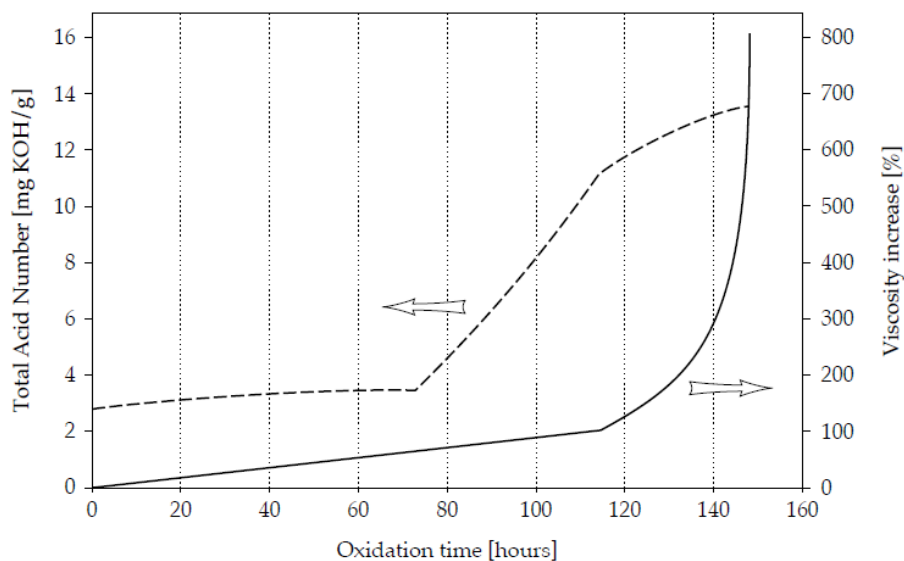


Figure 2.29: Effects of oil oxidation on acid number and viscosity of mineral oil [44].

2.4.3.1 Mechanism of vegetable oil autoxidation

Oxidation stability of vegetable oils is influenced by the level of unsaturated bonds. Vegetable oils with a higher level of unsaturated fatty acids are more easily oxidised. The presence of a double bond in the carbon chain of the fatty acid serves as an active area for the oxidation reaction [121]. In addition, a more double bond exists in the carbon chain of a vegetable oil, the more susceptible the oil is to oxidation [122]. The general oxidation mechanism is shown in Table 2.7 [123].

At the initial stage of the vegetable oil oxidation process, free radicals are formed from hydrocarbon molecules by removal of hydrogen atom from the methylene group next to the double bond. The presence of oxygen will then accelerate the reaction with free radicals to form peroxy radicals. Hydroperoxide with another free radical can then be formed when the peroxy radicals attack the hydrocarbon molecule. This propagates the oxidation process.

Table 2.7: Mechanism of oil autoxidation (adapted from [123])

Radical formation	$RH \rightarrow R^\circ + H^\circ$
Peroxide formation	$R^\circ + O_2 \rightarrow ROO^\circ$
Hydroperoxide formation (propagation)	$ROO^\circ + RH \rightarrow ROOH + R^\circ$

Note: RH is a hydrocarbon; R is a radical; R° is a free radical; H° is a hydrogen ion; ROO° is a peroxy radical and ROOH is a hydroperoxide radical (an organic acid)

2.4.3.2 Oil oxidation impact on lubrication

The study of the effects of hydroperoxides on the tribological performance of vegetables is very limited. The increase in wear scar diameter with ageing of coconut oil and soybean oil was found to be strongly related to the formation of hydroperoxides. The formation of hydroperoxides in coconut and soybean oil was influenced by ageing (Figure 2.30) [124] in which the hydroperoxide level for soybean oil rose significantly after 28 days compared to coconut oil. The increased level of hydroperoxides has shown a significant effect on wear (Figure 2.31).

The difference of hydroperoxide level in coconut and soybean oil has been explained in terms of their fatty acid composition [124]. Coconut oil, which is enriched with saturated fatty acids, is better in oxidation stability compared to soybean oil, which has a higher level of unsaturated fatty acids. The double bonds in unsaturated fatty acids are highly susceptible to oxidation, leading to the destruction of triglyceride structure and the formation of various oxidation products. As hydroperoxide builds up, some of them decompose forming various secondary products [123]. It is believed that the increase of wear was due to a continuous reaction between these hydroperoxides and its derivatives with the surface [124].

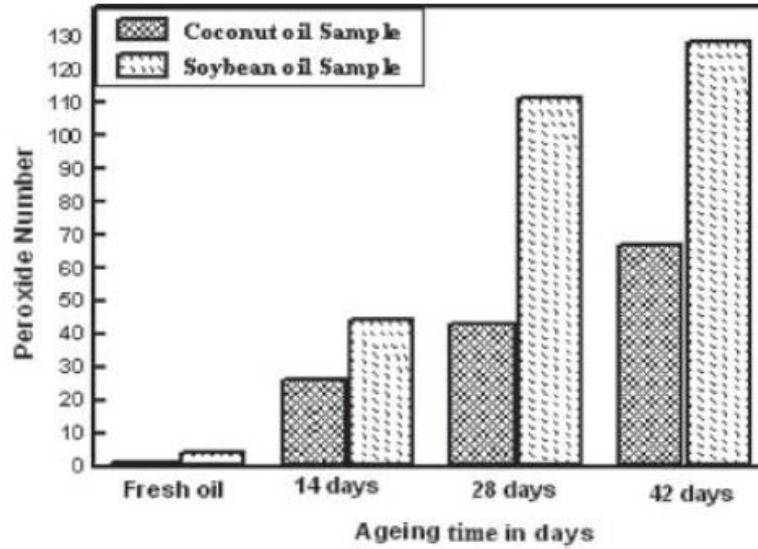


Figure 2.30: Effect of ageing on peroxide number for coconut and soybean oil [124].

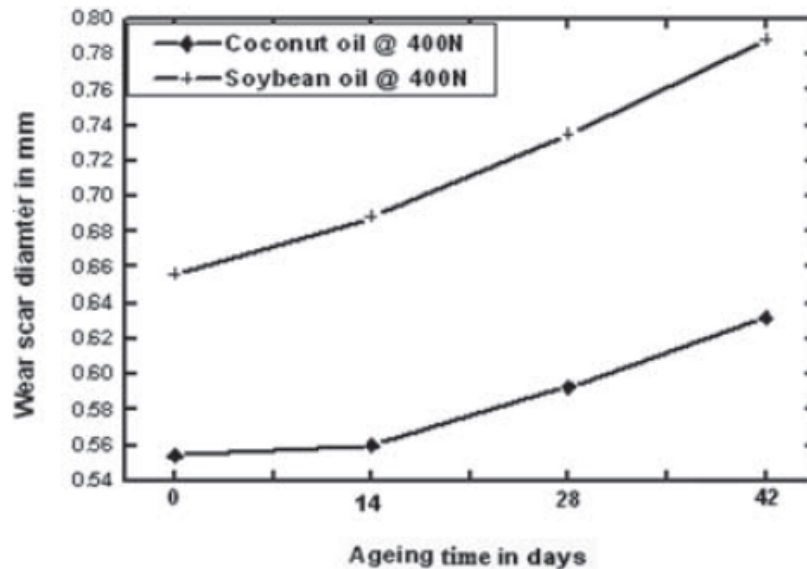


Figure 2.31: Effect of ageing on wear for coconut and soybean oil [124].

The impact of hydroperoxides on the lubrication performance of mineral oils has been studied by Newley et al. [125] and Habeeb and Stover [126]. A close relationship was observed between increased wear and peroxide accumulation (Figure 2.32) [125]. However, the wear and level of hydroperoxide was reduced when an anti-oxidants, peroxide decomposers and radical scavengers added into the lubricant reduced both peroxide accumulation and wear [125]. The role of hydroperoxides in engine wear with anti-oxidant package (zinc dialkyl dithiophosphate) in commercial engine oil has been investigated [126].

While there was a little wear observed in fresh oil, addition of hydroperoxides caused a tremendous increase in wear which was related to the concentration (Figure 2.33). The increase in wear was suggested to be due to oxidative attack on the metal surfaces [126].

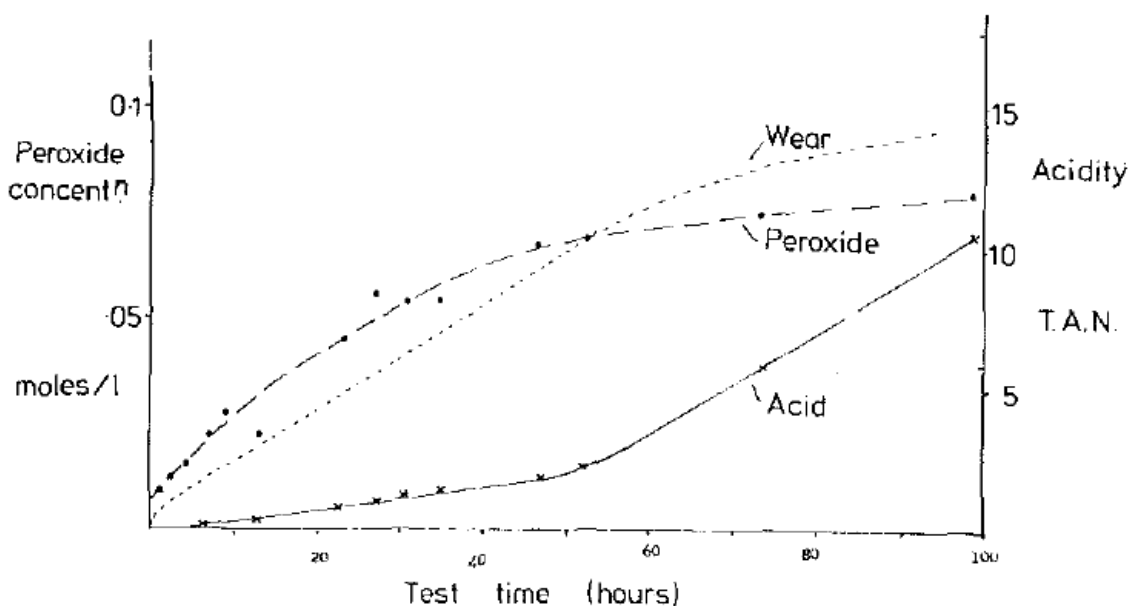


Figure 2.32: Influence of wear on hydroperoxide level in lubricant oil [125].

2.5 Tribological performance of vegetable oil lubricants

Tribological performances of vegetable oils as biolubricants have been reported in many experimental studies mainly by bench experiments. The tests can be classified into four areas (depending on nature of oil) typically comprising pure oil [9-19]; blended with other oil [20-22]; formulated with additives [12, 16, 24-28] and with modification through chemical synthesis [18, 28, 35-39].

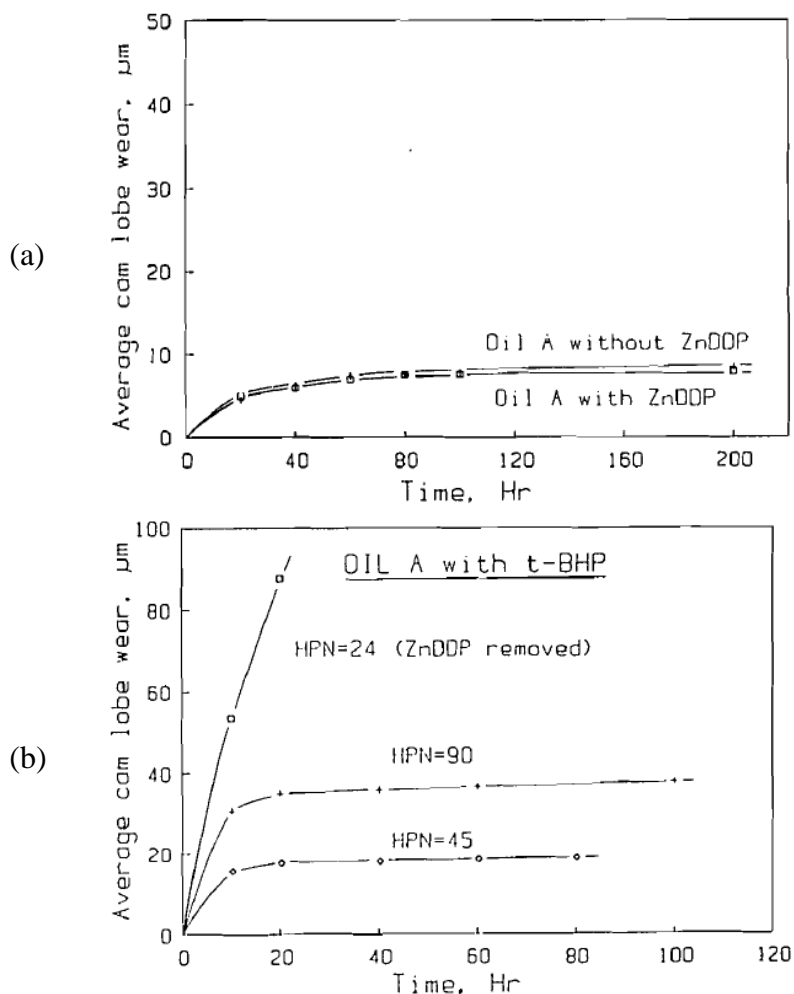


Figure 2.33: (a) Wear of fresh engine oil and (b) the effect of hydroperoxide (t-BHP) at difference concentration (HPN) on wear [126].

2.5.1 Performance of pure vegetable oil lubricants

The essential step in assessing the potential of vegetable oils as biolubricants is by running the test in their pure oil state. This is important because base stocks have a strong influence on the fluid lubricant chemical and tribological properties [127]. The pure vegetable oils that have been evaluated tribologically include; coconut oil [12], safflower oil [10], corn oil, rapeseed oil [128], jojoba oil [129], olive oil [14], castor oil [14], palm oil [15] and soybean oil [38]. Of the various tribological experiments conducted on vegetable oils, very few of them provide a scientific explanation in supporting their friction and wear results.

A comparative study of sixteen commercial pure vegetable oils with mineral lubricant and synthetic esters was conducted using a reciprocating ball-on-disc tribometer by Gerbig et al. [14]. Gerbig simulated two wear mechanisms with a ball-on-disc contact; the adhesive mechanism by using same material for ball and disc (AISI 52100) and abrasive mechanism by using alumina (Al_2O_3) as the disc. It was found that under the tests representative of adhesive wear, only linseed, olive, walnut and safflower oils showed a stable low friction coefficient (COF \sim 0.11) while the rest of the oils presented unstable friction curves. While olive and safflower oils gave the lowest friction, their wear result also gave the lowest value in wear resistance. However, the vegetable oils were far behind from the mineral oil and synthetic esters in terms of friction and wear performance. Under abrasive wear conditions, all oils showed steady and low friction values (COF = 0.11 to 0.13). However, in terms of wear, significant differences were found in which sesame and castor oils showed the least abrasive wear damage. Gerbig's tests concluded that the tribological performance of the vegetables oils depends strongly on the tribosystem (material used and contact condition).

Another comparative study of vegetable oils performance has been that of Reeves et al. [130] on the influence of fatty acids on tribological performance. Using pin-on-disc testing at ambient conditions, their investigation attempted to link the fatty acids composition with the friction and wear in eight types of vegetable oils. Reeves provided a standard for quantifying the fatty acid concentrations in vegetable oils by defining unsaturation number (UN) which refers to the average number of double bonds. It was found that the avocado oil with the lowest in unsaturation level (UN = 0.985) shown the best tribological performance with the lowest friction (COF= 0.0201) and wear (0.1037 mm^3) when compared to other vegetable oils (Figure 2.34). Contrary to this, soybean oil with UN = 1.451 showed higher friction (COF= 0.4059) and wear (0.3839 mm^3). They concluded that the friction and wear

could be reduced through formation of a monolayer which serves to minimise the metal-to-metal contact by saturated and monounsaturated fatty acids (oleic acid in avocado oil) [131]. More double bond presence in the fatty acids (linoleic acid in soybean oil) however, decreased the density of the fatty acid monolayer [130].

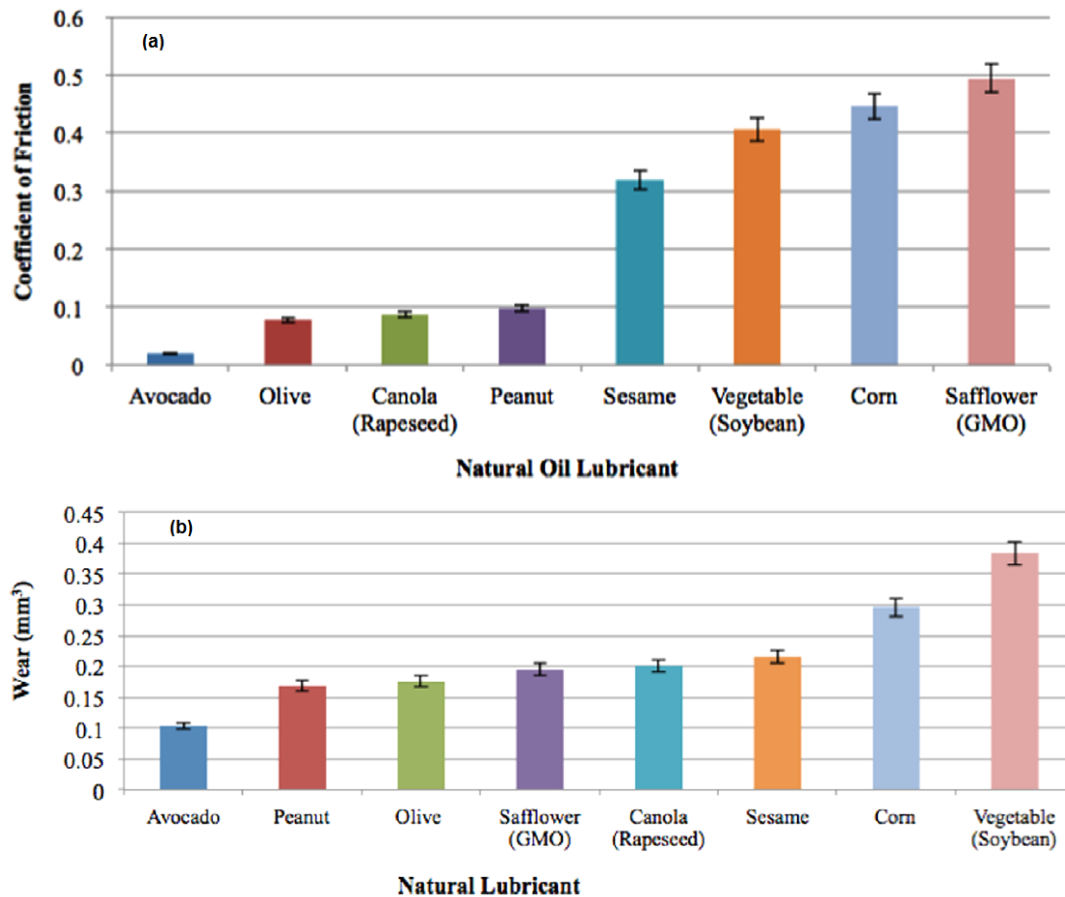


Figure 2.34: (a) Friction and (b) wear results of eight vegetable oils using pin-on-disc tester performed at ambient temperature by Reeves et al [130].

The hypothetical explanation of Reeves et al. [130] regarding the influence of fatty acids on the formation of monolayer was supported by experimental results of saturated and unsaturated fatty acids in sunflower oil conducted by Fox et al. using a ball-on-plate test rig [131]. It was reported that increasing an unsaturation level in the fatty acids (stearic, oleic, linoleic in ascending order), which means increasing number of double bonds, has increased the wear and friction in boundary lubrication (Figure 2.35). Fox suggested that the stearic

acid which has no double bond is aligned linearly on the surface thus, it was closely packed and served as a strong protective layer. On the other hand, the presence of double bonds in both oleic and linoleic acids will force a bend in the chain and they become more difficult to pack close together, resulting in a weaker protective layer.

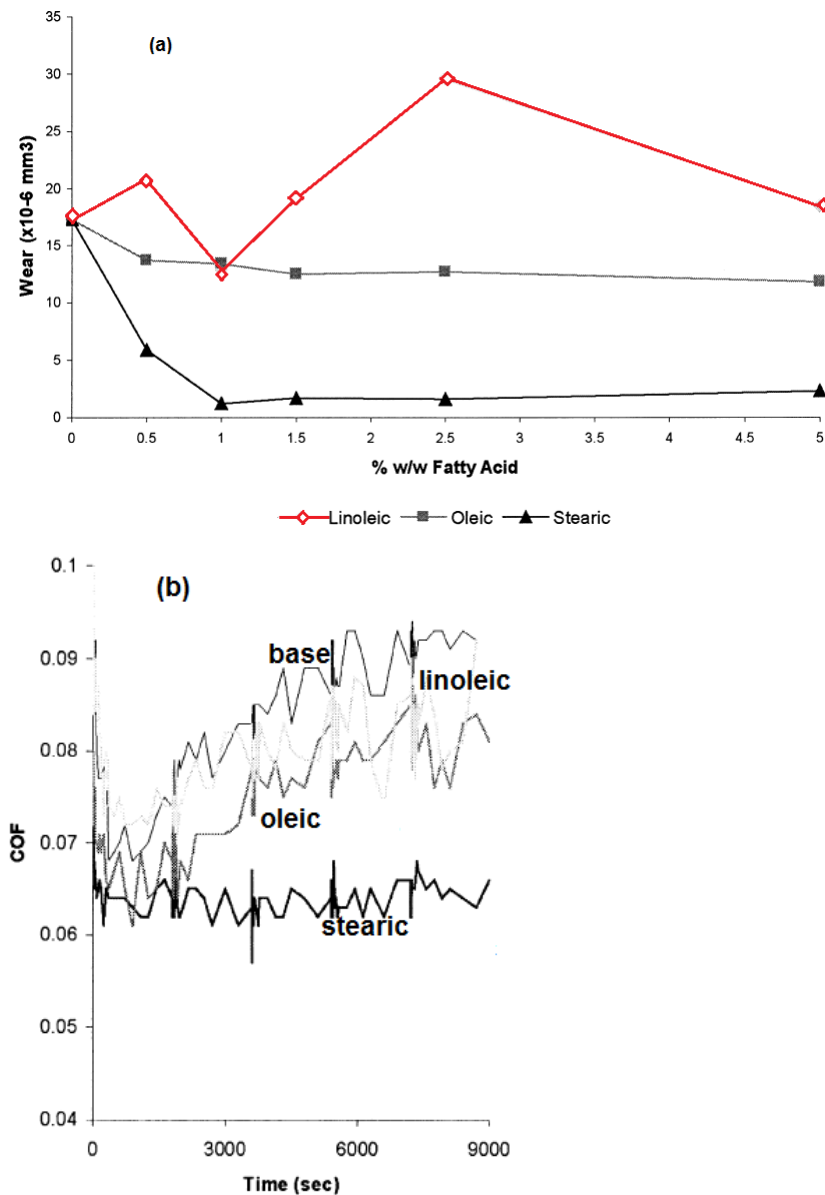


Figure 2.35: (a) Effect of saturated (stearic) and unsaturated fatty acids (oleic and linoleic) in sunflower oil on wear and (b) friction at 1% weight of fatty acids in sunflower oil (adapted from Fox et al. [131]).

The explanation provided by Reeves et al. [130] and Fox et al. [131] however, contradicts with the adsorption test result of unsaturated fatty acids on steel conducted by Lundgren et al. [132]. It was revealed that the amount of unsaturated fatty acids in two spreading solvents (hexadecane and heptamethylnonane) adsorbed on steel surfaces was increased with increasing in unsaturation of the fatty acids (Figure 2.36). Lundgren analysed the area per molecule and collapse area of fully protonated fatty acids [133] and linked them with the adsorption result; these area increased as the unsaturation of fatty acids increases [132]. In another test of Lundgren et al. [134], using surface force apparatus, they investigated the influence of unsaturation in fatty acids on friction on mica surfaces. It was however, reported that the friction coefficient increased with increasing unsaturation (Table 2.8) which agreed with the two different load regimes seen for linoleic acid.

Table 2.8: The influence of unsaturated fatty acids on friction coefficient (μ) and film thickness (D) running at different speed (0.4, 4 $\mu\text{m/s}$) and adsorption time (1, 24 hours) [134]. Note: Linoleic acid showed two regimes of friction coefficient with increasing load, corresponding to two different film thicknesses.

System	D (Å)	Ads. time (h)	μ	
			$v = 0.4 \mu\text{m/s}$	$v = 4 \mu\text{m/s}$
<i>n</i> -Hexadecane	5–8	1, 24	0.11 ± 0.01^a	
Stearic acid	46–54	1, 24	0.055 ± 0.005	
Oleic acid	50–55	1, 24	0.16 ± 0.01	
Linoleic acid	20–25	1	0.50 ± 0.02	1.1 ± 0.1
		24	0.58 ± 0.03	1.5 ± 0.1
	12–15	1	0.16 ± 0.01^a	0.60 ± 0.02^a
		24	0.14 ± 0.01^a	0.60 ± 0.05^a
Dehydroabietic acid	13–15	1	0.30 ± 0.01	

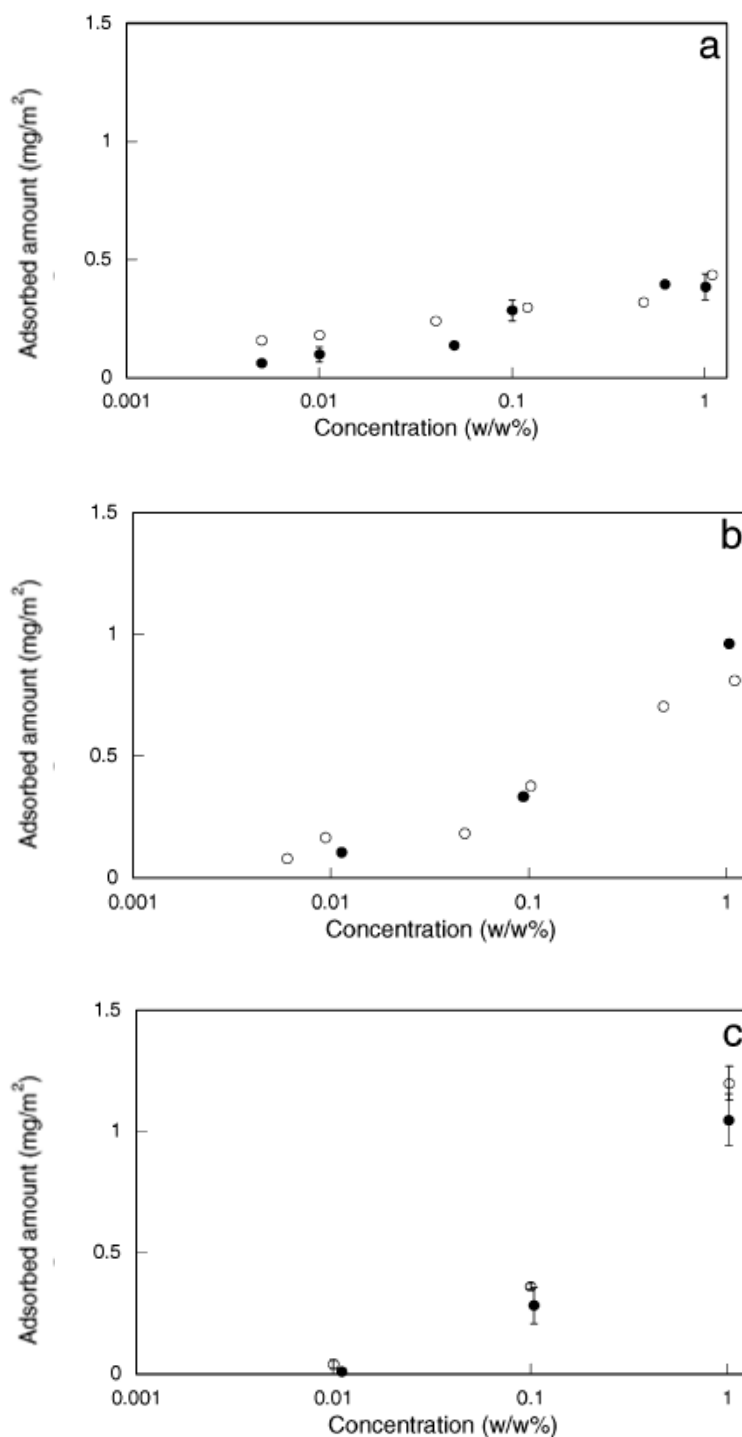


Figure 2.36: The amount of (a) oleic acid, (b) linoleic acid and (c) linolenic acid in n-hexadecane (●) and heptamethylnonane (°) solutions adsorbed on steel surface [132].

Interest in investigating the effect of vegetable oil oxidation on wear and friction performance also arises among researchers. Using a four-ball-tribotester, Jagadeesh et al. [11] was comparing five types of vegetable oils with their oxidised version on boundary

lubrication. It was observed that the oil viscosity, peroxide level, fatty acid composition and wear scar diameter were increased with ageing duration and oil temperature. However, Jagadeesh reported that the friction coefficient for oxidised oils was reduced. He linked this situation with the build-up of free fatty acids during oxidation and thus, facilitating the formation of metallic soaps with low shear strength.

2.5.1.1 Tribological performance of palm oil and soybean oil

Palm oil (PO) and soybean oil (SBO) are the two types of vegetable oil that have the highest consumption globally (1995 to 2015) when more than 100 million metric tons were produced [135]. Chemically, these two oils differ by virtue of different fatty acid makeup (both type of and percentages of) (Table 2.5). PO has a higher level of saturated fatty acids compared to soybean oil. Saturated fatty acids that exist in palm oil like palmitic acid and stearic acid have no double bond in their carbon chain and are thus less reactive to oxidation. PO has exhibited outstanding oxidation stability when tested at 180°C [136]. SBO, on the other hand, has a higher level of unsaturated fatty acids which contain carbon double bonds in their chemical structure and thus is vulnerable to oil oxidation [137, 138]. However, these unsaturated fatty acids (linoleic acid and alpha-linolenic acid) could increase the melting point, thus SBO has higher liquidity at a lower temperature than PO.

Research works in comparing the tribological performance between PO and SBO are limited to a four-ball-tribotester [9, 11] and results were not consistent between researchers. For example, Jagadeesh [11] reported that, at 400N of load and 75 °C of oil temperature, PO has lower coefficient of friction (COF) and produced less wear compared to SBO. However, at lower loads of 147 N and 392 N (ASTM D4172) Syahrullail [9] found that although the PO has a lower COF than SBO, in terms of wear resistance, SBO performed better than PO.

Contrary to this, it was seen that the SBO produced lower COF and less wear than PO at higher load (1236 N) [9].

Of many studies on PO and SBO lubricating performance, very limited work was found applicable to the lubrication system of an internal combustion engine. It was Masjuki et al. [15] who tested the lower and upper piston ring on plates made from grey cast iron (GCI) and compared the PO with a mineral oil (MO) based lubricant using a reciprocating test. However, the test was performed at low load, 10 N (3.0 MPa contact pressure) and room temperature. It was found that, although the PO produced higher COF than the MO based lubricant, the wear resistance of PO was found to be better (example of upper piston ring results are shown in Figure 2.37). In their investigation, Masjuki et al. identified although the abrasive wear was the main wear mechanisms on both piston rings, the levels of wear were different for each ring. While more grooves, pits and material transfer was observed on lower piston ring, small cracks were present on upper piston rings (Figure 2.38).

More recent development on the palm oil lubrication research was focused on the chemical modification of palm oil. For example, Zulkifli et al. [37] reported on the tribological performance of the palm oil based trimethylolpropane ester (TMP). This lubricant oil was produced from the transesterification process of palm oil methyl ester with trimethylolpropane in order to improve the oxidative and thermal stability [139]. Using a four-ball-tribometer, he conducted a friction and wear test at extreme pressure. He compared various ratios of TMP in paraffinic oil and found that both friction and wear were better than paraffinic oil at various load.

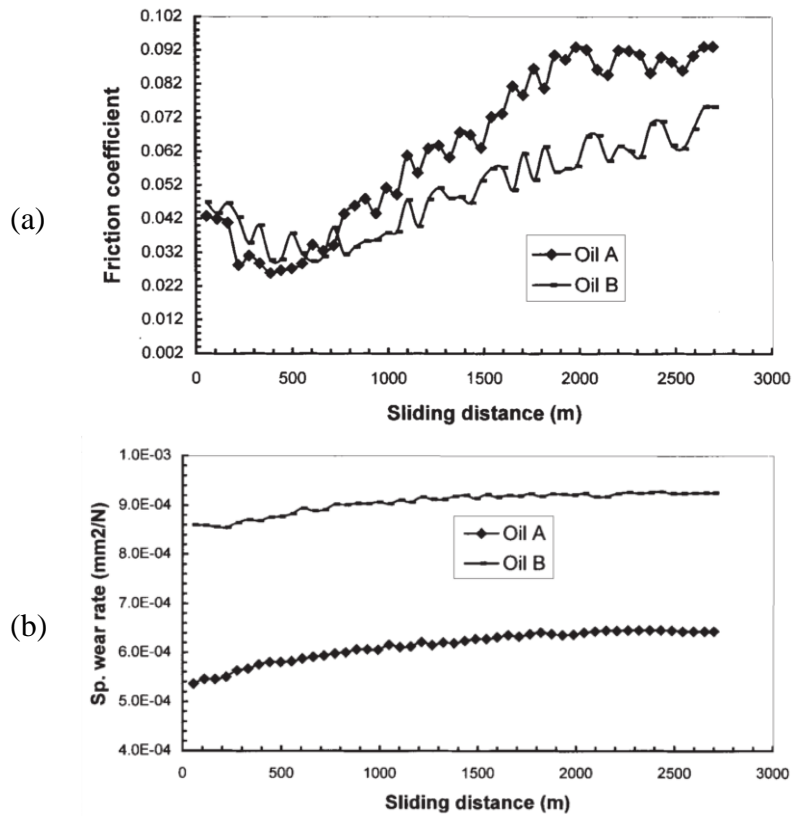


Figure 2.37: (a) Friction performance and (b) wear rate of upper piston ring lubricated with palm oil (Oil A) and mineral based lubricant (Oil B) (adapted from [15]).

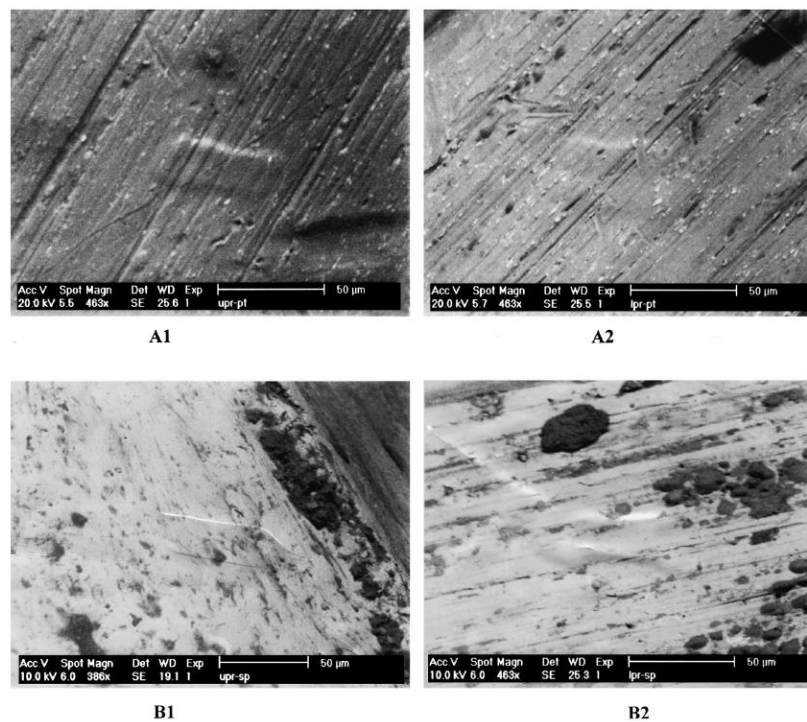


Figure 2.38: Scanning electron microscopy images of lower piston ring (1) and upper piston ring (2) under palm oil (A) and mineral base lubricant (B) [15].

2.5.2 Performance of vegetable oil-mineral oil blends

A blend of oil can be created by mixing of two or more oils to achieve the anticipated performance, for example, a mix of two vegetable oils (palm oil and olive oil) shared the fatty acid composition and physicochemical properties like melting point, viscosity and iodine value which is related to the blend ratio [140]. A commercial mineral engine oil was found to perform well in wear [12, 14], friction [15], and oxidation stability [8] compared to vegetable oil. However, this oil is relatively expensive compared to pure vegetable oil. By blending both of these oils, the cost of the lubricant can be reduced and furthermore the total dependency on petroleum base stock can also be decreased. The superior performance of mineral engine oil especially in wear resistance over vegetable oils [14] has led to an interest in understanding on its tribological response, after an amount of vegetable oil is added into it.

A mixture of mineral oil with vegetable oil exhibited different responses at different blend ratio [20] and material combination [22]. Using four-ball-tribotester, Jabal et al. [20] reported that a blend of palm oil and mineral oil (SAE 40) demonstrated the lowest friction coefficient (0.053) at a 60:40 blend ratio while the wear resistance was the best at a 80:20 blend ratio (Figure 2.39). Contrary to this, when the mineral oil (SAE 40) blended with jatropha oil tested by pin-on-disc (aluminium pin and cast iron disc), Shahabuddin et al. [22] found that the friction coefficient and wear were lowest at a 0:100 ratio which means the addition of vegetable oil gave no improvement in friction. However, by using a different test rig (four ball tester – chromium steel ball), a mineral oil-jatropha oil blend showed the best performance in friction and wear at a 10:90 ratio when tested at an extreme pressure conditions [22].

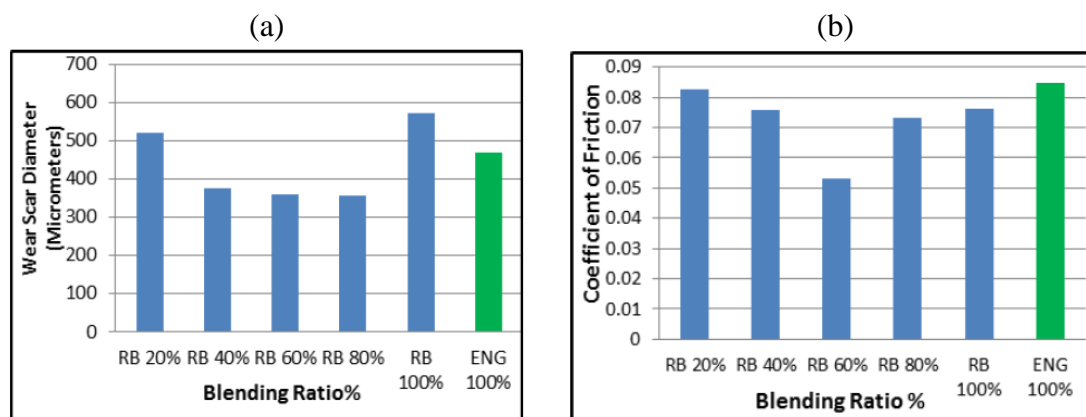


Figure 2.39: The effect of blending ratio of palm olein-mineral oil (SAE40) on (a) wear scar diameter and (b) coefficient of friction [20].

2.5.3 Performance of vegetable oil with anti-wear additives

To enhance some properties of lubricants, additives are added which typically represent about 1 to 25% of a base oil [64]. For example, anti-wear agents in lubricants are added to improve the wear resistance characteristics of contacting surfaces. They form a protective layer to prevent metal-to-metal contact by adsorption of their molecules on the substrate surface through physical adsorption or chemical adsorption processes [44]. Among the most commonly used as anti-wear agents in commercial engine oils are zinc dialkyl dithiophosphate (ZDDP) and Boron compounds (hexagonal boron nitride) which their chemical structure are shown in Figure 2.40.

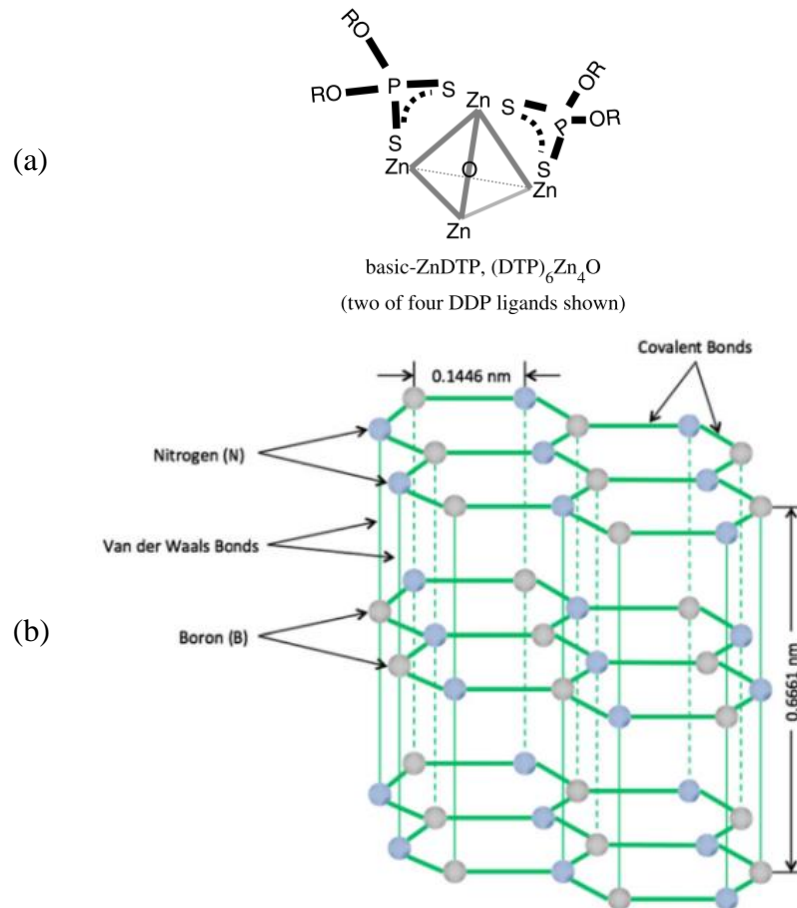


Figure 2.40: Chemical structure of (a) ZDDP and (b) hexagonal boron nitride (adapted from [95] and [34]).

There are three main mechanisms were proposed by which the ZDDP may act as an anti-wear agent in oil: by forming a protective film as a barrier to metal-to-metal contact; by removing corrosive oxidation products; and by absorbing the iron oxide particles thus limiting abrasion [95]. A number of studies have reported on the ZDDP tribofilms formation. However, it is generally accepted that ZDDP may form a series of pad-like structure (separated by valley) on the surface of the bearing (Figure 2.41) [96]. The main composition of the pad is a glassy, mixed iron and zinc phosphate. This phosphate glass is covered by a zinc polyphosphate in outer layer (≈ 10 nm thick). On the metal surface below these pads there are a mixture of sulphur-rich layer (zinc or iron sulphide) which fix the pad to the metal surface.

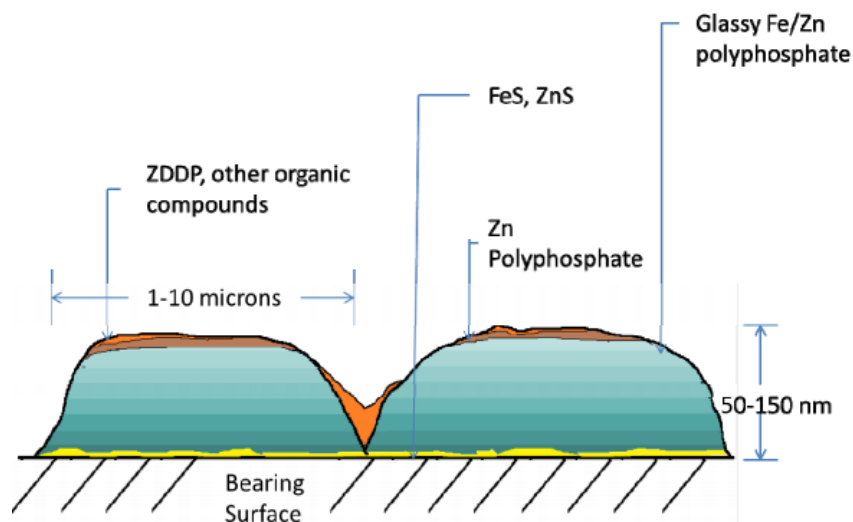


Figure 2.41: Schematic of ZDDP tribofilm pad structure and composition [96].

Other than working as an anti-wear agent, ZDDP is also very effective as an anti-oxidant. The anti-oxidant characteristic that exists in ZDDP has made it a potential substance to be mixed with vegetable oils since a limitation of vegetable oils is that they are very susceptible to oxidation [138]. A hydroperoxide which is typically formed in oxidised oil may increase wear which is related to the degradation of oil and producing strongly corrosive element [123].

A number of researchers have reported the tribological performances of ZDDP mixed with various vegetable oils including with coconut oil [12], soybean oil [28], karanja oil [29], palm oil [141], corn oil [142], canola oil [142] as well as modified vegetable oil like palm oil based trimethylolpropane ester [30]. Many researchers found that the 2% of ZDDP in vegetable oils gave the best tribological results [12, 29, 142], particularly the friction and wear results from 2 % ZDDP in coconut oil were better compared to a commercial lubricant (SAE 20W50) when tested by in a four-ball-tester (Table 2.9) [12]. Similar tribological performance was also achieved by a four-ball-tester when karanja oil mixed with 2% ZDDP

was compared to mineral oil (SAE 20W40) [29]. The ZDDP performance of palm kernel oil and palm stearin has been investigated using a pin-on-disc tribometer at room temperature [141]. The friction and wear results showed that the palm kernel oil exhibited better performance with 3% of ZDDP while the palm stearin was superior at 5% ZDDP [141]. Both corn oil and canola oil were also seen to give an improvement of friction coefficient at 2% ZDDP when tested by pin-on-disk tribometer [142]. Evaluation of the addition of ZDDP in lubricating oil was also conducted using a four-ball-tribotester with 52100 steel balls.

Table 2.9: Coefficient of friction and wear scar diameter of coconut oil, coconut oil with 2% ZDDP as comparison to commercial lubricant (SAE 20W50).

Oil	Coefficient of friction (μ)	Wear scar diameter (mm)	Weld load (N)
Coconut oil	0.07	0.54	1236
SAE 20W50	0.08	0.36	1962
Coconut oil+2% AW/EP additive	0.06	0.34	2453

Chemically modified palm oil, palm oil-based trimethylolpropane (TMP) and the base oil for synthetic lubricants, poly-alpha-olefin (PAO) [30] were tested. There was no improvement seen in friction behaviour for both TMP and PAO added with ZDDP at 1% although the wear resistance was better for a blend of TMP and PAO. It has also been reported that the addition of ZDDP to soybean oil gives improved wear resistance at higher sliding speeds when compared to tests with the pure oil [28]. The results presented by a number of authors suggest that varying levels of a particular additive are required in different types of vegetable oil to achieve the tribological improvement.

Boron nitride is also used as an anti-wear additive in mineral engine oil and is a ceramic lubricant that works efficiently in improving wear resistance, especially at high temperature [143]. Many improvements were found in the tribological performance of mineral oil mixed with hexagonal boron nitride (hBN) [144-146]. Attempts have also been made to use the boron nitride as a vegetable oil additive such as in canola/rapeseed oil [34] and jatropha oil [147]. It was found that 0.05% of boron nitride in modified jatropha oil reduced the friction coefficient and wear scar diameter when tested at 75 °C in a four-ball-tribotester, but any further increase in the concentration resulted in the friction and wear performance being inferior to that of the base oil [147]. The tribological performance of hBN in canola oil was affected by the surface roughness and the particles shape and size of hBN. Smaller particles (typically spherical) easily merge in the asperity valleys to produce a protective film on smooth surfaces whereas larger particles (typically plates) behave as a third body abrasive due to their size and geometry (Figure 2.42) [34].

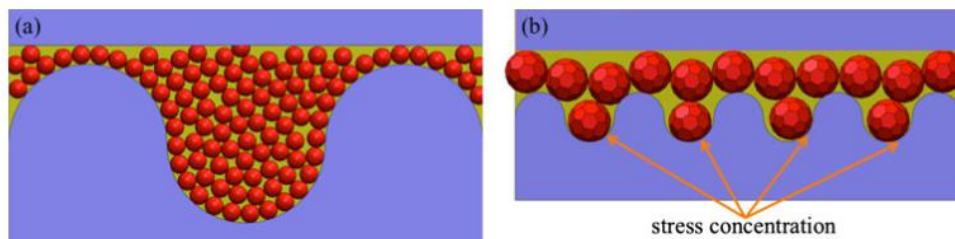


Figure 2.42: Schematic of boron nitride on aluminium disc (surface roughness, $R_a = 0.3 \mu\text{m}$) with canola oil at difference particulate size; (a) 70 nm (b) $0.5 \mu\text{m}$ [34].

2.6 Grey cast iron

Grey cast iron (GCI) has been known for its good tribological properties such as low friction and high wear resistance, for example, it is a common material for the piston ring and

cylinder liner contact in internal combustion engines [148]. Typically comprising iron, silicon, manganese, sulphur, phosphorus and 2.5 to 4.0% carbon [149] in the form of flake graphite. It provides a solid lubrication film, that gives excellent wear and friction characteristics under a dry sliding contact [150].

2.6.1 Tribological performances of grey cast iron

Investigation on friction and wear performance of grey cast iron is a fundamental classical research were studies were mainly focused on the influence of carbon content [151] which affected the flake size of graphite [152]. Using a ball-on-flat contact under dry sliding test, Donald [151] investigated the effects of varying carbon content on friction and wear of grey cast iron as a comparison to white cast iron. Donald reported that at a lower carbon content (2.12 %), thin graphite flakes are sparsely distributed in a pearlitic matrix and these flakes are greater and coarser at higher carbon content. Donald also found that the friction and wear were reduced with an increase of carbon content in which the friction is sensitive to moisture (Figure 2.43). However, the graphite was found to be smeared out on the worn surfaces where some time is needed for this process occurs. As a result, friction was initially higher and decreased before reach to a steady state value when the graphite layer uniformly covered the surface.

A more recent study was performed by Prasad [153] when he investigated the wear and friction of grey cast iron in both dry and lubricated surfaces. He linked some of the test parameters such as applied load, sliding speed and test environment on the sliding specimens of a grey cast iron. Prasad reported that the graphite flakes in the microstructure of grey cast iron was presence in the interface of ferrite and pearlite matrix (Figure 2.44a). Higher wear loss in dry surfaces was seen by Prasad as a cracking tendency from decohesion of graphite

flakes (Figure 2.44b) and higher frictional heating. However, in the presence of lubricant the worn surface was smoother and the cracking tendency was suppressed in which the oil decreased the severity of frictional heating. Prasad suggested that delamination assisted adhesion was the main wear mechanism. The presence of microcracks and an indication of wear induced plastic deformation on the worn surfaces substantiated Prasad justification (Figure 2.45).

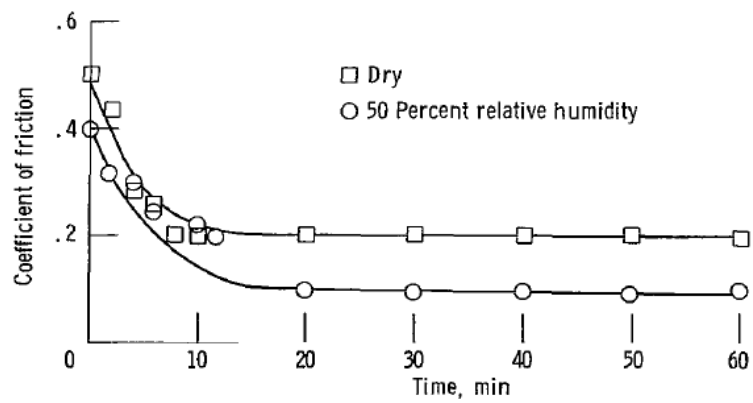


Figure 2.43: Effect of moisture on the friction of grey cast iron [151].

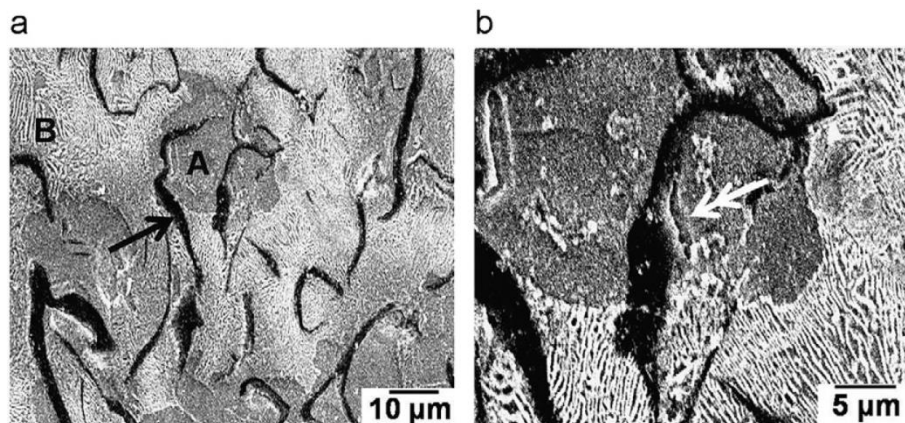


Figure 2.44: (a) Microstructure of the grey cast iron shows the presence of graphite flakes (shown by single arrow) in a ferrite (A) and pearlite (B) matrix interface and (b) Decohesion of graphite flakes on worn surface (shown by single double arrow) [154].

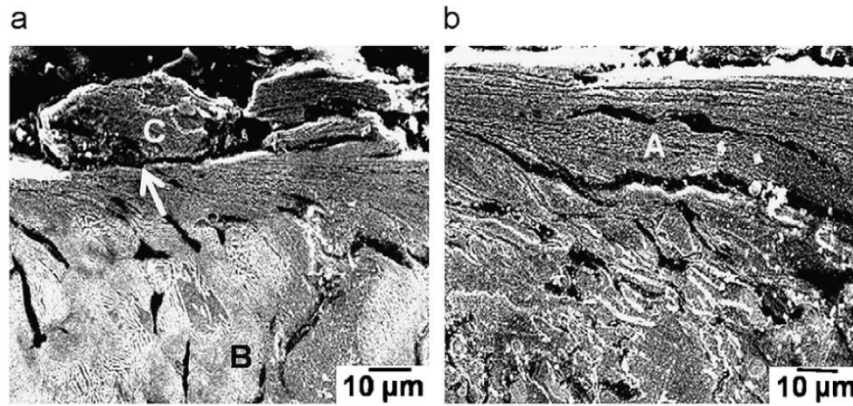


Figure 2.45: Subsurface images of the grey cast iron specimens tested at (a) 500 and (b) 1500 rpm (A= fine microconstituents and flow/ orientation of graphite in the matrix along the sliding direction, B: undeformed bulk structure, arrow: micocrack and C: region in a process of separation from the bulk) [153].

2.6.2 Influence of hardness on tribological performance of grey cast iron

The effects of metal hardness on tribological performance in dry, or lubricated, contacts are well reported [155-157]. It was shown that in a dry contact, pure materials with high hardness gave lower friction than softer materials [158]. The high hardness is attributed to the presence of stronger atomic bonds increasing the resistance to adhesion [158]. Furthermore, the low hardness material allowed more indentation to the surface thus increasing the track width and ploughing force [159]. However, Mokhtar [160] reported that in a lubricated contact, the friction coefficient for heat treated carbon steel was independent of specimen hardness, while in dry contact, friction was lower for harder material (Figure 2.46).

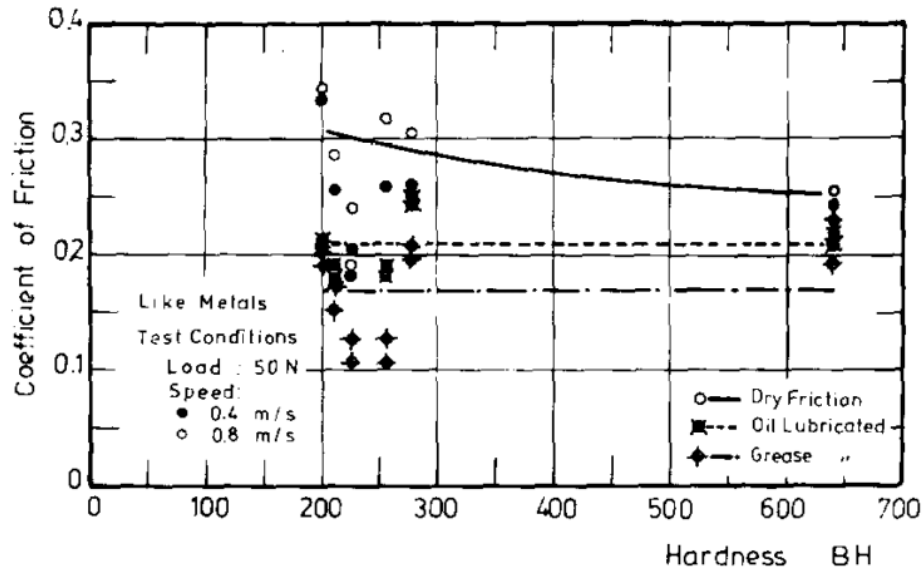


Figure 2.46: Influence of hardness on coefficient of friction for heat treated carbon steel (0.54 % C) for dry and lubricated surfaces [160].

The variation of reported hardness, even in ‘standard’ GCI is high. The difference between maximum and minimum hardness value of GCI grades designated within EN 1561 is 60 HB [161]. Shturmakov [162] also found that GCI ASTM 35B (equivalent to EN 1561 EN-GJL 250) produced the same range (59.4 HB) (Figure 2.47). Others presented the hardness value for this material in various ranges, such as 220-240HV and 207-255 HB [163, 164]. However, there are a few reports ignoring this range and using a bulk value of GCI hardness as a single value (265 HV [150] and 195 HB [165]) of hardness to further conducting their tribological test. The wide range of GCI hardness is typically attributed to the heterogeneous microstructure [149] and the uneven size and distribution of flake graphite [166] caused by the different cooling rate of material during the solidification process in the mould tool [167]. It was reported that differences in cooling rate in compact castings affected to the final strength. For example, the tensile strength and hardness were higher at the more rapidly cooled corners than in the more slowly cooled centre (Table 2.10) in a cross-section of a 76 mm square bar (Figure 2.48) [166].

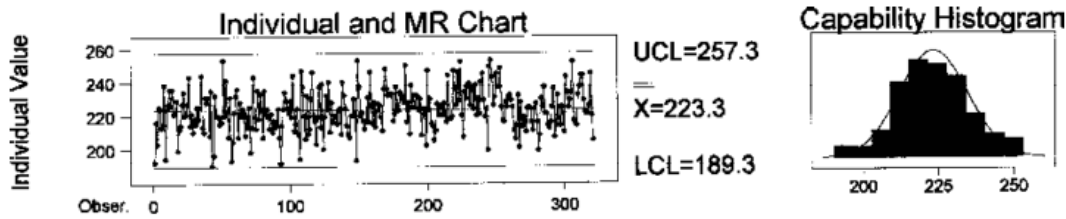


Figure 2.47: Brinell hardness (y-axis) versus observation number (x-axis) of grey cast iron GCI ASTM 35B (adapted from [162]).

Table 2.10: Brinell hardness of grey cast iron bar related to the position of specimen

Bar size: 3 in (76 mm) square × 16 in (406 mm)		Analysis: TC 3.35%, Si 1.15% Mn 0.62%, S 0.04% P 0.026%, CE value 3.79					
Position of specimen	Centre	1×1 in (25.4 × 25.4 mm) Corner	$\frac{1}{2} \times \frac{1}{2}$ in (12.7 × 12.7 mm) Corner	$\frac{1}{4} \times \frac{1}{4}$ in (6.4 × 6.4 mm) Corner			
	Diameter of specimen, in	0.564	0.798	0.399	0.226	0.173	0.177
Diameter of specimen, mm	14.3	20.3	10.1	5.7	4.4	4.5	
Tensile strength, ton/in ²	13.2	14.9	15.3	15.0	15.0	15.5	
Tensile strength, N/mm ²	204	230	236	232	232	239	
Brinell $\left\{ \begin{array}{l} 3000/10 \\ 750/5 \\ 120/2 \end{array} \right.$	171	182	193	194	194	199	

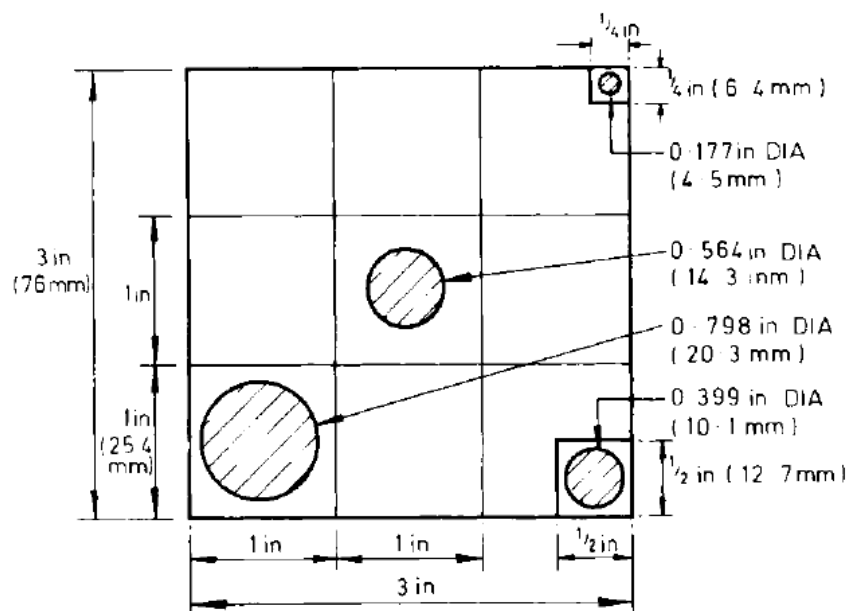


Figure 2.48: Cross section of 76 mm square bar of grey cast iron [166].

The effect of cast iron specimen hardness on friction and wear has been reported [168] mainly under dry sliding contact condition but the specimen hardness is presented as specific bulk value and the nature of the hardness measurement is not mentioned. Sugishita [168] performed friction tests (pin-on-disc) on different heat treated spheroidal graphite cast irons (hardness range 300 ~ 1000 HV) and found the friction coefficient (0.11 ~ 0.21) was inversely proportional with material hardness in the solid lubrication condition when the hardness was less than 400 HV. However, when the hardness was more than 400 HV, the friction coefficient was proportional to material hardness [168].

The lubrication effects of vegetable derived oils on cast irons have been studied, but the works are limited to palm oil and jatropha oil and the hardness of the specimens is not specified [15, 21]. The tribological performance of soybean oil and its chemically modified oils also have been reported, but the tests mainly using a four-ball-tribometer [38, 169, 170] which is based on a rotating steel ball pressed against three fixed steel balls. The hardness effects of GCI on friction and wear would be an interesting subject if it is further studied with vegetable oil (soybean oil) as a biolubricant under reciprocating sliding contact with rigorous hardness characterisation of the counterface.

2.7 Piston Ring and Cylinder Liner Materials

2.7.1 Piston rings

Piston rings serve to fulfil several important tasks in an internal combustion engine such as providing lubrication to the cylinder liner surface, sealing the combustion chamber from leakage of gasses into the crankcase, and to transfer heat that builds up in the piston to

the cylinder surface. Materials for the piston ring should be able to accommodate several requirements such as high wear resistance and low friction in boundary lubrication, good mechanical strength, good elastic behaviour, good heat conductivity, good corrosive resistance and good machinability.

Some pistons are assembled with three types of piston rings (Figure 2.49) known as a compression ring, scraper ring and oil control ring. The compression ring is usually attached at the top point of the piston and its main function is to seal the cylinder from leakage of gases produced during the combustion process. The scraper ring is placed below the compression rings. Its main function is to disperse the oil on the cylinder walls so that the compression rings are properly lubricated and also to wipe off the oil left behind by the oil control ring. The oil control ring is placed at the bottom of the piston. It ensures oil is evenly spread on the cylinder walls, scrapes the excessive oil off the walls and sends it to the crankcase.

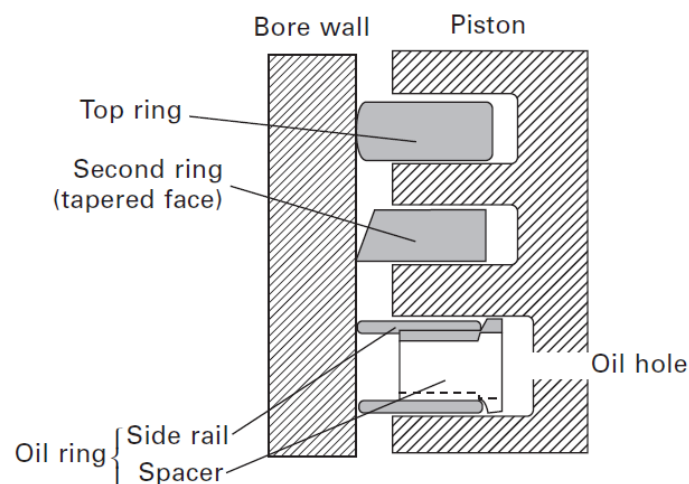


Figure 2.49: Three types of piston rings [171].

2.7.2 Piston ring materials

Typical materials used for a piston ring include grey (lamellar graphite) cast iron, ductile (nodular/spheroidal graphite) cast iron and tempered steel or stainless steel [172]. For many years, grey cast iron was the most popular piston ring material. Its tribological characteristics, cost competitiveness and material availability has made it the optimal material for the piston rings [148]. In addition, the flake graphite in the grey cast iron is useful in acting as an oil reservoir that supplies oil at dry starts or temporary loss of lubricant [173].

Grey cast iron is a standard material for compression and oil control rings in gasoline and diesel engines which is specified under subclass 13 according to ISO 6621-3 [172]. Its material composition is close to the standard grey cast iron EN-GJL-250 (BS EN 1561:2011) [174]. The pearlite microstructure and the lamellar graphite structure in the grey cast iron are excellent characteristics for a piston ring material that keep the friction and wear to a minimum level in oil control rings. In special cases, where greater wear resistance is required, an alloyed grey cast iron (subclass 25 according to ISO6621-3) can be used [172]. In order to improve their mechanical properties, alloyed grey cast irons are normally heat-treated and their microstructure is primarily martensitic.

Nodular cast iron (BS EN 1563: 2011) has mechanical properties between those of grey cast iron and steel. However, its friction properties are slightly higher than grey cast iron [175]. This material is recommended for compression rings and oil control rings, where the required strength is better than that of lamellar grey cast iron [171]. For applications where greater wear resistance is needed with the higher mechanical strength, the nodular cast iron alloyed with niobium is usually recommended [172, 176].

Steel can also be used to manufacture many types of piston rings (compression ring, scraper ring and oil control ring). Steel has advantages over grey cast iron in terms of its high mechanical strength, fatigue resistance, heat resistance and good corrosion resistance. Steel, however, has poor friction properties compared to grey cast iron. For this reason, steel piston rings are normally coated and or surface treated. The main purposes of surface treatments on the piston ring are to improve initial wear during running-in and to enhance durability, where very long life is required. For example, it was reported that the hard chrome electroplating reduces friction and increases wear resistance of the cylinder working surface, thereby increasing the service life of engines up to 20,000 hours [177].

Typical surface treatments for piston rings include nitriding [178], electrochemical plating, e.g., chrome plated [179, 180], ceramic coating [181] and thermal spraying e.g. plasma-sprayed molybdenum [182]. Surface coatings and treatments intended to provide good oxidation resistance, such as tin-plating, black-oxidizing and phosphating are available for specific applications. Polymer coatings are among the latest solutions for protection against microwelding of the cast iron and steel piston rings [183, 184] but still need development.

2.7.3 Cylinder liner

The cylinder liner is a removable component, inserted into an engine block to form a cylindrical wall. It provides a surface for its partner, i.e., piston rings, to slide against and carry out the lubrication and sealing job in the combustion chamber. Due to the reciprocating motion between the piston rings and the cylinder liner, its surface is susceptible to friction and wear.

Wear occurs particularly at the upper reversal point of the piston rings (top dead centre) because of change in direction of the moving parts causes a transition through zero velocity and likely lubrication starvation [185]. The wear behaviour of the running surface and the piston rings is substantially determined by the material pairing selected for the two components [186]. In order to reduce wear, the running surface should be smooth and the lubrication between the sliding the cylinder liner and the piston ring must be adequate. The type and quality of the running surface effects oil consumption as well as the wear of the two components [187, 188].

2.7.4 Cylinder liner materials

Most cylinder liners are made of grey cast iron of BS1452 grade 250 [148] (equivalent to EN 1561-GJL-250), aluminium alloys and steels. Aluminium liners are typically coated while the steel liners can be hardened, reinforced or spray-coated [172]. Cylinder liners made of aluminium have the advantage of a higher thermal conductivity and lower specific gravity compared to grey cast iron. Steel, on the other hand, stands out for its high strength and stiffness.

Grey cast iron is typically used for cylinder liners due to its cost effectiveness and tribologically beneficial. The graphite phase in the material provides good dry lubricating effect and serve as a reservoir to supply oil at dry start or during oil starvation situations [173]. Lamellar gray cast iron (GJL) with a pearlite microstructure is manufactured to provide a hardness and strength range as shown in Table 2.11. For higher strength requirements, lamellar gray cast iron (GJL) with a bainite base microstructure or cast iron with vermicular graphite (GJV) can be used (Table 2.11). In order to improve the wear

resistance of the cylinder liner surface, the grey cast iron can also be coated with a hard chromium layer [189] or ceramic metal composite. It was reported that the wear resistance improved as the grey cast iron cylinder liners are coated with a ceramic-metal composite (chromium oxide, Cr_2O_3 and molybdenum, Mo) by low pressure plasma spraying [190].)

Excellent thermal conductivity and lower density make aluminium alloys a suitable alternative to grey cast iron in the fabrication of cylinder liners. Thermal spray coating methods can be used to protect the sliding surface of aluminium liners in order to improve the tribological characteristics with low cost and short processing time [191]. Compared to cast iron liners, ferrous thermal spray coatings on cast aluminium components have some advantages such as lighter weight and improved scuffing resistance [192]. For example, it was reported that at high load and high velocity, the wear rates decreased when the aluminium alloys were thermally sprayed by carbon steel coatings [193]. Other developments on the aluminium liners include the usage of metal matrix composite (aluminium alloys made up of at least two distinct phases) combine with reinforcement ceramic materials like zirconium dioxide (ZrO_2) for achieving greater fuel economy [194].

Several efforts have also been made to study surface coating technology for cylinder liners. The tribological behaviour of titanium suboxide (TiO_x) coatings for grey cast iron cylinder liners under different conditions was evaluated [195]. It was found that a thermally sprayed titanium suboxide coating for cylinder liners outperforms the wear resistance of uncoated grey cast iron cylinder liners. Stainless steel balls with diamond-like carbon (DLC) coatings were also used to simulate the cylinder liner-piston ring material by four-ball-tribometer [196]. It was reported that the coated balls exhibit better friction and wear performance than uncoated stainless steel balls. Other evaluation of the wear resistance on the

chrome plated cylinder liner compared to non-plated cylinder liner revealed that the wear results were improved by almost 50% [197].

Table 2.11: Properties of cast iron for cylinder liners [172].

Properties	Cast iron with lamellar graphite (GJL)		Cast iron with vermicular graphite (GJV)	
	Perlite	Bainite and very fine perlite	Perlite	
Basic microstructure	Perlite	Bainite and very fine perlite	Perlite	
Hardness [HB]	180–300	270–330	240–300	
Tensile strength [MPa]	200–350	400–600	500–650	
Young's modulus [GPa]	100–120	120–140	130–160	
Chemical composition (weight %)	C	2.8–3.3	2.6–2.8	3.0–3.6
	Si	1.8–2.1	1.4–2.0	1.8–2.9
	Mn	0.6–1.0	Max. 0.8	0.2–0.8
	P	Max. 1.0	Max. 0.08	Max. 0.4
	S	Max. 0.12	Max. 0.08	Max. 0.01
	Cr	0.1–0.3	–	–
	Mo	Max. 0.6	1.0–1.5	–
	Cu	Max. 0.8	–	Max. 0.8
	B	Max. 0.07	–	–
	Ti	–	–	Max. 0.06
	Ni	Max. 1.2	1.0–1.5	–

2.8 Summary

Vegetable oil based lubricants are renewable resource and biodegradable product which provides them with strong advantage over commercial mineral oils. Although vegetable oils have been demonstrated as a potential candidate for biolubricants, there is no evidence so far that confirming their suitability to be applied in automotive engine lubrication system through a series of small-scale test that have been conducted previously. This is because, many of the previous studies, were limited to a certain kind of test rig (either four-ball tribometer or pin-on-disc) and test condition (some oil are tested at room temperature).

Thus, further systematic research that confirms the potential of vegetable oil based lubricants in an automotive engine must be performed. This can be done through a different means of testing which could involve their performance closer to contact motion in an internal combustion engine systems (piston ring motion).

The lubrication effects across a wide range of grey cast iron hardness is another interesting area that should be considered accordingly in conjunction with tribological performance of vegetable oils. Using a rigorous hardness characterisation of the counterface could produce more reliable and robust data for investigation of vegetable oils performance on wear and friction.

Chapter 3: Experimental methodologies

3.1 Introduction

This chapter describes the materials and methodologies used in setting up the experiments. The friction and wear test rigs, measurement equipment, specimens, lubricants, inspections and analysis methods that were used in this research are explained. Some theoretical calculations used to determine the lubrication regimes are also stated.

3.2 Experimental Equipment

3.2.1 Friction and wear test

A Phoenix Tribology/Plint TE77 test rig (Figure 3.1) was used for measuring the friction force by means of a calibrated load cell. The coefficient of friction (COF) was then calculated based on the friction force and the normal load applied. A schematic of the machine is shown in Figure 3.2. The linear reciprocating motion on the test rig resembles the motion of a piston ring in an internal combustion engine. However, a point contact (ball-on-flat) was chosen in this study in order to eliminate misalignment problems at the counterface of the contacting bodies.

All of the tests were run at a temperature of 100 ± 2 °C by means of programmable temperature controller. This was to replicate the oil temperature in the oil sump in an internal combustion engine [198]. A mean sliding speed of 0.13 ± 0.01 m/s and a maximum stroke length of 15 ± 0.1 mm was selected and the test duration was 1 hr. All test parameters (Table

3.1) were selected based on preliminary experiments conducted to ensure the production of measurable and comparable wear scars between the specimens lubricated with vegetable oils and mineral oil. Thus, a normal load 40 N (yield to a 1.7 GPa Hertzian contact pressure) applied to the ball was selected based on trial and error. The scope of this research was to run the test at only one set of test conditions so that the study could be focused on the response of the lubricants on friction and wear.

The wear behaviour of specimens was identified by mass loss measurement. Specimen masses were measured before and after the test and the difference recorded as the mass loss of the specimen. The tests were run for three repetitions for each lubricant and the average mass loss and friction coefficient were then calculated. The standard deviation was plotted in the graphs as an error bar.

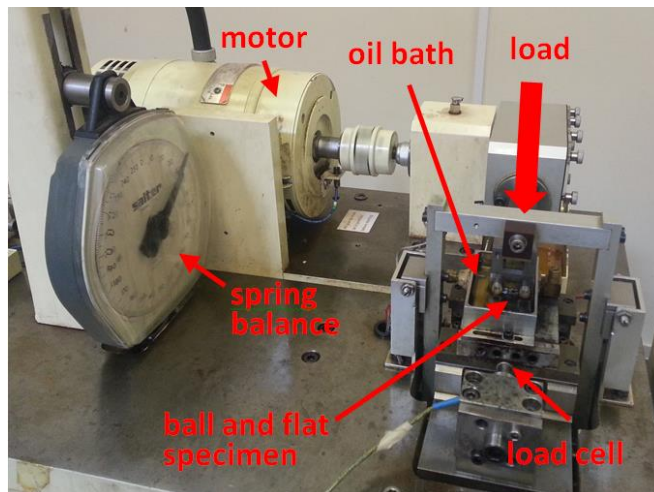


Figure 3.1: Phoenix Tribology/Plint TE77 test rig

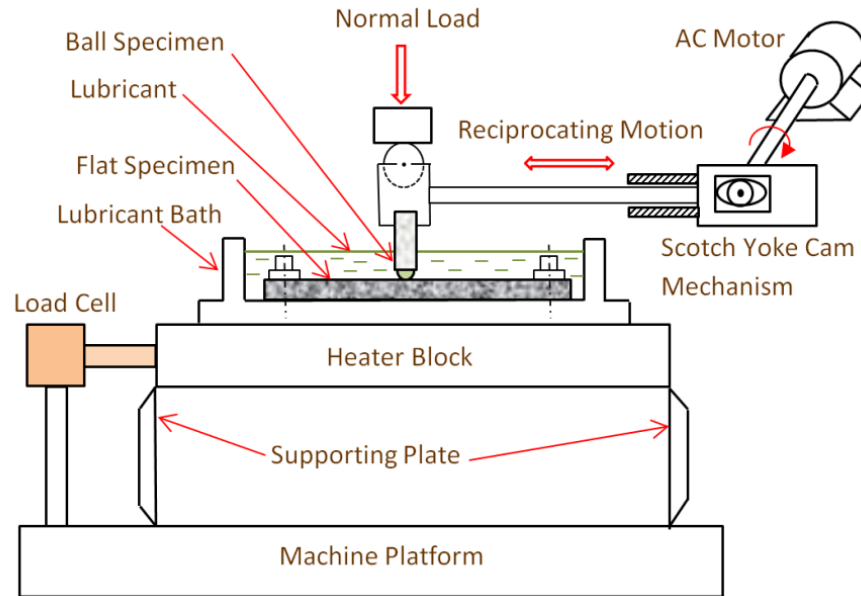


Figure 3.2: Schematic of friction and wear test rig

Table 3.1: Test parameters

Test parameters	Value
Normal load	40 ± 1 N
Hertzian contact pressure	1.7 GPa
Lubricant temperature	100 ± 2 °C
Lubricant volume	25 ± 1 ml
Sliding stroke	15 ± 0.1 mm
Mean sliding speed	0.13 ± 0.01 m/s
Experiment time	60 min

3.2.1.1 Justification of Test Method

The friction and wear tests performed in this study aimed to simulate the environment in the piston ring and cylinder liner movement in an internal combustion engine. However, due to limitations of time, test conditions and parameters were chosen on the Plint TE77 reciprocating test rig that may represent extreme contact conditions of a piston ring and a

cylinder liner. The description below explains the justification for the test conditions and the selection of the experimental parameters.

(a) Type of Contact

A point contact (ball-on-flat) was chosen in order to avoid misalignment issues during the setting up of the specimens. This is important in order to produce reliable initial data of tribological performance of a new lubricant as misalignment of specimens may create inconsistency in friction and wear. Although many researchers were using cut out specimens of piston ring and cylinder liner, it is susceptible to the inconsistency in the matching the conformal curvatures between the piston ring and liner surfaces. This furthermore tends to produce inconsistent wear data between tests. The cut out specimens, however, could be used for verification of the data after the ball-on-flat test is conducted.

(b) Specimen Materials

Grey cast iron was used for flat specimens (EN-1561-GJL-250). This is a common material for piston rings and cylinder liners [148, 172]. The use of chrome steel ball (AISI 52100) as a moving part is also acceptable because some of the piston rings are made from a chromium steel material [199].

(c) Normal Load and Contact Pressure

In general, vegetable oil lubricants were produced much higher wear compared to mineral engine oil. Thus, a trial and error method for determining a suitable load for comparing the wear performance of vegetable oils and mineral engine oil was performed. It

was found that 40 N is an optimum load. A lower load than 40 N produced too small a wear scar on mineral engine oil specimens and this made the weight loss measurement impossible. This 40 N load furthermore produced very high contact pressure (1.7 GPa) leading to severe contact conditions which are beyond the typical contact pressure of the piston rings and cylinder liners (10^4 - 10^5 Pa) [189].

(d) Mean Sliding Speed

The motor rotational speed of the Plint TE77 machine is controlled by a dial indicator on the controller panel and the value was tuned to 100 (no unit). This produced a motor speed of 260 rpm (by measurement). Based on the motor speed, the linear speed is calculated (0.13 m/s) which is a function of stroke and rotational speed [200]. Although the mean sliding speed in this study is lower than the typical mean piston speed of a car engine (16 m/s) [200], low speed test rigs are best used to simulate wear and scuffing behaviour of piston rings at top dead center. For example, Petra et al. conducted tests where the reciprocating motion of a grey cast iron liner and chromium plated piston ring was at a sliding speed of 0.18 m/s [201].

(e) Sliding Stroke

The sliding stroke is chosen at a value of 15 mm due to the maximum value that the Plint TE77 machine can provide. Typical piston stroke length for a car engine is around 50 mm to 90 mm [202]. A higher sliding stroke is also useful to investigate the influences of friction and wear over the wide hardness range of the grey cast iron specimens.

(f) Experiment Time

The 60 minute experiment time was chosen based on the evaluation of steady state friction results in the tests. From the outcome of the friction tests, the steady state friction was achieved around 30 to 40 minutes after the test started. Thus, a 60 minute experiment time is reasonable.

(g) Lubricant Temperature

The lubricants temperature in an engine varies from ambient temperature (just before the start-up) to the maximum operating temperature. The lubricant temperature applied in this study is assumed to be continuously supplied from the oil sump to the contacting surfaces at steady state temperature. Thus, the temperature was chosen at 100 °C as this is a typical temperature of oil in the sump of an internal combustion engine running at steady state [203, 204].

(h) Surface roughness of specimens.

The average surface roughness, R_a , of flat specimens (grey cast iron) after the grinding process was controlled around 0.15 μm . This value is close to the cylinder liner surface roughness after it has gone through a 'medium' polishing process ($R_a = 0.15 \mu\text{m}$) [205].

3.2.1.2 Limitation of the friction and wear test

The use of a laboratory test rig in this study represents a basic tribological test that attempts to duplicate the key factors in an engine particularly in simulating the contact conditions near to those in the piston ring motion on the cylinder liner. While it is appropriate for the purpose of assessing the potential use of vegetable oils as biolubricants, the limitations of the friction and wear tests method must be recognised.

The use of a friction and wear test rig with a ball-on-flat configuration is suitable to provide initial data on the performance of lubricants. It also eliminates the misalignment issues on the counterface and thus, minimises the error of the experiments. However, the use of a point contact is not replicating the real contact of the piston ring and cylinder liner and thus, limits the extent to which the results of this test can be related to real-life applications. Therefore, in order to improve the study, it is suggested to repeat the test using the cutout specimens of the actual piston ring and cylinder liner components.

In reality, it is very difficult to exactly predict the conditions in the engine as the operating environment is always changing. For example, in the actual application of the internal combustion engine, parameters such as engine speed, sliding duration and temperature of the lubricating are extremely varied. It is therefore, suggested that the study can be improved by running tests using variable parameters. However, there are a number of parameters such as sliding speed and the contact pressure that can join together to create frictional heating. Frictional heating, in turn, can affect the tribological performance of contacting surfaces. Therefore, a change in one parameter may affect several other factors. This makes it difficult to perform a friction or wear test in which only one parameter is considered as the independent variable and everything else is fixed.

Also in this work, it is not possible to perform the wear rate in situ. This perhaps could be conducted by measuring the instantaneous ball wear scar or flat specimens' mass loss after some period of time which requires stopping the machine for a while. However, when stopping the test rig for periodic wear measurement, there is a possibility of inducing an unintentional error in alignment at the contact surfaces when reassembling the ball specimen into the test rig for the second and subsequent times.

3.2.2 Hardness Test

Prior to the friction and wear tests, the hardness of the flat specimens was measured on the intended wear scar region. The wide range of hardness that grey cast iron specimens have may influence the consistency of data for the friction and wear results.

A microhardness test (Vickers Limited, England) was used in order to minimise the indentation size on the specimens. A 20 kg applied load was used on the GCI flat specimens to measure the hardness within the intended wear scar area (Scar 1, Scar 2 and Scar 3) as shown in Figure 3.3. On each of the intended wear scar regions, the hardness test was performed at three points along the centre line of the scar (labelled as hardness measurement points in Figure 3.3). These three points were 5 mm apart which was enough to represent the hardness at front, middle and back of the wear scar region along the sliding direction. The average hardness based on these three points was then calculated to characterise the hardness of each wear scar area before testing.

Next, the hardness measurements were performed on three wear scar regions on either side of specimen surfaces. This meant there were 6 average hardness data points for one specimen (3 scar regions x 2 surfaces). A total of 71 flat specimens were used in this

measurements work which meant there were 426 average hardness data points in total (71 x 6). An example of a hardness measurement data sheet is shown in Appendix 1.

In order to facilitate the friction/wear test and analysis in next chapter (Chapter 4), 9 measurement data points were then selected and divided into 3 groups (low, medium and high hardness) based on their hardness value. The friction and wear tests were then conducted on these 9 specimens.

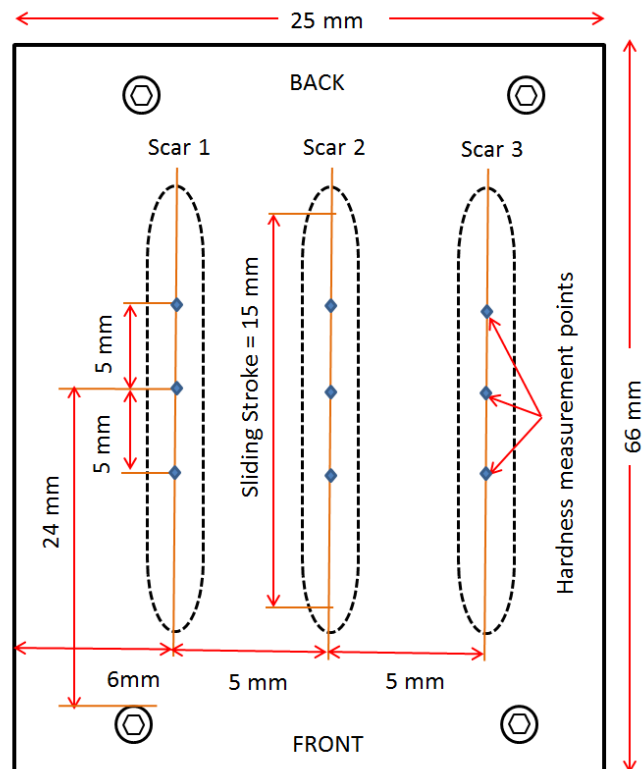


Figure 3.3: Measurement of hardness on intended wear scar region

3.3 Materials

3.3.1 Specimens

To evaluate the tribological performance of the biolubricants, a reciprocating sliding point contact (ball-on-flat) was chosen throughout this research. The moving specimen was a ball (6 mm diameter) made of high chrome steel (AISI 52100) with average surface roughness, $R_a = 0.03 \mu\text{m}$, and held firmly to prevent rotation by a brass tube. This type of steel ball is typically used as a ball bearing component.

The fixed specimen was flat in geometry, made of grey cast iron (EN1561-GJL-250) with a rectangular dimension 66 mm x 25 mm x 4 mm. The grey cast iron has a lamellar graphite microstructure and typically used as a piston ring and cylinder liner material. The surface of the flat specimen was ground to an average surface roughness, $R_a = 0.15 \mu\text{m}$ which is close to the surface roughness of the top compression ring of a piston ring in a four-stroke gasoline engine ($0.10 \mu\text{m}$) [206]. Both specimens are pictured in Figure 3.4 with the primary dimensions presented.

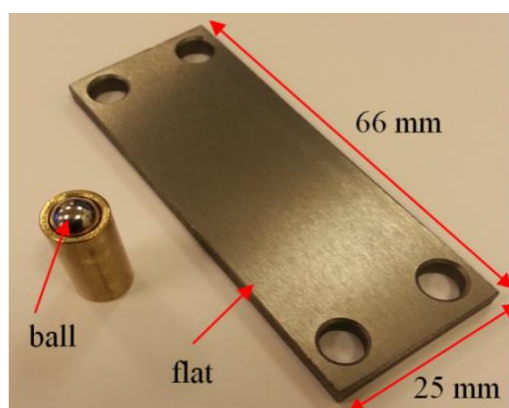


Figure 3.4: Ball and flat specimens

3.3.2 Lubricants

Three types of lubricants were used in this study (Figure 3.5):

- (i) the biolubricants (vegetable oil)
- (ii) the mineral oil
- (iii) the blended lubricants

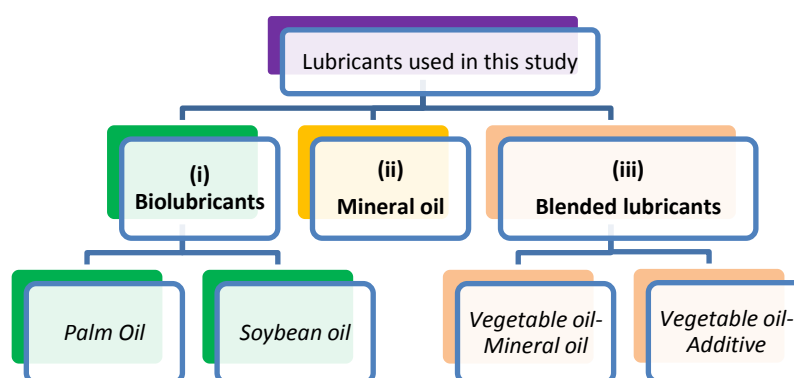


Figure 3.5: Summary of the lubricants used in this study

3.3.2.1 Biolubricants

The biolubricants used in this study were those from vegetable oils in their pure oil state. The vegetable oils consisted of palm oil (PO) and soybean oil (SBO). These two vegetable oils were selected because they make up most of the global consumption of vegetable oil (1995 to 2015) [207]. The PO used was an ordinary cooking oil (Vesawit, Malaysia) which had undergone manufacturing processes like refining, bleaching and

deodorising (also known as palm olein). A commercial SBO (Clearspring, Italy) was used from the organic type which had undergone a cold pressing process and was also suitable as a culinary oil. Unrefined SBO was chosen because it is more oxidatively stable than the refined oil [208]. Some of the important properties of PO and SBO that were measured in this study are listed in the Table 3.2. The images of these lubricants are shown in Appendix 2.

3.3.2.2 Mineral oil

Mineral oil (MO) mainly was used for benchmarking purposes in order to compare the tribological performance between the vegetable oils and the commercial lubricant. The MO sample was a commercial mineral engine oil (Shell Helix HX5) with SAE viscosity grade 15W40. Some of the important properties of this lubricant that were measured in this study are listed in the Table 3.2. The image of this lubricant is shown in Appendix 2.

Table 3.2: Properties of lubricants

Lubricants	Absolute Viscosity (cP)		Acid Number (mgKOH/g)
	40 °C	100 °C	
Mineral Oil (MO)	92.45	12.32	2.24
Palm Oil (PO)	38.08	7.78	0.24
Soybean Oil (SBO)	30.72	7.10	0.98

3.3.2.3 Blended lubricants

The blended lubricants were comprised of two types:

- (i) blend of the vegetable oil with mineral oil
- (ii) mixture of anti-wear additive in vegetable oil.

3.3.2.3.1 Vegetable oil-mineral oil blend

The vegetable oils (palm oil and soybean oil) were mixed individually at 50% by volume with the MO which corresponds to a 1:1 blend ratio. This equal ratio was selected in order to investigate the potential dominance of a particular oil against another on the tribological performance of oil mixture.

The mixed oil was stirred by an agitator for 10 minutes just before the test began. The uniformity of each blend was judged by visual appearance of the oil in which no significant layer or different colour was seen in the oil blends. Figure 3.6 shows the appearance for MO and PO in a pure oil state (a and b) and the mixture of MO and PO before the stirring process (c). It can be seen that there are two layers formed from the mixture of these two oils. The blend of MO-PO was then stirred for 10 minutes and left 24 hours (d). This was to ensure that the stirring process was reliable. The details of all vegetable oil-mineral oil blended lubricants used in this study are shown in Table 3.3. In addition, the PO was also mixed with SBO by the same ratio for comparison purposes.

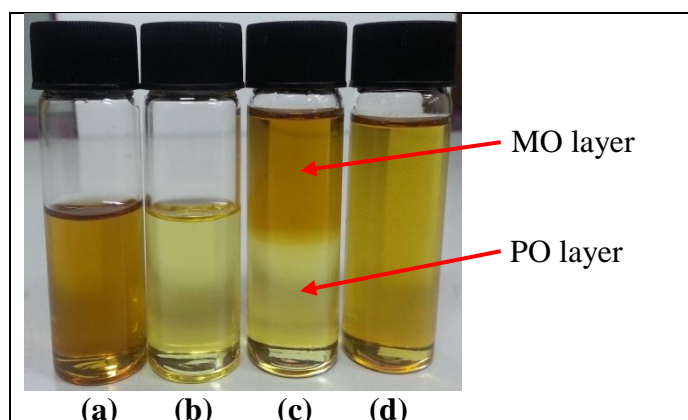


Figure 3.6: (a) Appearance of mineral oil and (b) palm oil in pure state. The significant layer is seen in MO-PO blended oil before the stirring process (c) and eliminated after the stirring process and left for 24 hours (d)

Table 3.3: Vegetable oil- mineral oil blended lubricants used in this study

Vegetable oil- Mineral Oil Lubricants	Absolute Viscosity (cP)		Acid Number (mgKOH/g)
	40 °C	100 °C	
50% MO + 50%PO (MO: PO)	54.97	9.26	0.97
50% MO + 50% SBO (MO: SBO)	46.44	8.77	1.13
50% PO + 50% SBO (PO: SBO)	32.98	7.10	0.68

3.3.2.3.2 Vegetable oil-additive blend

Two commercial additives were used in this study; zinc dialkyl dithiophosphate (ZDDP) and hexagonal boron nitride (hBN). The ZDDP (ZDDPlus, USA), with a chemical formula $Zn[(S_2P(OR)_2)_2]$, is a liquid at room temperature but the hBN, with particle size 0.5 μm or less (Ceratec, Germany) was dispersed in mineral oil as a carrier fluid by the manufacturer.

An amount of 2% of ZDDP and 6% of hBN in mineral oil was then added in the vegetable oils as these are the ratios (by volume) that are recommended by their respective manufacturer for optimum performance based on their product information sheet (Appendix 3 and Appendix 4). The oil with the additive was then stirred by an agitator for 10 minutes in order to ensure a uniform blend was formed. The appearance of each oil mixture was observed at the end of the stirring process. In order to determine that a uniform blend was produced, the oil was checked for the formation of a noticeable layer of different density components, or a colour difference as described in Section 3.3.2.3.1. The details of all blended lubricants used in this study are shown in Table 3.4.

Table 3.4: Blended lubricants used in this study

Vegetable oil- Additive Lubricants	Absolute Viscosity (cP)		Acid Number (mgKOH/g)
	40 °C	100 °C	
2% ZDDP + PO (ZD: PO)	38.31	7.98	1.98
2% ZDDP + SBO (ZD: SBO)	30.60	7.36	2.53
hBN in mineral oil + PO (hBN: PO)	38.59	7.85	0.44
hBN in mineral oil + SBO (hBN: PO)	30.43	7.08	1.21

3.4 Material Analysis

3.4.1 Surface morphology evaluation

After each test was completed, the flat specimens were removed from the test rig. An ultrasonic cleaner was used to clean the specimens for 5 minutes with acetone. In typical ultrasonic cleaning method, most particles are removed within the first 30 seconds [209]. The specimens were then rinsed in isopropanol to remove any carbon deposits on the specimens that may have formed due to exposure to acetone.

The specimens were then inspected under an optical microscope in order to obtain images of the wear scars in a broader view. Scanning electron microscopy (SEM) was used to inspect the worn specimens at a much higher magnification than the optical microscope. The images taken from both microscopes were then used for analysing the underlying wear mechanisms on the surfaces. The electron dispersive analysis of X-rays (EDX), coupled with SEM, was also used in analysing the elements that exist on the worn surfaces.

3.4.2 Surface topography evaluation

The unexpected formation of wavy-shaped wear scars after the tests (Figure 3.7) that mainly occurred on the specimens lubricated with the vegetable oils and their blends, has driven the importance in evaluating the surface topography. The wear scars on flat specimens were characterised by surface roughness, R_a and surface waviness. These measurements were performed with a profilometer (Mitutoyo Surftest, SJ-500). The surface roughness was taken at several different points (Figure 3.8) across the sliding direction in order to investigate the potential influence of the wavy-shaped wear scar on roughness.

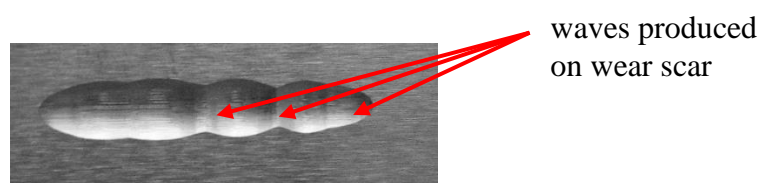


Figure 3.7: Wavy-shaped wear scar produced on specimens lubricated with vegetable oils and their blends.

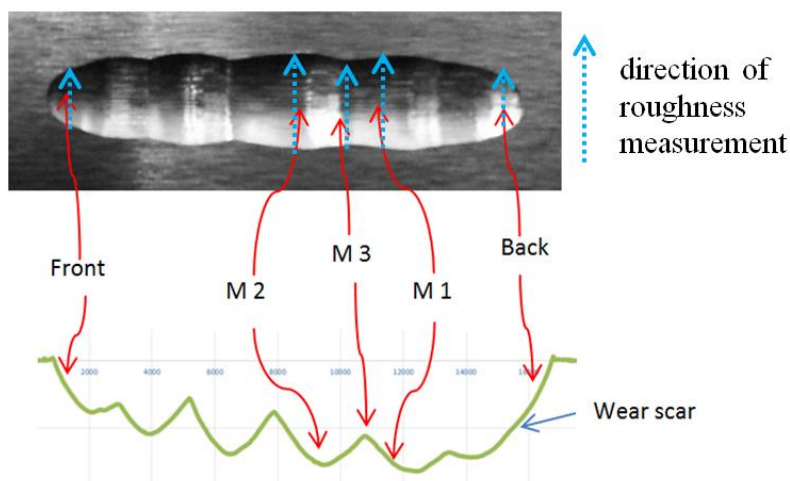


Figure 3.8: The different points (front, back, M1-M3) indicating where surface roughness measurements were taken.

The measurements of primary profile and surface waviness were taken along the sliding direction and in the middle of the scars. The primary profile traces the undulating

shape along the worn specimens and was recorded by several points in terms of X and Y coordinate at a particular position. Based on these points, a graph was plotted to represent the actual profile of the wavy-shaped wear scars. The surface waviness method was performed in order to provide measurable data so that the wavy-shaped wear scar between specimens could be compared quantitatively.

The surface waviness, W_a is derived from the primary profile evaluation in which the shorter wavelength components, λ_c and longer wavelength components, λ_f are suppressed through a band-pass filter [210]. This process was performed automatically by the profilometer software when the type of profile (primary profile, waviness or roughness) is changed by the user. The idea of these three profile measurements is depicted in Figure 3.9 in which the measurements were performed on the same surface. The cut-off values (λ_c , λ_f and λ_s) are illustrated in Figure 3.10 (ISO 4287) and used by the filter to isolate the wavelength band. The transmission characteristic (50% transmission at the cut-off) is defined in ISO 11562.

In this evaluation, a single value of surface waviness, W_a was recorded when the shorter wavelength components, $\lambda_{c(waviness)}$ and longer wavelength components, $\lambda_{f(waviness)}$ value were chosen at 0.025 and 0.8 mm (software default value). Table 3.5 shows the details of the parameters used in the profilometer software between the primary, waviness and roughness profile throughout this study.

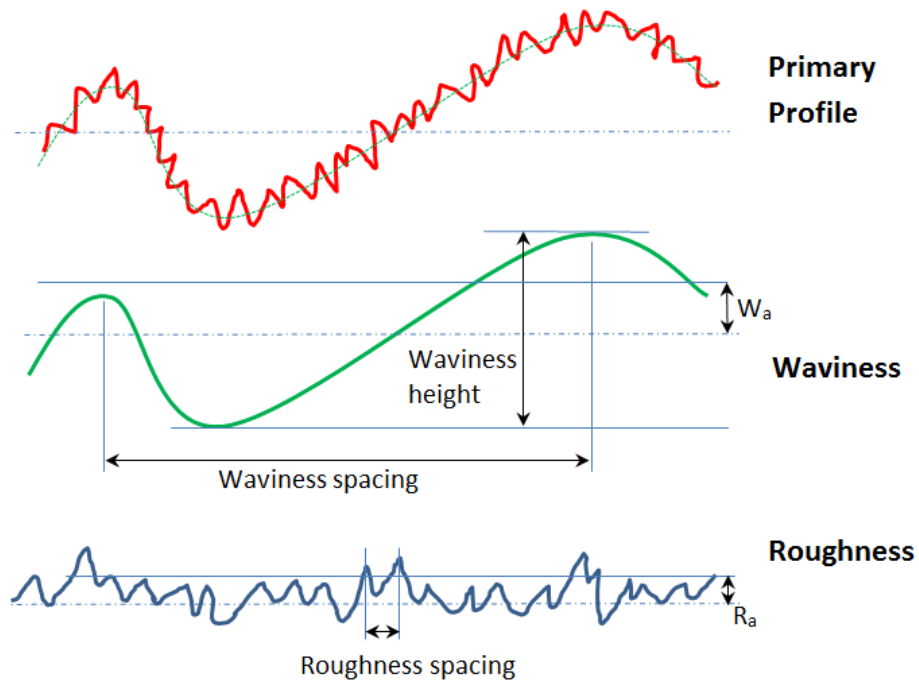


Figure 3.9: Primary, waviness and roughness measurement profile

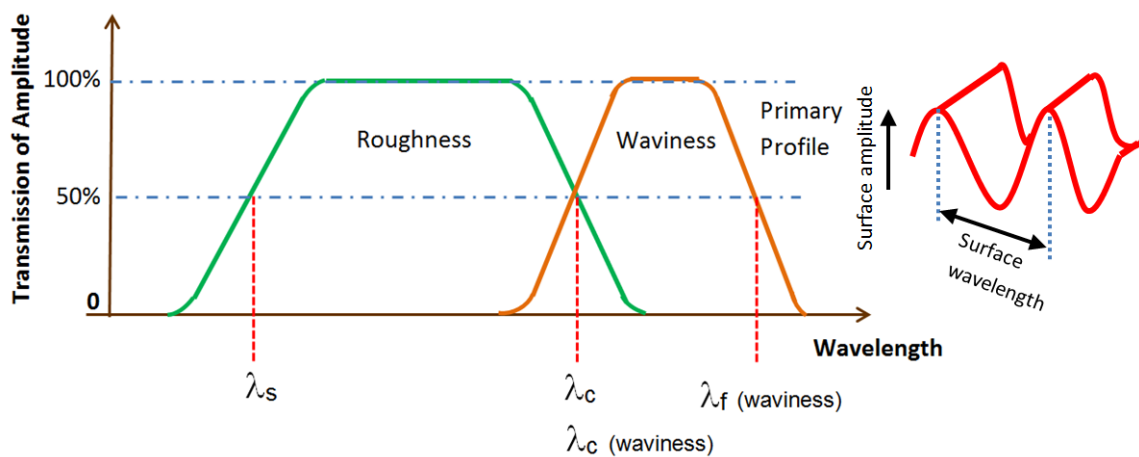


Figure 3.10: Filter transmission and cutoff for primary profile, roughness and waviness measurement. λ_s and λ_c represent the short wavelength cutoff and long wavelength cut-off for roughness.

Table 3.5: The differences of parameters between the primary profile, waviness profile and roughness profile. The grey cells indicate that the values are entered by the user. The white cells are those values given by the software

Software Parameter	Primary Profile	Waviness Profile	Roughness Profile
Kind of Profile	P_ISO	W_ISO	R_ISO
Number of Evaluation Length, nl_m	1	1	1
Sampling Length, l_e (mm)	0.8	0.8	0.08
Number of sampling length, nl_e	20	20	20
Pitch (μm)	0.5	5.0	0.1
Evaluation length, l_m (mm)	16.0	16.0	1.6
Cut off value (ISO 4287), λ_s (mm)	0.0025	-	0.0008
Cut off value (ISO 4287), λ_f (mm)	-	0.8	-
Cut off value (ISO 4287), λ_c (mm)	-	0.025	0.08
Stylus Speed (mm/s)	0.5	0.5	0.1

3.5 Lubricant Analysis Methods

3.5.1 Oxidation test

A rotary pressure vessel oxidation test (RPVOT) was conducted on the main lubricants and their blends according to ASTM D2272-14a by an oxidation stability test rig (Koehler, K70200). The oil was poured into a pressure vessel with a copper coil as a catalyst and then pressurised by oxygen gas at 90 psi (0.62 MPa). The oil in the pressure vessel was then heated in a silicon fluid bath at 150 °C and the pressure was observed. The pressure in the pressure vessel was then increased and reached a maximum value due to the heating process.

The oxidation stability was judged based on how much time (in minutes) the pressure took to drop to more than 25.4 psi (0.17 MPa) below the peak pressure. The dropping value of pressure in the pressure vessels indicates that an amount of oxygen has been absorbed into the oil. This is a starting point where the oil starts to be oxidised.

3.5.2 Oil viscosity test

The dynamic viscosity of the lubricants was measured by a rotary viscometer (Brookfield, LVDV1). Measurements were performed at 40 and 100 °C by means of a silicon fluid bath. Measurement of industrial oil viscosity at 40 °C is a common method which is based on the ISO viscosity grading system (ISO 3448). For most engine oils, the viscosity is typically measured at 100 °C in relation to the reference in SAE engine oil classification system (SAE J300).

The lubricants were poured into a small sample adapter which was able to measure the viscosity in a small volume of 6.7 ml. The viscometer measures the viscosity by measuring a torque required to rotate a spindle in the small sample adapter. This torque was then translated into a viscosity unit in centipoise (cP) by the viscometer software. In this study, the viscosity was measured for; fresh oil used oil taken from the oil bath of the test rig after 60 min used, and oxidised oil after the oxidation test.

3.5.3 Acid number test

The acid number (AN) of the lubricant was determined by a titration method (GRScientific, Aquamax MicroTAN titrator), according to ASTM D664-11a. It is an evaluation of oil acidity that measures how many milligrams is needed of the potassium

hydroxide (KOH) in order to neutralise one gram of acid in the oil which yields in a unit of mgKOH/g. An amount of titrant reagent, potassium hydroxide was titrated into the oil sample with titration solvent (mixture of water, isopropanol and toluene in a ratio of 5:495:500) by using the AN test rig. The AN test rig evaluates the AN by measuring the difference of voltage of the solution in its initial condition and at the end of titration process. This was performed by an electrode which soaked into the solution.

Increases of AN value in the oil could be an indicator of oil oxidation. In this study, the AN measurement was conducted for fresh oil samples, used oils taken from the test rig and those oils taken from the oxidation stability test.

3.5.4 Spectrochemical test

Spectrochemical analysis (mass spectrometry) was performed on the oil samples in order to identify the elements that existed in the oil such as calcium, zinc, phosphorus, molybdenum, boron etc. in parts per million (ppm). Typically, the procedure of mass spectrometry is started by bombarding the electrons into the sample until it is ionised. These ions are then separated and detected by their mass in a magnetic field. In this work, the oils samples were sent to an external laboratory (The Oil Lab Ltd, United Kingdom) for the testing and analysis.

3.5.5 Gas chromatography test

A gas chromatography test was performed on selected oil samples in order to identify the composition of fatty acids as a weight percentage (%) of the vegetable oils. This test is also to investigate any possible changes in the fatty acid composition of the vegetable oils

after an amount of additive was added into it. Typically, in a gas chromatography test, the sample solution is injected and carried by a moving gas into a separation tube known as the column. The components of the solution that exit from the column at different times are then identified by the detector and be compared with the result of a standard solution. In this study, the oil samples were sent to an external laboratory (Reading Scientific Services Ltd, United Kingdom) for testing and analysis.

3.5.6 Lubrication regime determination

In order to evaluate the contact conditions on the lubricated specimens, the estimation of their lubrication regime (hydrodynamic, elastohydrodynamic or boundary) is needed. This is performed by calculating the minimum film thickness, h_{min} based on the formula developed by Hamrock et al. [211] ((Equation 3.1).

$$H_{min} = 3.63U^{0.68}G^{0.49}W^{-0.073}(1 - e^{-0.68k}) \quad (\text{Equation 3.1})$$

where;

$$H_{min} = \frac{h_{min}}{R_x}, \quad \eta_o \tilde{u} = \frac{\eta_o \tilde{u}}{E' R_x}, \quad G = \alpha E', \quad W = \frac{w}{E' R_x^2}, \quad k = \left(\frac{R_y}{R_x}\right)^{2\pi}$$

h_{min} = minimum film thickness, m

R_x, R_y = effective radius in x and y direction, m

$U = \frac{\eta_o \tilde{u}}{E' R_x}$ = dimensionless speed parameter

η_o = absolute viscosity at atmosphere pressure and constant temperature, Pa.s

$\tilde{u} = \frac{u_1+u_2}{2}$ = mean velocity in x direction, m/s

u_1, u_2 = velocity in x direction, m/s

G = dimensionless material parameter

α = pressure-viscosity coefficient, m^2/N

W = dimensionless load parameter

w = applied load, N

$E' = 2 \left(\frac{1-\nu_1^2}{E_1} + \frac{1-\nu_2^2}{E_2} \right)^{-1}$ = effective elastic modulus, Pa

k = ellipticity parameter (for point contact, $k = 1$)

In order to determine the lubrication regimes of the sliding metals, the ratio between the minimum film thickness and root mean square of surface roughness, λ was calculated based on formula given by Ian [212] ((Equation 3.2):

$$\lambda = \frac{h_{min}}{\sigma^*} \quad (\text{Equation 3.2})$$

where $\sigma^* = \sqrt{R_{q1}^2 + R_{q2}^2}$ = root mean square (r.m.s) of two surfaces, m

R_q = r.m.s of surface roughness, m

The value of λ provides information about the lubrication regime (Figure 3.11). For $\lambda > 3$, the lubrication regime is termed hydrodynamic where full film lubrication prevents both metal-to-metal contact. However, in the case of $1 < \lambda < 3$, the lubrication regime has fallen into a partial elastohydrodynamic regime (mixed lubrication) where some contact between asperities occurs. For λ less than 1, only boundary lubrication is presented. The detailed calculation of the minimum film thickness and lambda values is depicted in the Microsoft Excel sheet in Appendix 5 (example for Mineral Oil) and Appendix 6.

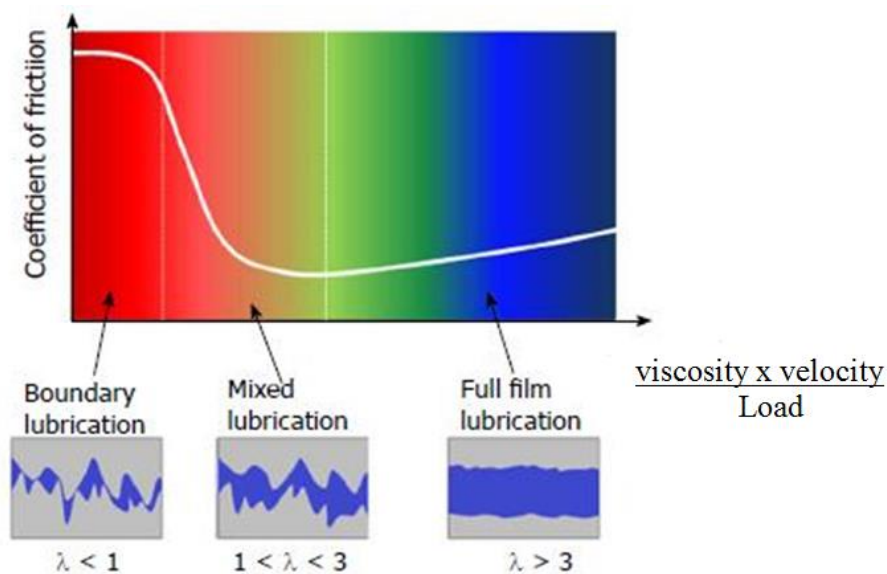


Figure 3.11: A Stribeck curve indicates the lubrication regime

In a piston ring contact, the lubrication regime changes depending on the crank angle. Boundary lubrication occurs during the first half of the power stroke [65]. In this study, boundary lubrication was preferred as it usually resembles a more severe contact condition.

3.6 Statistical analysis

The one-way analysis of variance (ANOVA) was used to determine the significance of friction and wear data with a 95% significance level which calculation was performed by Microsoft Excel. In this analysis, the null hypothesis is defined as: “all means of experimental data are equal”. The probability of obtaining this null hypothesis is defined as P in which lower P-value is an indication of strong evidence to reject the null hypothesis. In this study, data points are statistically significant if the significance level, P-value < 0.05. The details of this analysis ANOVA is depicted in the Microsoft Excel sheet in Appendix 7 (example for analysis of COF for Mineral Oil, Palm Oil, Soybean Oil lubricated specimens).

3.7 Summary of test method

Investigations to assess the potential use of vegetable oils as biolubricants in an automotive engine require an extensive type of testing which includes the evaluation of friction and wear performance, surface analysis of worn specimens and chemical analysis of oils. In this study, a total of ten lubricants were tested which include the mineral engine oil, vegetable oils (palm oil and soybean oil), vegetable oil-mineral engine oil blends and vegetable oil-additive blends.

It seems unfair to compare the performance of untreated vegetable oils with the fully formulated commercial mineral engine oil. However, on the basis of establishing the tribological data that comparing the worst case scenario with the best one, it is practically beneficial. The reference data of friction, wear and oil oxidation produced from the fully formulated commercial mineral engine oil is important and useful. This data provides a

targeted benchmark for the improvement to be achieved in the future. In addition, it is also expected that there would be some new knowledge that can be learned from the superior characteristics shown by the fully formulated mineral oil such as the additives used in the oil. Efforts have also been made to get the original untreated mineral oil from the oil manufacturer but this was not possible as this could be one of their key secrets in sustaining their business in the mineral lubricants area.

Following a replication test of a piston ring motion on a cylinder liner of an internal combustion engine, a reciprocating sliding point contact was chosen in order to minimise the error that may come from misalignment of specimens. A steel ball and a grey cast iron flat specimen (EN-1561-GJL-250) were selected as rubbing materials for evaluating the friction on the counterface. The justifications for the test parameter choice on the friction test rig have been described in detail. A mass loss measurement was implemented to evaluate the wear performance of lubricated specimens.

In view of wide hardness range of grey cast iron specimens, a technique to characterise the hardness on intended wear scar prior to the test is crucial. This was conducted by measuring the Vickers hardness at three points on the intended wear scar before the test. This step is important in ensuring the repeatability of wear result and thus, provides more robust tribological data.

Several techniques were also selected to investigate the effects of lubricants on the wear scar surface after the friction and wear tests such as surface topography and surface morphology. The surface topography investigation was conducted on the wear scar area in order to analysis the surface roughness and waviness value. The surface morphology analysis on the worn surfaces was performed by wear scar imaging. The optical microscope was used

for analysing the main wear mechanism in a broader view while the scanning electron microscopy was used for evaluating the wear mechanism on the very specific area and elemental analysis (EDX) on the worn surfaces.

For chemical analysis, selected oil samples were tested by spectrochemical analyser and gas chromatography tester in order to determine the possible elements and fatty acid composition that exist in the oil. In addition to this, the acid number and the oil viscosity were measured to determine the oxidation level of the used oil after the friction test. The oxidation stability tests of the fresh oil samples were also conducted by using the rotary pressure vessels oxidation test.

The limitations of the friction and wear test were also described, highlighting their role as only the beginning of a more intensive testing in the future that is required to fully characterise the performance of vegetable oils under a variety of test conditions. Finally, issues related to the reliability of the test data was verified by performing the statistical calculation using the single variable of ANOVA.

Chapter 4: Hardness characterisation of grey cast iron and its tribological performance in a contact lubricated with soybean oil

In this chapter the friction and wear response to a wide hardness range of the EN1561-GJL-250 grey cast iron (GCI) specimens lubricated with soybean oil are presented. The specimens are divided into 3 groups according to their hardness on intended wear scar regions, i.e. low, medium and high hardness. The results were analysed and discussed based on the related literature. The conclusions of the study are then presented.

4.1 Introduction

Grey cast iron is a common material for piston rings and cylinder liners, which are one of the main components of internal combustion engines. Its tribological performance relies on its flake graphite content, which gives good friction and wear performance. Nevertheless, the variation of reported hardness even in ‘standard’ grey cast iron is high. This may lead to variation of friction and wear results with this material. It is very important to consider this factor before a performance evaluation of vegetable oils lubrication is implemented.

In view of this, in this work, the hardness of the grey cast iron specimens was measured in the intended locations of the wear scars before testing commenced. The behaviour of friction and wear across a high variation of hardness was then investigated with the soybean oil as the biolubricant. Friction and wear tests were also performed on unlubricated specimens for comparison.

4.2 Hardness properties of grey cast iron

The hardness data of the specimens in the intended locations of the wear scars on Point 1, Point 2 and Point 3 at Scar 1, Scar 2 and Scar 3 (Section 3.2.1.1 Figure 3.3) with the average value, depicted in Appendix 1 (number of hardness measurements per wear scar regions = 426). This average value was then summarised in tabular form (hardness class versus frequency) as shown in Table 4.1. The data were then plotted as a bar graph in Figure 4.1 which shows the distribution of average hardness per wear scar regions on the GCI specimens before the friction and wear testing. Based on Figure 4.1, the hardness range of GCI specimens was found to be 65HV (lowest value 185 HV to highest value 250 HV). The majority of the hardness values were in the range 205 HV-209 HV (79 measurements) and 210 HV-214 HV (78 measurements). Based on the hardness examination results, nine wear scars, with hardness in these ranges, were selected for use in the friction and wear tests. To facilitate the experiment, these nine wear scars were then grouped into three classes and labelled as low, medium and high hardness (Table 4.2).

The distribution of GCI hardness value was as expected in which the high hardness range is comparable to previous literature (189.3-257.3 HB) [162] and in the standard (70 HB in range) (BS EN1561:2011). The hardness range from this work (65 HV) is similar to the GCI / ASTM 35B which is about 65 HB (65 HV) [162]. Hardness of GCI depends on factors such as element composition, size of flake graphite and distribution on the metal matrix and processing variable such as the casting cooling rate [166, 213].

Table 4.1: The frequency of average hardness per wear scar region that grouped based on hardness class. Total frequency (426) is equal to the total of wear scars where hardness were measured.

Hardness class	Frequency
180-184	0
185-189	10
190-194	23
195-199	38
200-204	46
205-209	79
210-214	78
215-219	39
220-224	25
225-229	27
230-234	17
235-239	15
240-244	17
245-249	8
250-254	4
255-259	0
Total	426

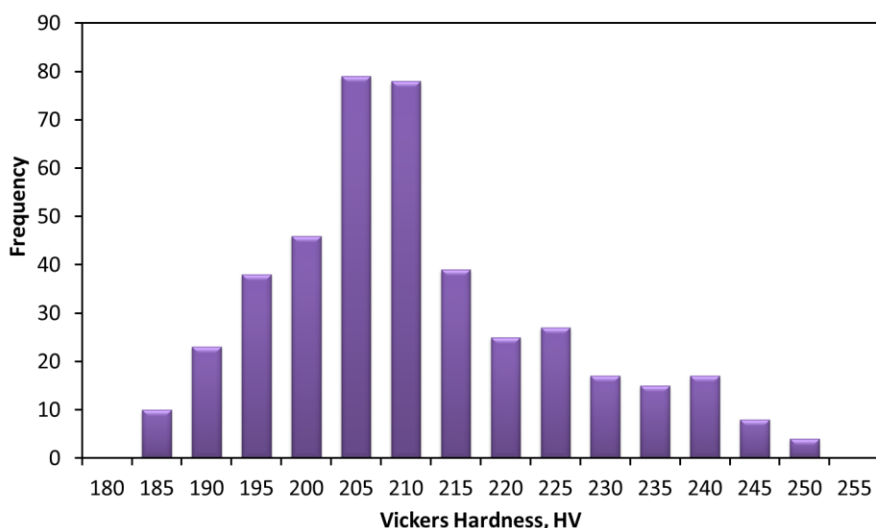


Figure 4.1: Distribution of average hardness per wear scar region on GCI specimens measured on intended wear scar regions before testing. The frequency denotes the number of wear scars where the average hardness measurements were performed.

Table 4.2: Hardness of nine selected wear scars of GCI grouped into low, medium and high hardness.

Number	Wear Scar Hardness (HV)	Average Group Hardness (HV)	Hardness group
1	207.7	206.5	low
2	206.7		
3	205.0		
4	224.3	223.4	medium
5	224.3		
6	221.7		
7	240.0	245.5	high
8	248.7		
9	247.7		

Cast iron that experiences a slow cooling rate produces lower hardness than rapidly cooled material. For example, different position in the same specimen in a casting bar (centre and corner position) produced different hardness (about 30 HB (30 HV)) due to the different cooling rate [166]. In addition, the cooling rate affects the microstructure of GCI by influencing the flake graphite size. A low cooling rate promoted bigger graphite size and produced lower hardness [167].

The wide hardness distribution of GCI specimens found in the results above has driven an interest to study its influence to the tribological performance. This is very important in order to ensure more robust and consistent data of friction and wear is produced in evaluating the biolubricant performance.

4.3 Friction analysis

The COFs for soybean oil lubricated GCI specimens are plotted in Figure 4.2a. Unlubricated GCI specimens (low hardness) were also tested for comparison. This specimen started with a high COF (0.292), which slowly reduced in magnitude. In contrast, for lubricated specimens, there was a low COF (about 0.09) at the beginning (running-in period), which increased gradually and then finally reached a steady state condition after about 45 minutes. Significant COF differences were observed for unlubricated and lubricated specimens for low hardness when compared to others. However, the differences of COF for lubricated specimens at medium and high hardness were not clearly observed so in order to show this difference in detail, Figure 4.2b was plotted using the COF at 60 min.

The COF for lubricated specimens is 13% lower at high hardness (0.122) compared to low hardness (0.140). Soybean oil lubricant was found to reduce the friction by 24% between lubricated (COF = 0.140) and unlubricated (COF = 0.185) specimens at low hardness. The ANOVA analysis of COF for all four above conditions (low, medium, high hardness and unlubricated specimens) were found to be significantly different ($P < 0.05$, Table 4.3). However, for medium and high hardness specimens, the COFs were not significantly different ($P > 0.05$, Table 4.4).

The COF profiles from this work are similar to those categorised by Blau [47]. A possible reason for the running-in behaviour for the unlubricated specimen is the reorientation process of random crystal texture on the contact surface [47]. During the initial sliding process, the rearrangement of random atoms in the crystalline solids (lattice structure) occurs at near-surface area. The preferred texture is gradually achieved which is a steady state of microstructure resistance to sliding. The sliding resistance at this condition is less

than the initial unworn surface of random orientation. A detailed discussion about this process has been previously discussed by Rigney and Hirth [214].

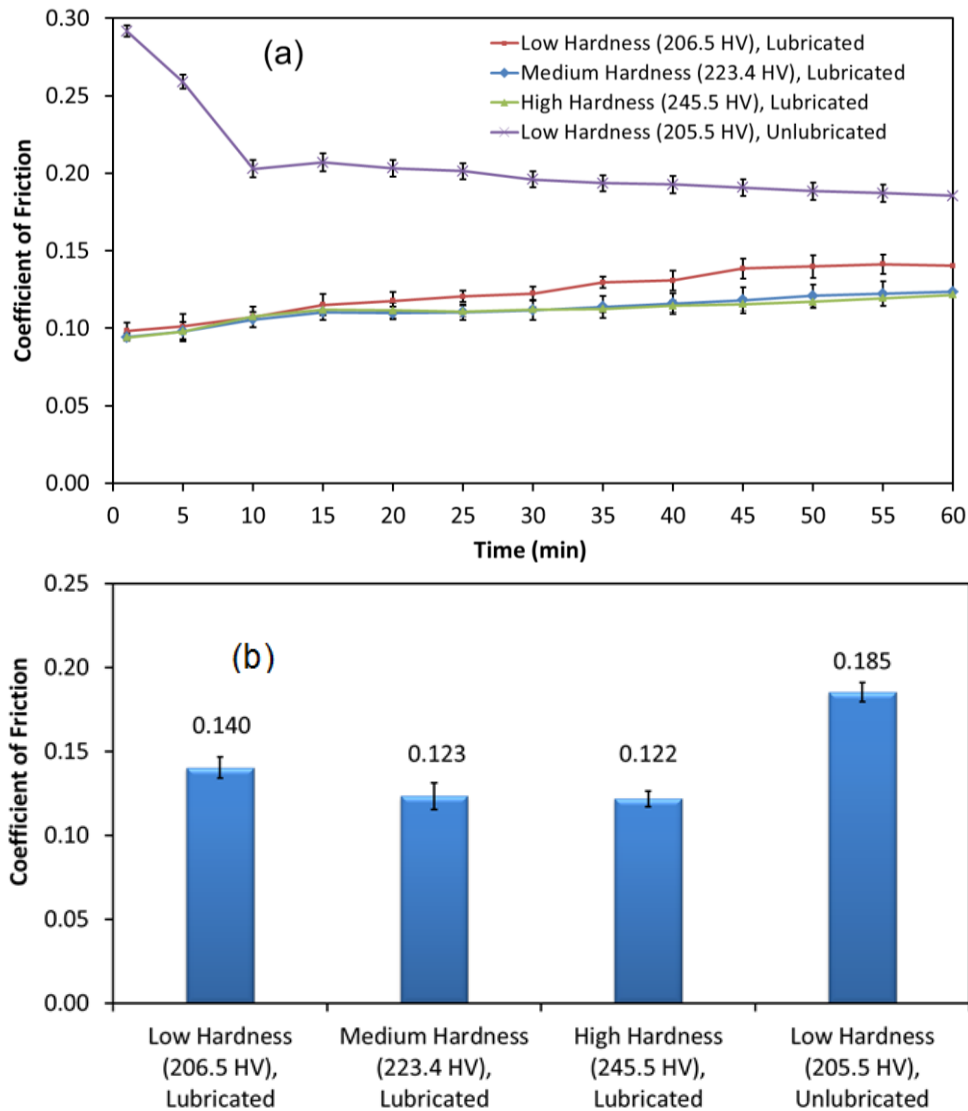


Figure 4.2: (a) Coefficient of Friction versus time and (b) Coefficient of Friction value at 60 minutes of specimens with low, medium and high hardness.

The COF profile for unlubricated GCI in this study is also similar with unlubricated GCI specimens tested at 0.8 m/s by Sugishita [150] in which the higher COF at the beginning was explained to be due to the partial detachment of graphite at the start of the test. In addition, in the case of flake graphite cast iron, it takes some time for the graphite to be near-

uniformly distributed across the surface in order to reach a steady state value of friction coefficient which is lower than the initial value [151].

Table 4.3: ANOVA analysis of COF for low, medium and high hardness specimens with unlubricated specimens

		<i>Count</i>	<i>Sum</i>	<i>Average</i>	<i>Variance</i>		
Groups	Low	3	0.421	0.140	3.81E-05		
	Medium	3	0.370	0.123	6.35E-05		
	High	3	0.365	0.122	2.19E-05		
	Unlubricated	3	0.557	0.185	2.62E-05		
ANOVA	<i>Source of Variation</i>	<i>SS</i>	<i>df</i>	<i>MS</i>	<i>F</i>	<i>P-value</i>	<i>F_{crit}</i>
	Between Groups	0.007983	3	0.002661	71.1270	4.14E-06	4.0661
	Within Groups	0.000299	8	3.74E-05			
	Total	0.008283	11				

Table 4.4: ANOVA analysis of COF for medium and high hardness specimens

		<i>Count</i>	<i>Sum</i>	<i>Average</i>	<i>Variance</i>		
Groups	Medium	3	0.370	0.123	6.35E-05		
	High	3	0.365	0.122	2.19E-05		
ANOVA	<i>Source of Variation</i>	<i>SS</i>	<i>df</i>	<i>MS</i>	<i>F</i>	<i>P-value</i>	<i>F_{crit}</i>
	Between Groups	4.49E-06	1	4.49E-06	0.1052	0.7618	7.7086
	Within Groups	0.000171	4	4.27E-05			
	Total	0.000175	5				

It is possible that the running-in behaviour of lubricated specimens is due to the removal of lubricious contaminants from the contact surface [48] and the disruption of the surface oxide layer by increasing the size of the metallic contact [50]. The removal of the graphite film due to the presence of the lubricant was also reported by Sugishita [150] which

reduces the solid lubrication effect during the running-in process. Therefore, the response of COF to different material hardness is subject to the breakdown of oxide films near the contact surface [215]. The high hardness specimens deform less, therefore, it is possible in preventing the excessive breakdown of the oxide film. This is shown by the amount oxygen element that retained on the worn specimen of high hardness specimen compared to the low hardness counterpart (this is discussed further in Section 4.8, Element analysis, Figure 4.11) and thus, the lower friction is produced as shown by COF of high hardness specimens.

The friction force is defined here as the summation of adhesive force and ploughing force as expressed by Bowden and Tabor [159]. The low hardness specimen is prone to deeper indentation by the steel ball thus, producing a wider track width and more deformation. The wider track width promotes a higher ploughing force to displace material, which accumulates in front of the slider (pin), and this increases the ploughing component of friction [159]. Furthermore, based on the Bowden and Tabor's formula, it can be shown that the plastic flow (close to the indentation hardness) may influence the adhesive component of friction in which low substrate hardness will produce a higher friction coefficient.

4.4 Wear analysis

Figure 4.3 shows the mass loss of GCI specimens after testing both with the contact lubricated with soybean oil and also unlubricated, for the three different hardness groups. At low hardness, soybean oil slightly reduced the wear by 7% (50.38 mg of mass loss) compared to unlubricated specimens (54.38 mg). The wear was inversely proportional to the hardness. For lubricated specimens, the mass loss is higher at low hardness (50.38 mg) compared to high hardness (12.90 mg), a difference of 74%. This shows that the difference in wear of

lubricated specimens (between low and high hardness) is very significant and greatly influenced by the wide range of surface hardness of the GCI specimens.

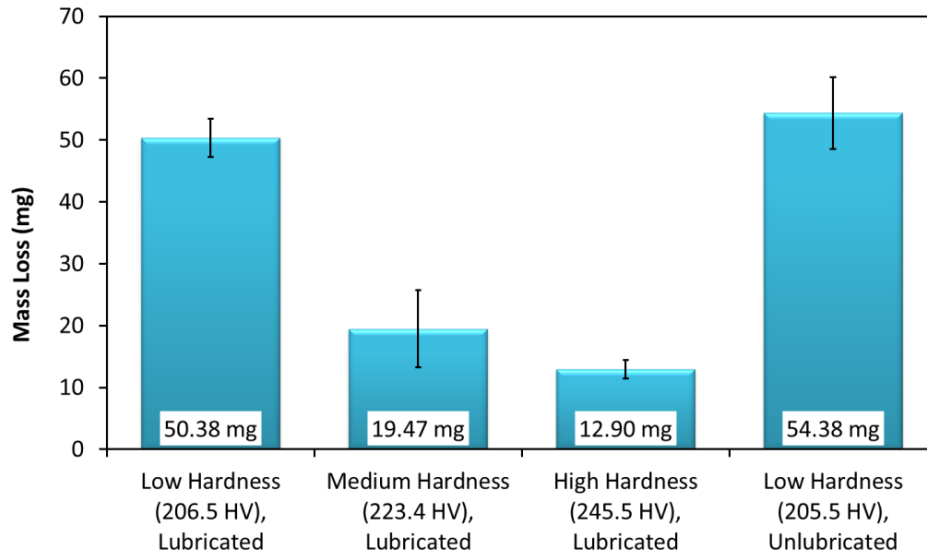


Figure 4.3: Mass Loss of specimens with low, medium and high hardness

The minimum film thickness, h_{min} , was calculated (Appendix 6, SBO lubricant to be 2.19×10^{-9} m and the lambda ratio, λ was 0.011). Based on this lambda value ($\lambda = h_{min}/\sigma^*$), which is significantly less than 1, it is clearly shown that the minimum film thickness was much lower than the surface roughness. This means that the lubrication film was too thin to provide total surface separation therefore, it is suggested that the lubrication regime was boundary [212].

The main wear mechanisms for all of specimens were found to be abrasive in nature (Figure 4.13). In abrasion, microcutting is the most efficient way to remove material [216] and penetrate into the specimen surface. This depends on the hardness of surface where a softer surface has lower penetration resistant.

Based on ANOVA analysis, no significant difference in wear was found between low hardness specimens of lubricated and unlubricated ($P > 0.05$, Table 4.5), and also between medium and high hardness specimens with lubrication ($P > 0.05$, Table 4.6). However, the mass loss for all three specimens (low, medium and high hardness) are significantly different ($P < 0.05$, Table 4.7).

Table 4.5: ANOVA analysis of mass loss for low hardness and unlubricated specimens

		<i>Groups</i>	<i>Count</i>	<i>Sum</i>	<i>Average</i>	<i>Variance</i>		
Groups		Low (Lubricated)	3	151.14	50.38	9.51		
		Low (Unlubricated)	3	163.13	54.38	33.91		
ANOVA		<i>Source of Variation</i>	<i>SS</i>	<i>df</i>	<i>MS</i>	<i>F</i>	<i>P-value</i>	<i>F_{crit}</i>
		Between Groups	23.96	1	23.96	1.1037	0.3527	7.7086
		Within Groups	86.83	4	21.71			
		Total	110.79	5				

Table 4.6: ANOVA analysis of mass loss for medium and high hardness specimens

		<i>Groups</i>	<i>Count</i>	<i>Sum</i>	<i>Average</i>	<i>Variance</i>		
Groups		Medium	3	58.41	19.47	39.29		
		High	3	38.71	12.90	2.17		
ANOVA		<i>Source of Variation</i>	<i>SS</i>	<i>df</i>	<i>MS</i>	<i>F</i>	<i>P-value</i>	<i>F_{crit}</i>
		Between Groups	64.68	1	64.68	3.12	0.1521	7.7086
		Within Groups	82.92	4	20.73			
		Total	147.61	5				

Table 4.7: ANOVA analysis of mass loss for low, medium and high hardness specimens

		<i>Count</i>	<i>Sum</i>	<i>Average</i>	<i>Variance</i>			
Groups		Low	3	151.14	50.38	9.51		
		Med	3	58.41	19.47	39.28		
		High	3	38.71	12.90	2.17		
ANOVA		<i>Source of Variation</i>	<i>SS</i>	<i>df</i>	<i>MS</i>	<i>F</i>	<i>P-value</i>	<i>F_{crit}</i>
		Between Groups	2403.05	2	1201.52	70.7158	6.74E-05	5.1432
		Within Groups	101.94	6	16.91			
		Total	2504.94	8				

4.5 Wear scar appearance

Figure 4.4a shows the wear scar appearance after 60 minutes while Figure 4.4b depicts the primary profile of the wear scar performed by profilometer. All wear scars have very similar formation, wavy-shaped scar indicating the onset of plastic deformation during sliding. The high hardness specimens produced the smallest wear scars.

The wavy-shaped wear scars in this study are similar to those seen in the work carried out by Plint involving a hard ball (AISI 52100) on soft tool steel plate (NSOH B01) [217]. However, an explanation for the formation of the wavy-shaped wear scar was not discussed. Thus, in this study, the mechanism of the formation of wavy-shaped wear scar at the initial sliding stage is proposed in Figure 4.5.

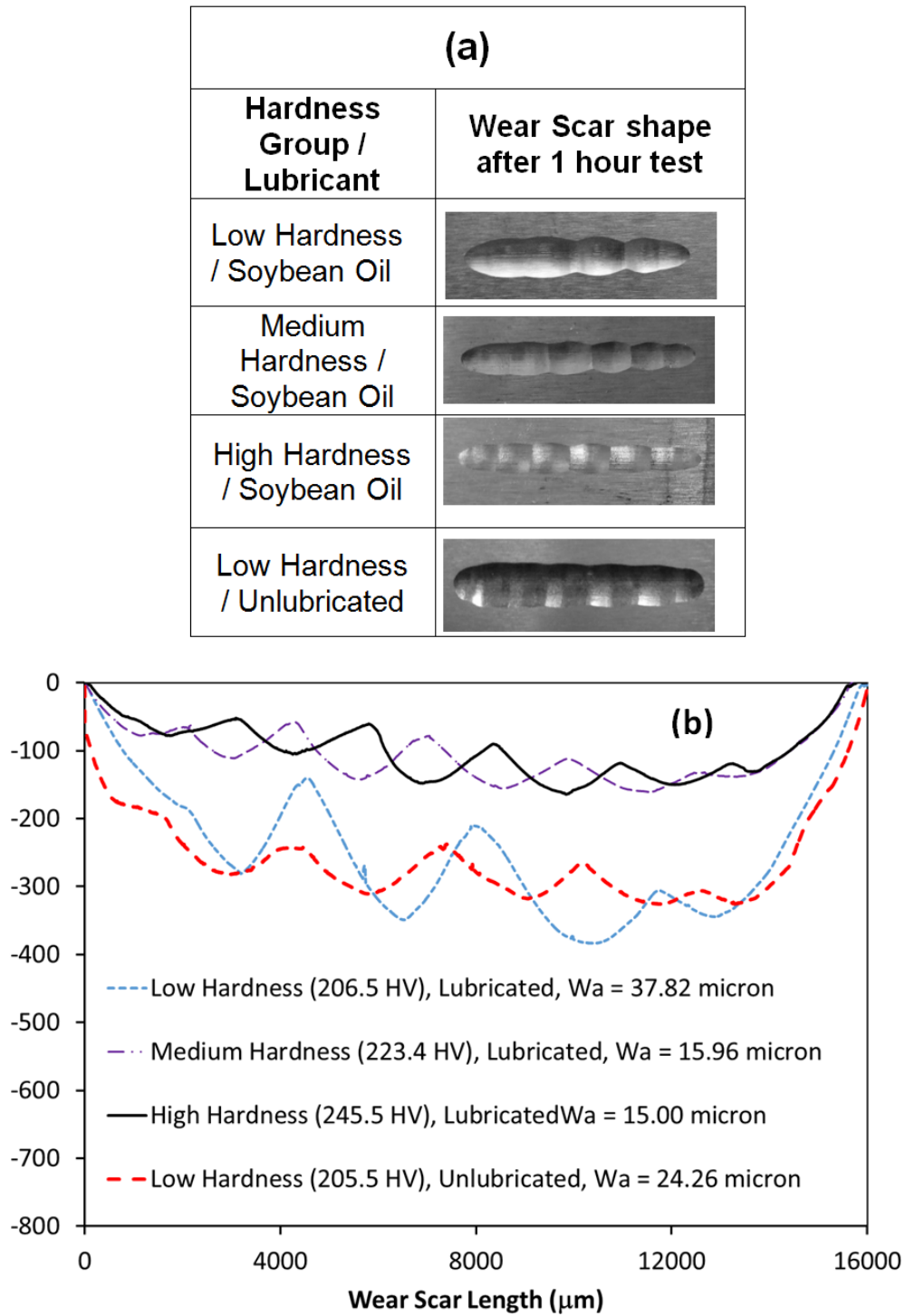


Figure 4.4: (a) Wear scar appearance and (b) Primary profile of specimens with low, medium and high hardness

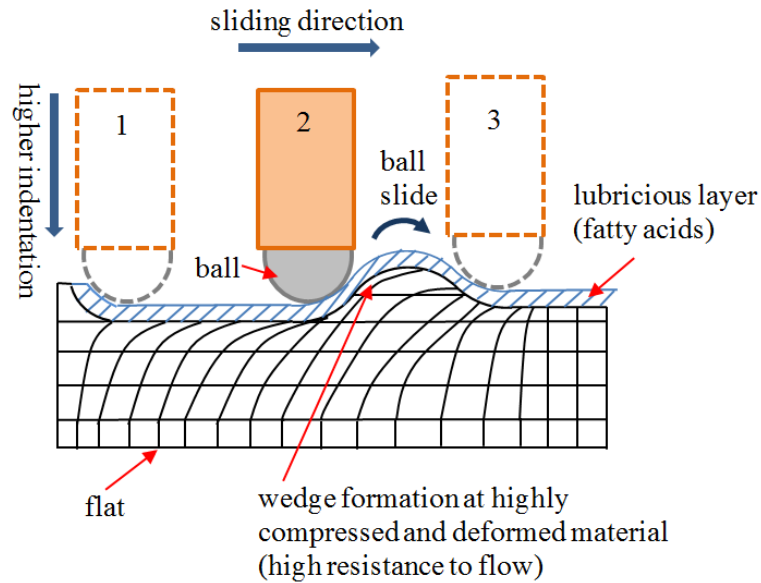


Figure 4.5: Formation of wavy-shaped wear scar at initial sliding stage

At high normal load, the ball indents into the flat specimen prior to sliding (Position 1, Figure 4.5). This ball then ploughs through the material and accumulates material against its sliding direction (Position 2, Figure 4.5). At Position 2, the ball has reached a point where the flow resistance is maximum (i.e. it has maximum resistance to its ploughing motion) and has started to develop a bulge on its front. The size of the bulge depends on the degree of penetration. At lower penetration, less material is ploughed with lower flow resistance and thus, a lower bulge can be formed. Due to the continuous tangential force produced by the test rig, the ball is then forced to move and slide on the bulge to the next position (Position 3, Figure 4.5) with the assistance of lubricious layer of fatty acids. The ploughing process was continued at this position where the bulge is formed again at its front of sliding direction.

The debris that were produced from the sliding process is trapped in the groove between bulge and the ball and acts as third-body abrasive particles (Figure 4.6). This debris could increase of deepness of the groove through the abrasion process. This whole process

was performed repetitively in both direction (reciprocating), and after some time, a considerable wavy-shaped wear scar could be seen.

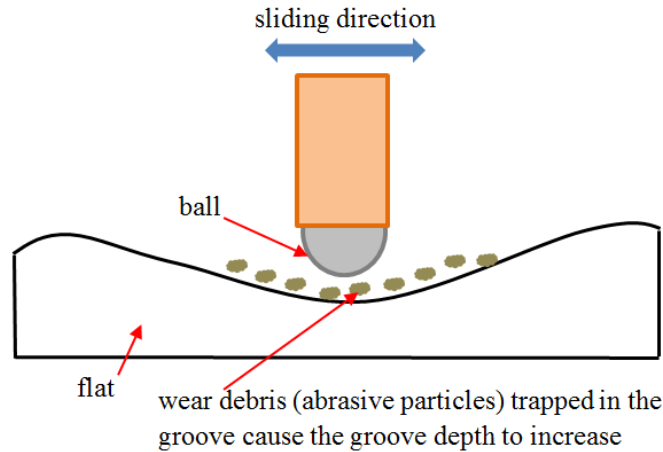


Figure 4.6: Propagation of depth at the undulating profile by the abrasion process attributed by the trapped debris

The phenomenon of the wave-shaped scars could also be explained by plastic ratcheting and the phenomenon known as shakedown limit. Ponter [218] described the relationship between Hertzian pressure to shear strength ratio and the COF (Figure 4.7). In this current study, the calculated Hertzian pressure was 1.7 GPa and the shear strength for GCI specimens was about 0.29 GPa (BS EN1561:2011). This yielded a Hertzian pressure-shear strength ratio of about 6. At COF = 0.12 (values taken from the COF of high hardness specimens) and Hertzian pressure to shear strength ratio of more than 6, Ponter [218] suggests that the material deformation will enter the plastic ratcheting region. This is shown by the red dotted line in Figure 4.7. Plastic ratcheting occurs when the applied load exceeds the plastic shakedown limit, in which the progressive plastic deformation of surfaces occurs during repeated sliding (Figure 4.8) [219]. In the ratcheting process, the large plastic strains are slowly accumulated and superimposed during each sliding cycle (i.e. forward and backward sliding direction of reciprocating motion) as proposed in Figure 4.9. This

accumulated plastic strain could translate into accumulated deformed material in the form of bulge. The position of bulge are different and its size increases on every repeated cycle (Figure 4.9 a-h).

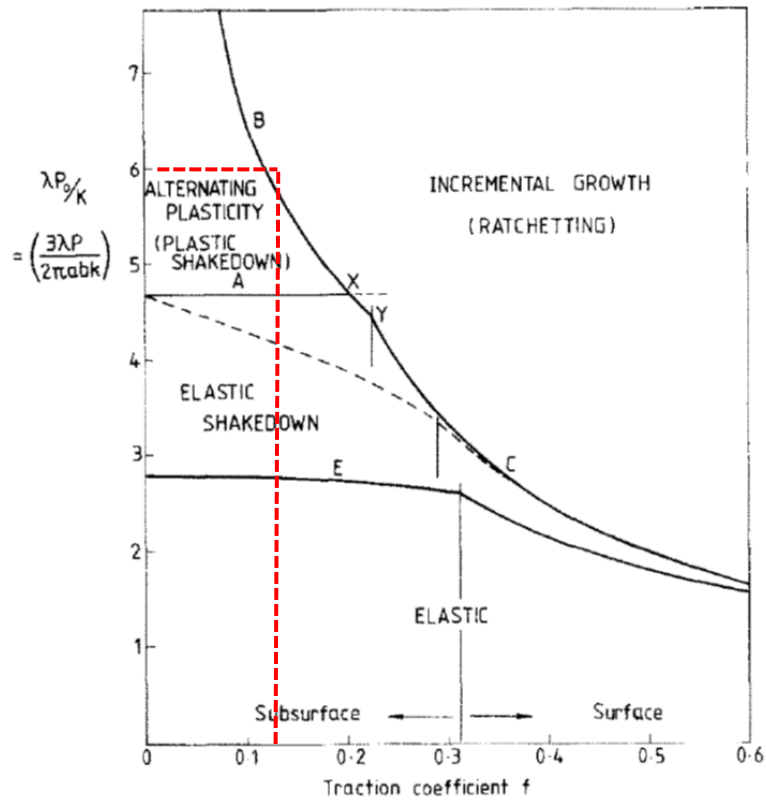


Figure 4.7: The elastic, elastic shakedown, plastic shakedown and ratcheting region associated with Hertzian pressure, P_0 -shear strength ratio, K on coefficient of friction, f for sliding point contact [218].

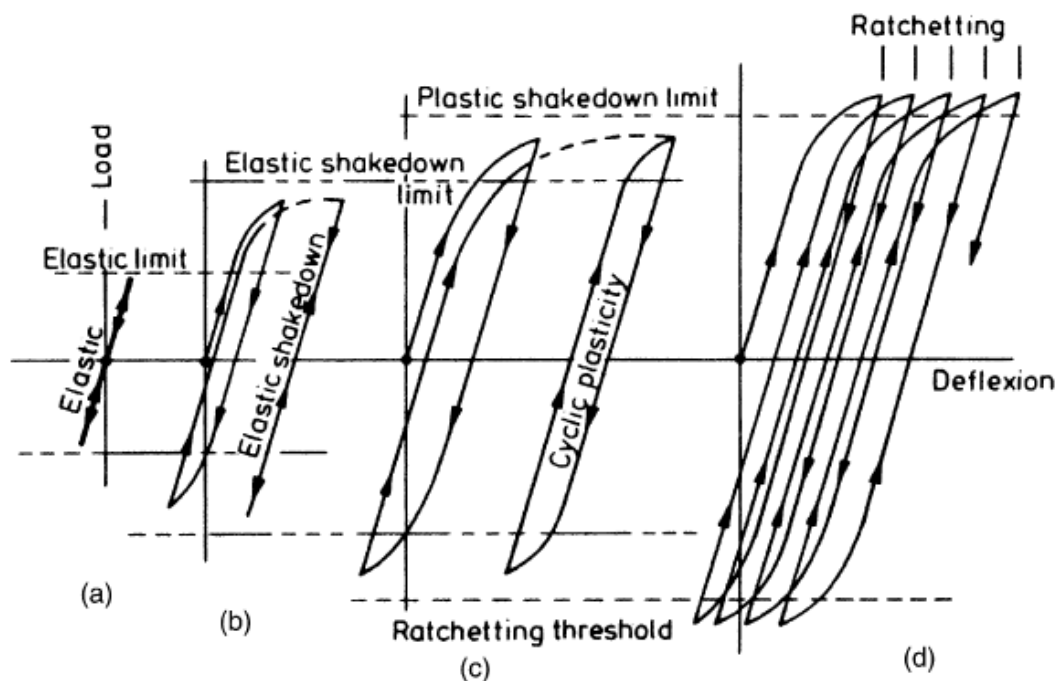


Figure 4.8: The different forms of structural response to cyclic loading: (a) elastic, (b) elastic shakedown, (c) plastic shakedown and (d) ratcheting [219]

In order to understand the microstructure of the wear scar, the worn specimens (with low and high hardness) sectioned along the length of the wear scar are shown in Figure 4.10. The graphite in GCI specimen is distributed heterogeneously with significant differences in form and distribution type. The graphite form for the high hardness specimen is similar to Form I with distribution C (as described in BS EN ISO 945 [220]) with a lamellar shape. However, for low hardness specimens the graphite form is found close to spheroidal shape (Form III, distribution D) which suggests undercooling of graphite occurred [220] and tends to produce bigger graphite size and lower strength. Although more fine flakes were seen in low hardness specimens, this morphology is unfavourable because it prevents the development of a fully pearlitic matrix [213] which may also reduce the material strength.

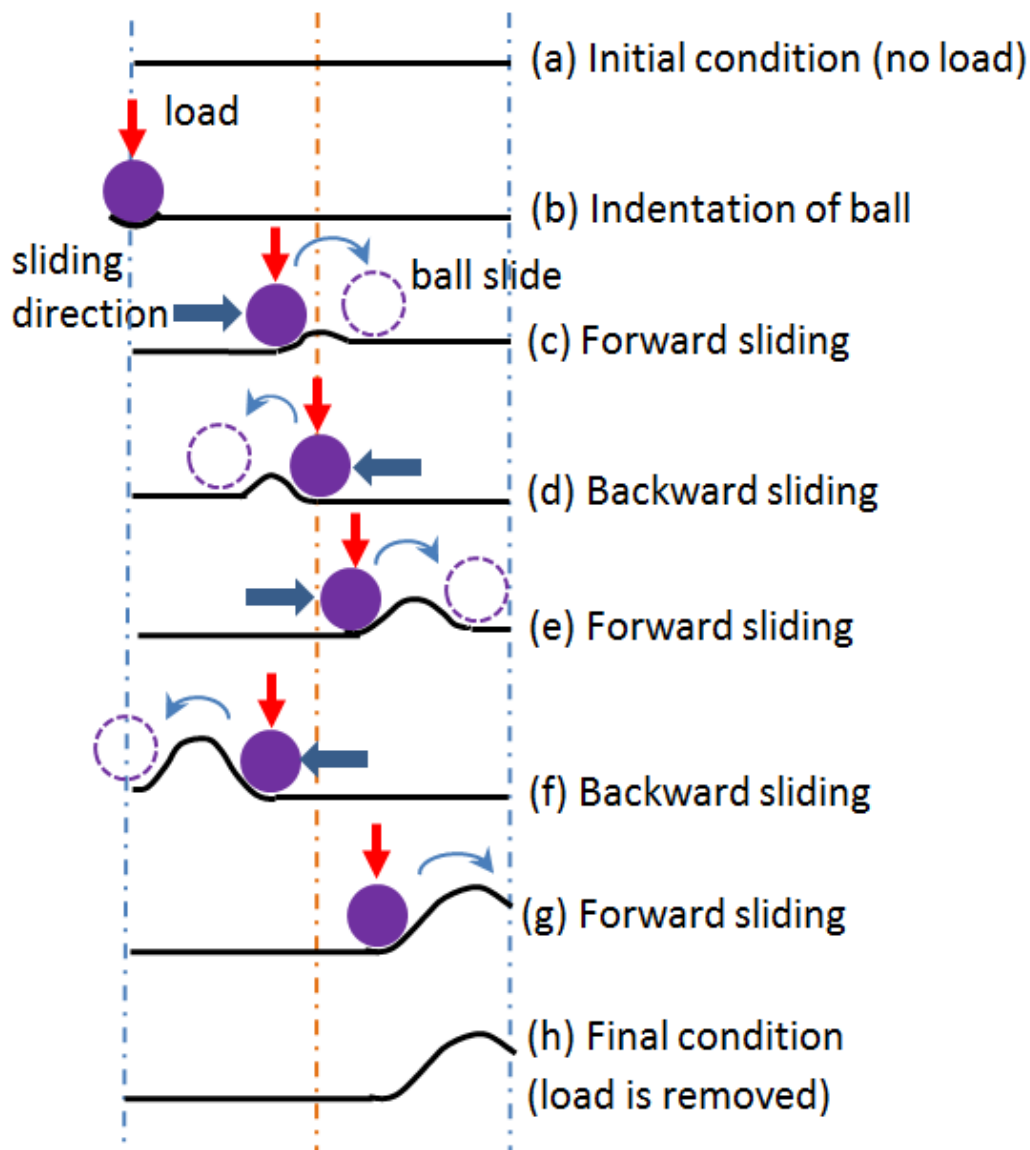


Figure 4.9: Accumulation of deformed material (in the form of bulge) during repeated sliding of ratcheting causes the changing in bulge position and size

The forms of graphite with a pearlite and ferrite matrix microstructure from this work are found to be similar with the GCI microstructure reported by Prasad in a pin on disc sliding test [154]. Further investigation near to contact surface (etched surface) of specimens of this current study revealed that a very high amount of ferrite matrix is found in the low hardness specimen while in the high hardness specimen, a pearlite matrix is found everywhere. This ferrite matrix has a lower hardness than the pearlite which contributes to its

lower strength. Furthermore, cracks and higher distortion of the pearlite matrix seen near to the worn surface for the low hardness specimen suggests that higher plastic flow occurred during the sliding process.

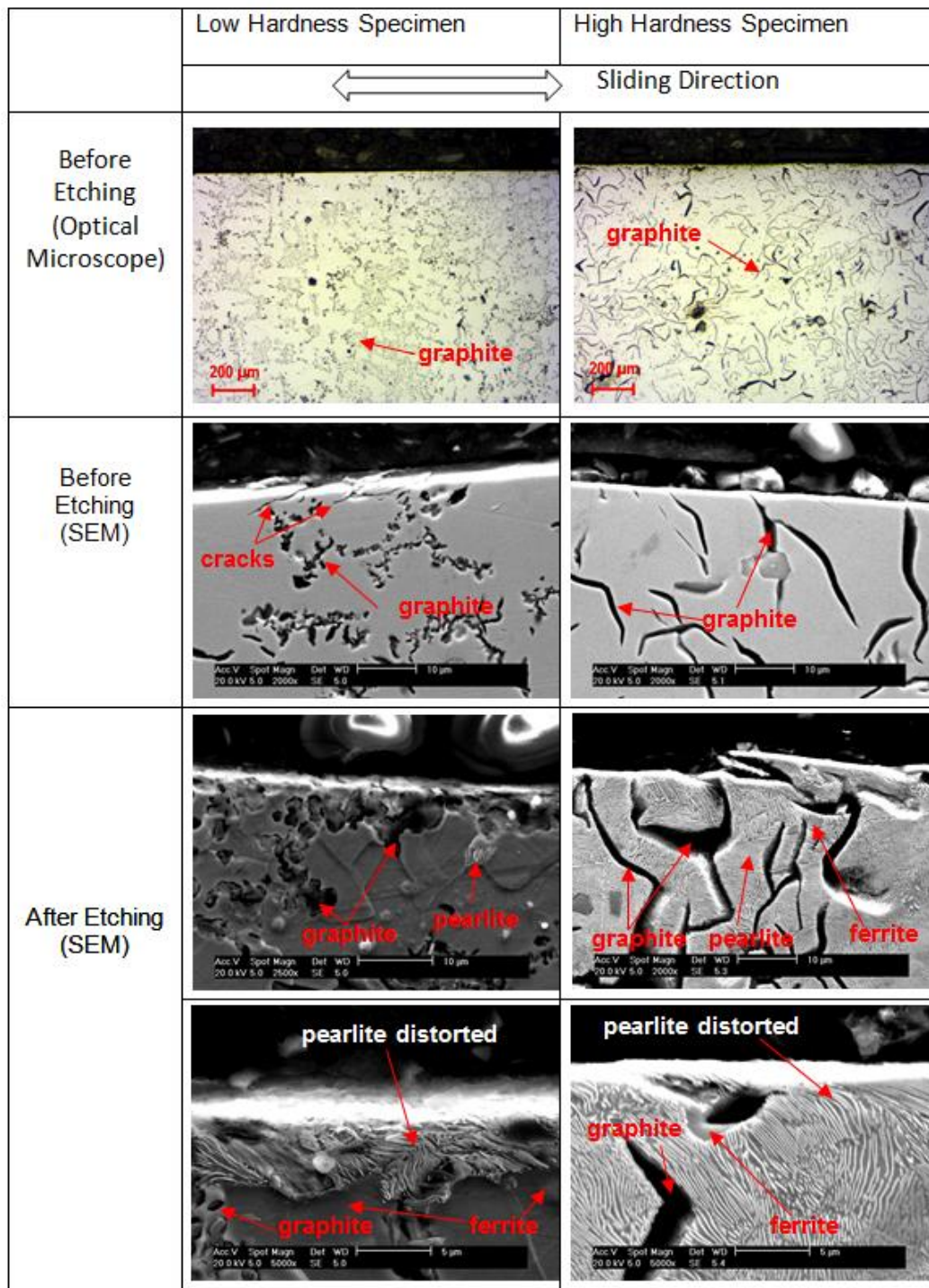


Figure 4.10: Sectioning images of wear scar for low and high hardness specimens.

4.6 Surface waviness analysis

To further investigate the influence of hardness on the formation of wave-shaped scars, measurements resulting in the primary profile and the waviness profile of the specimens were performed along the sliding direction in the middle of the scars. The typical primary profile result shown in Figure 4.4b shows that the medium and high hardness specimens have shallow depth compared to the low hardness specimen. The specimen with high hardness produced the lowest surface waviness ($W_a = 15.00 \mu\text{m}$) while the low hardness specimen generated the highest surface waviness ($W_a = 37.82 \mu\text{m}$). However, the unlubricated specimen (low hardness) is found to have lower surface waviness ($W_a = 24.26 \mu\text{m}$) than the lubricated counterpart.

Material with high hardness typically has higher yield strength and more resistance to plastic strain, and the measurements of waviness profile after test match this relationship. In the context of the wavy-shaped scar, the harder the specimen is the lesser the surface waviness formed in the wear scar. This is due to lower plastic strain accumulated for harder specimens during the plastic ratcheting process. Although the wear of the unlubricated specimen (low hardness) is higher than the lubricated counterpart (low hardness), in terms of waviness it shows a lower value compared to the lubricated specimen. The lower waviness value suggests that less plastic deformation occurred. This can be seen as less distortion of pearlite matrix occurred for high hardness specimen in Section 4.5, Figure 4.10.

The removal of the graphite film of GCI due to addition of lubricant was reported by Sugishita [150]. The result from elemental analysis (Figure 4.11) shows that more oxide layer (wt% of oxygen) is retained on the unlubricated specimen suggesting that the soybean oil

could disrupt the graphite film as solid lubricant in soybean oil lubricated specimens. The role of an oxide layer in reducing friction and wear rates was reported [50]. This oxide layer could act as a protective layer in decreasing the level of penetration from ball to flat specimens. Therefore, lesser plastic deformation may occur and the accumulation of plastic strain could be reduced.

4.7 Surface morphology

The images of the wear scar of GCI specimen after testing (Figure 4.13) were taken using the optical microscope at the different points (front, back and middle) shown in Figure 4.12a. The surface roughness also were measured similarly (Figure 4.12b). Generally, for the lubricated specimens (for all hardness), the wear mechanisms involved are similar.

The main wear mechanism for all specimens is abrasive wear with some evidence of plastic flow of material on the surface leading to cracks and spalling at Front and Back points. However, as the specimen hardness increased, the amount of abrasive wear is seen to be reduced. This is also shown by smoother surfaces on the Front and Back surfaces of high hardness specimens. The dark region on the unlubricated surfaces could indicate that the graphite was distributed across the surfaces (result is supported by high carbon content in elemental analysis, Figure 4.11). Severe abrasive wear was also observed to occur in the middle point of wear scar (unlubricated specimens). It can be noted that the abrasive wear was the dominant mechanism at the middle of the scar for both lubricated and unlubricated specimens.

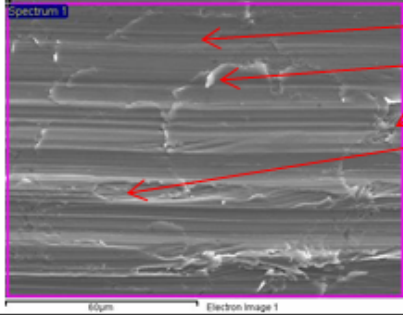
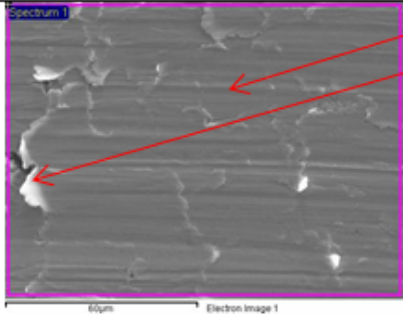
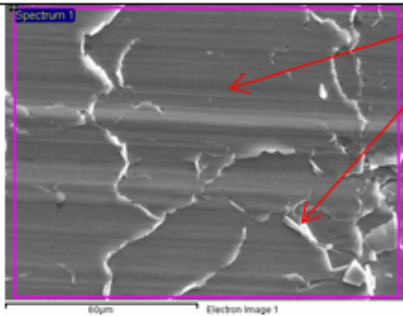
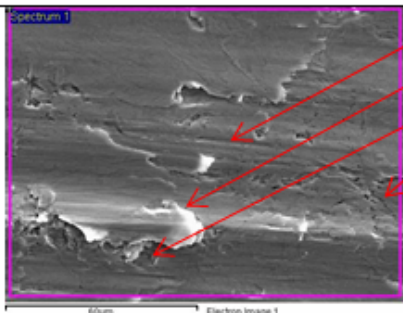
Hardness	Wear Scar Image	Wear Mechanism	Element Analysis		
			Element	Weight %	Atomic %
Low (205.0 HV) Lubricated		abrasion	C	3.77	14.56
		surface fatigue	O	1.43	4.15
		pitting	Si	2.91	4.80
		delamination	P	0.15	0.22
			S	0.00	0.00
			Mn	0.84	0.55
			Fe	90.91	75.56
Medium (221.7 HV) Lubricated		abrasion	C	3.27	12.53
		surface fatigue	O	2.44	7.03
			Si	3.30	5.41
			P	0.05	0.07
			S	0.01	0.01
			Mn	0.67	0.56
			Fe	90.26	74.38
High (248.7 HV) Lubricated		abrasion	C	3.88	14.63
		surface fatigue	O	2.49	7.03
			Si	3.00	4.84
			P	0.00	0.00
			S	0.04	0.05
			Mn	0.69	0.57
			Fe	89.90	72.88
Low (205.5 HV) Unlubricated		abrasion	C	7.13	23.33
		surface fatigue	O	5.27	12.95
		delamination	Si	2.84	3.97
		cracks	P	0.05	0.07
			S	0.05	0.06
			Mn	0.55	0.40
			Fe	84.12	59.23

Figure 4.11: Surface morphology under SEM (1000x) and elemental analysis

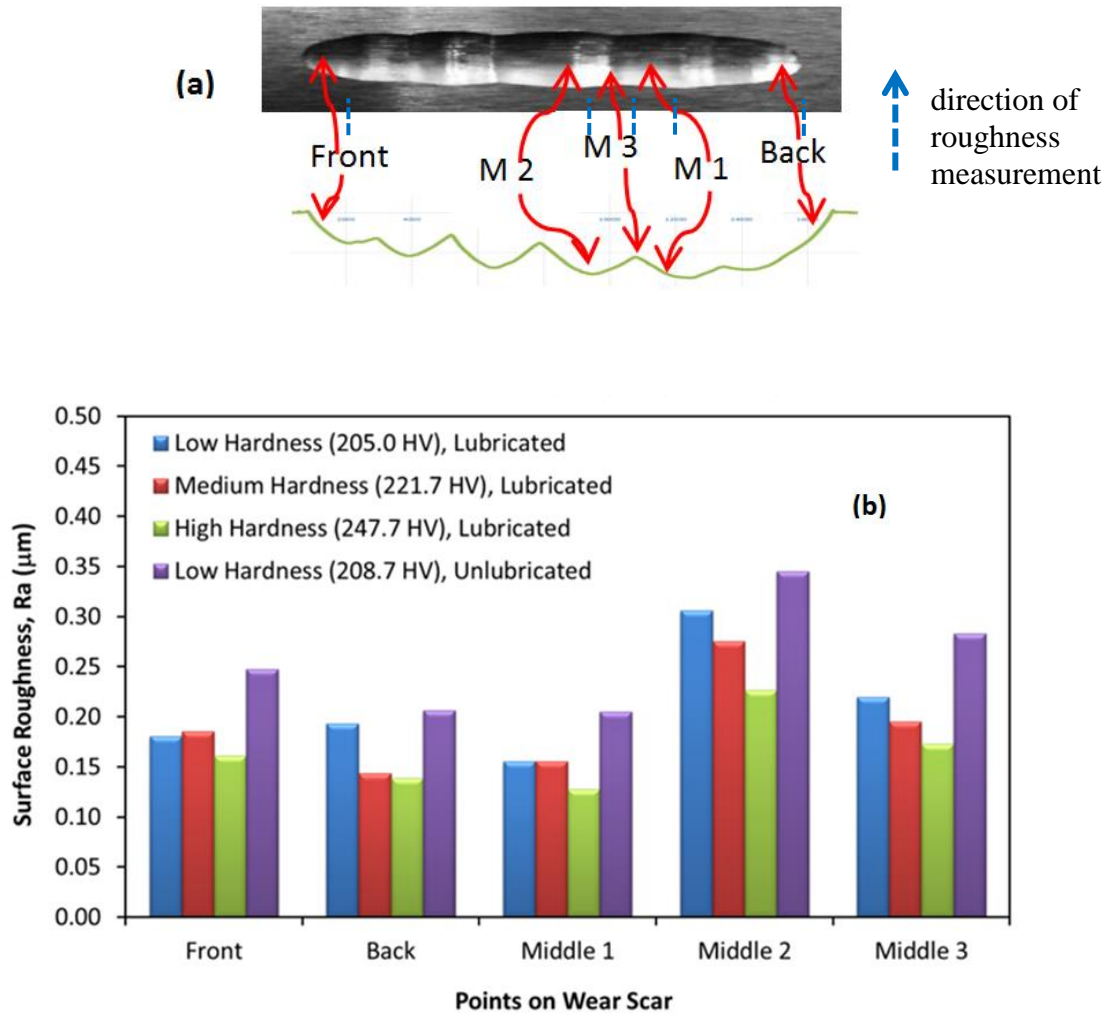


Figure 4.12: (a) Points on Wear Scar where the images and roughness are measured and (b) Surface roughness across wear scar taken at different points based on Figure 4.12a

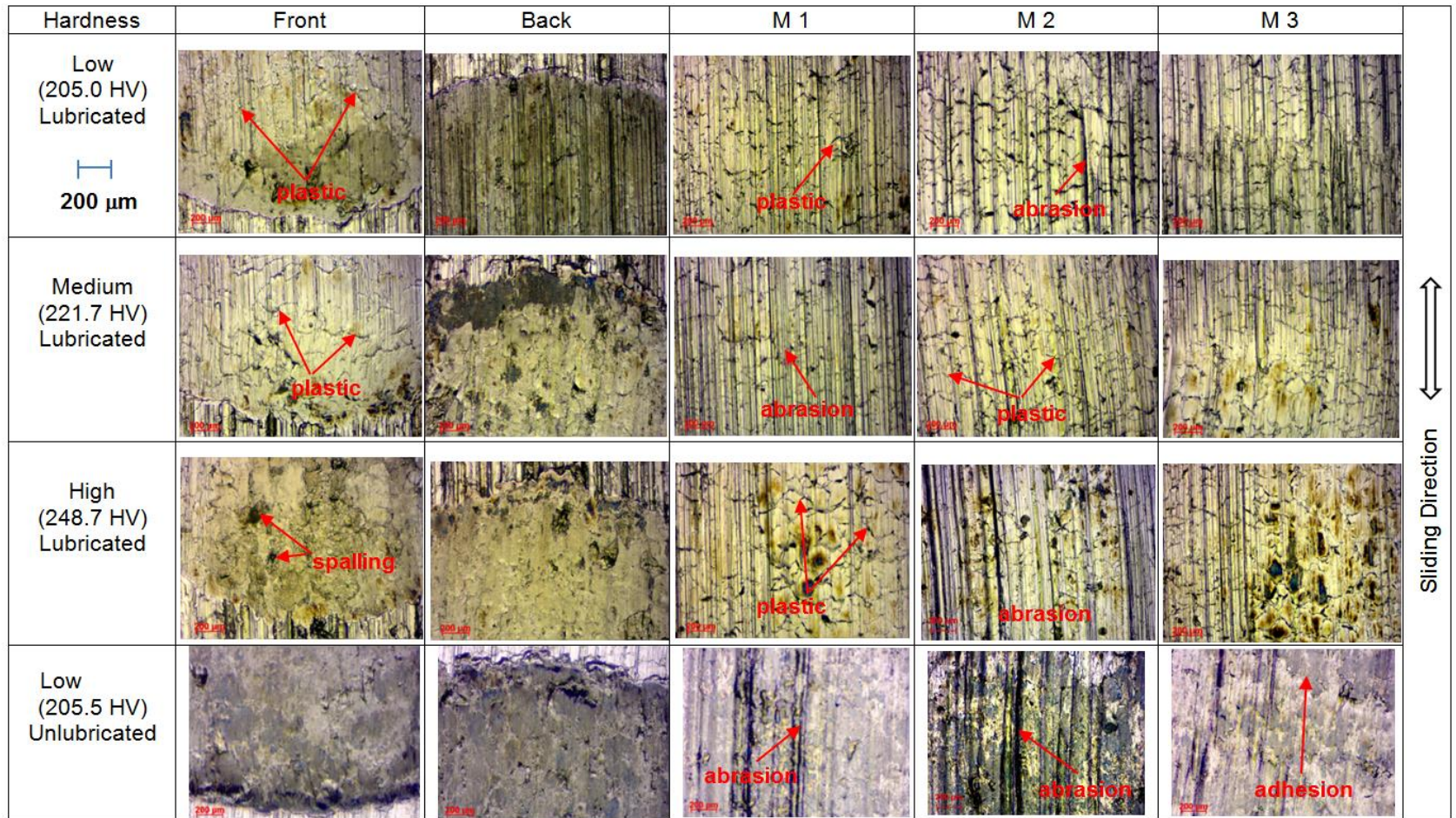


Figure 4.13: Wear scar images under optical microscope taken at different point (Figure 4.12a)

It has been reported that the material hardness and abrasive wear resistance are proportional [157], therefore, a GCI specimen with lower hardness is less resistant to abrasive wear and abrasion marks are more likely to form on the surface. Measurements of surface roughness after these tests (Figure 4.12b) confirmed this relationship (between hardness and abrasion) as reported that surfaces roughness decreases when hardness increases [155] which indicates that less abrasion occurs for harder specimens.

4.8 Elemental analysis

The surface morphology of specimens was inspected under SEM to further investigate the wear mechanism in a smaller area with higher magnification (1000x). EDX analysis also was used in order to analyse the elements on the surface (results were displayed in elements spectrum, Appendix 8 and weight/ atomic percentage, Figure 4.11). Generally, from the SEM images (Figure 4.11) the wear mechanisms found in all specimens were abrasive and surface fatigue, confirming the earlier observations. However, there was no clear evidence on the existence of adhesion wear on the specimens' surface. For lower specimen hardness (lubricated and unlubricated), some delamination, cracks and pitting were also observed.

In the EDX analysis, the level of oxygen present on each specimen surface was recorded to investigate the nature of the oxide layer on the surface. For the lubricated specimens, a higher amount of oxygen was detected on high hardness specimens compared to low hardness specimens. However, the amount of oxygen was found to be highest on unlubricated specimens compared to others because the oxide layer can continue to grow in an air environment after the material removal during sliding process.

Other work has reported that the metal oxide provides a protective layer during sliding [221]. In this study, the higher oxygen value that exists on high hardness specimens (lubricated) suggests that more oxide is retained on the surface compared to the low hardness specimens. This is due to less deformation occurring on the harder material thus preventing the oxide layer from breaking down. However, the lower amount of oxygen present on the lubricated specimen compared to unlubricated specimen suggests that the oxidation process of the lubricant (soybean oil) occurred during the sliding process. This seems particularly likely in this work as soybean oil is an unsaturated fatty acid with doubled bonded carbon atoms in the molecular structure and is therefore more susceptible to oxidation at elevated temperatures [114]. It was also noticed that higher carbon content produced in the unlubricated specimen compared to the lubricated suggests that the graphite is retained on the surface of GCI during the sliding process.

4.9 Conclusions and Summary

From the outcome of the experiments described in this chapter, the following conclusions can be highlighted:

- The use of single bulk hardness values to represent GCI specimen hardness should be avoided. This bulk hardness would misrepresent the friction and wear data as hardness differs very much across the surface of GCI specimens. The difference in specimen hardness of GCI revealed a great influence on the wear and friction test data. Inconsistent wear and friction results may be produced for repeated tests if the hardness characterisation of GCI specimen has not been performed properly. The wide hardness

range that GCI has, could also contribute to the non-uniform wear and friction at contact interface for machine parts made from this material.

- A hardness characterisation of GCI specimens close to the wear scar region prior to a test is very important in producing robust results of wear and friction. A high hardness of material should be selected in producing lower friction and high wear resistance.
- The influence of soybean oil over a wide range of GCI specimen hardness is significant. In terms of lubrication, the soybean oil showed less contribution to wear resistance (about 7%), but rather serves to decrease friction (about 24%) compared to an unlubricated surface.

The findings presented in this chapter have highlighted the importance of controlling the specimen hardness on the intended area of wear scar prior to the test. This is critical in the case of assessing the tribological performance of two lubricants where the differences in friction and wear are very small.

Chapter 5: Investigation into the tribological performance of palm oil and soybean oil in a reciprocating sliding contact at severe contact conditions

In this chapter, the friction and wear performance of pure vegetable oils is presented with mineral oil as a comparison. The performance assessment was carried out using a linear reciprocating sliding point contact with a 100 °C lubricant temperature and initial contact pressure of >1 GPa. Grey cast iron specimens, with tight hardness control in the intended area of wear scars, were used. Surface analysis of the specimens and chemical analysis of oils were performed to support the main experimental results.

5.1 Introduction

Palm oil (PO) and soybean oil (SBO) are the two types of vegetable oil that have the highest consumption of the world's vegetable oil production [222]. These two oils differ in the type and composition of fatty acids they contain. PO has a higher degree of saturated fatty acids compared to SBO. Saturated fatty acids that exist in PO, like palmitic acid and stearic acid, have no double bond in their carbon chain and thus, are less reactive to oxidation. The fatty acids that inherently exist in the vegetable oils make them a suitable candidate for biolubricants. In theory, the fatty acids act as lubricity agents in assisting the formation of protective films. This is due to a polar group (-OH) that is present at one end of the fatty acid molecule and reacts with the substrate surfaces through the mechanism of adsorption.

Based on the literature, most reports on the tribological performance of pure PO and SBO are insufficient to assess their potential use in machines (e.g. internal combustion engines and industrial equipment). Most of the tests were conducted at either room temperature with low applied load and/or by unidirectional test rigs (four-ball-tester and pin-on-disc). These are not applicable for simulating the motion in many machine element contacts, for example, the piston ring and cylinder liner, since the material in the tribo-pair and the nature of motion of the test specimens are not similar.

In view of this, the tribological tests in this chapter were performed on pure palm oil and soybean oil using a reciprocating test rig at a higher load and higher temperature with grey cast iron as the counterface. The friction and wear response of commercial mineral oil lubricated specimens and unlubricated specimens were also measured for comparison. All experiments include the friction and wear test as well as the elemental and oil analyses in this chapter and subsequent chapters were following the methods described in Chapter 3, Section 3.2-3.6.

5.2 Friction analysis

The average COF values for specimens lubricated with PO and SBO are shown in Figure 5.1a in which the MO and unlubricated GCI specimen results are also plotted as a comparison. The final COF value at 60 min uses is also depicted in Figure 5.1b. In general, the COF for lubricated specimens (PO, SBO and MO) started with a low value and increased gradually until it reached steady state. The unlubricated specimens, however, began with a high COF and then slowly reduced throughout the experiment. The palm oil lubricated specimen gave lower COF (0.105) than the soybean oil counterpart. The mineral

oil produced the lowest COF (0.093) while the unlubricated surface recorded the highest COF value. The difference between the COF of PO and MO lubricated specimens is about 11%. The PO lubricant, compared to unlubricated, achieved an improvement of 41% in friction. The result from single variable ANOVA analysis also showed that there is a significant different (P-value < 0.05, Table 5.1) between the COF for PO, SBO and MO.

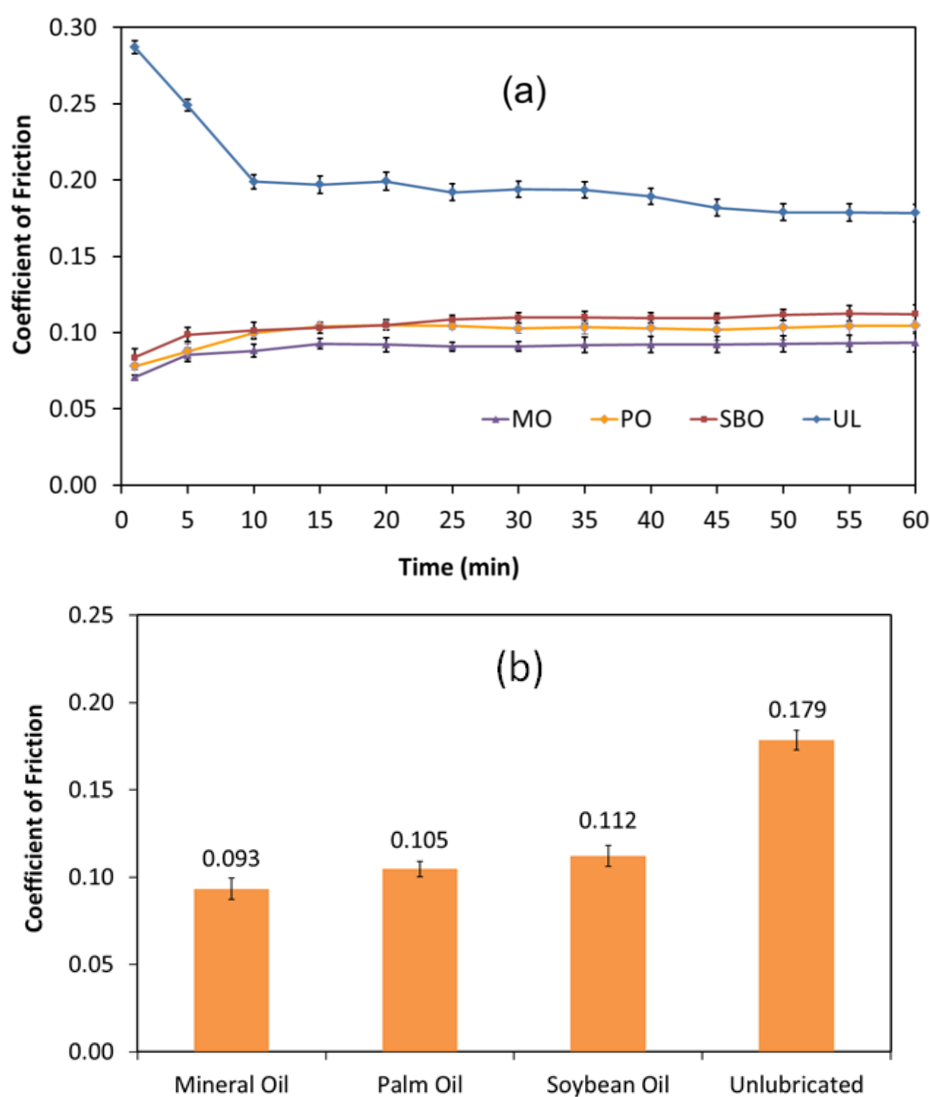


Figure 5.1: (a) Average coefficient of friction versus time for Palm Oil (PO), Soybean Oil (SBO), Mineral Oil (MO) and unlubricated specimen (UL) and (b) Coefficient of friction value at 60 minutes

Table 5.1: ANOVA analysis of COF for PO, SBO and MO lubricated specimens

		<i>Count</i>	<i>Sum</i>	<i>Average</i>	<i>Variance</i>		
Groups	MO	3	0.2799	0.093	3.71E-05		
	PO	3	0.3137	0.105	2.17E-07		
	SBO	3	0.3355	0.112	1.21E-05		
ANOVA	<i>Source of Variation</i>	<i>SS</i>	<i>df</i>	<i>MS</i>	<i>F</i>	<i>P-value</i>	<i>F_{crit}</i>
	Between Groups	0.00052	2	0.000261	15.81483	0.004054	5.143253
	Within Groups	9.89E-05	6	1.65E-05			
	Total	0.000620	8				

The effectiveness of fatty acids as a lubricant is well known [223]. The strong polarity of the fatty acids that exist in vegetable oils contributes to the formation of a mono-molecular layer through the attraction of carboxyl group (COOH) to the metallic surfaces [224]. Therefore, the PO and SBO reduced the COF compared to the unlubricated surface. The COF value for GCI lubricated with PO from this work is close to the COF value for grey cast iron (lower piston ring specimens) lubricated with PO reported by Masjuki (COF = 0.092) [15].

The difference between COF for PO and SBO could be influenced by the composition of saturated and unsaturated fatty acids that exist in vegetable oil. The results of gas chromatography for vegetable oil samples used in this study (Figure 5.2) have confirmed that a higher degree of unsaturated fatty acids exist in the SBO (oleic, linoleic and linolenic acids) compared to the PO counterpart which contains more saturated fatty acids (myristic, palmitic and stearic acids) in the oil samples.

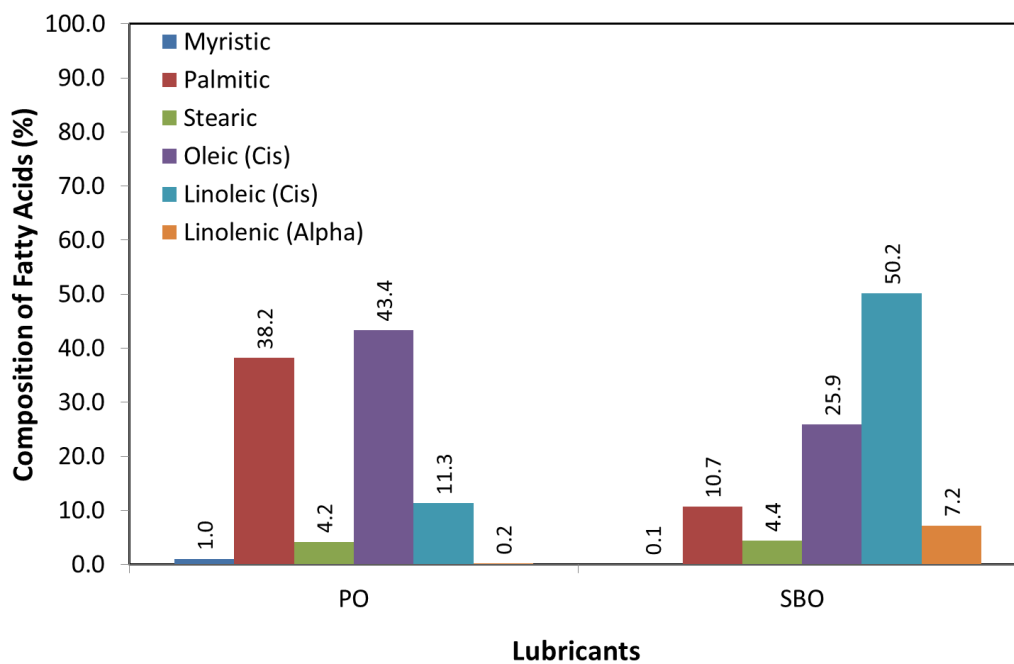


Figure 5.2: Composition of fatty acids for palm oil and soybean oil samples in this study tested by gas chromatography

Type of acid		Chemical structure
Saturated	Myristic (C ₁₄ H ₂₈ O ₂)	
	Palmitic (C ₁₆ H ₃₂ O ₂)	
	Stearic (C ₁₈ H ₃₆ O ₂)	
Unsaturated	Oleic (C ₁₈ H ₃₄ O ₂)	
	Linoleic (C ₁₈ H ₃₂ O ₂)	
	Alpha Linolenic (C ₁₈ H ₃₀ O ₂)	

Figure 5.3: Molecular structure of different type of fatty acids [108].

The COF rises with an increase in unsaturated fatty acids, where stearic acid (saturated acid) exhibits a lower friction coefficient than the oleic and linoleic acid (unsaturated acids) [134]. Saturated fatty acids contain no double bond in their carbon chain (Figure 5.3), thus the molecules can more easily align themselves in a straight chain and are closely packed on the surface to promoting a smooth interaction during motion (as discussed further in Section 5.3 and Figure 5.5). Unsaturated fatty acids, on the other hand, have double bonds and produce a bend in their chain (Figure 5.3), thus they are not as closely packed on the surface. SBO contains more unsaturated fatty acids (oleic and linoleic acids) than PO [114], and thus produces higher friction than PO.

The commercial MO lubricated specimens produced the lowest friction and this is likely due to the fact that its base oil has been treated by additive package that may function in part as a friction modifier. The existence of molybdenum in a spectrochemical analysis for the MO (Table 5.2) suggests that the additive could be from molybdenum-dithiophosphate or dithiocarbamate as these additives can reduce the friction in motor oil [225]. The existence of friction modifier in commercial lubricant is significant in reducing the friction as untreated MO (paraffinic MO) produced higher friction than PO at different normal load [226].

5.3 Wear analysis

Figure 5.4 shows the wear data (average mass loss) of the specimens lubricated with PO, SBO, MO and unlubricated. The unlubricated specimens produced the highest wear with 51.36 mg in mass loss. The soybean oil lubricated specimens has a slightly lower mass loss (42.73 mg) than the palm oil lubricated specimens (45.76 mg), a

difference of about 7%. However, the mineral oil showed superior wear resistance compared to vegetable oils in which the mass loss was 0.65 mg, about a 98% difference than the SBO lubricated specimens. The palm oil improved wear 16% compared to the unlubricated specimens.

Table 5.2: Elements in commercial MO in parts per million (ppm) from a spectrochemical test

Elements	Ca	Zn	P	Mo	B	Mg	Si	Al	Fe
ppm	2825	781	695	167	43	32	3	3	1

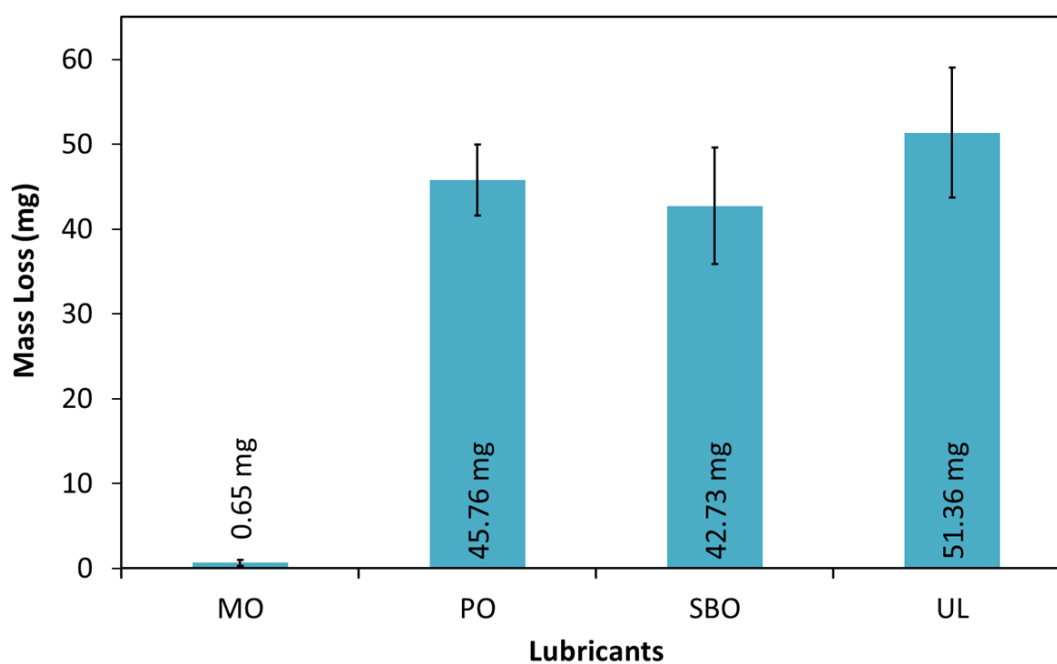


Figure 5.4: Average mass loss of specimens lubricated by palm oil (PO), soybean oil (SBO), mineral oil (MO) and unlubricated specimen (UL)

Table 5.3: Minimum film thickness, h_{\min} and lambda ratio, λ for all lubricants

Lubricant	Pressure-viscosity coefficient (Pa^{-1})		h_{\min} (nm)		λ	
	Initial	Final	Initial	Final	Initial	Final
Mineral Oil	1.39×10^{-8}	1.43×10^{-8}	3.617	3.709	0.018	0.039
Palm Oil	1.17×10^{-8}	1.19×10^{-8}	2.423	2.454	0.013	0.011
Soybean Oil	1.08×10^{-8}	1.09×10^{-8}	2.198	2.249	0.011	0.009

The calculated lambda ratio (λ) for all lubricants (Table 5.3) showed that the lubrication regime was boundary ($\lambda < 1$) (Appendix 6). The film thickness at the end of the test was also calculated based on the values of oil viscosity and surface roughness of specimens after 60 min of use. Slight increases in film thickness for all oils were noticed at the end of each the test due to an increase in viscosity of the oil. The existence of fatty acids play an important role in reducing the wear of material in boundary lubrication thus the specimen lubricated with vegetable oils (enriched with fatty acids) gave lower wear than the unlubricated specimen of GCI. From the results of COF (Figure 5.1b) and wear between PO and SBO, it can be seen that the wear and friction have no relation in vegetable oil lubrication. The lower wear result of specimen lubricated with SBO compared to PO is similar to the four ball test results reported by Syahrullail [9].

At this stage, it is interesting to discuss the theory of the role of the fatty acids' molecular chain structure in influencing both friction and wear as proposed in Figure 5.5. Figure 5.5a illustrates the linear structure of a saturated fatty acid chain that enriches in the PO composition. This linear chain makes it easier it to be aligned in parallel form after a polar group of carboxyl acid (-OH) is adsorbed to the metal surfaces (ball and flat). The straight and parallel arrangement of these carbon chains could promote a smoother

interaction during motion, particularly in the relative direction. However, due to its linearity, it might be possible for the chain to fill the gaps in between and increase metal-to-metal contact. SBO, on the other hand, has a higher degree of unsaturated acid which aligns themselves in a bent chain. Although the bent chain structure promotes higher motion resistance (due to ‘unsmooth’ interaction during motion), on the other hand, it provides better protection in minimising the metal-to-metal contact.

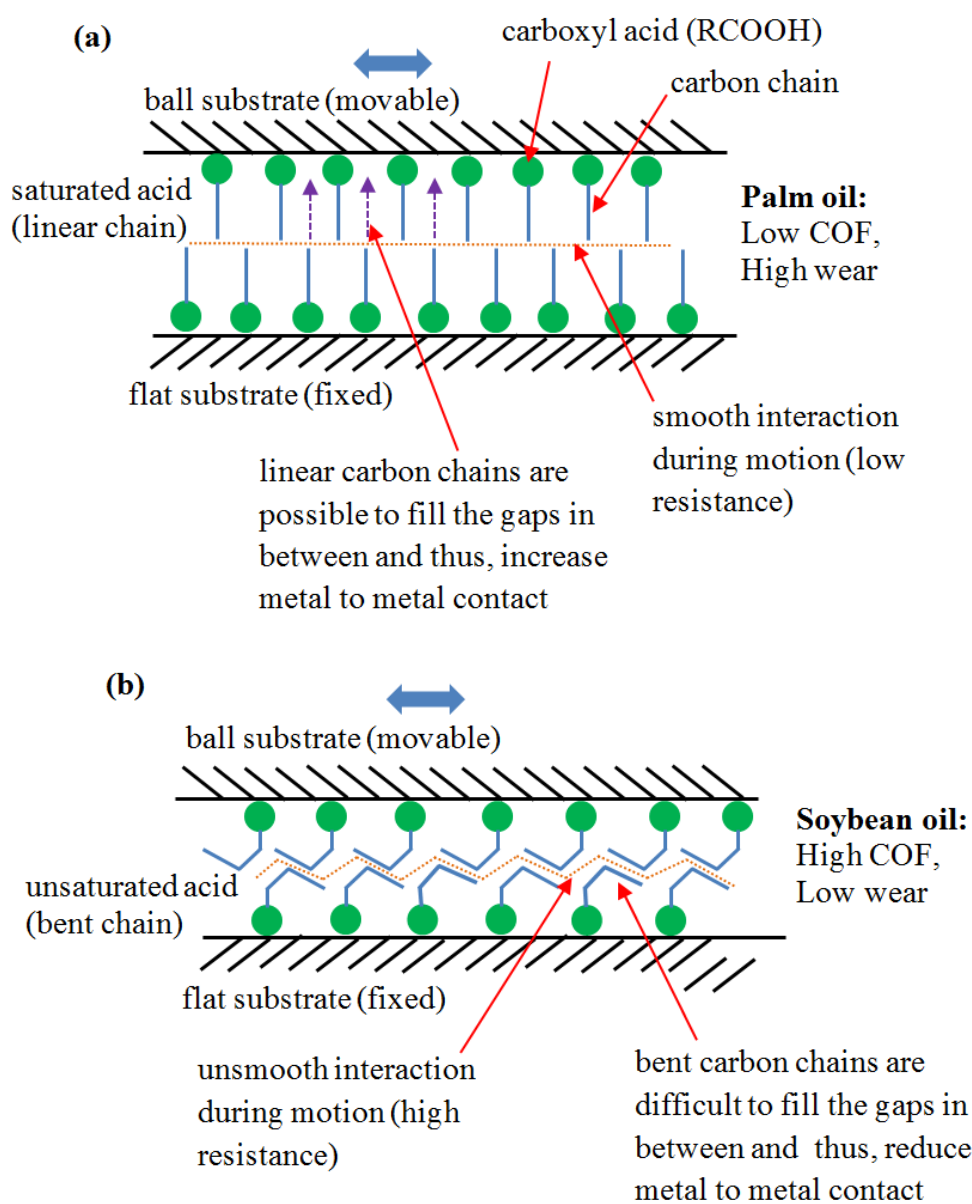


Figure 5.5: The molecular chain structure of (a) saturated and (b) unsaturated fatty acids

Further investigation of surface morphology (also discussed further in Section 5.6 and Figure 5.10) revealed that the PO lubricated specimen has a lower oxygen element than the SBO counterpart. This suggests that less oxide layer is retained by PO to prevent wear due to increasing in metal-to-metal contact. However, the statistical analysis of single variable ANOVA revealed that there is no significant different (P -value > 0.05 , Table 5.4) between the wear of the specimens lubricated with PO and SBO. Although it was reported that the untreated MO (paraffinic oil) produced lower wear than PO, however, the difference is 20% [226]. This indicates that the fully formulated MO used in this study has been improved by its manufacturer especially its wear protection characteristics.

Table 5.4: ANOVA analysis of mass loss for PO and SBO unlubricated specimens

		<i>Count</i>	<i>Sum</i>	<i>Average</i>	<i>Variance</i>		
Groups	PO	3	137.28	45.76	16.3291		
	SBO	3	128.19	42.73	37.4544		
ANOVA	<i>Source of Variation</i>	<i>SS</i>	<i>df</i>	<i>MS</i>	<i>F</i>	<i>P-value</i>	<i>F_{crit}</i>
	Between Groups	13.77135	1	13.7713	0.513782	0.51378	7.70864
	Within Groups	107.567	4	26.8917			
	Total	121.3383	5				

The superior wear resistance performance exhibited by the commercial MO over vegetable oils (98% difference) in this study could be attributed to the existence of an additive package that includes an anti-wear agent, zinc dialkyl dithiophosphate (ZDDP). This is shown by the detection of zinc in spectrochemical analysis (Table 5.2) and elemental analysis (as discussed further in Section 5.6, Figure 5.10). It has reported that at mild contact conditions (room temperature and 3.0 MPa contact pressure) the wear of palm oil lubricant was better than mineral oil [15], however, at severe contact conditions (i.e. this study) the wear when palm oil is the lubricant gave a much higher value than mineral

oil (more than forty orders of magnitude). This is due to the adsorption mechanism of the polar group of fatty acid (-OH) molecules in the vegetable oil in reducing metal-to-metal contact being only effective at low temperature and low load [224].

Further examination of the worn surfaces of the PO and SBO lubricated specimens suggests that a breakdown of lubrication occurred which led to severe wear. This is supported by the presence of a burn mark (visible under the optical microscope and as discussed further in Section 5.6, Figure 5.9) which is could be caused by frictional heat from metal-to-metal contact on the PO and SBO specimens. However, this appearance was not reported in normal (not severe) contact conditions [15]. To support this suggestion, the surface temperature obtained for specimens lubricated with the vegetable oils was estimated (Appendix 9) using test parameters, material properties and the COF [206]. The total contact temperature of the soybean oil lubricated surface was about 182 °C and 177 °C for PO lubricated specimens. The colour of burn marks on the worn specimens was then compared with the steel tempering colours [227] (Figure 5.6). As a result, it showed good agreement between the surface temperature and the tempering colour temperature. The brownish colour (burn marks) on the worn specimens of PO and SBO (Figure 5.9) were close to the colour of tempered steel at about 204 °C (Figure 5.6). This strengthened further the suggestion that the presence of burn marks on the worn specimens was due to the frictional heating caused by the breakdown of lubrication.

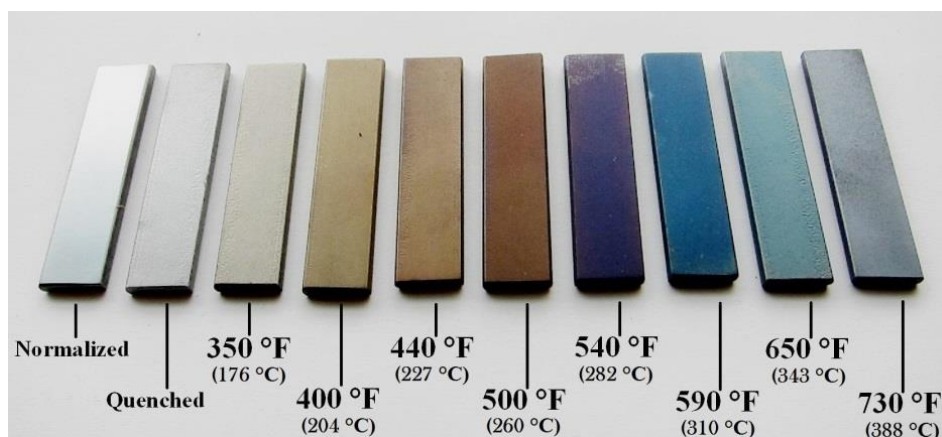


Figure 5.6: Tempering colours of steel [227]

5.4 Surface topography and waviness analysis

An indication of the typical wear scar appearance for all specimens after 60 min of testing is presented in Figure 5.7a. The primary profile and waviness measurement value are plotted in Figure 5.7b. The wear scar of MO (Figure 5.7a) has a narrow width and a smoother profile than the others. Compared to normal contact conditions test performed by Masjuki [15], at severe contact conditions, the vegetable oil lubricated specimens and unlubricated specimens in this study produced similar ‘unsmooth’ appearance (wavy-shaped scar). The unlubricated specimen has the deepest wear scar depth. In terms of surface waviness, the PO lubricated specimen produced the highest value ($W_a = 41.43 \mu\text{m}$) compared to SBO and unlubricated counterparts. The MO lubricated specimen produced the lowest surface waviness ($W_a = 1.40 \mu\text{m}$).

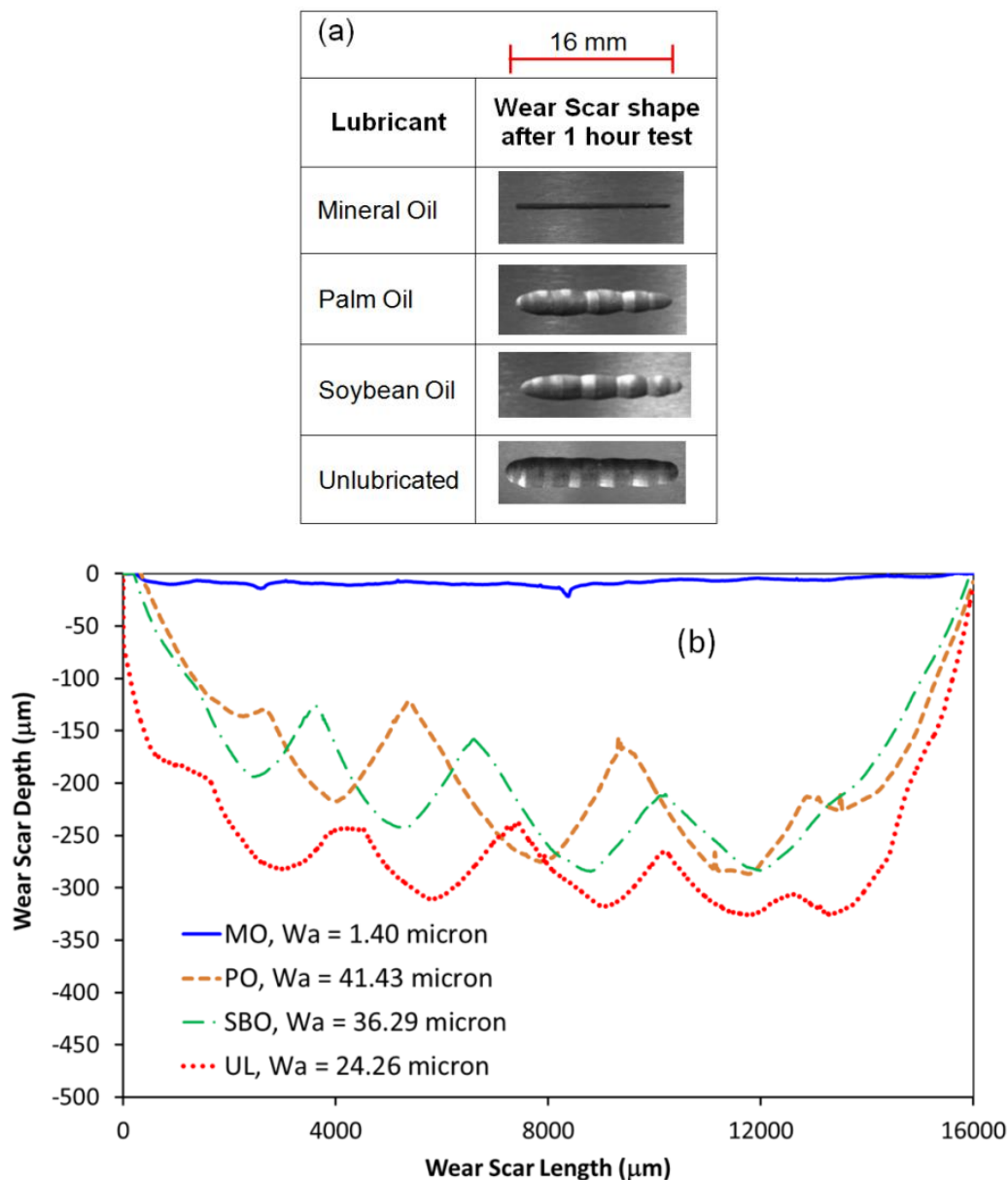


Figure 5.7: (a) Wear scar appearance and (b) Primary profile of specimens lubricated with mineral oil (MO), palm oil (PO), soybean oil (SBO) and unlubricated specimen (UL)

The formation of a wavy-shaped scar on unlubricated specimens and specimens lubricated with vegetable oils suggest that the shakedown limit was exceeded or plastic ratcheting occurred during the sliding process. This is caused by the high contact pressure that was applied. Due to higher normal load applied in this study, the contact condition entered the plastic ratcheting region [218] and produced accumulation of deformed material in the form of bulges (as discussed in Section 4.5 and Figure 4.7 – 4.9). However,

the relatively smaller and smoother wear scar produced by the MO lubricated specimens suggests that the anti-wear additive (ZDDP) that exists in the commercial MO performed very well in reducing the wear and preventing deeper penetration of the ball into the flat specimen. A lower degree of penetration could be equivalent to a contact condition with lower applied load, which may prevent the contact from passing the plastic shakedown limit and entering the ratcheting region. Although the PO lubricated specimen produced lower COF than the SBO and unlubricated counterpart, its surface waviness value showed the highest value ($W_a = 41.43 \mu\text{m}$). This shows that the COF was not significantly dominated by the surface waviness factor in the existence of vegetable oils as a lubricating agent.

5.5 Surface roughness analysis

The average surface roughness (Figure 5.8b), R_a , of specimens across the wear scar was measured at different points (Figure 5.8a). The MO lubricated specimen showed the lowest and most consistent surface roughness along the wear scar compared to vegetable oils and unlubricated counterparts. The unlubricated specimen demonstrated the highest roughness while the PO lubricated specimen produced lower roughness than the SBO. Points M2 and M3 were found to contribute rougher surfaces than other areas for PO, SBO and the unlubricated specimen. This suggests that both points (M2 and M3) experienced higher abrasive wear due to the debris that accumulated in the groove at point Middle 2. The surface roughness results across the wear scar correspond to COF values for all specimens as higher surface roughness may contribute to higher COF [228]. In this study, the lower surface roughness exhibited by the MO lubricated specimen has produced lower COF.

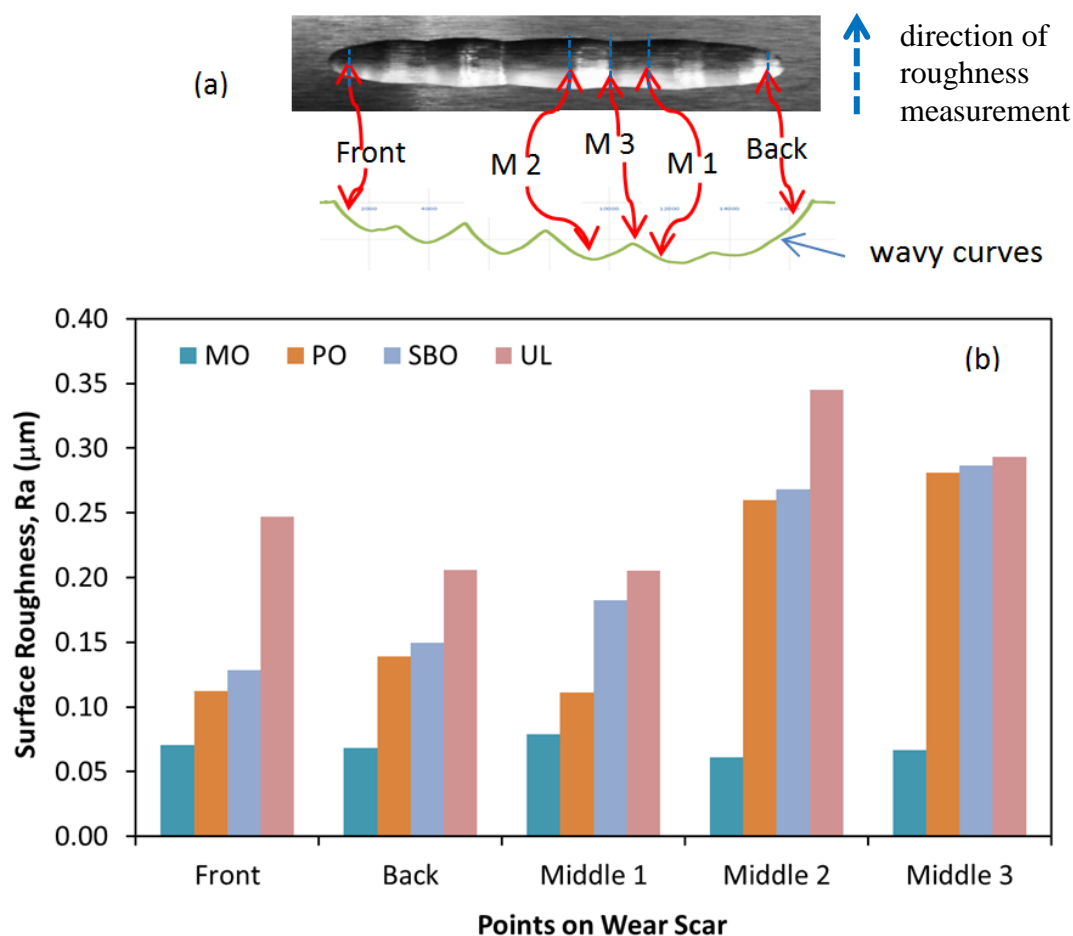


Figure 5.8: (a) Points on wear scar for inspection and (b) Surface roughness measured at different points

5.6 Surface morphology and elemental analysis

The surface morphology of wear scars under an optical microscope (Figure 5.9) after 60 min of testing are depicted at different points (Front, Back, M1, M2 and M3) in Figure 5.8a. The specimen lubricated with MO exhibited a similar appearance at each point with some pitting and spalling especially at points Front and Back which indicate more damage at the stroke ends. The same tendency has also been seen where more severe scuffing damage occurred at the stroke ends in reciprocating pin-on-pin for a fuel lubricated test [229]. In a reciprocating sliding test, the speed turns to minimum at stroke ends before changing the direction. The lower velocity at stroke ends causes a lower film

thickness and thus promotes scuffing. Further investigation of the MO lubricated surface by SEM (Figure 5.10) confirmed the existence of spalling (delamination) and cracks suggesting that the wear mechanism involved is fatigue wear.

For the specimens lubricated with PO and SBO, the main wear mechanism was found to be abrasive with some evidence of plastic deformation on the surface (Figure 5.9), especially at the stroke ends (Front and Back). The abrasive marks were smaller at points Front and Back for PO and SBO specimens compared to the middle points. This probably suggests that the wear particles accumulated at the middle points of PO and SBO specimens due to the wavy-shape of the wear scars, and thus contributed to third body abrasive wear. Some burn marks were also found on specimens lubricated with PO and SBO which suggests that high frictional heating occurred, probably due to breakdown of lubrication (Figure 5.9). The wear mechanism for the unlubricated specimens was found to be abrasive and fatigue wear, with the existence of a dark region on the surface suggesting that a graphite layer was formed.

The elemental analysis of lubricated specimens by EDX is presented in Figure 5.10. It was found that the oxygen element in the PO specimen was slightly lower than the SBO. A higher amount of oxygen and carbon was also noted in the unlubricated specimen. The specimen lubricated with MO has a higher content of sulphur (1.36 wt%) and phosphorus (0.72 wt%) compared to the unlubricated specimen. A higher percentage of oxygen and a small amount of zinc (0.90 wt%) were also detected at the MO specimen's surface.

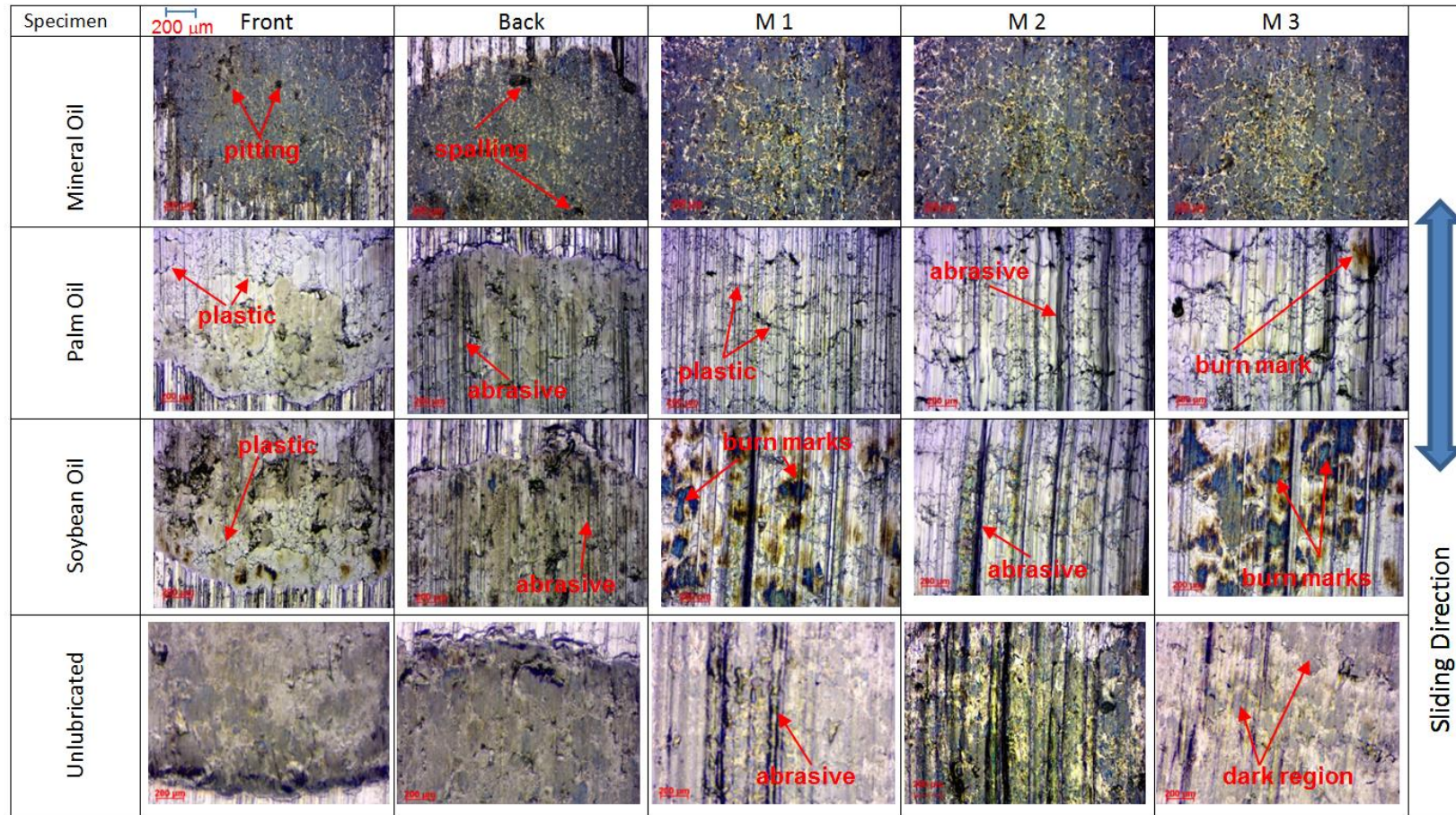


Figure 5.9: Optical microscope images of wear scar for all lubricants (20X magnification)

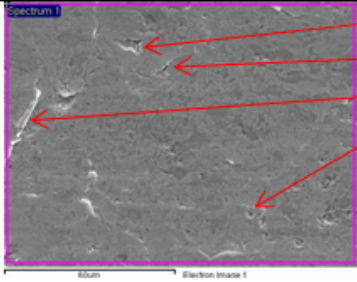
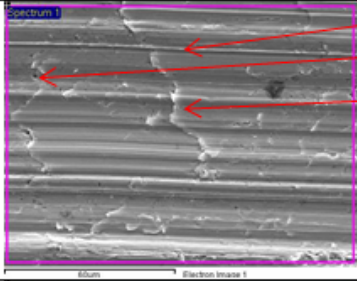
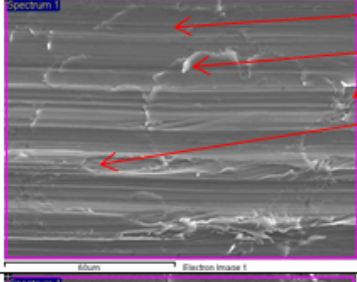
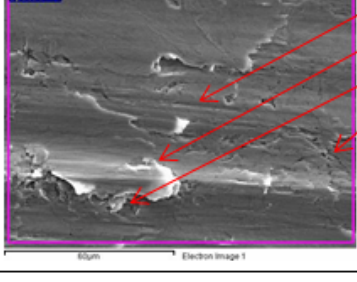
Lubricant	Wear Scar Image	Wear Mechanism	Element Analysis		
			Element	Weight %	Atomic %
Mineral Oil		delamination	C	3.38	10.96
		cracks	O	10.43	25.58
		surface fatigue	Si	2.70	3.77
		pitting	P	0.72	0.91
			S	1.36	1.66
			Mn	0.73	0.52
			Fe	79.80	56.06
Palm Oil		abrasion	C	3.79	14.67
		pitting	O	1.17	3.39
		surface fatigue	Si	3.29	5.44
			P	0.10	0.15
			S	0.04	0.06
			Mn	0.66	0.55
			Fe	90.95	75.73
Soybean Oil		abrasion	C	3.77	14.56
		surface fatigue	O	1.43	4.15
		pitting	Si	2.91	4.80
		delamination	P	0.15	0.22
			S	0.00	0.00
			Mn	0.84	0.71
			Fe	90.91	75.56
Unlubricated		abrasion	C	7.13	23.33
		surface fatigue	O	5.27	12.95
		delamination	Si	2.84	3.97
		cracks	P	0.05	0.07
			S	0.05	0.06
			Mn	0.55	0.40
			Fe	84.12	59.23

Figure 5.10: Scanning electron microscopy (SEM) images (1000X magnification) and elemental analysis of wear scar for all lubricants

The higher percentage of oxygen on the surface of the SBO specimen compared to the PO specimen suggests that more oxide layer is retained on the surface, so reducing the metal-to-metal contact, thus lower mass loss is produced in the SBO specimen. A similar reason could be applied to the specimen lubricated with MO in which a higher level of oxygen is

detected, suggesting that more oxide layer exists to prevent the metal-to-metal contact [221]. However, the lower amount of oxygen found in specimens lubricated with PO and SBO compared to the unlubricated specimen could be due to absorption of oxygen in the oil as vegetable oil is susceptible to oil oxidation [114]. The higher amount of carbon in the unlubricated specimen could be due to the formation and distribution of a graphite layer during the sliding process. The higher content of phosphorus in the MO specimen compared to others suggests that this element came from the MO (Table 5.2). The existence of zinc in the MO specimen suggests that the additive package contains this element. The most probable additive related to zinc is the anti-wear additive, ZDDP.

5.7 Acid number analysis

Figure 5.11 shows the acid number (AN) measurement result that characterises the lubricant degradation for MO, PO and SBO before and after the test. For fresh oil, the PO has a lower AN value than SBO while MO has the highest AN. It is clearly seen that all used oil after the test produced higher AN than new oil. The difference of AN for new and used oil (after wear test) is lowest for MO (0.16 mgKOH/g) than PO (0.21 mgKOH/g) and SBO (0.30 mgKOH/g). The AN values for all oil samples after rotary pressure vessel oxidation test (RPVOT) were greatly increased.

The higher AN value exhibited by SBO than PO suggests that the SBO sample used in this study is more acidic than the PO sample. The AN for MO in this study (2.24 mgKOH/g) is near to the UFA Super Engine Oil (15W-40) at 2.8 mgKOH/g [230]. Higher AN in MO compared to vegetable oil could be attributed to the existence of ZDDP additive as the ZDDP was found to increase the AN for base oil [231]. An increase in AN for the used

oils (both from wear test and RPVOT) in Figure 5.11 indicate that the oils have been undergoing a process of oxidation during the wear test as acids are formed during the oil oxidation process. The highest difference of AN before and after testing for SBO (0.30 mgKOH/g) compared to other oil showed that the SBO is more vulnerable to oxidation due to the higher unsaturation fatty acids (oleic, linoleic and linolenic acids) that exist in SBO. The lower oxidation stability of SBO could lead to higher COF as oil oxidation could increase the friction force [232].

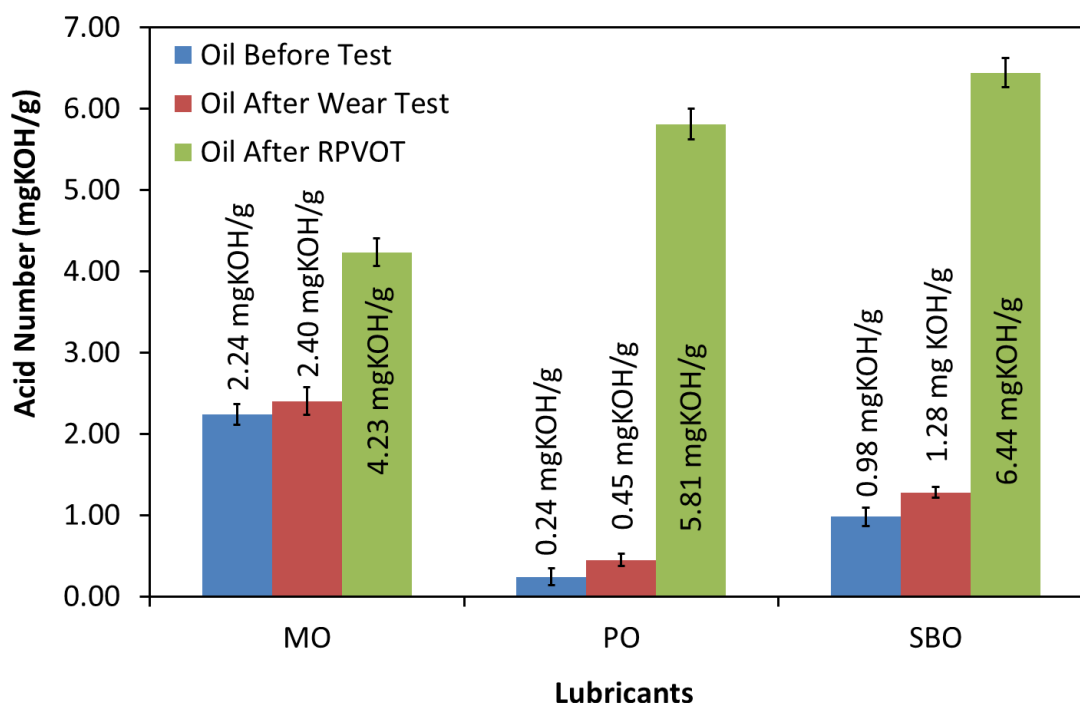


Figure 5.11: Acid Number for Mineral Oil (MO), Palm Oil (PO) and Soybean Oil (SBO) for fresh and used oil

5.8 Oil viscosity analysis

The dynamic viscosity for fresh oil, used lubricants (from wear test rig) and oil samples after RPVOT test were measured at 40 °C and 100 °C (Figure 5.12). For fresh oil at

100 °C, the MO showed highest viscosity (12.56 cP) followed by PO and SBO. A similar trend of viscosity was found for all fresh oils at 40 °C. All lubricants demonstrated decreasing viscosity at higher temperature, 100 °C compared to 40 °C. However, the vegetable oils showed more resilience to viscosity changes due to temperature than MO. This is due to the vegetable oils having a higher viscosity index than MO. It was shown by RPVOT samples that an increase in oil oxidation could increase the viscosity. Although the AN for used oils (from the wear test rig) in this study have increased which suggests they underwent an oxidation process, the viscosity difference for fresh and used oil is not significant. This shows that the oil oxidation process occurring during the test was not very severe.

The higher wear result on PO and SBO lubricated specimens compared to MO (Figure 5.4) could be due to the lower lubricant viscosity that they have. It was reported that with lower viscosity oils, piston rings also exhibited higher wear rates [233]. The viscosity result of PO and SBO could also be the possible reason to support why the PO specimen has lower COF than SBO (Figure 5.1b). The Stribeck curve shows that in the boundary lubrication regime [212], lower viscosity (with same speed and load) of lubricant causes higher friction. In this study, the PO has higher viscosity than SBO and therefore produced lower COF.

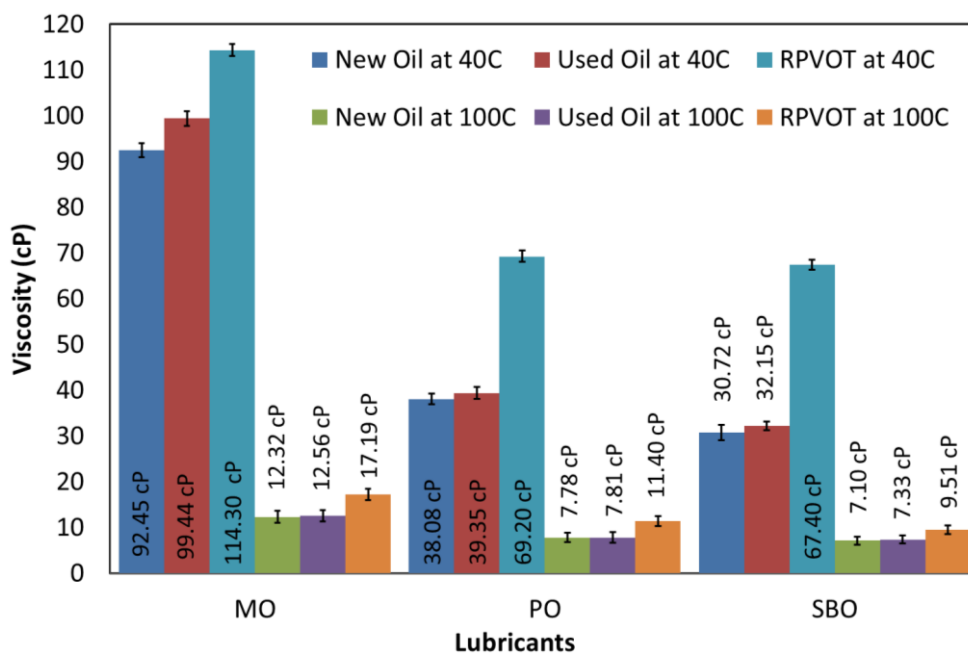


Figure 5.12: Viscosity of Mineral Oil (MO), Palm Oil (PO) and Soybean Oil (SBO)

5.9 Oxidative stability analysis

Figure 5.13 depicts the oxidation stability result which shows how fast the MO, PO and SBO oxidised in pressurised oxygen in a pressure vessel. Based on the oxidation time and the obtained peak pressure value, the MO has far greater stability than the vegetable oils. This could be due to the existence of anti-oxidant additive such as ZDDP in the MO, thus, prevent the rapid oxidation. The PO was more stable in oxidation than SBO. The lower oxidation time of SBO compared to PO is due to the existence of higher unsaturated fatty acids which may promote oxidation. The inferior performance of PO and SBO in the oxidative stability test compared to commercial MO supports the suggestion that a limitation in the vegetable oils' tribological performance is because oxidised oil could increase the wear [11].

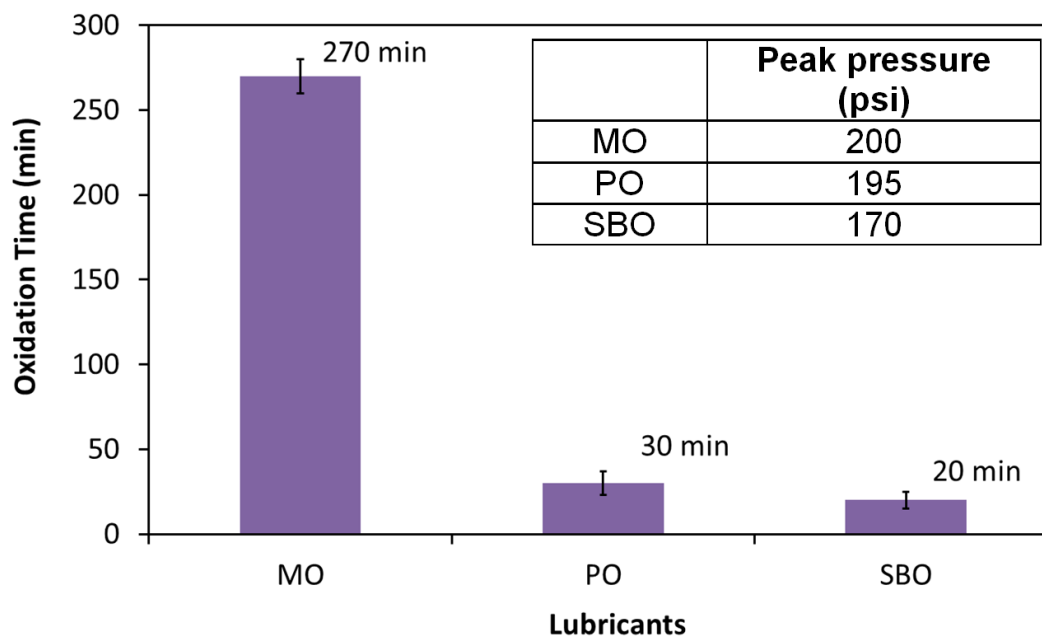


Figure 5.13: Rotary pressure vessel oxidation test (RPVOT) result for Mineral oil (MO), Palm Oil (PO) and Soybean Oil (SBO)

5.10 Conclusions and Summary

From the results of experiments conducted for vegetable oils at extreme condition, the following conclusions can be drawn:

- Pure palm oil exhibited lower friction coefficient than soybean oil, while soybean oil showed better performance of wear protection than palm oil. This showed that friction and wear is not directly related in vegetable oils lubrication.
- The lower viscosity and oxidative stability that the vegetable oils have could contribute to their poor wear resistance. At severe contact conditions, the vegetable oils are likely to breakdown and consequently produce a wavy-shaped profile of wear scar which indicates that the contact has entered the plastic ratcheting region. However, in terms of friction performance, pure palm oil is a potential base fluid for

biolubricant as it differs about 11% higher than commercial mineral engine oil (15W40).

The direct use of natural vegetable oils as a lubricant in automotive engine could potentially cause catastrophic damage to engine components. The superior tribological performance shown by the commercial mineral engine oil compared to vegetable oils (wear differ in 98%), especially in preventing wear, has resulted in an idea to investigate the friction and wear performance of the blending for these two oils (discussed in Chapter 6). This could reduce the dependency on mineral base lubricants, even if only by a few percentage points.

Chapter 6: Friction and Wear Performance of Vegetable Oil-Mineral Oil Blend in a Severe Reciprocating Sliding Contact

Following on from the discussion presented in Chapter 5, the work described here aims to build further understanding of the wear and friction response of a mineral oil-vegetable oil blend. The two vegetable oils considered (palm oil and soybean oil) were selected as they are produced in the highest in volumes globally [207]. These oils were blended individually with a commercial mineral engine oil (15W40) at a 1:1 ratio by volume. This ratio was chosen so that any domination of one oil over the other can be clearly seen. A blend of palm oil and soybean oil at the same ratio was also performed as comparison. The surface morphology was assessed and both surface elemental analysis and chemical analysis of the oil were also performed.

6.1 Introduction

It has been reported that it is feasible to blend vegetable oils together [140, 234] or with mineral oil [20, 22, 23] to modify their characteristics and performance. A blend of oil can be created by mixing of two or more oils to achieve the anticipated performance, for example, a mix of two vegetable oils (palm oil and olive oil) shared the fatty acid composition and physicochemical properties like melting point, viscosity and iodine value which is related to the blend ratio [140]. This indicates that in oil blends, the value of fatty acids and physicochemical properties are possible to be adjusted so that the value is in-between of the value of their pure oil. It has also been reported that an addition of a vegetable oil into mineral oil may cause reduction in the viscosity and of additive elements in the blended oil relative to the mineral oil [22].

From the experimental results in Chapter 5, the commercial mineral engine oil was found to greatly outperform the vegetable oils in terms of wear resistance, friction, and oxidation stability. However, this oil is relatively expensive and less environmentally friendly compared to pure vegetable oil. By blending both of these oils, the cost of lubricant can be reduced and furthermore the total dependency on petroleum base stock can also be decreased. The superior performance of mineral engine oil especially in wear resistance over vegetable oils has led to an interest in understanding on its tribological response, after an amount of vegetable oil is added into it.

Although the tribological performance of mineral oil-vegetable oil blends has been considered before, those studies were limited to particular test rigs (either four ball tester or pin-on-disc) and testing at room temperature [20, 22, 23]. Thus, a different means of testing is still needed especially involving performance closer to the contact motion found in real applications (for example an internal combustion engine systems). In view of this, a combination of a reciprocating sliding test rig with grey cast iron specimens performed at a higher temperature was applied to these oil blends. All experiments include the friction and wear test as well as the elemental and oil analyses in this chapter were following the methods described in Chapter 3, Section 3.2-3.6.

6.2 Friction Analysis

Figure 6.1a shows the coefficient of friction (COF) profile versus test duration (60 minutes) and Figure 6.1b highlights the average value of COF at the end of the test. Most lubricants started with a low initial COF which then increased gradually before reaching a steady state value at about 30 minutes. These COF trends are close to those categorised by

Blau [47] who suggested that this running-in behaviour might be due to the removal of lubricious contaminants from the contact surface [47] and disruption of oxide layer on the contact surface thus increasing the metal-to-metal contact [50].

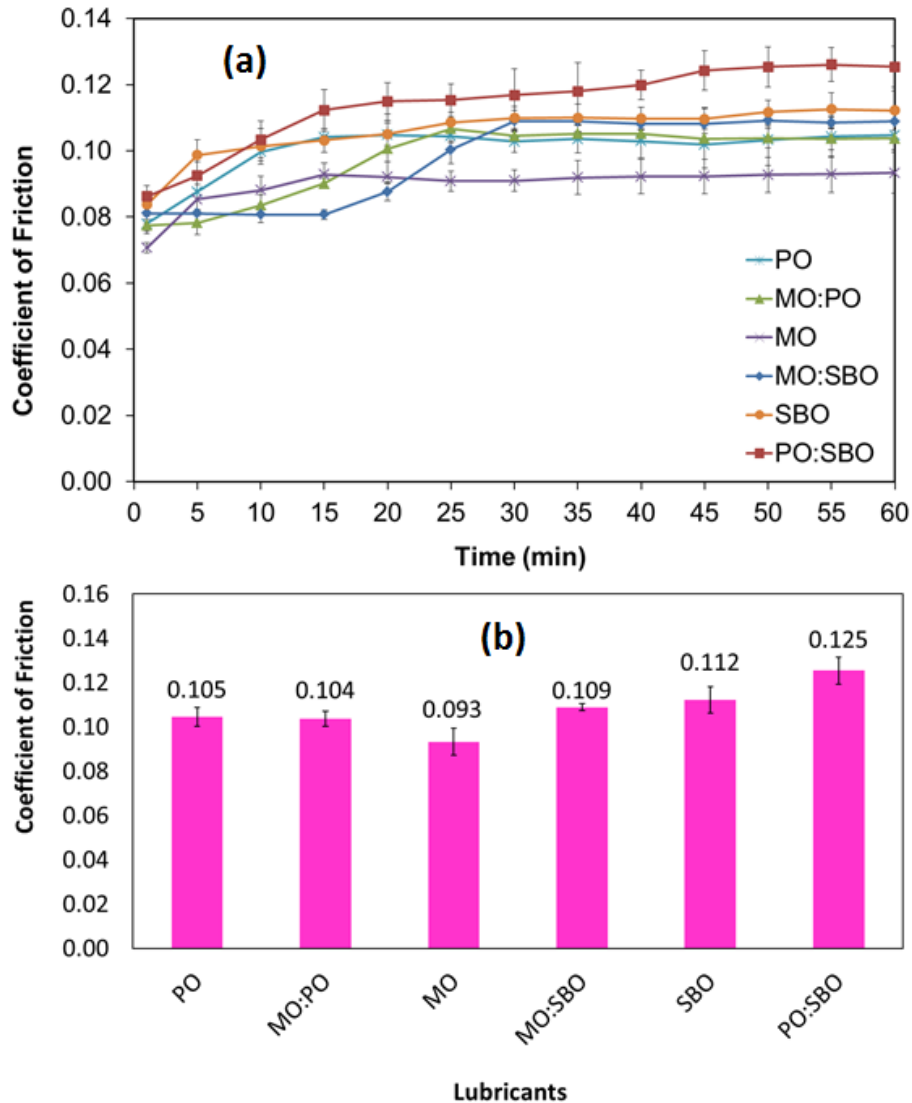


Figure 6.1: (a) Average Coefficient of Friction profile with experiment time and (b) Average Coefficient of Friction at 60 min. The error bars represent the standard deviation of the test data.

At the end of the test, the MO exhibited the lowest COF (0.093) while the blend of PO and SBO in 1:1 ratio (PO:SBO) produced the highest COF (0.125). The COFs for a blend of MO and vegetable oil generated a value in-between their pure oil states. Only a small

reduction is noted compared to their pure state. A blend of MO and PO (MO:PO) yielded a COF of 0.104, 1% less than pure PO (COF = 0.105). A slight improvement of COF was also found in a blend of MO and SBO (MO:SBO), in which the COF (0.109) only reduced 3% from pure SBO (COF = 0.112). A significant difference between the mean of the data for all lubricants in Figure 6.1b was also found through the ANOVA analysis (P-value < 0.05, Table 6.1).

Table 6.1: ANOVA analysis of COF for all lubricants

		<i>Count</i>	<i>Sum</i>	<i>Average</i>	<i>Variance</i>		
Groups	PO	3	0.3137	0.105	2.17E-07		
	MO:PO	3	0.3124	0.104	6.22E-06		
	MO	3	0.2799	0.093	3.71E-05		
	MO:SBO	3	0.3267	0.109	1.54E-08		
	SBO	3	0.3355	0.112	1.21E-05		
	PO:SBO	3	0.3761	0.125	0.000181		
ANOVA	<i>Source of Variation</i>	<i>SS</i>	<i>df</i>	<i>MS</i>	<i>F</i>	<i>P-value</i>	<i>F_{crit}</i>
	Between Groups	0.00052	2	0.00026	15.8148	0.00405	5.14325
	Within Groups	9.89E-05	6	1.65E-05			
	Total	0.00062	8				

Table 6.2 shows the spectrochemical analysis of all the lubricants tested in this study and expresses the existence of elements in parts per million. There are a number of elements abundantly detected in the MO (calcium, zinc, phosphorus, molybdenum, boron and magnesium) relative to other oils. This suggests that, as expected, it has been treated by an additive package which comprises of these elements. The lowest COF exhibited by the MO specimens could be influenced by a friction modifier in the oil, typically molybdenum-dithiophosphate or dithiocarbamate, as these class of additives aim to reduce the friction in engine oil [225].

Table 6.2: Elements detected in lubricants in part per million (ppm) from spectrochemical analysis

Elements	Lubricants					
	PO	MO:PO	MO	MO:SBO	SBO	PO:SBO
Calcium	0	1341	2825	1356	25	16
Zinc	1	389	781	393	3	3
Phosphorus	0	327	695	359	59	30
Molybdenum	0	80	167	80	0	0
Boron	2	20	43	20	1	1
Magnesium	0	6	32	13	17	8
Silicon	3	20	3	5	2	3
Aluminium	0	2	3	2	0	0
Iron	0	2	1	1	0	0
Sodium	2	7	0	7	3	3
Lead	0	1	0	1	0	0
Barium	0	1	0	0	0	0

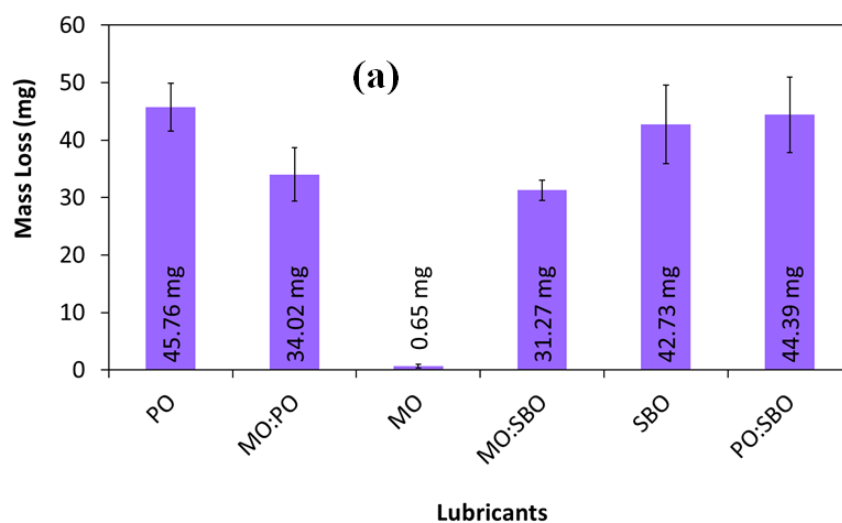
The analysis shown in Table 6.2 demonstrates that the composition of the elements that was detected in MO (calcium, zinc, phosphorus, molybdenum, boron and magnesium) was diluted into about 50% for vegetable oils-mineral oil blend (MO:PO and MO:SBO). This shows that the influence of the friction modifier (from molybdenum [225]) in the MO-vegetable oils blend have deteriorated. Thus, the COF for oil MO:PO and MO:SBO were recorded to be in-between their pure oil states.

It is also suggested that the base oil of vegetable oil influences the performance of the blend, for example, the MO:PO blend produced a lower COF than MO:SBO as the pure PO produced a lower COF than a pure SBO. The PO comprises more saturated fatty acids (containing no double bonds) than SBO, thus, it could be easier for the molecules to align themselves in a closely packed straight chain, on the metal surface. Thus, a smoother

transition during motion was created (as proposed in Figure 5.5, Chapter 5) in the MO:PO oil than MO:SBO.

6.3 Wear Analysis

Figure 6.2a shows the average mass loss of the specimens after 60 minutes of testing for each lubricant and their related wear scars. From the minimum film thickness (h_{\min}) estimation and the lambda value (λ), the lubrication regime for all lubricated specimens was boundary (Table 6.3). The highest average mass loss recorded was from the PO specimens (45.76 mg) while the MO specimens had a superior wear resistance with a lowest average mass loss of 0.65 mg. The specimens lubricated with MO and PO (MO:PO) generated a wear scar of a size in-between their pure oil states (mass loss = 34.02 mg). A similar result was also observed for specimens lubricated with a blend of MO and SBO (MO:SBO) in which the mass loss (31.27 mg) was again in-between the values for pure SBO and MO. It was observed that although the MO had a superior performance in preventing wear compared to the pure vegetable oils, the addition of 50% MO in both vegetable oils did not greatly influence the wear resistance result of the blended oils. For both cases of blended oil (MO:PO and MO:SBO), the mass loss differs by about fifty orders of magnitude compared solely to MO. It should also be noted that the type of vegetable oil influenced the wear result of its blended oil with MO. The MO:PO blend produced higher wear than the MO:SBO blend and this aligns with the fact that the PO generated higher wear than the SBO in their pure forms. The statistical analysis of single variable ANOVA also revealed that there is a significant difference (P-value <0.05, Table 6.4) between the mass loss of vegetable oils and their blends with MO studied here.



(b)	Wear scar shape
PO	
MO:PO	
MO	
MO:SBO	
SBO	
PO:SBO	

Figure 6.2: (a) Average Mass loss of lubricated specimens after 60 minutes and (b) Wear scar appearance after the test

Inspection of the wear scars after each test (Figure 6.2b) revealed a smooth shape and narrow scar width on the MO specimens. The existence of zinc (Table 6.2) in the MO, which is likely to include the anti-wear additive, zinc dialkyl dithiophosphate (ZDDP) could prevent the surface from suffering severe wear. Although the amount of zinc in the blended oil of MO and vegetable oils (MO:PO and MO:SBO) is reduced to almost half (Table 6.2), the wear resistance of both lubricants was not similarly reduced by this amount. This indicates that the

vegetable oil was dominant in influencing the wear performance of the vegetable oil blends with MO.

Table 6.3: Minimum film thickness, h_{\min} and lambda ratio, λ for all lubricants

Lubricants	h_{\min} (nm)		λ	
	Initial	Final	Initial	Final
Palm Oil (PO)	2.42	2.45	0.01	0.01
MO:PO	2.86	2.82	0.01	0.01
Mineral Oil (MO)	3.62	3.71	0.02	0.04
MO:SBO	2.67	2.65	0.01	0.01
Soybean Oil (SBO)	2.19	2.25	0.01	0.01
PO:SBO	2.25	2.31	0.01	0.01

Table 6.4: ANOVA analysis of mass loss for all lubricants

		<i>Count</i>	<i>Sum</i>	<i>Average</i>	<i>Variance</i>		
Groups	PO	3	137.28	45.76	16.33		
	MO:PO	3	102.06	34.02	21.53		
	MO	3	-	-	-		
	MO:SBO	3	93.82	31.27	3.17		
	SBO	3	128.19	42.73	37.45		
	PO:SBO	3	133.16	44.39	16.06		
ANOVA	<i>Source of Variation</i>	<i>SS</i>	<i>df</i>	<i>MS</i>	<i>F</i>	<i>P-value</i>	<i>F_{crit}</i>
	Between Groups	513.36	4	128.34	8.01	0.0036	3.478
	Within Groups	160.19	10	16.02			
	Total	673.54	14				

It should also be noted that all lubricants, except the MO, produced a similar wavy-shaped wear scar which suggests that there was plastic flow on the specimen surface. The

high mass loss produced by the blended oils showed that the role of the anti-wear additive that exists in the MO is diminished in the blended oil. The existence of only about 50% of zinc in the blended oil (from the MO) had failed in preventing the metal-to-metal contact between the ball and flat specimen, thus, promoting severe wear and causing the plastic flow observed.

Table 6.5: Elemental analysis of wear scar for all lubricants specimen by EDX

Element	Weight % (wt%)						Atomic % (at%)					
	Lubricants											
	PO	MO: PO	MO	MO: SBO	SBO	PO: SBO	PO	MO: PO	MO	MO: SBO	SBO	PO: SBO
C	3.79	4.41	3.38	4.27	3.77	3.18	14.67	16.44	10.96	15.93	14.56	12.35
O	1.17	2.21	10.43	2.38	1.43	1.95	3.39	6.2	25.58	6.66	4.15	5.67
Si	3.29	3.02	2.70	2.99	2.91	3.3	5.44	4.82	3.77	4.78	4.80	5.47
P	0.10	0.04	0.72	0.06	0.15	0.07	0.15	0.06	0.91	0.09	0.22	0.11
S	0.04	0.12	1.36	0.00	0.00	0.02	0.06	0.16	1.66	0.00	0.00	0.02
Mn	0.66	0.76	0.73	0.87	0.84	0.5	0.55	0.62	0.52	0.71	0.71	0.43
Fe	90.95	89.24	79.80	89.43	90.91	90.98	75.73	71.57	56.06	71.83	75.56	75.94
Zn	-	0.19	0.90	0.01	-	-	-	0.13	0.54	0.01	-	-

Further inspection of the worn surfaces of the specimens through an elemental analysis by EDX (Table 6.5) suggests that the wear of specimens could be associated with the retention of an oxide layer on the surface. This is shown by the surface lubricated with MO having the highest amount of oxygen (10.43 wt%) present and thus, a more protective layer is retained to minimise the metal-to-metal contact. However, for specimens lubricated with MO-vegetable oils blended in 1:1 ratio (MO:PO and PO:SBO), the oxygen appeared not to be greatly retained. For the blended oils, MO:PO produced 2.21 wt% while PO:SBO yielded 2.38 wt%. These oxygen amounts are about one-fifth of the amount of oxygen retained on MO lubricated surface. Furthermore, the amount of zinc detected on the blended oil surfaces

was relatively small compared to the MO specimens and this could have caused the low wear resistance.

The dominance of vegetable oil in influencing the wear for vegetable oil-mineral oil blend is proposed in the mechanisms in Figure 6.3 (comparison between PO, MO and MO:PO). The polarity of vegetable oil (carboxyl group in fatty acids molecules) has made it possible for them to adhere to metal surfaces (Figure 6.3a), but during sliding at severe contact conditions, these fatty acids molecules are removed and thus, produce severe wear (Figure 6.3b). In the case of MO, the anti-wear additives are effectively present on the surface to provide a protective layer in reducing metal-to-metal contact (Figure 6.3c), and this layer is retained even after sliding at severe contact conditions (Figure 6.3d). However, in the vegetable oil-mineral oil blend, the additives are unable to form a fully protective layer due to most of the surface is already covered by the carboxyl group of vegetable oil. This has affected to higher wear of MO:PO lubricated specimens compare to MO lubricated specimens, since only small amount of anti-wear additives are formed on the surface (Figure 6.3e).

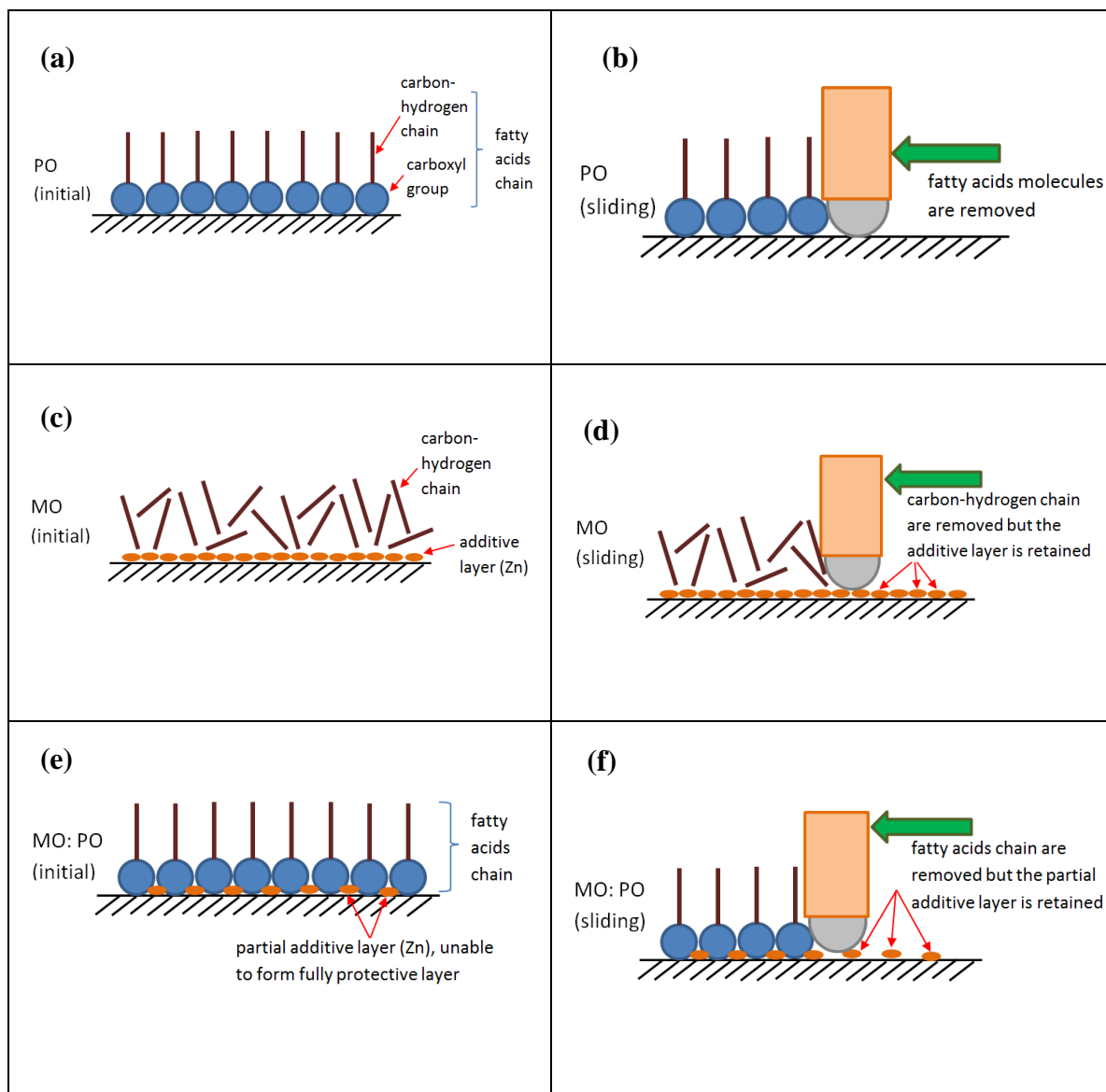


Figure 6.3: Mechanisms of vegetable oil (a and b), mineral oil (c and d) and vegetable oil-mineral oil blend (e and f) in influencing wear

6.4 Surface Topography Analysis

The average surface roughness, R_a across the wear scars after testing is shown in Figure 6.4a and where measurements were taken at different points in Figure 6.4b. The specimen tested with a blend of PO and SBO (PO:SBO) exhibited a higher surface roughness after testing while the MO lubricated specimen generated the lowest surface roughness. The surface roughness for the specimen lubricated with MO were found to be more consistent at

each point while others recorded different surface roughness at different points. The point where the highest surface roughness were recorded for most lubricants mainly occurred at the point Middle 2 (M2) and Middle 3 (M3). This suggests that the debris produced during the material removal process could be trapped in the groove area of point Middle 2 and thus promote higher levels of abrasive wear. The blend of MO and vegetable oils (MO:PO and MO:SBO) produced higher surface roughness compared to the MO specimen especially at the middle point. It is therefore suggested that the addition of 50% MO in vegetable oils did not greatly influence the reduction of surface roughness as a result of the wear process. Higher surface roughness measured on the specimens lubricated with a blend of PO and SBO (PO:SBO) reflects its highest of the recorded COF (Figure 6.1b).

In order to differentiate between the influence of each lubricant on the formation of wavy-shaped wear scars (Figure 6.2b), the primary profile and surface waviness, W_a were measured along the sliding direction in the middle of the scars. The surface waviness is derived from the primary profile measurement in which the shorter wavelength components and longer wavelength components are suppressed through a band-pass filter [210]. Figure 6.5 depicts the primary profiles for all specimens along the wear scar with their waviness value.

The MO specimen exhibited the shallowest profile and lowest surface waviness ($W_a = 1.40 \mu\text{m}$). The PO specimen however produced the highest value of surface waviness ($W_a = 41.43 \mu\text{m}$). Although the specimen lubricated with a blend of PO and SBO (PO:SBO) produced the highest COF (Figure 6.1b), its surface waviness value is relatively small compared to PO and SBO specimen. This suggests that the surface waviness is not related to the COF in lubrication with vegetable oils and their blend with MO.

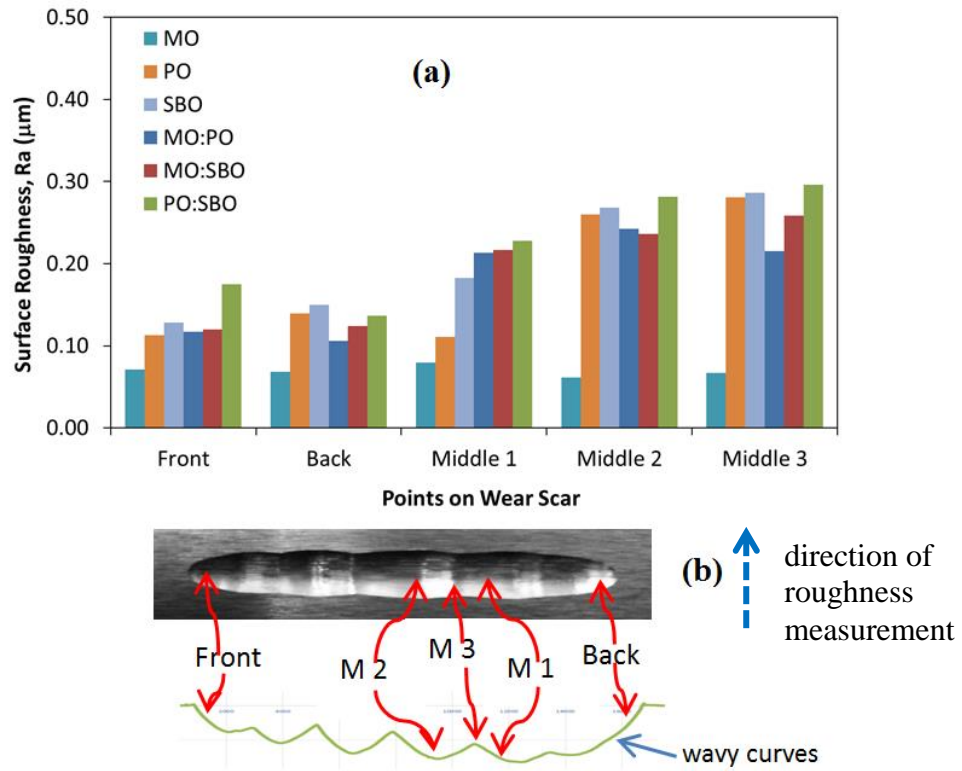


Figure 6.4: (a) Surface roughness of specimens across the wear scar at a point according to diagram in (b)

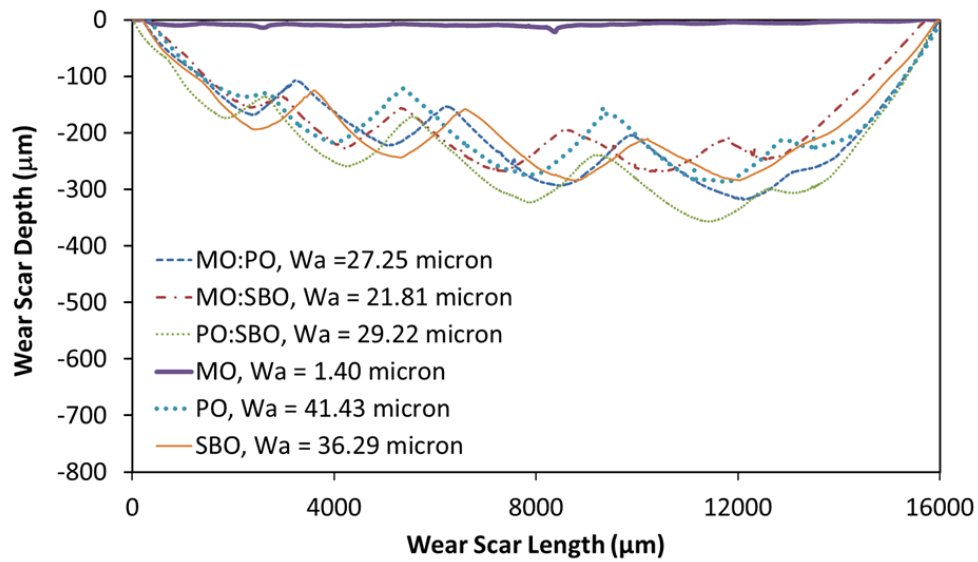


Figure 6.5: Primary profile and surface waviness, W_a of specimens measured along the wear scar.

6.5 Surface Morphology Analysis

Figure 6.6 contains typical images of worn specimens of all lubricants observed under an optical microscope at different points (Figure 6.4b). The two primary wear mechanisms for all specimens lubricated with vegetable oils and their related blends (PO, SBO, MO:PO, MO:SBO and PO:SBO) were abrasion, with some pitting, and plastic deformation at the surface. Also visible are some burn marks (features brownish in colour) found on the worn specimens used with these lubricants. This suggests that the surface underwent a frictional heating caused by metal-to-metal contact during sliding. This idea was discussed in more detail in the previous chapter (Chapter 5, Section 5.3 Wear Analysis).

Further investigation of specimens lubricated with vegetable oils and their blends using SEM techniques (Figure 6.7a, b, d, e and f) revealed some surface fatigue and evidence of delamination at worn surfaces. This indicates that the wear mechanism for these lubricants is a combination of abrasion and surface fatigue. However, the abrasive marks for vegetable oil–MO blends (Figure 6.7b and d) were found to be smaller compared to PO and SBO counterparts.

The appearance and wear mechanism of the MO lubricated specimen was consistent especially at the middle points (Figure 6.6, MO specimen at point M1, M2 and M3). There was some pitting and spalling, especially at points Front and Back which represent the end points of the reciprocating stroke. This could be due to the change of direction (and associated transition through zero velocity) at the stroke ends lowering the film thickness and promoting scuffing [229].

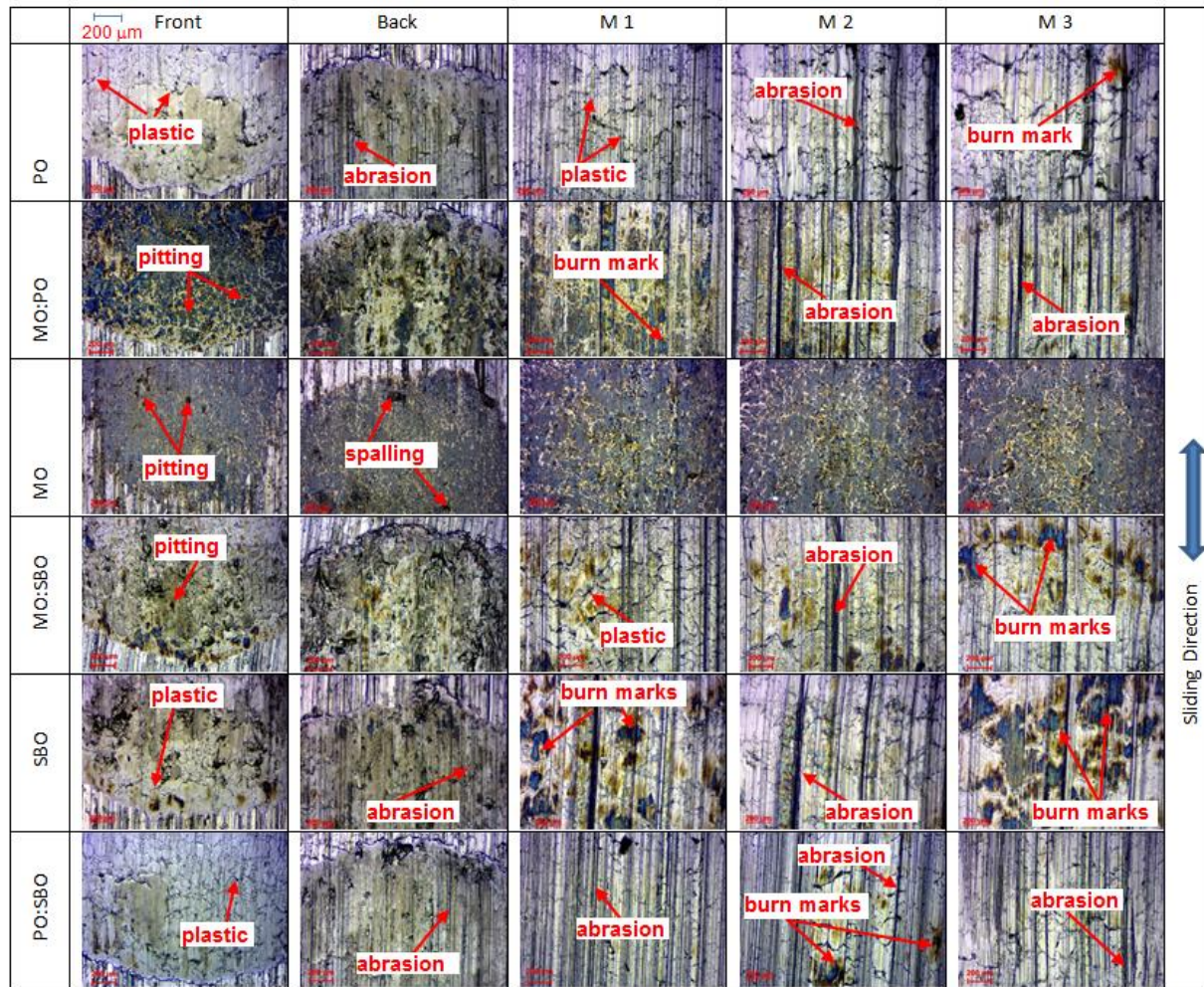


Figure 6.6: Optical microscope images of wear scar for all lubricants (20X magnification)

Further investigation of MO worn specimen under the SEM (Figure 6.7c) observed surface cracks as a result of surface fatigue which were induced by the repeated loading and unloading cycles. This indicates that the main wear mechanism for MO lubricated specimen was fatigue wear. The surface cracks and pitting on the MO lubricated specimen in this study are also similar to those seen on grey cast iron specimen lubricated with a commercial mineral engine oil (15W40) [235].

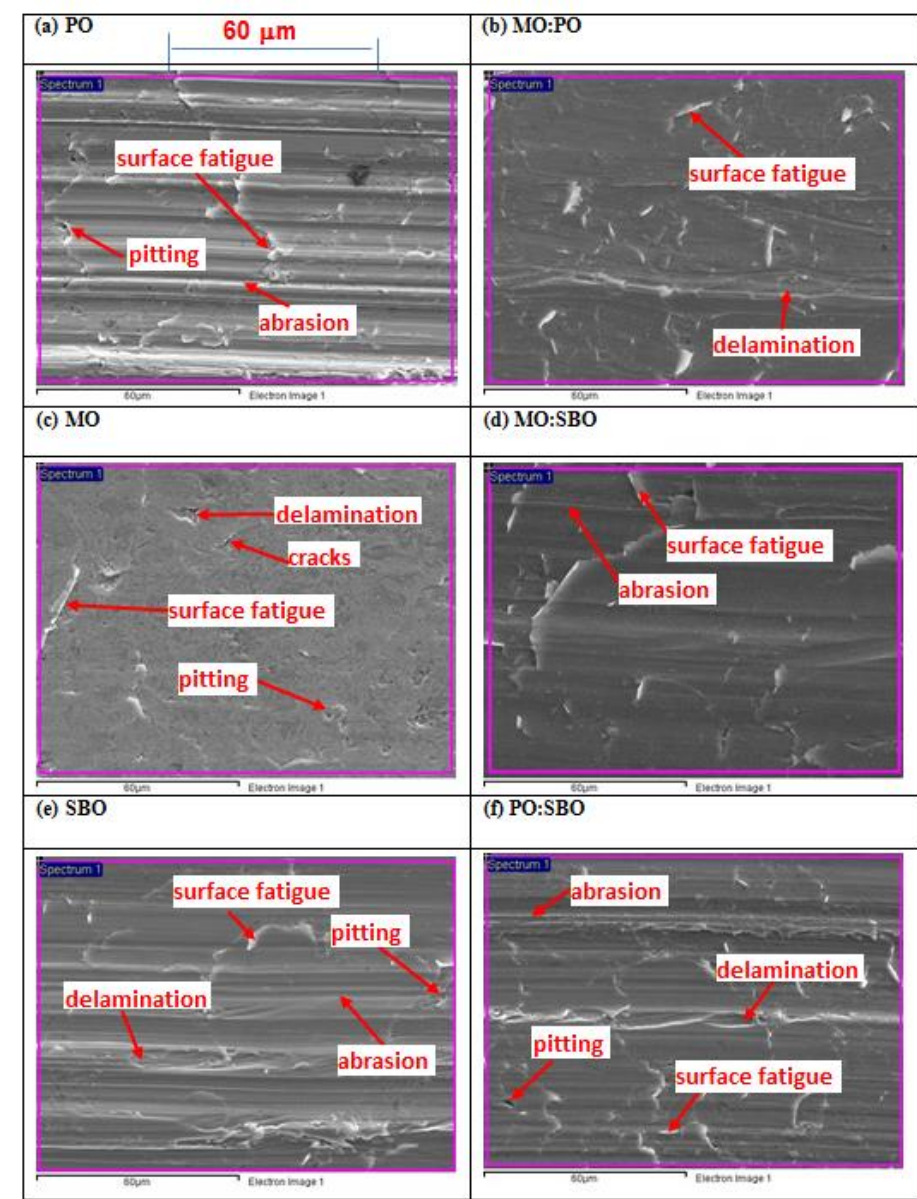


Figure 6.7: Scanning electron microscopy (SEM) images (1000X magnification) and elemental analysis of wear scar for all lubricants

6.6 Oxidative Stability Analysis

Figure 6.8 presents the results of the oil oxidation test implemented by RPVOT test rig with the maximum pressure achieved in the pressure vessels. It can be clearly seen that the MO significantly outclassed the other oils in terms of oxidative stability (270 minutes) and the peak pressure (200 psi). The lower performance of vegetable oils and their blends could have contributed to their lower wear resistance [11]. The SBO was found to have the lowest oxidative stability (20 minutes). An improvement in oxidative stability can be seen in vegetable oils blended with MO, probably due to existence of anti-oxidant additives from the MO. The PO blended with MO recorded 90 minutes of oxidation time while SBO-MO blend oil recorded about 35 min. The PO-MO blend oil demonstrated a significant improvement compared to other oils. The higher oxidation time of the PO-MO blends, when compared to SBO-MO blend, could be attributed to the higher saturated fatty acids that exist in PO which helps to delay the oxidation process.

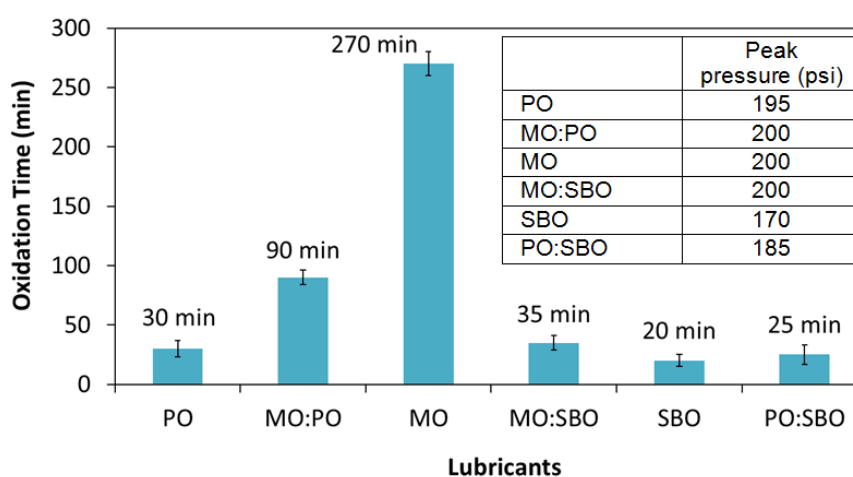


Figure 6.8: Rotary pressure vessel oxidation test (RPVOT) result for mineral oil (MO), palm oil (PO) and soybean oil (SBO) and their blended oils

The dominance of vegetable oils in oxidative stability results over the MO:PO and MO:SBO suggests that the existence of unsaturated fatty acids (with the presence of carbon double bond in their structure) in both PO and SBO promoted the rapid oxidation of vegetable oil-mineral oil blend. Although the PO is enriched with saturated fatty acids, the total percentage of unsaturated fatty acids composition in this oil (54.9%) was considerably high (Chapter 5, Figure 5.2) while in SBO, the total of unsaturated fatty acids made up 83.3% of its composition (Chapter 5, Figure 5.2).

6.7 Acid Number Analysis

Figure 6.9 shows the acid number (AN) for all lubricants that were tested as fresh oil, used oil (post-test from wear test rig), and oil from an oxidation test (RPVOT). In the case of fresh oil, the MO recorded the highest AN (2.24 mgKHO/g) compared to other lubricants. This higher AN could be due to the existence of anti-wear additives which includes zinc dialkyl dithiophosphate as this additive increased the AN value in base oil [231]. The higher AN produced by SBO (0.98 mgKOH/g) compared to PO (0.24 mgKOH/g) could be attributed to the higher acidity of free fatty acid that exists in unrefined oil (SBO) than refined oil (PO). The free fatty acids are removed by distillation during the refining process [236]. For blended oils (MO:PO, MO:SBO and PO:SBO), the AN values are generated in-between the values of their pure oils and were influenced by type of the vegetable oil in the blend (either PO or SBO). A higher AN for all lubricants from both the wear test and the RPVOT test indicate that the oils have been oxidised after the wear test. However, the difference in AN before and after the wear test for blended oils (MO:PO and MO:SBO) are smaller than pure PO and SBO. This is probably due to the the existence of anti-oxidant additive from the MO in the oil blend that assists in prolonging the oxidation process.

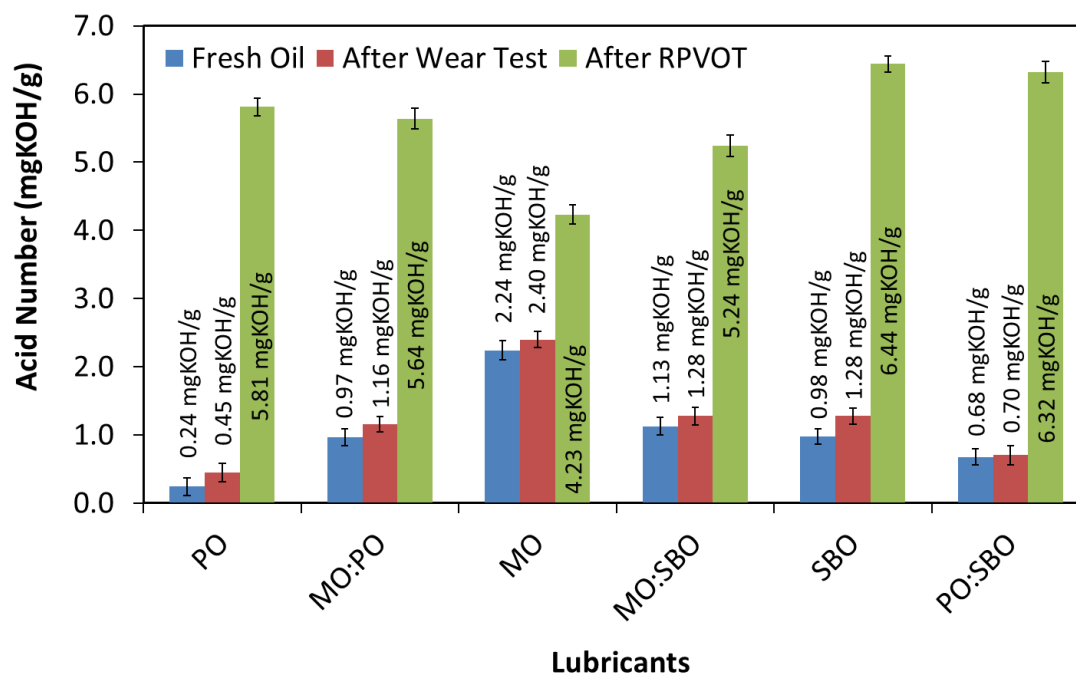


Figure 6.9: Acid Number for Mineral Oil, Palm Oil, Soybean Oil and their blended oils for fresh and used oils

6.8 Oil Viscosity Analysis

Figure 11 compares the results of dynamic viscosity measurements for all lubricants (fresh oil and used oil post-wear test) measured at 40°C and 100°C. It was found that the viscosity of MO is higher than vegetable oils at both temperatures. As expected, all oils produced a lower viscosity at a higher temperature, with MO recording a higher viscosity than vegetable oils at all temperatures. However, the viscosity of the vegetable oils (PO and SBO) is more stable with respect to temperature change than MO. This suggests that the vegetable oils have a higher viscosity index than MO. It should also be noted that the viscosities for fresh blended oils (MO:PO and MO:SBO) were reduced to a level where their viscosities are nearer to the values of the pure vegetable oils (PO and SBO) rather than to that of the MO. For example at 40°C, the fresh MO:PO oil produced viscosity 54.97 cP. This value is closer to PO viscosity (38.08 cP) rather than MO viscosity (92.45cP).

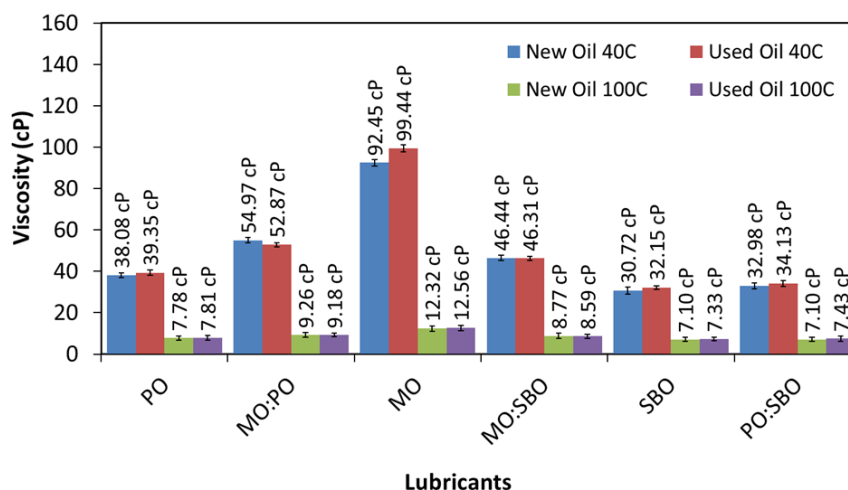


Figure 6.10: Viscosity of Mineral Oil (MO), Palm Oil (PO) and Soybean Oil (SBO) and their blended oils

The lower viscosity of the pure vegetable oils influences the viscosity of their blends with MO. The higher wear (Figure 4a) on specimens lubricated with vegetable oils and their blend with MO could be due to their lower viscosity. Previous work investigating viscosity of lubricants has reported that lower viscosity oils can promote higher wear rate [233] and that the oil viscosity increases with oxidation [237]. The values of viscosity for the used oils in this study were not greatly different when compared to fresh oils. This suggests that although the oxidation process occurred in the wear test rig (from AN result in Figure 10), the level of oxidation in the oils is considerably lower.

6.9 Conclusions and Summary

From the work testing vegetable oil-mineral oil blended lubricants (1:1) at severe contact conditions, the following conclusions can be drawn:

- The vegetable oils blended with commercial mineral engine oil exhibited tribological improvement in friction, wear resistance and oxidative stability compared to their pure oils.
- The tribological performance of lubricant formulated from vegetable oil-MO blend was highly dominated by tribological characteristics of the vegetable oil. Although the addition of 50% of MO in vegetable oil blends reduces the presence of additive elements by 50%, the deterioration in wear and oil oxidation performance were very significant.
- The selection of base oil for vegetable oil – MO blend is important because it influenced the tribological performance of the blend. The performance of friction and wear for MO:SBO oil compared to MO:PO blend were following the pattern of its pure oil.

Although the use of vegetable oil-mineral oil blends in lieu of pure mineral oil could reduce dependency on petroleum base stock, its tribological performance was very weak and not suitable for use in practical applications. The superior wear performance shown by the commercial mineral oil compared to pure vegetable oils was failed to influence the wear performance in the mineral oil-vegetable oil blend. Other methods are therefore required to improve the performance of the vegetable oils (and when they are used in blends), particularly to improve their role in reducing wear. The use of the anti-wear additives commonplace in mineral oil formulations in vegetable oil is worthy of further investigation.

Chapter 7: Improving the friction and wear performance of vegetable oils at severe contact condition through the use of additives

In view of the wear results produced from previous chapters, much work is needed in improving the wear resistance of grey cast iron when using vegetable oil lubricants, especially at severe contact conditions. One of the ideas is to mix the vegetable oil with commercial anti-wear additives that have been claimed by the manufacturer to perform well with mineral engine oil. Thus, in this chapter, the friction and wear responses of palm oil and soybean oil with two commercial anti-wear additives (zinc dialkyl dithiophosphate and boron compound) are investigated at a lubricant temperature 100 °C under severe contact conditions in a reciprocating sliding contact.

7.1 Introduction

An effective engine lubrication system is multifunctional which includes reducing friction and wear, transferring excessive heat, inhibiting corrosion and oxidation and removing wear debris and contamination. Base oils alone are not able to fulfil these requirements due to limited physicochemical properties and thus, they require modification. Recently, many studies on biolubricants have focused on the modification of vegetable oils in order to produce a better base oil. This can be performed through chemical synthesis [222, 238] or formulating the vegetable oils with additives [239].

Commercial lubricant manufacturers blend their base oils with additive packages which include a viscosity modifier, extreme pressure agent, corrosion inhibitor, dispersant, detergent, anti-foam agent, anti-oxidant and anti-wear agent. Among the most commonly

used as anti-wear agents in commercial engine oils are zinc dialkyl dithiophosphate (ZDDP) and boron nitride.

Although extensive research has been carried out on the performance of ZDDP and boron nitride additives on vegetable oils, they are limited to unidirectional sliding test rigs (four-ball-tester [12, 28-31] and pin-on-disc [34, 240, 241]) with steel and aluminium as counterface materials. In addition, many of the tribological tests reported were run at a lubricant temperature less than 100 °C [28-30, 34, 240] which is inappropriate for higher temperature lubricant applications such as in a sump of an internal combustion engine [40].

Therefore, in this work, the tribological response of two commercial anti-wear additives; ZDDP and boron nitride in palm oil and soybean oil were evaluated at a lubricant temperature 100 °C using a reciprocating test rig. A point contact with an initial contact pressure > 1 GPa was applied, leading to a severe contact condition. Grey cast iron specimens within a narrow hardness range on the intended wear scar were used. Surface morphology, elemental analysis and chemical analysis of oils were also presented to support the main results. The tribological results were also compared with the commercial mineral engine oil. All experiments including the friction and wear test as well as the elemental and oil analyses were carried out following the methods described in Chapter 3, Section 3.2-3.6.

7.2 Friction Analysis

The average coefficient of friction (COF) for all lubricants is plotted against time (60 minutes) in Figure 7.1a. Figure 7.1b highlights the final average value of COF taken at the end of the test. The error bars show how much the final value differs from the mean value of the data. All lubricants exhibited a similar running-in behaviour in which they started with a lower COF value at the beginning that gradually increased before reaching a steady state value after about 30 minutes. The running-in behaviour in Figure 7.1a might be caused by the pressure drop due to an increase in the area of contact during the sliding process. The COF is inversely proportional with the mean contact pressure [242]. Other possible reasons could possibly be the removal of lubricious contaminants from the contact surface [47] or the disruption of an oxide layer on the counter-face leading to an increase in metal-to-metal contact [50].

The COF for the MO lubricated specimens (Figure 7.1b) showed the lowest value (0.093) while the highest COF was from specimens lubricated with hBN:SBO (0.116). Based on Figure 7.1b, the ZDDP blended with vegetable oils (ZD:PO and ZD:SBO) gave a reduction in COF while the hBN in vegetable oils (hBN:PO and hBN:SBO) did not show any improvement compared to the pure oil state. In the pure oil state, the PO showed a lower COF (0.105) compared to SBO (0.112). This result seems to be similar for PO and SBO with additives. For example, the ZD:PO exhibited a lower COF (0.095) compared to the ZD:SBO lubricated surface (COF=0.099). An interesting COF result was noted on the ZD:PO lubricant in which it presented a very competitive value (0.095) compared to the MO (0.093). All COF data in Figure 7.1b show a significant difference between the mean values when tested by ANOVA analysis of single variable (P-value < 0.05, Table 7.1).

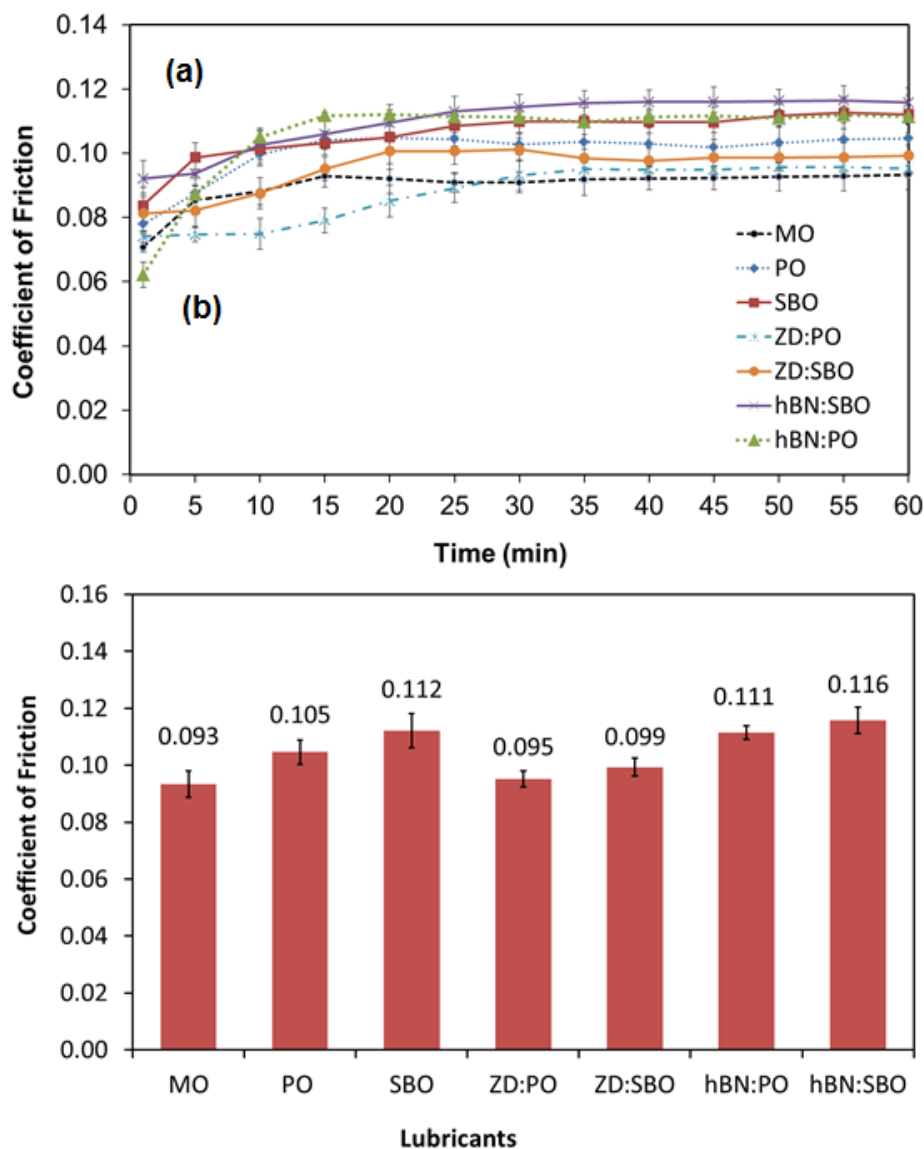


Figure 7.1: (a) Average coefficient of friction profile versus experiment time and (b) Average coefficient of friction at 60 minutes

The spectrochemical analysis of elements for all lubricants is shown in Table 7.2. The amount of various elements (in ppm) in pure vegetable oils (PO and SBO) is relatively small compared to other lubricants. It is interesting to note that the pure SBO contained calcium (25 ppm), phosphorus (59 ppm) and magnesium (17 ppm). These metallic elements are typically found in natural soybean oil and are used to determine the quality of the vegetable oil before converting it to a biodiesel [243].

Table 7.1: ANOVA analysis of COF for all lubricants

		<i>Count</i>	<i>Sum</i>	<i>Average</i>	<i>Variance</i>		
Groups	MO	3	0.279	0.093	3.71E-05		
	PO	3	0.313	0.105	2.17E-07		
	SBO	3	0.335	0.111	1.21E-05		
	ZD:PO	3	0.286	0.095	4.20E-05		
	ZD:SBO	3	0.297	0.099	9.89E-05		
	hBN:PO	3	0.333	0.111	1.51E-05		
	hBN:SBO	3	0.347	0.116	4.80E-05		
ANOVA	<i>Source of Variation</i>	<i>SS</i>	<i>df</i>	<i>MS</i>	<i>F</i>	<i>P-value</i>	<i>F_{crit}</i>
	Between Groups	0.00136	6	0.000227	6.618	0.001	2.847
	Within Groups	0.00048	14	3.43E-05			
	Total	0.00184	20				

The existence of the additive package in the commercial MO sample may be seen as detected elements in the MO column. These include calcium, zinc, phosphorus, molybdenum, boron and magnesium in the sample. Calcium (calcium hydroxide) is mostly used as lubricant detergent (to clean and neutralise oil impurities) due to its lower cost [100]. The impurities in oil can cause deposits (oil sludge) on engine components. The molybdenum in the MO sample is from molybdenum-dithiophosphate (MoDDP) or molybdenum-dithiocarbamate (MoDTC) additives, as these additives act to reduce the COF in engine oil [225]. These additives could also exist in the MO sample in this study and thus lead it to produce the lowest COF.

The addition of 2% commercial ZDDP in both PO and SBO has led to a significant difference in the amount of elements (calcium, zinc and phosphorus) compared to their pure oil state. The addition of ZDDP in PO and SBO has lowered the COF compared to their pure oil state which is typical for other vegetable oils (e.g., coconut, karanja, corn and

canola oil) [12, 29, 142]. Contrary to the lower friction result found in the ZDDP mixture with vegetable oils, the existence of ZDDP alone in base oil increases the friction compared to the oil without ZDDP due to increases in roughness on metal surfaces [244, 245]. This work revealed (Figure 7.1b) that ZDDP, besides being known as an anti-wear agent and an anti-oxidant agent, also acts as a friction modifier for vegetable oils.

Table 7.2: Elements detected in lubricants in part per million (ppm) from spectrochemical test

Elements	Lubricants						
	MO	PO	SBO	ZD:PO	ZD:SBO	hBN:PO	hBN:SBO
Calcium	2825	0	25	25	49	120	147
Zinc	781	1	3	1153	1129	65	65
Phosphorus	695	0	59	879	917	51	106
Molybdenum	167	0	0	0	0	350	352
Boron	43	2	1	3	0	342	357
Magnesium	32	0	17	0	16	3	19
Silicon	3	3	2	8	65	5	3
Aluminium	3	0	0	0	0	5	6
Iron	1	0	0	0	0	0	0
Sodium	0	2	3	5	2	4	5
Lead	0	0	0	0	1	0	0
Barium	0	0	0	0	0	0	0

The existence of boron and molybdenum elements are abundantly observed in the vegetable oils (PO and SBO) blended with commercial boron based additive. The small amount of zinc and phosphorus that were found in the hBN:PO and hBN:SBO may come partly from the mineral oil as this oil was used by the manufacturer as a carrier fluid for the hBN additive.

Although boron was detected in the spectrometer results from analysing the hBN:PO and hBN:SBO (Table 7.2), it did not appear on the worn specimens surfaces as analysed by EDX (Table 7.5). Detection of a light element (boron) by EDX is somewhat difficult due to low photon energy that it has which may lead to a high absorption in the specimen and in the EDX detector [246]. Another possibility was that the boron elements had been removed from the counterface during the sliding process and thus failed to perform their function as an effective lubricious film. The particle size of boron nitride used in this study ($0.5\ \mu\text{m}$) was relatively larger than the average surface roughness of the flat specimens ($R_a = 0.15\ \mu\text{m}$). This could be the reason why the boron was not merging in the asperity valleys of the contact surfaces. Larger particles act as a third body abrasive products and this may increase the friction [34] where the hBN particles were prevented from settling on the surface.

7.3 Wear Analysis

Table 7.3 shows the calculated minimum film thickness (h_{\min}) and lambda value (λ). It is found that the lubrication regime for all lubricated specimens was boundary ($\lambda < 1$). The differences of minimum film thickness between the start and the end of test were calculated and mainly attributed to the differences of oil viscosity before and after the test (Figure 7.9). It was found that all lubricants experienced an increase in film thickness except for ZD:PO and ZD:SBO. However, the lambda values for most of lubricants did not change.

Table 7.3: Minimum film thickness, h_{\min} and lambda ratio, λ for all lubricants

Lubricant	h_{\min} (nm)		λ	
	Initial	Final	Initial	Final
MO	3.62	3.71	0.02	0.04
PO	2.42	2.45	0.01	0.01
SBO	2.19	2.25	0.01	0.01
ZD:PO	2.45	2.42	0.01	0.01
ZD:SBO	2.21	2.16	0.01	0.01
hBN:PO	2.44	2.46	0.01	0.01
hBN:SBO	2.19	2.22	0.01	0.01

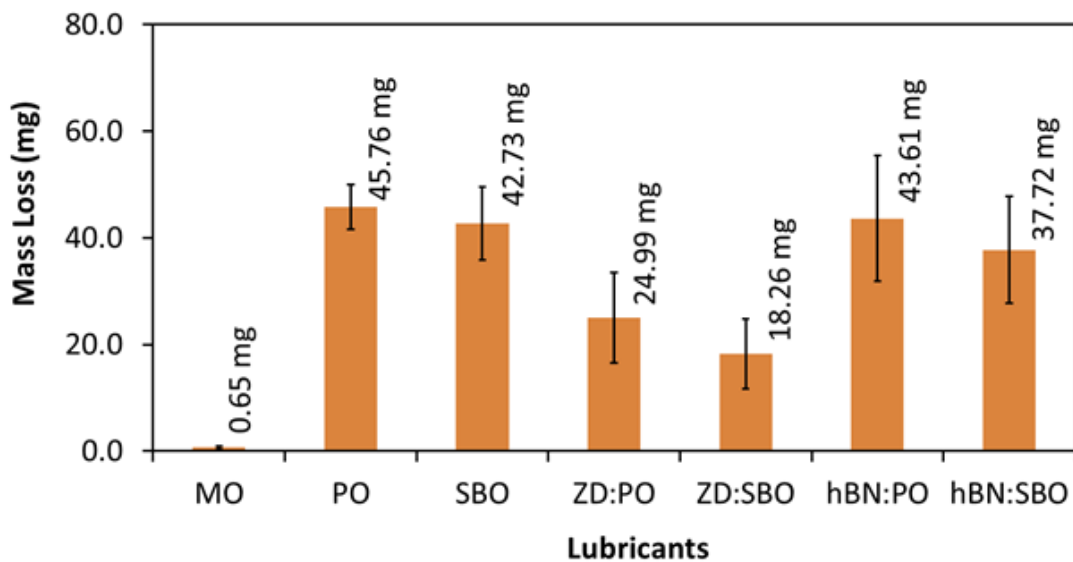


Figure 7.2: Average Mass loss of lubricated specimens after 60 minutes

Figure 7.2 shows that the mixture of ZD:SBO (mass loss=18.26 mg) improved the wear about 57% compared to pure SBO (mass loss=42.73 mg) while the ZD:PO (mass loss=24.99 mg) gave a wear reduction of about 45% compared to pure PO (mass loss=45.76 mg). However, only a small amount of mass loss was found in boron compound additives blended with vegetable oils. The hBN:SBO (mass loss=37.72 mg) recorded about a 12% improvement compared to the pure SBO state while hBN:PO (mass

loss=43.61 mg) only improved about 5% compared to PO alone. The mass loss results for all biolubricant lubricated specimens showed a significant difference between the mean of data when tested by the single variable ANOVA analysis (P-value <0.05, Table 7.4).

Table 7.4: ANOVA analysis of mass loss for vegetable oils and vegetable oil-additive blends

		<i>Count</i>	<i>Sum</i>	<i>Average</i>	<i>Variance</i>		
Groups	MO	-	-	-	-		
	PO	3	137.28	45.76	16.32		
	SBO	3	128.19	42.73	37.45		
	ZD:PO	3	74.97	24.99	3.26		
	ZD:SBO	3	54.78	18.26	6.14		
	hBN:PO	3	130.84	43.61	22.32		
	hBN:SBO	3	113.17	37.72	44.99		
ANOVA	<i>Source of Variation</i>	<i>SS</i>	<i>df</i>	<i>MS</i>	<i>F</i>	<i>P-value</i>	<i>F_{crit}</i>
	Between Groups	1907.96	5	381.59	17.54	3.79E-05	3.1058
	Within Groups	261.049	12	21.75			
	Total	2169.01	17				

The superior performance in wear of the MO indicates that the anti-wear additives have successfully acted as an efficient lubricant in preventing severe damage to the sliding surface at the severe contact condition applied in this study. This suggests that the anti-wear additives (possibly ZDDP) that exist in the MO are capable of maintaining a protective layer in preventing metal-to-metal contact throughout the test. The existence of ZDDP in the MO sample could be shown by a high amount of zinc and phosphorus detected by the spectrometer (Table 7.2). Although lower zinc concentrations (781 ppm) were found in the MO compared to ZD:PO (1153 ppm) and ZD:SBO (1129 ppm), the MO produced lower wear and friction than these two lubricants. This suggests that the existence of another element in the MO like molybdenum (from MoDDP or MoDTC

additive) could potentially act together with the ZDDP in improving the wear and friction performance of MO. The molybdenum, however, was not significantly present in both ZD:PO and ZD:SBO.

Vegetable oils on the other hand, even though they presented competitiveness in friction coefficient; were still far behind in wear resistance performance compared to MO, especially in a severe test condition. In considering ZDDP as an additive in vegetable oils, both PO and SBO appear to have the capability to provide for the formation of a protective layer on the surface of grey cast iron. In a typical lubricant oil with the ZDDP additives, the phosphate layer is commonly found on the wear scar and serves as a wear reducing layer [247-249], which was also reflected by the highest phosphorus amount found on MO lubricated specimens (0.72 wt%, Table 7.5). Although the phosphorus amount on vegetable oils-ZDDP was higher (spectrochemical analysis, Table 7.2), it was discovered that the amount of this element (P) detected in worn specimens of ZD:PO and ZD:SBO were not significantly different when compared to their pure oil state (EDX analysis, Table 7.5). This suggests that, with vegetable oil, a different mechanism of formation of protective layer from ZDDP (other than phosphorus layer) could occur on the surface.

Zinc may also play this role on the counterface in order to minimise metal-to-metal contact. This is shown by the detection of zinc element during EDX analysis (Table 7.5) of worn specimens for ZD:PO and ZD:SBO lubricants. In order to determine that the wear improvement was solely due to the ZDDP additive, a test of fatty acids composition on PO, SBO, ZD:PO and ZD:SBO oils was performed by gas chromatography (Figure 7.3). It was noted that there were no significant differences found on the fatty acid composition of vegetable oil-ZDDP mixtures compared to their pure oil state. This indicates that the fatty acids compositions in the vegetable oil were not influenced by the existence of ZDDP.

Table 7.5: Elemental analysis of wear scar for all lubricant specimens by EDX

Element	Weight %							Atomic %						
	Lubricants													
	MO	PO	SBO	ZD:PO	ZD:SBO	hBN:PO	hBN:SBO	MO	PO	SBO	ZD:PO	ZD:SBO	hBN:PO	hBN:SBO
C	3.38	3.79	3.77	2.87	3.71	3.45	3.81	10.96	14.67	14.56	11.20	13.94	13.44	14.65
O	10.43	1.17	1.43	2.25	2.85	1.52	1.71	25.58	3.39	4.15	6.59	8.04	4.43	4.93
Si	2.70	3.29	2.91	2.99	2.90	3.05	2.64	3.77	5.44	4.80	4.99	4.67	5.07	4.34
P	0.72	0.10	0.15	0.16	0.13	0.00	0.14	0.91	0.15	0.22	0.25	0.20	0.00	0.21
S	1.36	0.04	0.00	0.00	0.09	0.12	0.10	1.66	0.06	0.00	0.00	0.13	0.18	0.14
Mn	0.73	0.66	0.84	0.81	0.73	0.63	0.75	0.52	0.55	0.71	0.69	0.60	0.53	0.63
Fe	79.80	90.95	90.91	90.88	89.50	91.23	90.85	56.06	75.73	75.56	76.26	72.37	76.34	75.10
Zn	0.90	-	-	0.03	0.09	-	-	0.54	-	-	0.02	0.06	-	-

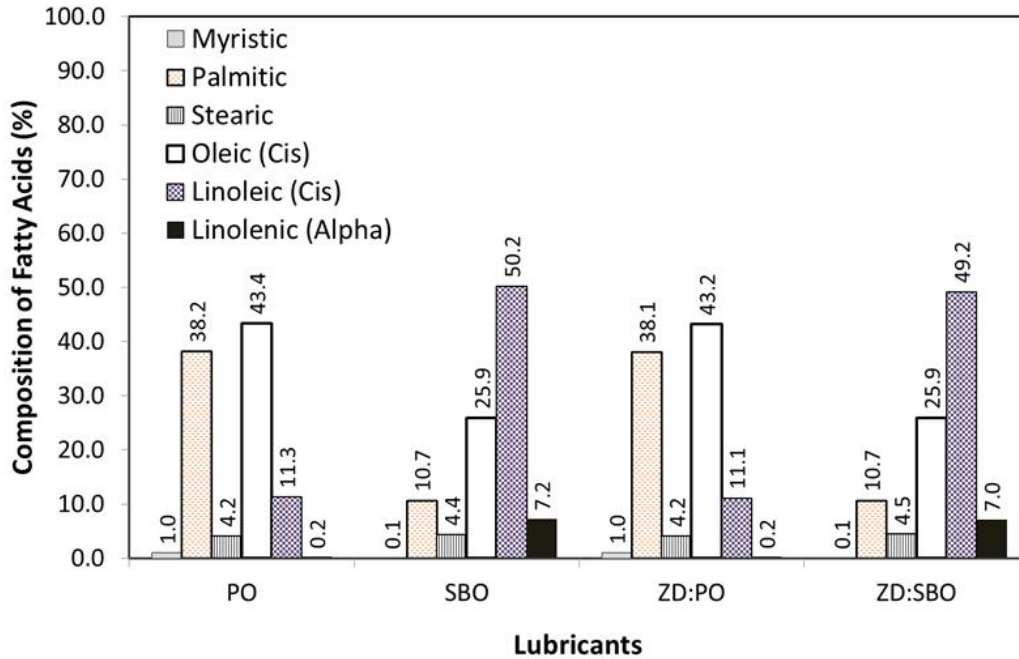


Figure 7.3: Composition of fatty acids on selected oils extracted from gas chromatography test

7.4 Surface Topography Analysis

The shape of wear scar after each test was examined visually (Figure 7.4a). The specimen lubricated with MO produced a straight narrow wear scar with a shallower depth compared to specimens lubricated with vegetable oils. The additive packages that exist in MO could possibly act as a barrier in preventing deeper indentation of ball into the specimen. However, specimens lubricated with vegetable oils and their mixtures with additives showed catastrophic damage with the formation of wavy-shape scars and a wider width. The formation of wavy-shaped scars could also suggest that there was plastic flow due to ratcheting on the contact surface during sliding as a result of the high contact pressure. Ratcheting is likely to occur when the normal load applied is beyond the plastic shakedown limit [218]. Although the vegetable oil lubrication exhibited poor performance in wear resistance at extreme contact condition, the addition of the ZDDP additive in both

PO and SBO has seen an improvement in wear scar appearance in which narrower wear scars were produced.

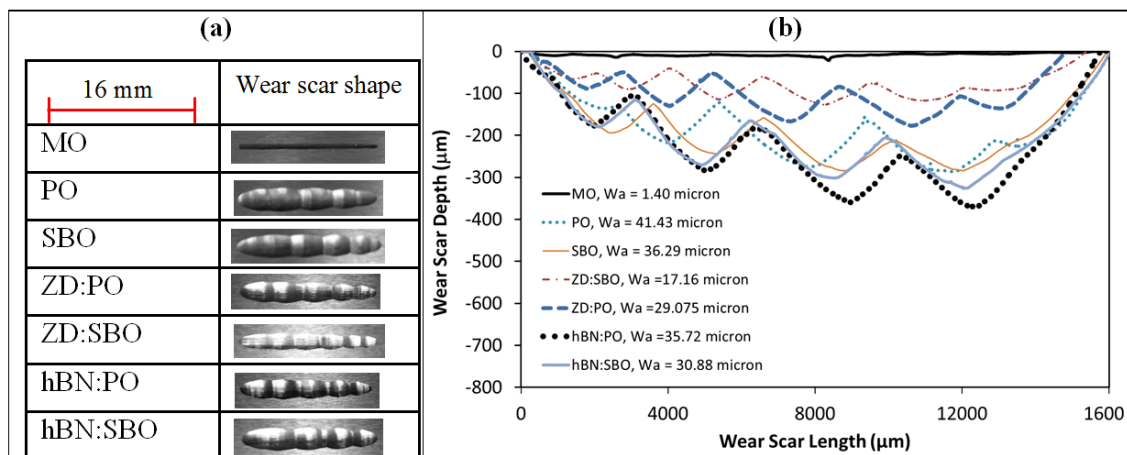


Figure 7.4: (a) Wear scar shape for all lubricated specimens and (b) Primary profile and surface waviness, W_a of specimens measured along the wear scar

In order to further understand the characteristics of these wavy-shape wear scars, Figure 7.4b was plotted. This figure shows the primary profile of wear scars which represents the shape and depth of the worn surfaces measured by a two-dimensional profilometer along the wear scar. Surface waviness measurements (resembling surface roughness in macro scale) were also recorded by altering the wavelength components of the primary profile in the profilometer software [210]. It can be seen that the shallowest profile and lowest surface waviness was from MO lubricated specimen ($W_a = 1.40 \mu\text{m}$). The highest surface waviness was from specimen lubricated with PO ($W_a = 41.43 \mu\text{m}$). It can also be noted that the addition of ZDDP in vegetable oils (ZD:PO and ZD:SBO lubricants) has caused the formation of shallower wear scars and lower surface waviness values. However, deeper penetration was found on specimens lubricated with hBN:PO and hBN:SBO and it was noted that the penetration of wear scar depth produced was dependent on the relative position of the waves. Where there is a higher penetration of the

ball into the flat specimens (as shown by hBN:PO specimens compared to PO and ZD:PO in Figure 7.4b), the peaks of waviness shift within the length of the wear scar.

Figure 7.5a shows the surface roughness (R_a) measured across the wear scars of worn specimen after testing performed at different points (Figure 7.5b). It was noted that the MO lubricated specimen exhibited the lowest and more consistent surface roughness throughout the wear scar. However, for specimens lubricated with vegetable oils and vegetable oil-additive mixtures, the surface roughness varies along the wear scars. Higher roughness was recorded, especially at middle points (Middle 1(M1), Middle 2(M2) and Middle 3(M3)) compared to the MO specimen's roughness. The higher roughness at middle points was likely influenced by the undulating profile that provides a reservoir and promotes accumulation of wear debris. More debris is likely to be trapped at deeper points on a wear scar (Middle 2) and thus, will act as a third-body abrasive. The higher surface roughness commonly led to a higher COF and this was shown by the specimen lubricated with hBN:SBO which recorded the highest COF and roughness.

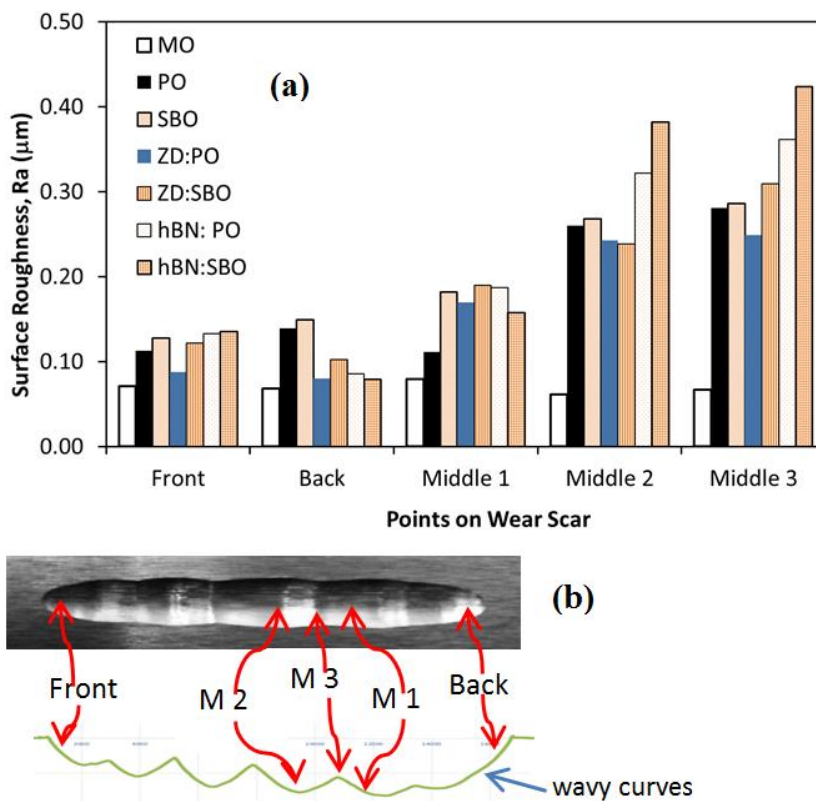


Figure 7.5: (a) Surface roughness of specimens across the wear scar at a point according to diagram in (b)

7.5 Surface Morphology Analysis

The wear scar images of worn specimens taken at different points (Figure 7.5b) for all lubricants under optical microscope are shown in Figure 7.6. A more consistent appearance was seen for the MO worn specimen at each point compared to specimens lubricated with vegetable oils and vegetable oil-additive blends. Some pitting and spalling were found at end points (Front and Back) on the MO specimen indicating a different wear mechanism having occurred at the stroke ends of the reciprocating motion when compared to the middle of the scar. In a reciprocating motion, the speed turns to zero at the stroke end at the moment of changing its direction and this will lower the film thickness, due to the lower velocity, and thus, promote scuffing. These wear mechanisms at the stroke ends

are similar to the pattern from a reciprocating sliding test for pin on pin (a cylinder contact on a cylinder perpendicularly) with steel material and fuel lubricated in which severe scuffing was reported [229]. Detailed examination of the MO worn specimens under SEM (Figure 7.7a) showed surface cracks and delamination and this suggests that the wear mechanism for the MO specimen was fatigue wear.

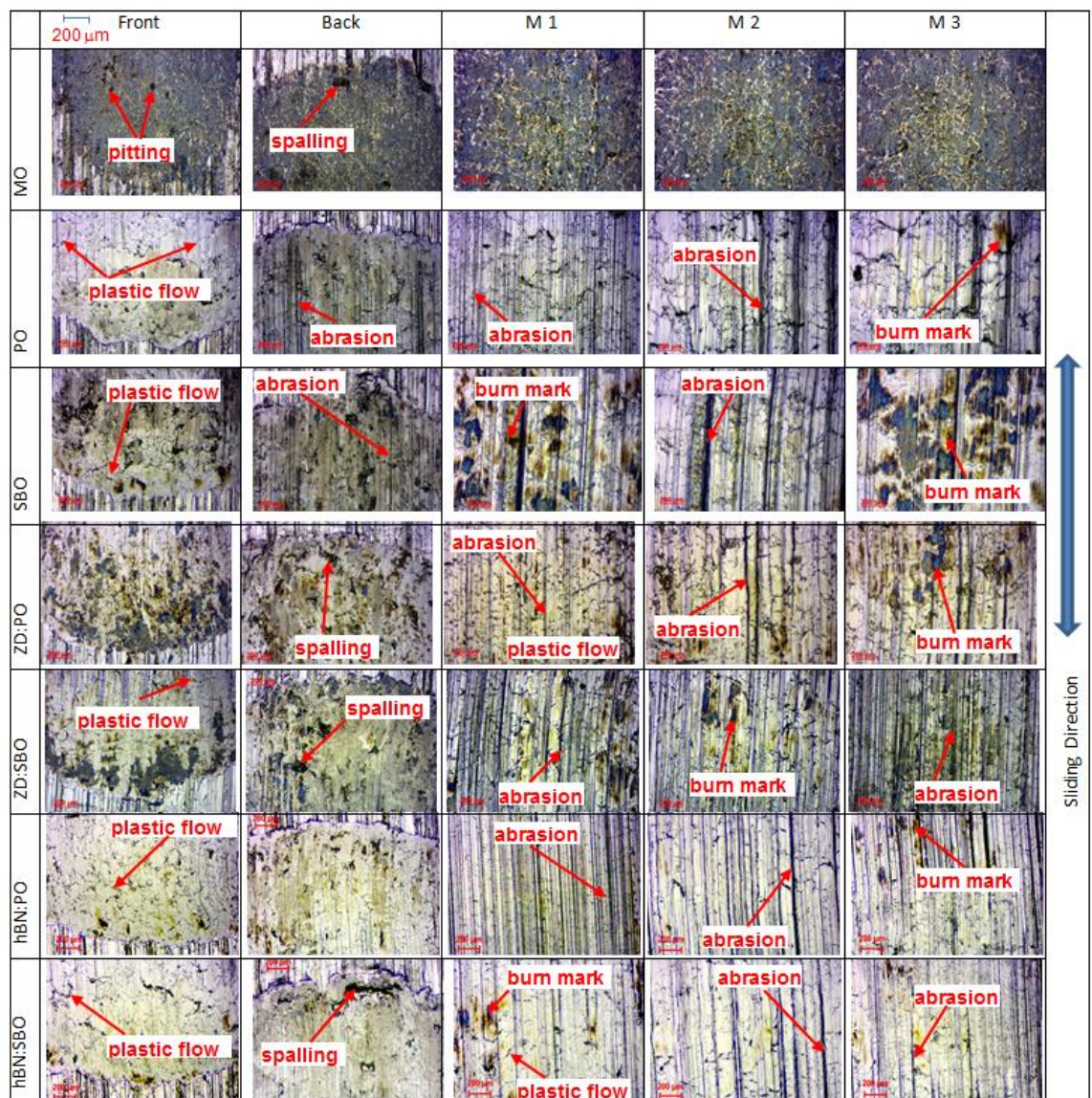


Figure 7.6: Optical microscope images of wear scars for all lubricants (20X magnification)

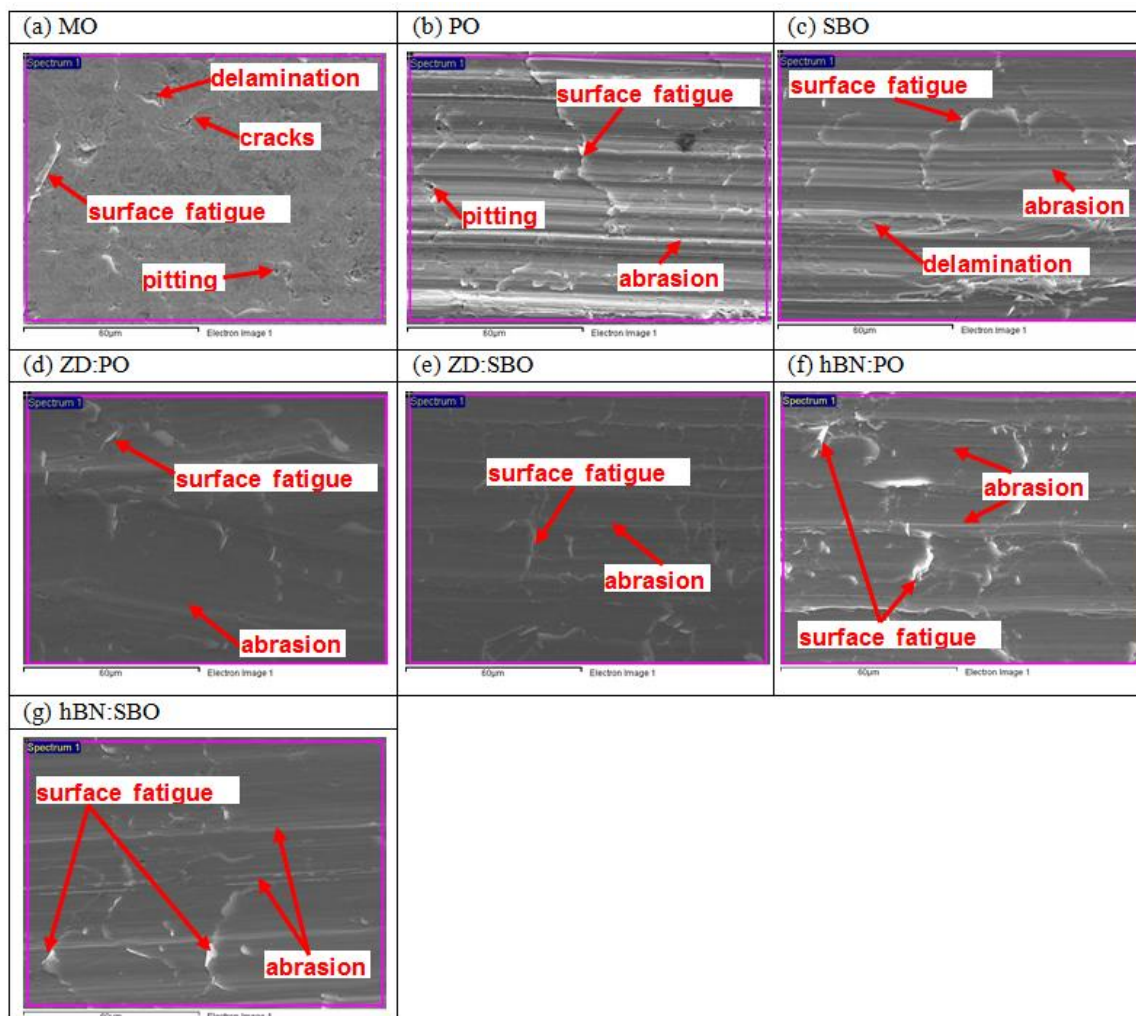


Figure 7.7: Scanning electron microscopy (SEM) images (1000X magnification) and elemental analysis of wear scars for all lubricants

The main wear mechanism for specimens lubricated with vegetable oils and vegetable oil-additive mixtures was observed to be abrasive. This can be clearly seen by the abrasive scratch marks on the worn surfaces especially at the middle points of the wear scar (Figure 7.6). This supports the previous claim that most of the debris was trapped at the middle point due the undulating profile that was generated during the sliding process. It was also noted that at the stroke ends (Front and Back) more plastic flow can be seen on the surface which suggests that this occurred during the sliding process on the contacting surfaces. The addition of ZDDP in vegetable oils has seen a slight improvement on abrasive wear. Less abrasion with smoother surfaces was seen on ZD:PO (Figure 7.7d) and

ZD:SBO (Figure 7.7e) specimens under detailed examination with SEM when compared to their pure oil state (Figure 7.7b and Figure 7.7c). Less abrasion was also seen in the specimen lubricated with hBN:PO and hBN:SBO (Figure 7.7f and Figure 7.7g) with more surface fatigue likely to occur.

Some burn-like marks (brownish colour) could also be seen mainly at middle points on the worn surface for all specimens lubricated with vegetable oils and vegetable oil-additive mixtures (Figure 7.6). These marks possibly occur as a result of the process of frictional heating caused by metal-to-metal contact which may raise the temperature at the counterface. To support this idea, a calculation of surface temperature was performed based on the material properties and test parameters [206]. The estimated surface temperature was then compared to the tempering colour of steel which indicates the brownish colour was likely to appear when the temperature was close to 200 °C [227]. It was found that for the SBO lubricated specimen, the total contact temperature was around 182 °C. Based on this temperature, a good agreement was found between the colour of burn-like marks on worn specimens and the steel tempering colour. Thus, it is reasonable to suggest that the higher wear produced by vegetable oils and vegetable oil-additive mixtures compared to MO in this study were due to the breakdown of the lubricants. The burn-like marks were not observed with the mineral oil suggest that the anti-wear additives were working efficiently with this oil to minimise metal-to-metal contact.

7.6 Elemental Analysis of Worn Specimens

EDX analysis was performed on worn specimens for all lubricants (Table 7.5). The amounts of oxygen and zinc that were detected on the specimens were easily

distinguishable and this could be the best basis for explaining the wear resistance results. The existence of oxygen could be related to retention of an oxide layer after the sliding process which influences to the friction and wear reduction [221]. The presence of zinc element was to form a protective layer by creating a barrier to prevent metal-to-metal contact. Both oxide layer and zinc protective layers are important in minimising the metal-to-metal contact between contacting bodies [50, 245].

The amount of oxygen in the MO lubricated specimen was the highest (10.43 wt%) when compared to others. This is associated with the lowest mass loss that the MO specimen produced. However, the amount of oxygen in the specimen lubricated with vegetable oils and vegetable oils-additive mixtures was not greatly retained. The amount of oxygen was slightly higher (1.43 wt%) found in the SBO lubricated specimen compared to the PO counterpart (1.17 wt%) and this was reflected in the result of the SBO wear performance, that was slightly better than PO. Although the oxygen detected in specimen lubricated with ZD:PO (2.25 wt%) and ZD:SBO (2.85 wt%) was higher than their pure oil state, they are about five orders of magnitude less than the oxygen amount detected in the MO lubricated surface and this is the reason why the higher wear was still produced. Furthermore, the amounts of zinc detected on the specimen lubricated with ZD:PO (0.03 wt%) and ZD:SBO (0.09 wt%) were relatively small compared to the MO specimen (0.9 wt%) and thus a thinner protective layer was thought to have formed. There was also a distinguishable amount of oxygen detected in hBN:PO (1.52 wt%) and hBN:SBO (1.71 wt%) compared to their pure oil state which presented a slight wear reduction in their specimens. However, no boron compound was detected on the worn specimens, which proves that the hBN particles have been flushed out in the lubricant during the sliding process. The relationship between the mass loss and the wt% of O and Zn is shown in

Figure 7.8. It shows a non-linear relation between the mass loss and the weight % for both elements. Based on the graph (Figure 7.8), the small amount of zinc in weight % tremendously reduced the mass loss compared to oxygen, suggesting that the protective layer was more influenced by the zinc.

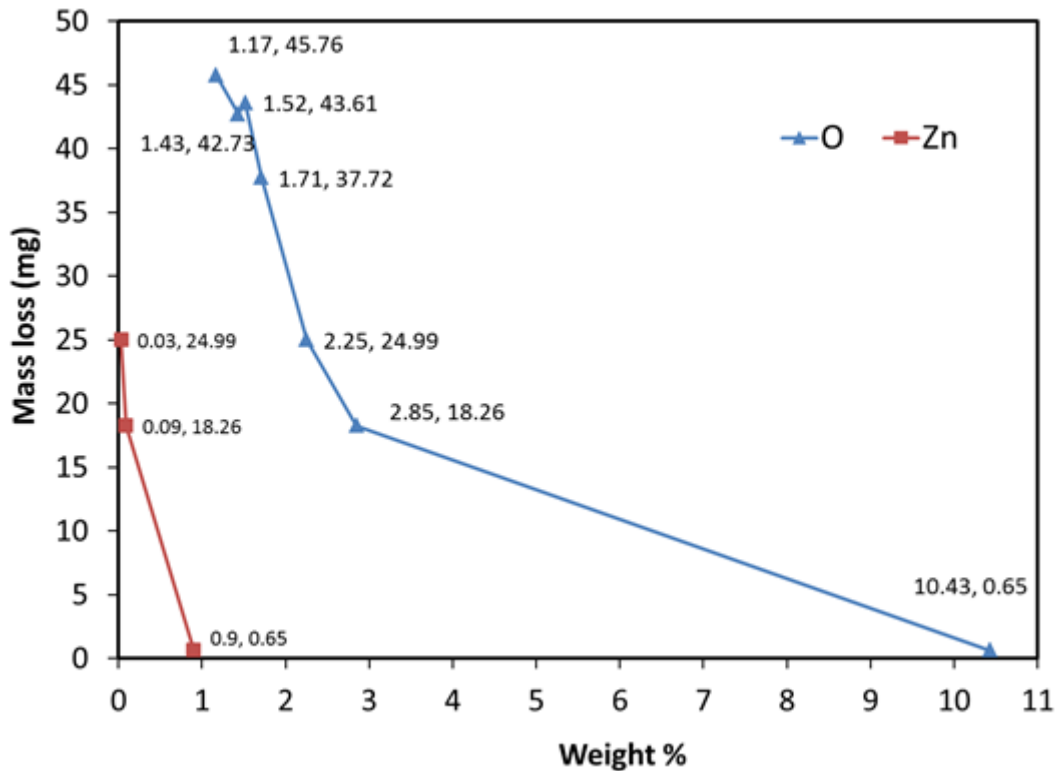


Figure 7.8: Relation between the weight % of oxygen and zinc to the mass loss of specimens in relation to EDX analysis results in Table 7.5.

7.7 Oil Viscosity Analysis

Figure 7.9 shows the dynamic viscosity results measured at 40°C and 100 °C for fresh oil and used oil from the wear test rig. At both temperatures, the MO samples showed a higher viscosity compared to vegetable oils and vegetable oil-additive mixtures. As expected, all lubricants showed a viscosity changes with temperature in which their value drops from a low temperature to a high temperature. However, the changes in

viscosity over temperature for vegetable oils and vegetable oil-additive mixtures were found to be lower than from the MO sample. This lack of influence of temperature on viscosity for vegetable oils compared to MO suggests that the vegetable oils have a strong interaction between molecules that are resilient to temperature change.

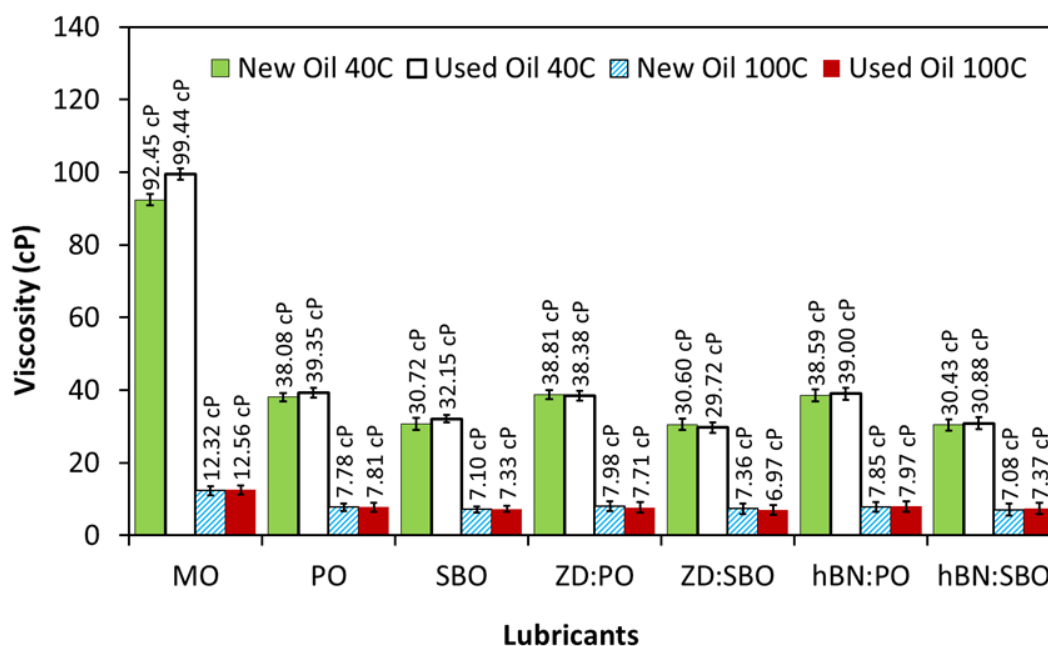


Figure 7.9: Viscosity of Mineral Oil (MO), Palm Oil (PO), Soybean Oil (SBO) and their blends with additives for fresh and used oil.

The viscosity value for all used oils after the wear test was not greatly changed which indicates that little or no oil thickening process occurs during a sliding test. It is also noted that the addition of additives in the vegetable oils has not caused any significant changes in the oil viscosity value. A higher wear rate was reported for a sliding test in lower viscosity lubricant oil [233]. Thus, the lower value of viscosity in vegetable oils compared to MO sample could be the reason to the lower wear resistance of their lubricated specimens. The minimum film thickness formula [211] is dependent on the oil viscosity, where higher viscosity oil promotes higher film thickness.

7.8 Oxidative Stability Analysis

The results of the oxidation stability tests for all lubricants performed using the rotary pressure vessel oxidation test (RPVOT) test rig are depicted in Figure 7.10. It was found that the MO sample showed the highest stability in oil oxidation (270 min) and recorded a higher peak pressure (200 psi) compared to the vegetable oils. The anti-oxidant additive that exists in MO (ZDDP) could prevent the rapid oxidation process.

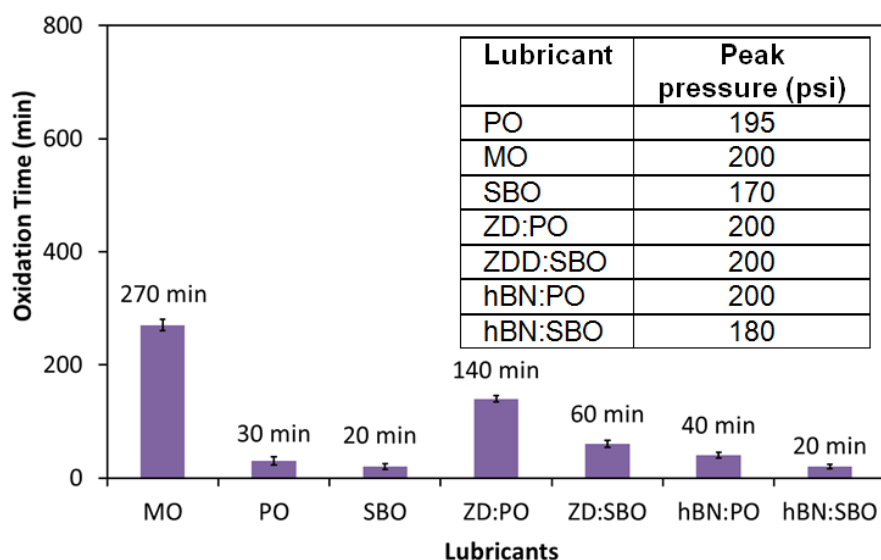


Figure 7.10: Rotary pressure vessel oxidation test (RPVOT) result for mineral oil (MO), palm oil (PO), soybean oil (SBO) and their blends with additives.

The lower oxidation stability that the vegetable oils have may cause their poor wear performance [11]. The lowest oxidation stability and lowest peak pressure indicates that the oxygen, that was pressurised in the pressure vessel of the machine, has reacted more quickly with the oil. In its pure oil state, SBO exhibited the lowest oxidation stability (20 min) with the lowest peak pressure (170 psi). The higher amount of unsaturated fatty acids in SBO compared to PO has made it more susceptible to oxidation. The higher unsaturated fatty acids in SBO compared to PO has made it more susceptible to oxidation. The

additions of additives in vegetable oils have led to an improvement in oxidation stability, especially in ZD:PO. This clearly indicates that the ZDDP was actively performing as an anti-oxidant agent in delaying the oxidation process in vegetable oils. The higher oxidation stability of ZD:PO could probably be the main factor that influenced to the reduction of wear. However, the oxidation stability of ZD:PO is relatively lower than the MO sample which recorded about 50% less than the MO's oxidation time.

The higher oxidation stability of ZD:PO compared to ZD:SBO was influenced by their base oil performance. The pure PO has higher oxidative stability compared to pure SBO. The oxidation results for ZD:PO and ZD:SBO was also exhibited a similar trend (ZD:PO was higher than ZD:SBO). A slight improvement in oxidation stability was also seen in hBN:PO which is likely attributed to the small volume of mineral oil in the mixture that acted as a carrier fluid for the hBN additive. Mineral oil performed well in oxidation stability. In addition, there is no evidence found in literature that the hBN may act as an anti-oxidant agent.

7.9 Acid Number Analysis

The acid number (AN) for all lubricants tested in the form of fresh oil, used oil from wear test rig and used oil from the RPVOT test rig is depicted in Figure 7.11. AN is a measurement of oil acidity that is to quantify the amount of potassium hydroxide (KOH) in miligram needed to neutralise one gram of oil. Measurement of AN is important in lubricant studies in order to monitor the oil oxidation level (ASTM D664-11a).

In an oxidised oil, the hydroperoxide which is formed during propagation stage, may form oxygenated compounds like aldehydes and ketone which then may react further

to form organic acids with the existence of oxygen [250]. It can be seen that the pure vegetable oils (PO and SBO) exhibited the lowest AN compared to MO and their vegetable oil-additive mixtures in fresh oil state. It is also noted the MO sample and vegetable oil-additive mixtures recorded a higher AN. All of the used oils from the wear test rig have also shown an increase in AN. However, the AN values for used oils from the wear test rig were relatively small compared the AN after RPVOT.

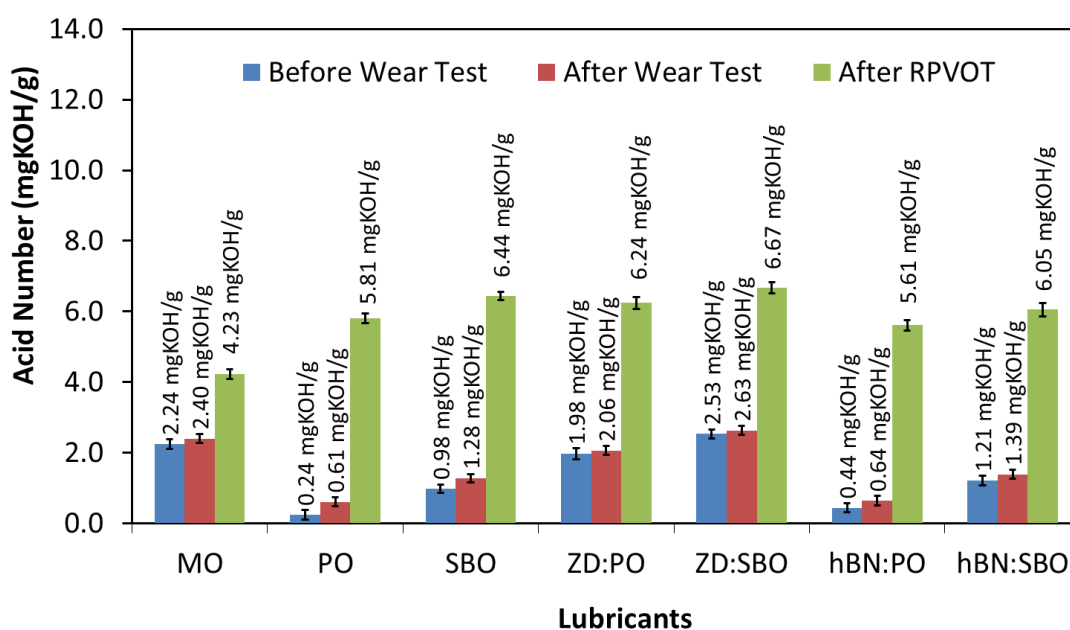


Figure 7.11: Acid number for all lubricants.

The higher AN value from fresh SBO (0.98 mgKOH/g) relative to PO (1.98 mgKOH/g) is possibly due to the higher acidity of the free fatty acid that is inherent in unrefined oil (SBO). During the refining process, most of the free fatty acids are removed [251]. The higher AN in the MO sample and vegetable oil-additive mixtures could be attributed to certain additives like ZDDP that exist in lubricating oils that may increase the AN in a base oil [252]. This was confirmed by the AN value of ZD:PO and ZD:SBO where significant increases in AN were seen when the ZDDP was added to pure PO and SBO. The highest AN recorded for oil samples taken from RPVOT test rig have confirmed

that acids were produced during the oil oxidation process. This reinforces the earlier notion that an oxidised oil has a higher AN than the fresh oil sample and that the oils have been oxidised or started to oxidise after the wear test. This may also have contributed to higher wear in ZD:PO and ZD:SBO compared to MO as ZDDP is less efficient as anti-wear agent when it reacts with the peroxy radical that builds up in oxidised oil [253].

7.10 Conclusions and Summary

From the results presented of experiments conducted at severe contact conditions involving vegetable oils and their blends with additives (combined together and summarised in Table 7.6), the following conclusions can be drawn:

- The addition of 2% ZDDP in vegetable oils did not influence the fatty acid composition in vegetable oils. However, this level of additive has led to a significant improvement in wear, friction and oxidation stability.
- The amount of oxygen detected on worn specimens was found to be related to the amount of mass loss and the amount of zinc found on the worn surface was significantly related to the level of wear.
- The oxidative stability of oil and the surface waviness of the worn specimens are the factors most strongly related to the mass loss of specimens. The level of change in surface roughness of the specimen in the wear scar region was dependent on the friction coefficient during a particular test. The higher the friction, the higher the surface roughness.

Table 7.6: Summary of friction and wear results in relation to other experimental data

Lubricants	Mass loss (mg)	COF	Surface Waviness, Wa (μm)	Surface Roughness at M2 point, Ra (μm)	Viscosity at 100 °C (cP)	Oxidation Time (min)	TAN (mgKOH/g)	Zn (wt%)	O (wt%)	Zn (ppm)	B (ppm)
MO	0.65	0.093	1.4	0.06	12.32	270	2.24	0.9	10.43	781	43
ZD:SBO	18.26	0.099	17.16	0.23	7.36	60	2.53	0.09	2.85	1129	0
ZD:PO	24.99	0.095	29.08	0.24	7.98	140	1.98	0.03	2.25	1153	3
hBN:SBO	37.72	0.116	30.88	0.38	7.08	20	1.21	-	1.71	65	357
SBO	42.73	0.112	36.29	0.27	7.1	20	0.98	-	1.43	3	1
hBN:PO	43.61	0.111	35.72	0.32	7.85	40	0.44	-	1.52	65	342
PO	45.76	0.105	41.43	0.26	7.78	30	0.24	-	1.17	1	2

- The ZDDP was found to perform three tribological functions when used as an additive in vegetable oils: as an anti-wear agent, as an antioxidant, and as a friction modifier.
- Of the additive-vegetable oil mixtures, the ZD:PO oil provided the best friction reduction while the ZD:SBO provided the best wear resistance.
- The tribological performance of vegetable oil-additive blends was dependent on the tribological performance of its base oil.
- The function of hexagonal Boron Nitride as an anti-wear additive is less effective when the particles size is greater than the surface roughness.

In view of the presence of molybdenum and zinc and their contribution to the performance of the MO, a combination of ZDDP with MoDDP or MoDTC additive should be considered for future work aiming to improve the tribological performance of vegetable oil. Much more development is also needed to be carried out on formulating vegetable oil based lubricants for them to be viable alternatives to hydrocarbon-based lubricants

Chapter 8: Discussion of the tribological performance of vegetable oils

This chapter aims to highlight and connect the main tribological results found in the Results and Discussions chapters. Each chapter (Chapters 4-7) that was represented individually in this thesis are linked together here to show their commonality that drives the overall outcomes of this study. A brief description of the rationale and the needs of the testing described in each chapter is presented, underlining the key issues, along with possible explanations and issues interconnected to the next part of the work (i.e. the next chapter). Some of the evidence collected from the friction and wear tests, specimens' analyses and oil analyses have been used as the basis for the discussion and they are cross-referenced with the relevant published literature where necessary. A final summary covering the overall findings and discussion of the study as a whole is also included.

8.1 Responses of grey cast iron specimens' hardness on friction and wear of vegetable oil

Before evaluating the tribological performance of vegetable oils, it is important to assess the possibility of producing an unintentional error during the experiment. This kind of error may come from several sources and may affect the reliability of the measured data. It includes the errors that come from materials (non-uniformity of specimens' strength), test rig (machine vibration, load cell calibration, test set-up etc.) and the lubricants (composition of elements).

In this study, during the trial and error run of grey cast iron specimens lubricated with vegetable oil, it was found that the mass loss data varied considerably between tests.

Further investigation was conducted by means of checking the hardness of the grey cast iron specimens and comparing with the value published in the relevant standard (BS EN1561:2011) and previous literature [162]. It was found that the hardness of grey cast iron specimens varied greatly, even within the same specimen (Appendix 1). To minimise the experimental error that may come from the variations in the material properties, the grey cast iron specimens used in this study have been strictly examined. This was done by measuring the hardness directly on the intended wear scar region and the average hardness was taken based on hardness value at three points on the intended wear scar. The friction and wear response of different specimens hardness (low, medium and high hardness) with the soybean oil were then performed as described in Chapter 4.

Through analysis of the hardness measurement results on the intended location of the wear scar of the grey cast iron specimens, the hardness range was found to be very high (65 HV; lowest value 185 HV to highest value 250 HV). Based on this hardness range, the specimens were then classified into three groups to represent low, medium and high hardness (Table 4.2). This classification is important in order to evaluate the response of specimens' hardness on the friction and wear performance of vegetable oils. It should also be noted that the majority of the specimens' hardness on the intended wear scar was in the range of 200 HV-210 HV. Thus, the specimens in this hardness range are the most suitable to be used for conducting the experiments described in Chapter 5, 6 and 7.

The wide hardness range of grey cast iron specimens produced in this study (65 HV) was reliable data as this value is close to the standard (70 HB in range, BS EN1561:2011) and similar with the hardness range found in the previous work (65 HB) [162]. The factors that influence the variation of hardness in the grey cast iron specimens may include the element composition, size of flake graphite and distribution on the metal

matrix and processing variable in the foundry such as the casting cooling rate [166, 213]. The graphite size on the different position of the material (either at centre or corner position) is very much influenced by the casting cooling rate [166]. A slow cooling rate (typically occurs at the centre position) tends to produce bigger graphite size in grey cast iron microstructure thus, promoting lower hardness [166, 167]. In addition, it was reported that higher cooling rates are associated with the dendrite fineness as a result of the decreasing in the distance between the dendritic arms in GCI specimens which produce higher hardness [254]. Results found on the further examinations on the material cut out of the specimens were agreed with this idea. The differences in graphite size and graphite distribution are shown by low and high hardness specimens (Figure 4.10) as well as the metal matrix distribution (pearlite and ferrite) support the former explanation [166, 167, 254] that the material hardness in the grey cast iron was influenced by the graphite size and distribution which associate with the casting cooling rate.

From the results of friction and wear tests conducted at the different specimen hardnesses (low, medium and high hardness) on the intended wear scar region by soybean oil, it was found that the tribological results were significant. The differences of the friction coefficient between the low and high hardness specimens were about 13%, but for wear it was much higher (74%). The results show that the wide hardness range issue in grey cast iron specimens is a very important aspect to be considered before conducting the friction and wear test especially involving vegetable oil with reciprocating sliding point contact. The hardness then needs to be properly measured and controlled on the intended wear scar before the test begins. In this study, the hardness was measured on the intended wear scar by three points that have about 5 mm gaps in between (Figure 3.3). If the hardness measurement is not taken seriously or the specimen hardness is assumed as a

bulk value, it may contribute to the producing of unreliable tribological test data (produce higher data variation between tests) especially for evaluation of reciprocating sliding point contact with the vegetable oils.

Despite GCI specimens having a great influence on the assessment of the tribological performance of vegetable oil in reciprocating sliding point contact, many reports published previously ignored the wide range of hardness and used bulk value as a single value (for example, 265 HV [150] and 195 HB [165]) of GCI hardness prior to conducting their tribological test. They also did not highlight any issues regarding the variation in their friction and wear test data as has been emphasised in this study. This was probably due to their type of contact being different from the one used in this study, i.e., they were using a conformal contact like pin-on-disc [150] and curved surface on a rotating ring [165]. This conformal contact could be less sensitive in responding to the wide hardness distribution on the GCI specimen surface compared to the point contact. In a conformal contact, the two surfaces have closely matched curvatures with each other with a high degree of geometrical conformity. As a result, the load is carried over a large area of surface interaction and the localised pressure concentration at the interface is low. Thus, the variance in the tribological performance, especially on the wear resistance, due to wide hardness distribution on the surface could not be seen significantly.

Another possible reason might be due to the amount of load applied in the previous cases [150, 165] resulting in a very low contact pressure compared to the pressure applied in this study (1.7 GPa). For example, it is estimated that the maximum pressure applied in both cases above were 0.19 GPa [150] and 0.935 MPa [165] which produce a pressure to shear strength ratio to 0.7 and 0.003 respectively (calculations based on Figure 4.7). These lower contact pressures show that the wear process could occur in the elastic region

(Figure 4.7) and possibly far from the limit of severe wear. Thus, they are not very sensitive in responding to the wide distribution of hardness on the surface, especially to the lower hardness area. Compared to this study, the 1.7 GPa contact pressure applied was very high (beyond the plastic limit in Figure 4.7) and could be very sensitive to the lower hardness area and thus, sufficient enough to produce severe wear.

In summary, the wide range of grey cast iron specimens' hardness have shown evidence of producing high difference in the tribological performance when tested with the vegetable oil, particularly by reciprocating sliding point contact. They may produce a high standard deviation for friction and wear results between specimens with different hardness. This hardness issue has to be taken into consideration in the remainder of the work presented here as it may lead to producing false results especially in the case of comparing two lubricants with small differences in their friction and wear performance. Thus, a tight material characterisation has been implemented throughout the study (as presented in Chapters 5-7) by only allowing the specimens that have a hardness on the intended wear scar in the range of 200-210 HV.

8.2 Tribological performance of pure vegetable oils

In conducting research on vegetable oils as biolubricants, it is important to establish their base line performance in friction and wear before any improvement is made to them. Further to this, an understanding of the compositions of pure vegetable oils and their lubrication mechanisms is also needed. As such, tribological tests involving palm oil and soybean oil in its pure state were conducted by a reciprocating sliding point contact in Chapter 5. It is well known that commercial lubricants used in automotive engines have

been developed by formulating base oil with additive packages that provide excellent engine protection. As a reference for future improvement work, it is also important to include data that shows how much the friction and wear of these pure vegetable oils are different from that of the commercial oils. Thus, a similar tribological test was also conducted on the mineral engine oil (15W 40). As the issue of grey cast iron specimens hardness has been identified, the specimens with a tight hardness range of 200 HV-210 HV on the intended wear scar have been used in this study.

In comparing both vegetable oils, the friction performance shown by pure PO and SBO is not much different in which the pure PO (COF=0.105) exhibited slightly lower friction than the SBO (COF=0.112). The difference in COF could be explained by the types and composition of fatty acids in both oils. The COF increases with increasing in unsaturation of fatty acids in which the saturated acid exhibited lower friction coefficient than the unsaturated acids [134]. In this case, higher degrees of saturated fatty acids (dominant in PO) are consisting of a straight chain molecular structure. When they are adsorbed on the surface, they tend to align themselves in a linear fashion on the surfaces. This adsorbed structure could then produce a smoother interaction of molecules between surfaces during relative motion and thus, minimise the friction (Figure 5.5a).

The lower friction result shown by PO compared to SBO, however, is not similar to the result found in wear resistance. The PO, recorded higher mass loss (45.76 mg) compared to SBO (42.73 mg). This fact discloses that in vegetable oil lubrication, friction and wear are not related, leading to a suggestion that a base oil selection is very important in aiming for either friction or wear improvement. Previous studies on the tribological performance of vegetable oils also show that their relationship between friction and wear with vegetable oils is commonplace [9, 130, 255]. For example, it was recorded by a four-

ball-tester that soybean oil produced higher friction than palm oil, but in terms of wear resistance, it was reversed [9]. Similarly, by pin-on-disc machine, the soybean oil produced higher wear compared to corn oil, but for friction, it was lower [130]. However, these authors did not discuss the reason for this observation.

In this study, it is suggested that this opposite relation between friction and wear in vegetable oils was due to their amount and molecular chain structure of fatty acids. PO and SBO are different in terms of fatty acid types and compositions. It is proposed (Figure 5.5) that the saturated fatty acids which are enriched in PO may form in a linear orientation and thus smooth the motion on the surface. However, this linear orientation tends to produce spaces in between carbon chains and these spaces may be easily filled up by other carbon chains from the opposite surface and thus promote metal-to-metal contact. SBO, on the other hand, is enriched with unsaturated fatty acids, which consist of bent carbon chains. These bent chains could increase the resistance of motion on the surfaces when they are interacting during sliding. However, when the contacting surfaces are loaded during sliding motion, the bent chain may be overlapped and thus provide an extra protective layer and minimise metal-to-metal contact. The same reason proposed above might also be used in comparing the performance of pure soybean oil and corn oil as reported in the previous study [130]. Although the amount of saturated acids in both oils (soybean oil and corn oil [256]) are almost similar, they differ in the amount of unsaturated fatty acids (corn oil has higher oleic and linoleic acids). Higher unsaturated acids in the corn oil compared to soybean oil could produce higher friction, but possibly lower the wear due to more bent carbon chains existing in the oil.

In relation to the COF of mineral engine oil (15W 40) that is used as a reference oil in this study, the COF produced by the vegetable oils is competitive (Figure 5.1). The pure

PO, although it produced higher COF than fully formulated MO, the difference is only 11%. This shows that the pure vegetable oils have a potential characteristic as a base oil for biolubricants development. Fatty acids that exist in the vegetable oil are polar molecules which are easily attracted to the metal surfaces by the mechanism of chemisorption and thus provide a layer to minimise friction [111].

In terms of wear performance, both vegetable oils exhibited inferior wear compared to the MO (about 98% differences, Figure 5.4). The SBO mass loss (42.73 mg) was more than fifty orders of magnitude higher compared to MO (0.65 mg). Catastrophic damage (the wavy-shape wear scars) can also be observed in vegetable oils lubricated specimens compared to the MO counterpart. Through examination, under the optical microscope, of the worn surfaces, it can be seen that there are several burn-like marks visible at some areas (brownish colour, Figure 5.9). These burn-like marks may be produced by frictional heating due to metal-to-metal contact during sliding at some asperities. The frictional heating could increase the surface temperature and thus, may change the surface colour.

To verify this suggestion, a surface temperature calculation was carried out (Appendix 9) and compared with the image of heat treated steel (Figure 5.6). It was found that a good agreement is achieved between the surface temperature values (204 °C for SBO), the colour of steel heat treated images (brownish colour at about 204 °C) and the colour of burn-like marks image suggested that the vegetable oils experienced a lubrication breakdown at severe contact conditions. In addition to this, the appearances of severe abrasion on the worn surfaces of PO and SBO compared to MO (SEM images, Figure 5.10), could also be used to support the claim of lubrication breakdown. A complete

breakdown of the wear surface is evidenced by the appearance of smearing and tearing of the steel surface with grooving up to 200 μm [257] and this value is almost similar with the depth of wear scar found in PO and SBO specimens (more than 200 μm , Figure 5.7).

The poor wear performance results exhibited by both vegetable oils in this study is as expected because the protective film on the surface formed by their fatty acid molecules is easily removed under extreme operating conditions [44, 258]. However, the question of how much the protection layer has been removed during sliding is something interesting to be highlighted here. This is prompted by the indication that the large percentage difference shown by the vegetable oils compared to the mineral engine oil in wear resistance (about 98%) did not seem to be reflected in the friction coefficient differences (about 11%). Although the wear performance of vegetable oils was extremely poor, the friction performance is fair relatively to the fully formulated mineral engine oil. A similar result was reported by Gerbig (using reciprocating test by steel materials) [14] who indicated that vegetable oils are competitive in terms of friction coefficient rather than wear resistance when compared with the mineral oil and synthetic esters. This brings about a suggestion that the protective layer formed by fatty acids was not completely removed during sliding, but rather leaving a small part of its working layer on the surface to improve the friction as shown through the friction results. This could possibly happen in certain areas, especially in the middle space between asperities where there is no metal-to-metal contact exist.

Other factors that may contribute to the higher wear of vegetable oil lubrication are the oxidation of the oil. The increase of hydroperoxide level in oxidised vegetable oils has shown a significant effect on wear [124]. It was exhibited that the oxidative stability of vegetable oils in this study is very poor compared to the MO counterpart (Figure 5.13).

Similarly, it was found that the oil viscosity and the acid number were slightly increased after the experiment (Figure 5.11 and Figure 5.12) suggesting that the oil in the test rig experienced mild oxidation [44, 120]. Higher wear resistance results in MO lubricated specimens are likely to be linked with the additive packages that exist in its formulation. The existence of elements like zinc, molybdenum and boron in the MO sample (Table 5.2) suggest that its base oil has been treated with an anti-wear additive, antioxidant and friction modifier which may include zinc dialkyldithiophosphate, boron nitride and molybdenum dithiocarbamate or dithiophosphate.

Another observation that is important to be discussed here was the formation of the wavy shape of wear scar on the specimens produced by the pure vegetable oils after the wear test. This could be a sign of catastrophic damage which is caused by the breakdown of vegetable oil lubricants at severe sliding contacts conditions. This wavy-shaped wear scars are similar to the appearances of wear scar found on the test of hard steel balls (AISI 52100) on soft steel plates (NSOH B01) carried out by Plint [259]. However, the reason for the formation of this shape after the sliding process was unexplained. It was also suggested that this phenomenon occurred due to the applied load in this study having entered the plastic ratcheting region which is beyond the shakedown limit (Figure 4.7) [218]. In the plastic ratcheting region, large plastic strains are slowly accumulated and superimposed during each sliding cycle (forward and backward sliding motion) as proposed in Figure 4.9.

In summary, the results found in this part of the study (Chapter 5) have provided baseline data for the friction, wear and oxidation stability of the pure vegetable oils (palm oil and soybean oil) with regard to a commercial mineral engine oil. The friction coefficient of pure vegetable oils shows competitiveness and indicates potential

opportunities for future development. This friction coefficient result has also motivated a question on how efficiently the fatty acids layer is removed from the surfaces during the sliding process at severe contact conditions.

However, the direct use of pure vegetable oils as a lubricant in the automotive engine could be disastrous to the engine components as they produced very high wear due to the breakdown of lubrication. The lubrication mechanism of pure vegetable oils, influenced by the molecular structure of the saturated and unsaturated fatty acids, has been proposed. Apart from the high levels of wear, the protective layer of vegetable oils formed by their fatty acids is thought not to be entirely removed during the extreme sliding conditions, but rather leaving some space for the layer to encounter the friction. The test results of palm oil and soybean oil also reveal that the friction and wear are not related. That said, in prioritising either friction or wear improvement, a base oil selection is significant.

The large differential in wear resistance result of the MO compared to pure vegetable oils creates great opportunities for improvement. The element compositions traced in the MO have triggered an interesting idea to be studied on what will happen if they exist in the vegetable oils. These trace elements which include the additive packages in the MO are believed to be a major contributor to its lubrication effectiveness. However, the investigation on the effects of the each traced additive element found in the MO sample in the vegetable oil could be a long term research. One alternative of this could be by formulating a mixture of lubricant which combines both mineral engine oil and vegetable oil at 1:1 blend ratio. In this blend ratio (vegetable oil-mineral oil blend), the additives packages that exist in the MO are still in the oil blend where the amount is assumed to be reduced by about 50% from the original concentration of the MO. In this formulation, a

half volume of MO is mixed with another half volume of vegetable oil (from the original volume of lubricant in the oil bath of the test rig) with a half concentration of MO additives. The effect of MO additive packages in the vegetable oils could produce a friction and wear data in between of the MO and the pure vegetable oil and the middle value is expected as a hypothesis of the test.

8.3 Tribological Performance of vegetable oil-mineral oil blend

The mineral engine oil used in Chapter 5 is a fully formulated oil with an additive packages which includes an anti-wear additive. As a result, it the MO depicted a superior tribological performance when compared to the pure vegetable oils particularly in wear resistance. In view of the wear result gap between the MO and vegetable oils (98% in differences), an idea has been triggered to observe on how much improvement can be made on the vegetable oils performance with the help of MO.

The first attempt to find the improvement on the tribological performance of the vegetable oils is made by blending them with a commercial mineral engine oil at an equal blend ratio (Chapter 6). Apart from finding an improvement, the idea of this blending is to evaluate the response of the additive packages that exist in the MO sample in the vegetable oils. This method could be the simplest and quickest way as it did not require any complex chemical process or formulation. However, the additive packages contained in the vegetable oil-mineral oil blend are expected to be diluted to about half of their concentration as compared to the original volume of the MO. The effectiveness of the additive packages in the vegetable oil is judged based on the expected tribological results, i.e., the blended oil could at least achieve a middle value in between the tribological

performance shown by pure vegetable oil and MO. This hypothesis is based on the previous literature on the two vegetable oils blend [140] and vegetable oil-mineral oil blends [22] which achieves a mean value of fatty acid compositions [140] and mean value of additives concentration [22] in their oil blends at 50:50 ratio.

As expected, the spectrochemical result for the vegetable oil-mineral oil blends at 1:1 blend ratio exhibited that all additive elements in MO have reduced into about 50% in their concentration (ppm, Table 6.2). For example, the value of zinc element in MO was 781 ppm and when the MO is blended into PO, it has reduced to 389 ppm. The reduction of about 50% in additive concentration found in this study is similar to the result reported by Shahabuddin et al. [22], i.e., when a jatropha oil is blended with a commercial lubricant (SAE 40) at 50:50 blend ratio. As a result, the 50% reduction of the additives in the half volume of MO used in the blended oils has influenced to their tribological performance (Figure 6.1 and Figure 6.2). In addition to this, the tribological results found in the vegetable oil-mineral oil blends have produced a value in between the value of MO and vegetable oil in its pure state.

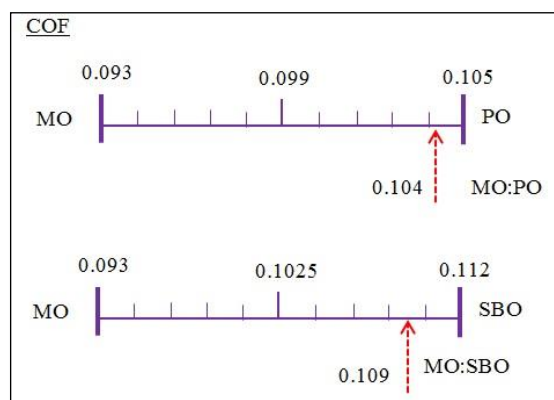


Figure 8.1: Coefficient of friction results for MO:PO and MO:SBO compared to their pure oil state.

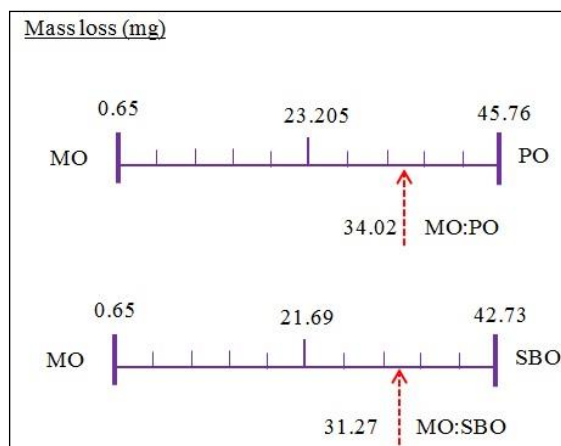


Figure 8.2: Mass loss results for MO:PO and MO:SBO compared to their pure oil state.

The detailed data of the friction, wear and oxidation stability of the blended oils, however, have shown a biased result where the values were nearer to the vegetable oils side (Figure 8.1, Figure 8.2 and Figure 8.3). It is interesting to note that although the MO exhibited a superior result in wear resistance compared to its vegetable oil counterpart, the addition of 50% of MO in the vegetable oils failed to contribute similarly to the wear resistance enhancement (differences in wear is more than 40 orders of magnitude compared to MO). It is recorded that the mass losses for MO:PO specimens (34.02 mg) are much closer to the mass losses of the PO specimens (45.47 mg) compared to MO specimens (0.65 mg). In the same way, the friction improvement found in the vegetable oil-mineral oil blends was very small. The COF for PO:MO blend has 1% lesser than the COF of PO. Similarly, the SBO:MO blend only reduced the friction by 3% compared to SBO in its pure state. This indicates that in a 1:1 blend ratio of vegetable oil-mineral oil, the vegetable oil has a strong domination and very much impacts in influencing the friction and wear performance. The higher wear and friction results presented by the MO-vegetable oil blends in this study have shown a similar trend when a mix of 50% jatropha oil with 50% of commercial lubricant (SAE 40) was tested by pin-on-disk tester [22].

However, in that study [22], the author was not comparing the performance with the pure jatropha oil and the reason behind the higher friction and wear results at a particular percentage of 50% was unexplained.

The strong dominance shown by the vegetable oils in the vegetable oil-mineral oil blends in friction and wear results may indicate the failure of MO additives to be fully adsorbed on the surfaces. This is probably because of there are some areas on the surfaces that are still covered by the fatty acid molecules as suggested in the above section (Section 8.2) which hinders the MO additive activities on the surface. A previous study by Vizintin et al. [258] on the addition of extreme pressure (EP) additive in rapeseed-based oil could be used to back-up this claim. Vizintin et al. [258] found that at a low contact pressure (1.0-2.5 GPa) the wear performance for rapeseed oil-EP additive has no significant difference from the rapeseed oil alone. However, at a higher contact pressure (3.17 GPa) the wear for rapeseed oil with the EP additive dropped a lot. Vizintin et al. [258] suggest that the EP additive only started to work at higher contact pressure, i.e., when the adsorption film of the rapeseed oil was completely breaking down. Another possible reason for the failure of MO additives to effectively work on the surfaces lubricated by the vegetable oil-MO blend might be due to the competition of additives on the surfaces. Studt [260] found that the increase in the amount of polar compounds in oil could reduce the adsorption of additives on the metal surface due to competitive adsorption, which leads to the inefficiency of anti-wear additives. Similarly, due to the high polarity of the fatty acid molecules in the vegetable oil, which strongly adsorbed on the surface, the MO additives that exist in the oil blend are incapable of settling down on the surface; the efficiency of anti-wear additives is thus decreased.

The similar trend of the vegetable oil domination in the friction and wear results of vegetable oil-mineral oil blend was also found in the oxidation stability test (Figure 8.3). Contrary to this, it was reported in the previous study that when two vegetable oils are blended at 50:50 volume ratio, the oxidation behaviour is produced in between (mean value) of their pure oil value [140]. In this study, the oxidation time in MO:PO (90 min) is closer to the oxidation time of PO (30 min) and far lower compared to MO (270 min). Similarly, for MO:SBO, the oxidation time (35 min) was closer to its pure SBO (20 min). This shows that the existence of unsaturated fatty acids (with the presence of carbon double bond in their structure) in both PO and SBO are very strong in promoting the rapid oxidation of the vegetable oil-mineral oil blend. The total percentage of unsaturated fatty acids in PO (54.9%) and SBO were high (83.3%) (Figure 5.2) and this could lessen the effect of the anti-oxidant that exists in the oil blends. The carbon double bond in unsaturated acids is more reactive [256] and this has made the MO:SBO blend more unstable to oxidation compared to PO:SBO.

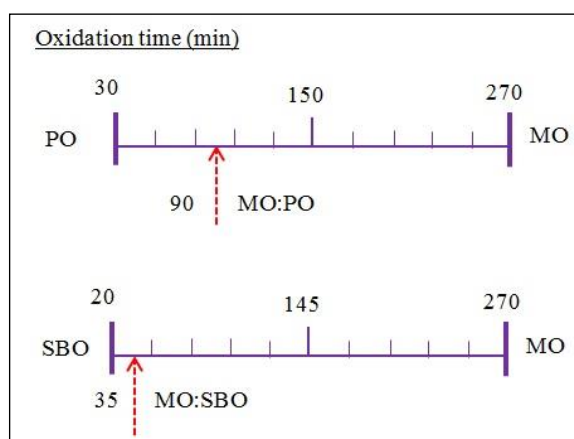


Figure 8.3: Oil oxidation results for MO:PO and MO:SBO compared to their pure oil state.

Another observation found from the friction result could mean that the COF for vegetable oil-mineral oil blend was following the trend of COF for its pure state. For instance, the PO has lower COF than the SBO and this trend is followed by the PO:MO blend where it has lower COF than the SBO:MO. Similarly, the higher mass loss exhibited by MO:PO compared to MO:SBO was related with the mass loss result of PO which is higher than the SBO. Based on these findings, it is clearly shown that the performance of vegetable oil-mineral oil blends was influenced by the type of base oil (vegetable oil) used in the oil blend. This suggests that the lubrication mechanism (proposed in Figure 5.5) that explains the phenomenon of opposite relation between friction and wear of PO and SBO may be still valid in the blended oils. The existence of the base oil of the MO with the additive packages in the vegetable oil-mineral oil blends possibly did not change the molecular structure of fatty acids that were attracted to the surfaces.

In view of the tribological results found in Chapter 6, a lubrication mechanism for vegetable oil-mineral oil blend was proposed in Figure 6.3 (comparison between PO, MO and MO:PO). This explains how the vegetable oil could play an important role in influencing the wear in the vegetable oil-mineral oil blend. It is suggested that due to the polarity of vegetable oil, the carboxyl group in fatty acids molecules are possibly attracted to the metal surfaces, thus, blocking some of the antiwear additives from the MO settling down on the contacting surfaces. Furthermore, this has prevented the formation of a fully protective layer by the MO anti-wear additives and thus contributed to higher wear. The elemental analysis of the worn specimens lubricated by the blended oils and MO support this proposal (Table 6.5). It should also be noted that the zinc element detected in MO:SBO specimens (0.01 wt%) was too little compared to the one detected in MO

specimens (0.90 wt%) despite the zinc concentration was reduced by only about 50% in the MO:SBO (spectrochemical analysis, Table 6.2).

In summary, the formulation of vegetable oil-mineral oil blended lubricants at a 1:1 ratio has failed to achieve the targeted tribological improvement, at least to attain a mean value of the tribological performance in between the value of vegetable oil and mineral oil. The use of diluted additive packages in the oil blends has shown ineffective functionality in improving friction and wear due to the presence of vegetable oil. This is probably due to the existence of the fatty acid layer on the surface even though after sliding and their polarity characteristic that might be blocking and preventing the additives from settling down on the surfaces. The use of a single anti-wear additive in higher concentration (compared to the concentration in the vegetable oil-mineral oil blends) in the vegetable oil alone might be able to verify this suggestion, as well as to improve the overall tribological performance.

8.4 Tribological Performance of vegetable oil-anti-wear additive blend

The outcome of blending the mineral oil with the vegetable oils at a 1:1 volume ratio, besides evidencing their poor tribological performance, is to trigger an initial clue about how the conventional anti-wear additives will work on a surface lubricated by the vegetable oils. In Chapter 6, the vegetable oils have shown their dominant factor in influencing the friction and wear of the oil blends. Although the elements of MO additives were detected in high amounts in the vegetable oil-mineral oil blends, their amount in elemental analysis of worn specimens was relatively little. It is also proposed in Chapter 6

that the fatty acid's polarity in the vegetable oils might have lessened the role of the anti-wear additive on the surface.

In Chapter 7, the main idea of the work was focusing on the final objectives of this research, i.e., to find the tribological improvement of vegetable oils through the use of additives. Thus, the direct blend of a single anti-wear additive in the pure vegetable oil is implemented in Chapter 7. Apart from seeking a tribological improvement and investigating the additive response in the vegetable oil, it also can be used to verify the earlier suggestion that was proposed in Chapter 6 (Figure 6.3) that said, the polarity of fatty acids in the vegetable oil has prevented the additives from being adsorbed onto the surface. The antiwear additives used in Chapter 7 are those from commercial additives that have been claimed to perform well with the commercial mineral engine oil by the manufacturer (zinc dialkyl dithiophosphate and boron compound).

The PO and SBO blended with the ZDDP additive showed positive results in friction reduction and a similar response was observed when the ZDDP was mixed with other vegetable oils [12, 29, 142]. It should be noted that the ZD:PO lubricant presented a very competitive COF value (0.095) compared to the COF of MO (0.093). The lower COF of MO than ZD:PO could be caused by the molybdenum element detected in the MO sample. The existence of molybdenum element suggests that this oil may contain either molybdenum-dithiophosphate (MoDDP) or molybdenum-dithiocarbamate (MoDTC) additives as these additives reduce the COF in engine oil [225]. It is generally accepted that the role of ZDDP in lubricant oil is to form a series of pad-like structure on the surface which comprises a glassy, mixed iron and zinc phosphate layer [96]. This layer may serve as a protective film in minimising the metal-to-metal contact and thus, reducing friction in the vegetable oil.

One interesting outcome shown by the friction results in this study is the addition of 2% ZDDP into the pure PO, where the friction level of the oil blend has been reduced to a level comparable to the fully formulated MO (contains molybdenum based friction modifier). There are at least two logical reasons that can be used to explain this result. Firstly, it can probably be linked to the claim made in Section 8.2 above. That said, the protective layer of vegetable oils formed by their fatty acids is not entirely removed at the 1.7 GPa applied in this study, but leaves some area for the protective layer to lower the friction (explanation was based on the result of extreme pressure additive in rapeseed oil at low and high contact pressure conducted by Vizintin et al. [258]). This unremoved fatty acid layer could still be intact on the surface and thus, may serve as a friction modifier in reducing the friction (also shown by the small difference of 11% in the pure PO and MO friction result presented in Chapter 5). In addition, the saturated acids such as palmitic acid that is comprised plentifully in the PO have a well-known history as effective friction modifiers [67]. Therefore, it can be seen that although with the absence of the molybdenum based friction modifier in the blended oil, the friction in the ZD:PO was comparable to the fully formulated MO. Secondly, the concentration of the zinc found in the ZD:PO oil blend (1153 ppm) was relatively very high compared to the MO (781 ppm). Although the earlier claim suggests that the polarity of the fatty acids might prevent the MO additives from being adsorbed on the surfaces, the use of higher concentration might be able to allow more additive to attract onto the surface. In addition, it was reported that the concentration of an extreme pressure additive on the surface and its absorbability is increased as the concentration in the bulk oil increases [260]. Further to this, it was also reported that the friction coefficient for the canola oil with 2% concentration of ZDDP was lower compared to the 1% concentration and pure canola oil [261]. A higher concentration means higher chances for the additives to be adsorbed onto the surface.

Contrary to this, the boron nitride has failed to lower the COF of oil blends compared to their pure oil state. The blending of hBN:SBO exhibited the highest COF. The size of boron nitride particles used in this study (0.5 μm) is much higher than the average surface roughness of the specimens ($R_a = 0.15 \mu\text{m}$). They could possibly fail to coalesce into the spaces between asperities and become a third-body abrasive product. They are easily abraded from the surfaces during the sliding process and increase the friction and wear [34]. This idea could be supported by the elemental analysis of worn specimens (Table 7.5). Despite the higher concentration of boron element found in the vegetable oil-boron nitride blended oils (hBN:PO and hBN:SBO in Table 7.2), it did not appear on the worn specimens surfaces as analysed by EDX (Table 7.5). That said, the boron element has failed to stay on the surface after the sliding process.

The existence of ZDDP in both PO and SBO is significant in wear resistance improvement. The improvement in wear was about 57% for ZD:SBO and 45% for ZD:PO compared to their pure oil. However, in the case of vegetable oil-boron nitride blends, a smaller amount of wear resistance improvement was recorded, i.e., 12% for hBN:SBO and 5% for hBN:PO compared to their pure oil. It is suggested that the mechanism (effect of particle size) that causes higher friction is also responsible for the wear behaviour of vegetable oil-boron nitride blends. The wear reduction in the ZD:PO and ZD:SBO specimens compared to their pure oil counterpart indicates that the response of the anti-wear additive in vegetable oil was positive.

The ZDDP additive (detected as zinc and phosphorus elements in the spectrochemical test, Table 7.2) serves as a protective layer in preventing metal-to-metal contact during sliding. However, the higher concentration of zinc found in the ZD:PO (1153 ppm) and ZD:SBO (1129 ppm) compared to MO (781 ppm), was not reflected in its

impact in wear reduction. Although the amount of zinc concentration in MO is much lower than those found in the vegetable oil-ZDDP blends, its wear performance was better, proposing that the wear reduction was not only caused by the ZDDP alone. It is suggested here that the existence of another additive element in the MO might synergistically act as combined function as antiwear and friction modifier. This may include the molybdenum (from MoDDP or MoDTC additive) which potentially acts together with the ZDDP in improving the wear and friction performance of MO.

It should also be emphasised at this point that the amount of zinc and phosphorus detected in the worn specimens of ZD:PO and ZD:SBO was very little compared to the one found in the MO specimens (EDX analysis, Table 7.5) despite the higher amount of zinc and phosphorus established in their oil blends compared to MO (spectrochemical analysis, Table 7.2). This supports the earlier suggestion (Chapter 6, Figure 6.3) that the additive in the vegetable oil blends might not be able to settle down on the surface due to the polarity of fatty acids that cover most of the areas. As a result, the formation of phosphate layer in the vegetable oil that serves as a wear reducing layer in typical lubricant oil with the ZDDP additives[247-249] might be restrained and thus lessen the wear protection characteristic. The adsorption results of ZDDP in both polar and non-polar base oil on steel surface reported by Suarez et al. [262] may be used to support this claim. Suarez et al. [262] found that when ZDDP is blended in a non-polar base oil, the additive molecules have better access to the steel surface (a thicker layer is formed), leading to higher absorption rates than when ZDDP is blended in a polar oil. Suarez et al. [262] suggest that this is due to the higher affinity of the polar base oil molecules on the steel surface, which limits the access of the additive molecules to the surface and therefore their ability to attach and react with it to form a protective reaction layer.

The friction, wear and oxidation stability results for the vegetable oil blending with additive also were following the previous trend, i.e., their tribological performance was influenced by the base oil. For example, in a pure oil state, the PO showed a lower COF (0.105) compared to SBO (0.112). This result seems to be similar for PO and SBO with additives, i.e., the ZD:PO exhibited a lower COF (0.095) compared to the ZD:SBO lubricated surface (COF=0.099). Similarly, the mass loss for vegetable oil-additives blend is found to be parallel to the mass loss of their pure oil state, which is clearly agreed to the fact that base oil very much influences the friction and wear behaviour of a lubricant [263]. These results could also indicate that the differences in type and composition of fatty acids that exist in the pure PO and SBO (which influence to the friction and wear) did not change in their blended oils.

With reference to the elemental analysis on the surface, the amount of wear was found to be inversely proportional to the amount of oxygen and zinc detected on the surface. That said, the lower the wear, the higher of amount oxygen and zinc detected on the worn surfaces which connected to the retention of the oxide layer and ZDDP protective layer on the surface. The amount of zinc, however, was greatly influenced by the level of wear compared to oxygen. Another important finding that could be highlighted here is that the ZDDP is an agent that may work simultaneously in three uses in the vegetable oils; as an anti-wear agent, anti-oxidant agent and friction modifier. Contrary to this, it was previously reported that the ZDDP alone in base oil was not efficient as a friction modifier as it increases the friction compared to the oil without ZDDP due to increases in roughness on metal surfaces [244, 245].

In summary, the formulation of ZDDP in the vegetable oils has shown improvements in friction, wear and oil oxidation. The result with a boron nitride additive

in the vegetable oils, however, was not encouraging, probably due to the particle size used. The friction coefficient performance by vegetable oil-ZDDP blends was very good and their value is comparable to the commercial MO. This is probably due to some of the fatty acids layer that adsorbs on the surface could not be removed completely during sliding and thus, acts as a friction modifier to lessen the friction. The poor wear resistance of these lubricants, on the other hand, may be attributed to the inability of the anti-wear additive to work efficiently on the surface. The lack of enough anti-wear additive remaining on the worn specimen of vegetable oils was strengthened to the earlier suggestion that some of the anti-wear additives may be hindered to be adsorbed on the surface due to the polarity of fatty acids molecule which is stronger to attract on the surface. The superior wear performance of MO which contains less concentration of ZDDP than the oil blends could also indicate that the wear protection is not only performed by the ZDDP alone. The combination of few additives in vegetable oils should be extended in the future research to prove this suggestion. This includes a combination of ZDDP with MoDDP or MoDTC at an appropriate concentration as they act synergistically as friction modifier and anti-wear additive in the commercial MO.

8.5 Summary

The friction and wear results obtained from testing GCI specimens with vegetable oils have raised awareness toward the specimens' hardness in regards to the reciprocating sliding point contact. Specimen hardness is one of the most important aspects to be considered in minimising the experimental error. It is suggested that the use of bulk hardness that typically to represent the overall specimen hardness is no longer valid, particularly for testing involving reciprocating sliding point contact using vegetable oil.

The assumption that the bulk hardness may be a fair representation of the entire GCI specimen hardness leads to a higher deviation in the friction and wear data as local hardness differs significantly in GCI specimens. This is troublesome especially in the case of assessing two lubricants that have very small differences in their friction and wear data. Thus, in order to produce more robust tribological results, hardness characterisations of GCI specimens on intended wear scar region prior to the test have been implemented and this method is applied throughout this research.

The tribological results found in pure vegetable oils and commercial mineral engine oil has established a baseline data for the friction and wear improvement work in the future. The good tribological characteristics found in the vegetable oils, particularly the competitiveness in friction coefficient over the MO, has raised strong motivation that their base oil has a potential to be further developed. The opposite friction and wear results between PO and SBO are proposed due to their molecular chain structure of fatty acids between saturated and unsaturated acids. A deeper meaning for this is that, in selecting the base oil for biolubricant, it is important to identify which performance should be prioritised (either friction or wear) as different base oils have different characteristics on friction and wear. From the poor wear resistance results, the pure vegetable oils need to undergo a proper treatment process before they are viable as an alternative to the commercial mineral engine oil such as the use of additives or the base oil treatment process.

The performance of the vegetable oils was found to be dominant in influencing friction, wear and oil oxidation in the vegetable oil-mineral oil blends at 1:1 blend ratio. The 50% contribution of the MO in the oil blends has failed to bring down the friction and wear value to a targeted value (a middle value between their pure oils) suggesting that the

additives' role was hindered. It is believed that the adsorption of MO additives has been limited by the existence of fatty acids that were not removed completely from the surface due to inadequate contact pressure during sliding. The polarity effect of fatty acids have made them stay on the surface thus, may block and lessen the additives role.

The friction coefficient performance shown by the vegetable oil-ZDDP blends was comparable to the fully formulated MO which supports the claim that the fatty acids layer might have not been removed entirely during sliding and subsequently acts as a friction modifier. The friction and wear result performed by boron nitride additive in the vegetable oils, however, was not positively improved and this could be due to the particle size used. The existence of ZDDP in the vegetable oil has the capability to form a protective layer on the surface of grey cast iron in minimising wear. However, the lower wear resistance and the lower amount of ZDDP detected on the surface shown by the vegetable oil-ZDDP blends may be caused by a competition of the ZDDP additive with the fatty acids on the surface. It is also suggested that the wear protection could not only be performed by the ZDDP alone. The combination of other additives such as molybdenum based additives with the ZDDP at appropriate concentration could act synergistically in reducing both wear and friction in the MO.

Chapter 9: Conclusions and suggestions

In this final chapter, the outcomes of the study are presented as a reflection against the project aim objectives defined in Chapter 1. Summaries of findings related to the project objectives are highlighted point by point and the project aims are then concluded. Recommendations for future work, publications arising from this work and the scientific contributions are also stated.

9.1 Achievement on Objective 1

It was determined that the EN1561-GJL-250 grey cast iron has a wide range of hardness as measured on its surfaces. This wide range of hardness greatly influences the friction and wear results when tested with soybean oil as a lubricant. In view of the friction and wear response toward the grey cast iron specimens, the use of single bulk hardness values to represent GCI specimen hardness should be avoided and hardness measurements performed on intended wear scar regions prior to testing in order to produce more robust data for friction and wear.

The findings presented here emphasise the significance of this in the case of assessing the tribological performance of two lubricants where the differences in friction and wear are very small. Repeatability and reproducibility of tribological results especially on wear performance related to vegetable oil lubricants could also very difficult to achieve when hardness is assumed to be uniformly distributed on the grey cast iron specimens.

9.2 Achievement on Objective 2

The friction coefficient of palm oil against grey cast iron was found to be competitive to the commercial mineral engine oil within 10%. However, in terms of wear, the mineral engine oil was far superior compared to vegetable oils (98% difference). Other than friction and wear, vegetable oil lubricants were also found to have lower oxidation stability (about 9 order in magnitude) and lower viscosity compared to mineral engine oil. The inferior wear performance shown by the vegetable oil lubricants is likely due to its inability to prevent metal-to-metal contact at severe contact conditions as a result of lubricant breakdown.

In view of this, significant further work should be conducted to investigate improving the vegetable oil based lubricants before it is deemed feasible as an alternative to mineral oil in real applications. A key investigation should be to blend a commercial antiwear additive in vegetable oil and assess its subsequent performance.

9.3 Achievement on Objective 3

The addition of mineral oil to the vegetable oils improved their friction, wear and oxidation performance relative to pure vegetable oil. However, the tribological performance of vegetable oil-mineral oil blends was dominated by the tribological characteristics of the vegetable oil. The addition of 50% mineral oil in the vegetable oil did not give a friction and wear result close to a middle value between the vegetable oil and mineral oil in their pure oil state. Instead, the friction and wear were biased towards the performance of the pure vegetable oil.

More specifically, the tribological performance of vegetable oil-mineral oil blends at an equal ratio was very poor compared to mineral oil. The nominally superior tribological characteristics of mineral oil failed to compensate the poor performance of the vegetable oil. Another method is needed particularly in improving the wear resistance of vegetable oil. The use of commercial antiwear additives in vegetable oil was implemented in the next investigation.

9.4 Achievement on Objective 4

The tribological performance of vegetable oils has been improved by addition of an anti-wear additive. The addition of 2% ZDDP in vegetable oils improved the friction (COF of PO differ 2 % with MO), wear resistance (mass loss improved 57% in SBO) and oxidative stability (oxidation time of PO improved about four order in magnitude). In vegetable oil-additive lubricants, the friction and wear also were not related to each other. The tribological performance of vegetable oil-additive blends was dependent on the tribological performance of its base oil. The ZD:PO gave the best friction improvement in vegetable oil-additive blend, the ZD:SBO performed the best in wear resistance.

The amount of wear is inversely related to the amount of oxygen detected on the worn surface. A small amount of zinc on the surface greatly improves the wear resistance. Although ZDDP significantly improves the tribological performance of vegetable oils, the function of hexagonal Boron Nitride as an antiwear additive appears to be less effective, possibly due to the particle size used in this study being greater than the surface roughness. This is an obvious area of further investigation.

9.5 Achievement on Project Aim

Overall, the tribological performance showed by the biolubricants considered in this study indicates that the potential use of these lubricants in practical applications (e.g. automotive engines, industrial machines etc.) is clearly possible. However, much work is required before it is technically and commercially feasible. Two areas should be given priority; improving the wear resistance and improving the oxidative stability of vegetable base oil.

9.6 Contribution to scientific knowledge and industrial field

The scientific contribution of this work can be summarised as follows:

1. At severe contact conditions, the pure vegetable oils could breakdown resulting metal-to-metal contact, severe wear and catastrophic damage to the sliding surfaces. This damage manifests as a wavy-shaped wear scar, as a result of plastic ratcheting and shakedown limit due to high contact pressure. A mechanism of formation for the wavy-shaped wear scar was proposed in this thesis (Section 4.5).
2. The friction and wear performance shown by vegetable oils was shown to be not directly related to each other. Higher friction in one vegetable oil could produce lower wear. This could relate to the type of fatty acids in the oil. Saturated fatty acids (enriched in palm oil) has a linear chain and uniformly arranged on the surfaces and thus, provide a smoother transition during motion compared to unsaturated fatty acids (enriched in soybean oil). The unsaturated fatty acids have bent chains and are not uniformly arranged on the surface, therefore providing

more resistance to motion. However, the bent chains could serve as a better protective layer, compared to the linear chains that the saturated fatty acid has. The mechanisms of friction and wear for palm oil and soybean oil were proposed in this thesis (Section 5.3).

3. The dominance of the vegetable oil in influencing the wear in vegetable oil-mineral oil blend was significant. The carboxylic group in the fatty acids covers the surfaces limiting the additive (ZDDP) to settle in efficiently on the surface and form a fully protective layer. The mechanisms of vegetable oil, mineral oil and vegetable oil-mineral oil blend in influencing wear were also proposed in this thesis (Section 6.3).

The results of this study provide an important contribution to the lubrication industry because it has been discovered that at severe contact conditions, the commercial antiwear additive, ZDDP with pure vegetable oils have shown a positive response to the friction performance and wear resistance. This may lead to the discovery that other commercial additives such as friction modifier, viscosity enhancer, extreme pressure agent and detergent might also work efficiently with vegetable oil based lubricants. This could also inspire the additive manufacturers to develop “greener” additives in line with the vegetable oils.

9.7 Recommendations for future work

Based on the outcomes of this study, vegetable oils are indeed a potential candidate as alternative lubricants in automotive engine applications. Besides the inherent

advantages that they have, like renewable basestocks, biodegradability and non-toxic oils, vegetable oils have shown competitiveness in friction coefficient over mineral engine oil and exhibited a positive response to both friction and wear resistance when treated with an antiwear additive.

Research considering vegetable oils as biolubricants are continuously being performed with an increasing number of studies directed toward improvement being published. Besides, a number of improvements are already available in this field, further research that confirms the capability of vegetable oils in the automotive engine must be conducted systematically. Results from this study provide a base data for the tribological performance of palm oil and soybean oil, and can also be used to support the establishment of biolubricants from the other vegetable oils as well as encourage ongoing research on using renewable natural sources as alternative lubricants. Some future works to further evaluate the lubrication mechanism and feasibility of vegetable oil as biolubricants are suggested in this section which include:

- The comparable result of friction coefficient found in this study between the ZDDP alone in the vegetable oil and the fully formulated MO has suggested that the fatty acids layer is not completely removed from the surface, but rather acting as an additional friction modifier. The role of ZDDP alone in the vegetable oil, however, was found insufficient to reduce wear equivalent to the MO. Thus, a synergistic effect on the combination of ZDDP and molybdenum based friction modifier at appropriate concentration that is implemented in the MO is believed to be beneficial in further reducing the friction and wear of vegetable oil.

- Chemical syntheses of modified vegetable oils has shown improvement in their tribological performance [18, 28, 35-39]. Based on the positive tribological response shown by the vegetable oils with antiwear additive conducted in this study, it is not too much to hypothesise that the behaviour of the modified vegetable oils combined with several other additives would also produce a positive impact. This can be performed by blending modified vegetable oils (chemically synthesis) with additive packages that are commercially used in the manufacture the fully formulated mineral engine oil. The results produced from the bench test then should be verified by testing the same lubricants in a real engine. The tribological, engine and emission performance should also be evaluated in order to strengthen the findings.
- The lubrication mechanism served by the vegetable oils at contacting surfaces needs to be verified. The current theory is mainly based on the adherence of polar fatty acids on the surfaces to provide metal-to-metal separation [256]. In this study, the lubrication mechanism of two vegetable oils that gave the opposite result of friction and wear was proposed which is influenced by the molecular structure of fatty acids. In addition, the lubrication mechanisms of vegetable oil-mineral oil blend were also proposed which explain that the vegetable oil is dominant in influencing wear in the oil blend. However, these theories were proposed based on the limited findings found in this study. A better methodology in understanding on this theory is still needed. This can be performed by conducting the test using a series of vegetable oils which consist a range of saturated and unsaturated oil groups and the test can be run at variable parameters.

- The positive response of vegetable oil lubricants in this study could generate an interesting idea for them to be tested in other applications. To increase the marketability of the vegetable oil lubricants in the future, the investigation on the potential use of palm oil and soybean oil and their blend with additive should also be performed to other industrial applications such as in a manufacturing processes. This includes the use of vegetable oils as a lubricating agent (e.g. stamping oil) and cooling agent (e.g metal cutting coolant). The replacement of traditional metal working fluids with biolubricants is likely to bring environmental benefits (e.g. disposal and operator health) with similar frictional performance, and their poor wear resistance performance is much less crucial. In metal forming operations like stamping, the vegetable oils performance can be evaluated in the area of interface friction between workpiece and tool surfaces, metal flow and tool life. While in metal cutting, the investigation can be performed in the area of tool life, thermal deformation and surface finish.

9.8 Publications arising from this work

1. Bahari, A., Lewis, R., Slatter, T., 2017, “Friction and wear response of vegetable oils and their blends with mineral engine oil in a reciprocating sliding contact at severe contact conditions.” *P I Mech Eng J-J Eng*, (ISSN 1350-6501) (DOI: 10.1177/1350650117712344).
2. Bahari, A., Lewis, R., Slatter, T., 2017, “Friction and wear phenomena of vegetable oil based lubricants with additives at severe sliding wear conditions.” *Tribol T*, (ISSN 1547-397X) (DOI: 10.1080/10402004.2017.1290858).

3. Bahari, A., Lewis, R., Slatter, T., 2016, “Hardness characterisation of grey cast iron and its tribological performance in a contact lubricated with soybean oil.” P I Mech Eng C-J Mec (ISSN 0954-4062) (DOI:10.1177/0954406216675895).

References

1. Mercurio, P., K.A. Burns, and A. Negri, *Testing the ecotoxicology of vegetable versus mineral based lubricating oils: 1. Degradation rates using tropical marine microbes*. Environmental Pollution, 2004. **129**(2): p. 165-173.
2. Emmanuel, O.A. and O. Mudiakeoghene, *Biodegradation of mineral oils – A review*. African Journal of Biotechnology, 2009. **8**(6): p. 915-920.
3. *Long-term world oil supply scenarios*. 2000 [cited 10/11/2016; Available from: http://www.eia.gov/pub/oil_gas/petroleum/feature_articles/2004/worldoilsupply/oil_supply04.html].
4. Bentley, R.W., *Global oil & gas depletion: An overview*. Energy policy, 2002. **30**(3): p. 189-205.
5. Aleklett, K. and C.J. Campbell, *The peak and decline of world oil and gas production*. Minerals and Energy-Raw Materials Report, 2003. **18**(1): p. 5-20.
6. HS, G. *Chemical Building Blocks of Life*. [cited 2016 18 Dec]; Available from: <http://science.halleyhosting.com/sci/ibbio/chem/notes/chpt3/triglyceride.htm>.
7. Aluyor, E.O., K.O. Obahiagbon, and M. Ori-jesu, *Biodegradation of vegetable oils: A review*. Scientific Research and Essay, 2009. **4**(6): p. 543-548.
8. Luna, F.M.T., et al., *Assessment of biodegradability and oxidation stability of mineral, vegetable and synthetic oil samples*. Industrial Crops and Products, 2011. **33**(3): p. 579-583.
9. Syahrullail, S., S. Kamitani, and A. Shakirin, *Tribological Evaluation of Mineral Oil and Vegetable Oil as a Lubricant*. Jurnal Teknologi, 2014. **66**(3): p. 37-44.
10. Carlton, J.R., et al., *The influence of fatty acids on tribological and thermal properties of natural oils as sustainable biolubricants*. 2015. **90**: p. 123-134.
11. Mannekote, J.K. and S.V. Kailas, *The Effect of Oxidation on the Tribological Performance of Few Vegetable Oils*. Journal of Materials Research and Technology, 2012. **1**(2): p. 91-95.

12. Jayadas, N.H., K.P. Nair, and G. Ajithkumar, *Tribological evaluation of coconut oil as an environment-friendly lubricant*. Tribology International, 2007. **40**(2): p. 350-354.
13. Syahrullail, S., S. Kamitani, and A. Shakirin, *Performance of Vegetable Oil as Lubricant in Extreme Pressure Condition*. Procedia Engineering, 2013. **68**: p. 172-177.
14. Gerbig, Y., et al., *Suitability of vegetable oils as industrial lubricants*. Journal of Synthetic Lubrication, 2004. **21**(3): p. 177-191.
15. Masjuki, H.H., et al., *Palm oil and mineral oil based lubricants - their tribological and emission performance*. Tribology International, 1999. **32**(6): p. 305-314.
16. Quinchia, L.A., et al., *Tribological studies of potential vegetable oil-based lubricants containing environmentally friendly viscosity modifiers*. Tribology International, 2014. **69**: p. 110-117.
17. Sharma, B.K., et al., *Lubricant properties of Moringa oil using thermal and tribological techniques*. Journal of thermal analysis and calorimetry, 2009. **96**(3): p. 999-1008.
18. Shashidhara, Y. and S. Jayaram, *Tribological Studies on AISI 1040 with Raw and Modified Versions of Pongam and Jatropha Vegetable Oils as Lubricants*. Advances in Tribology, 2012. **2012**.
19. Syahrullail, S., M. Izhan, and A.M. Rafiq, *Tribological investigation of RBD palm olein in different sliding speeds using pin-on-disk tribotester*. Scientia Iranica. Transaction B, Mechanical Engineering, 2014. **21**(1): p. 162-170.
20. Jabal, M.H., F.N. Ani, and S. Syahrullail, *The Tribological Characteristic of the Blends of Rbd Palm Olein with Mineral Oil Using Four-ball Tribotester*. Jurnal Teknologi, 2014. **69**(6): p. 11-14.
21. Imran, A., et al., *Study of Friction and Wear Characteristic of Jatropha Oil Blended Lube Oil*. Procedia Engineering, 2013. **68**: p. 178-185.
22. Shahabuddin, M., et al., *Comparative tribological investigation of bio-lubricant formulated from a non-edible oil source (Jatropha oil)*. Industrial Crops and Products, 2013. **47**: p. 323-330.

23. Shanta, S., G. Molina, and V. Soloiu, *Tribological effects of mineral-oil lubricant contamination with biofuels: a pin-on-disk tribometry and wear study*. Advances in Tribology, 2011. **2011**.
24. Choi, U., et al., *Tribological behavior of some antiwear additives in vegetable oils*. Tribology International, 1997. **30**(9): p. 677-683.
25. Elemsimit, H.A. and D. Grecov, *Impact of liquid crystal additives on a canola oil-based bio-lubricant*. Proceedings of the Institution of Mechanical Engineers, Part J: Journal of Engineering Tribology, 2014: p. 126-135.
26. Zulkifli, N.W.M., et al., *Experimental Analysis of Tribological Properties of Biolubricant with Nanoparticle Additive*. Procedia Engineering, 2013. **68**: p. 152-157.
27. Husnawan, M., H. Masjuki, and T. Mahlia, *The interest of combining two additives with palm olein as selected lubricant components*. Industrial Lubrication and Tribology, 2011. **63**(3): p. 203-209.
28. Cheenkachorn, K., *A Study of Wear Properties of Different Soybean Oils*. Energy Procedia, 2013. **42**: p. 633-639.
29. Mahipal, D., et al., *Analysis of lubrication properties of zinc-dialkyl-dithiophosphate (ZDDP) additive on Karanja oil (Pongamia pinnatta) as a green lubricant*. International Journal of Engineering Research, 2014. **3**(8): p. 494-496.
30. Zahid, R., et al. *Comparison of tribological performance of zinc dialkyldithiophosphate (ZDDP) in poly-alpha-olefin (PAO) and palm oil-based trimethylpropane (TMP) ester*. in *Proceedings of Malaysian International Tribology Conference 2015*. 2015. Malaysian Tribology Society, Kuala Lumpur, Malaysia.
31. Talib, N., R.M. Nasir, and E. Rahim. *Tribology characteristic of hBN particle as an additive in modified jatropa oil as a sustainable metalworking fluids*. in *Proceedings of Malaysian International Tribology Conference 2015*. 2015. Malaysian Tribology Society.
32. Farhanah, A., et al., *Modification of RBD palm kernel and RBD palm stearin oil with ZDDP additive addition*. Jurnal Teknologi, 2015. **74**(10).
33. Azhari, M.A., M.F. Tamar, and N.R. Mat Nuri, *Physical property modification of vegetable oil as biolubricant using ZDDP*. 2006.

34. Reeves, C.J., et al., *The influence of surface roughness and particulate size on the tribological performance of bio-based multi-functional hybrid lubricants*. Tribology International, 2015. **88**: p. 40-55.
35. Arumugam, S. and G. Sriram, *Synthesis and characterisation of rapeseed oil bio-lubricant - Its effect on wear and frictional behaviour of piston ring-cylinder liner combination*. Proceedings of the Institution of Mechanical Engineers, Part J: Journal of Engineering Tribology, 2013. **227**(1): p. 3-15.
36. Wu, X., et al., *Study of epoxidized rapeseed oil used as a potential biodegradable lubricant*. JAOCS, Journal of the American Oil Chemists' Society, 2000. **77**(5): p. 561-563.
37. Zulkifli, N.W.M., et al., *Wear prevention characteristics of a palm oil-based TMP (trimethylolpropane) ester as an engine lubricant*. Energy, 2013. **54**: p. 167-173.
38. Dodos, G.S., G. Anastopoulos, and F. Zannikos, *Tribological evaluation of biobased lubricant basestocks from cottonseed and soybean oils*. SAE International Journal of Fuels and Lubricants, 2010. **3**(2): p. 378-385.
39. N.W.M.Zulkifli, S.S.N.A., M.A.Kalam, H.H.Masjuki, R.Yunus, M.Gulzar, *Lubricity of bio-based lubricant derived from different chemically modified fatty acid methylester*. Tribology International, 2015. **93**: p. 555-562.
40. Hollinghurst, R., *High Temperature Lubrication Requirements of European Gasoline and Diesel Engines for Cars*. 1974, SAE Technical Paper.
41. Andersson, P., J. Tamminen, and C.-E. Sandström, *Piston ring tribology. A literature survey*. VTT Tiedotteita-Research Notes, 2002. **2178**(1).
42. Mate, C.M., *Tribology on the small scale: a bottom up approach to friction, lubrication, and wear*. 2008: Oxford University Press.
43. Bowden, F., A. Moore, and D. Tabor, *The ploughing and adhesion of sliding metals*. Journal of Applied Physics, 1943. **14**(2): p. 80-91.
44. Gwidon, W.S. and W.B. Andrew, *Engineering tribology*. 2nd ed. 2014, Oxford, UK: Butterworth-Heinemann.
45. Bowden, F.P. and D. Tabor, *The Friction and Lubrication of Solids*. 1950, London: Oxford University Press.

46. Menezes, P.L., et al., *Tribology for scientists and engineers*. 2013: Springer.
47. Blau, P.J., *Interpretations of the friction and wear break-in behavior of metals in sliding contact*. *Wear*, 1981. **71**(1): p. 29-43.
48. Blau, P.J., *Friction science and technology: from concepts to applications*. 2008: CRC press.
49. Furey, M., *Surface temperatures in sliding contact*. *ASLE Transactions*, 1964. **7**(2): p. 133-146.
50. Rabinowicz, E., *Lubrication of metal surfaces by oxide films*. *ASLE Transactions*, 1967. **10**(4): p. 400-407.
51. Mecklenburg, K.R., *The Effect of Wear on the Compressive Stress in the Sphere-on-Plane and Multiple-Flat-on-Curve Configurations*. 1973, DTIC Document.
52. Kenneth, H., et al., *Triboscience and tribotechnology superior friction and wear control in engines and transmissions. Scientific Report: European Cooperation in Science and Technology*. 2007, European Cooperation in Science and Technology: Brussels, Belgium.
53. Buckley, D.H., *Possible relation of friction of copper-aluminum alloys with decreasing stacking-fault energy*. 1967.
54. Rigney, D. and J. Hirth, *Plastic deformation and sliding friction of metals*. *Wear*, 1979. **53**(2): p. 345-370.
55. He, Y., et al., *Friction and wear behaviour of ceramic-hardened steel couples under reciprocating sliding motion*. *Wear*, 1995. **184**(1): p. 33-43.
56. Bhushan, B., *Modern tribology handbook*. 2000, Boca Raton, USA: CRC Press.
57. Stachowiak, G.W., *Wear: materials, mechanisms and practice*. 2006: John Wiley & Sons.
58. Blau, P.J., *How common is the steady-state? The implications of wear transitions for materials selection and design*. *Wear*, 2015. **332**: p. 1120-1128.

59. Ajayi, O.O. and R.A. Ereke, *Variation of Nominal Contact Pressure with Time during Sliding Wear*, in *International Joint Tribology Conference*. 2001: San Francisco.
60. Sharma, S., S. Sangal, and K. Mondal, *On the optical microscopic method for the determination of ball-on-flat surface linearly reciprocating sliding wear volume*. *Wear*, 2013. **300**(1-2): p. 82-89.
61. Totten, G.E., *Fuels and Lubricants Handbook : Technology, Properties, Performance and Testing*. 2003, USA: ASTM International.
62. Meurant, G., *Tribology: a systems approach to the science and technology of friction, lubrication, and wear*. Vol. 1. 2009: Elsevier.
63. Suh, N.P., *The delamination theory of wear*. *Wear*, 1973. **25**(1): p. 111-124.
64. Rizvi, S.Q.A., *A Comprehensive Review of Lubricant Chemistry, Technology, Selection and Design*. 1st ed. 2009, Pennsylvania, USA: ASTM International.
65. Priest, M., *Factors influencing boundary friction and wear of piston rings*. *Tribology series*, 2000. **38**: p. 409-416.
66. Tang, Z. and S. Li, *A review of recent developments of friction modifiers for liquid lubricants (2007–present)*. *Current opinion in solid state and materials science*, 2014. **18**(3): p. 119-139.
67. Spikes, H., *Friction modifier additives*. *Tribology Letters*, 2015. **60**(1): p. 5.
68. Campen, S., et al., *In situ study of model organic friction modifiers using liquid cell AFM; saturated and mono-unsaturated carboxylic acids*. *Tribology Letters*, 2015. **57**(2): p. 18.
69. Vilaro, J.S. and P.E. Mosier, *Carboxylic acid derivatives as friction modifiers in fuels*. 2009, U.S. Patent No. 20110162263.
70. DeBlase, F.J., et al., *Fatty sorbitan ester based friction modifiers*, U.S. Patents, Editor. 2010, U.S. Patent No. 9296969: U.S.A.
71. Suen, Y.F., *Lubricating composition containing friction modifier blend*. 2014,

U.S. Patent No. 8703680

72. Lundgren, S., *Fatty amine salts as friction modifiers for lubricants*. 2016, U.S. Patent No. 9487728
73. Holtmyer, M.D. and J. Chatterji, *Study of oil soluble polymers as drag reducers*. Polymer Engineering & Science, 1980. **20**(7): p. 473-477.
74. Campen, S., et al., *On the increase in boundary friction with sliding speed*. Tribology letters, 2012. **48**(2): p. 237-248.
75. Bray, U.B., C. Moore, and D.R. Merrill, *Improvements in diesel-engine lubricating oils*. 1939, SAE Technical Paper.
76. Mitchell, P.C., *Oil-soluble Mo-S compounds as lubricant additives*. Wear, 1984. **100**(1-3): p. 281-300.
77. Ma, Y., et al., *Impacts of friction-modified fully formulated engine oils on tribological performance of nitrided piston rings sliding against cast iron cylinder bores*. Tribology transactions, 2004. **47**(3): p. 421-429.
78. Kasrai, M., et al., *The chemistry of antiwear films generated by the combination of ZDDP and MoDTC examined by X-ray absorption spectroscopy*. Tribology transactions, 1998. **41**(1): p. 69-77.
79. Feng, X., et al., *Anti-wear performance of organomolybdenum compounds as lubricant additives*. Lubrication Science, 2007. **19**(2): p. 81-85.
80. Topolovec Miklozic, K., J. Graham, and H. Spikes, *Chemical and physical analysis of reaction films formed by molybdenum dialkyl-dithiocarbamate friction modifier additive using Raman and atomic force microscopy*. Tribology Letters, 2001. **11**(2): p. 71-81.
81. de Barros' Bouchet, M., et al., *Boundary lubrication mechanisms of carbon coatings by MoDTC and ZDDP additives*. Tribology International, 2005. **38**(3): p. 257-264.
82. Yamamoto, Y. and S. Gondo, *Friction and wear characteristics of molybdenum dithiocarbamate and molybdenum dithiophosphate*. Tribology Transactions, 1989. **32**(2): p. 251-257.

83. Parfenova, V., et al., *Molybdenum-containing dithiophosphates as multifunctional additives for mineral oils*. Chemistry and Technology of Fuels and Oils, 1986. **22**(1): p. 24-26.
84. Bakunin, V., et al., *Synthesis and application of inorganic nanoparticles as lubricant components—a review*. Journal of Nanoparticle Research, 2004. **6**(2): p. 273-284.
85. Wu, Y., W. Tsui, and T. Liu, *Experimental analysis of tribological properties of lubricating oils with nanoparticle additives*. Wear, 2007. **262**(7): p. 819-825.
86. Sunqing, Q., D. Junxiu, and C. Guoxu, *A review of ultrafine particles as antiwear additives and friction modifiers in lubricating oils*. Lubrication Science, 1999. **11**(3): p. 217-226.
87. Akbulut, M., *Nanoparticle-based lubrication systems*. Journal of Powder Metallurgy & Mining, 2012. **1**(1).
88. Joly-Pottuz, L., et al., *Ultralow-friction and wear properties of IF-WS 2 under boundary lubrication*. Tribology letters, 2005. **18**(4): p. 477-485.
89. Dong, J., et al., *Lubricant additives chemistry and applications*. 2003.
90. De Vries, L. and B. Kennedy, *Oxidation inhibited lubricating oil compositions with extreme pressure properties*. 1973, U.S Patent No. 3753908.
91. Wan, Y. and Q. Xue, *Effect of antiwear and extreme pressure additives on the wear of aluminium alloy in lubricated aluminium-on-steel contact*. Tribology international, 1995. **28**(8): p. 553-557.
92. Sakurai, T. and K. Sato, *Study of corrosivity and correlation between chemical reactivity and load-carrying capacity of oils containing extreme pressure agents*. ASLE TRANSACTIONS, 1966. **9**(1): p. 77-87.
93. Torrance, A., J. Morgan, and G. Wan, *An additive's influence on the pitting and wear of ball bearing steel*. Wear, 1996. **192**(1-2): p. 66-73.
94. Khorramian, B., et al., *Review of antiwear additives for crankcase oils*. Wear, 1993. **169**(1): p. 87-95.

95. Spikes, H., *The history and mechanisms of ZDDP*. Tribology letters, 2004. **17**(3): p. 469-489.
96. Johnson, D.W. and J.E. Hils, *Phosphate esters, thiophosphate esters and metal thiophosphates as lubricant additives*. lubricants, 2013. **1**(4): p. 132-148.
97. Zhang, Z., et al. *Tribofilms generated from ZDDP and DDP on steel surfaces: Part 1—growth, wear and morphology*. in *World Tribology Congress III*. 2005. American Society of Mechanical Engineers.
98. Zhang, Z., et al. *Tribofilms Generated From ZDDP and DDP on Steel Surfaces: Part 2—Chemistry*. in *World Tribology Congress III*. 2005. American Society of Mechanical Engineers.
99. Wong, V.W. and S.C. Tung, *Overview of automotive engine friction and reduction trends—Effects of surface, material, and lubricant-additive technologies*. Friction, 2016. **4**(1): p. 1-28.
100. Nehal S. A and Amal M. N. *Lubricating Oil Additives*. [cited 2016 15November]; Available from: <http://www.intechopen.com/books/tribology-lubricants-and-lubrication/lubricating-oil-additives>.
101. Canter, N., *Use of antioxidants in automotive lubricants*. Tribology & Lubrication Technology, 2008. **64**(9): p. 12.
102. Colclough, T., *Role of additives and transition metals in lubricating oil oxidation*. Industrial & engineering chemistry research, 1987. **26**(9): p. 1888-1895.
103. Lopes, A., et al., *Study of antioxidant property of a thiosphorated compound derived from cashew nut shell liquid in hydrogenated naphthenics oils*. Brazilian Journal of Chemical Engineering, 2008. **25**(1): p. 119-127.
104. Trivedi, H., N. Forster, and C. Saba, *Rolling contact fatigue testing of a 3 cSt polyolester lubricant with and without TCP and DODPA/PANA at 177 C*. Tribology Letters, 2004. **16**(3): p. 231-237.
105. Brown, J.R., et al., *Lubricant and concentrate compositions comprising hindered-phenol-containing diester antioxidant and method thereof*. 2009, U.S Patent No. 7538076.
106. Gui, M.M., K.T. Lee, and S. Bhatia, *Feasibility of edible oil vs. non-edible oil vs. waste edible oil as biodiesel feedstock*. Energy, 2008. **33**(11): p. 1646-1653.

107. Agriculture, U.S.D.o. *Oilseeds: World Markets and Trade*. 2016 [cited 2016 16 December]; Available from: <https://apps.fas.usda.gov/psdonline/circulars/oilseeds.pdf>.
108. Mang, T. and W. Dresel, *Lubricants and lubrication*. 2007: John Wiley & Sons.
109. James Baggot and NetBiochem. *General Features of Fatty Acid Structure*. [cited 2016 18 Dec]; Available from: http://library.med.utah.edu/NetBiochem/FattyAcids/3_3.html.
110. Stachowiak, G.W., *Engineering tribology*. 3rd ed. ed, ed. A.W. Batchelor. 2005, Burlington MA: Burlington MA : Elsevier Butterworth-Heinmann, 2005.
111. Allen, C. and E. Drauglis, *Boundary layer lubrication: monolayer or multilayer*. *Wear*, 1969. **14**(5): p. 363-384.
112. UFA, *Lubricant Handbook, Chevron lubricants*. 2008, Chevron: Edmonton, Canada.
113. Darfizzi Derawi and Jumat Salimon, *Palm olein based biolubricant basestocks: synthesis, characterisation, tribological and rheological analysis*. *Malaysian Journal of Analytical Sciences*, 2013. **17**(1): p. 153-163.
114. Lou A.T.H and E. Ritcher, *Biobased lubricants and greases: Technology and Products*. 1 ed. 2011, Chichester: John Wiley and Sons.
115. Kheang, L.S. and C.Y. May, *Influence of a lubricant auxiliary from palm oil methyl esters on the performance of palm olein-based fluid*. *Journal of Oil Palm Research*, 2012. **24**(AUGUST): p. 1388-1396.
116. Soya.be. *Information about Soy and Soya Products: Soybean oil production*. [cited 2016 18 Dec]; Available from: <http://www.soya.be/soybean-oil-production.php>.
117. Gunstone, F., *Vegetable oils in food technology: composition, properties and uses*. 2011: John Wiley & Sons.
118. Kummerow, F.A., *The Effects of Hydrogenation on Soybean Oil*. 2013: INTECH Open Access Publisher.

119. Neff, W.E. and G.R. List, *Oxidative stability of natural and randomized high-palmitic-and high-stearic-acid oils from genetically modified soybean varieties*. Journal of the American Oil Chemists' Society, 1999. **76**(7): p. 825-831.
120. Wurzbach, R. *Lubricant Oxidation Analysis and Control*. [cited 2016 17 Dec]; Available from: <http://www.machinerylubrication.com/Read/14/lubricant-oxidation>.
121. Adhvaryu, A., et al., *Oxidation kinetic studies of oils derived from unmodified and genetically modified vegetables using pressurized differential scanning calorimetry and nuclear magnetic resonance spectroscopy*. Thermochemica Acta, 2000. **364**(1–2): p. 87-97.
122. Sherwin, E., *Oxidation and antioxidants in fat and oil processing*. Journal of the American Oil Chemists' Society, 1978. **55**(11): p. 809-814.
123. Fox, N.J. and G.W. Stachowiak, *Vegetable oil-based lubricants-A review of oxidation*. Tribology International, 2007. **40**(7): p. 1035-1046.
124. Mannekote, J.K. and S.V. Kailas, *Studies on boundary lubrication properties of oxidised coconut and soy bean oils*. Lubrication science, 2009. **21**(9): p. 355-365.
125. Mecpherson, F., *Oxidative wear in lubricated contact*. Journal of Lubrication Technology OCTOBER, 1980. **102**: p. 539.
126. Habeeb, J. and W. Stover, *The role of hydroperoxides in engine wear and the effect of zinc dialkyldithiophosphates*. ASLE transactions, 1986. **30**(4): p. 419-426.
127. Srivastava, A. and P. Sahai, *Vegetable oils as lube basestocks: A review*. African Journal of Biotechnology, 2015. **12**(9).
128. Arnšek, A. and J. Vižintin, *Lubricating properties of rapeseed-based oils*. Journal of Synthetic Lubrication, 2000. **16**(4): p. 281-296.
129. Biresaw, G., A. Adhvaryu, and S. Erhan, *Friction properties of vegetable oils*. Journal of the American Oil Chemists' Society, 2003. **80**(7): p. 697-704.
130. Reeves, C.J., et al., *The influence of fatty acids on tribological and thermal properties of natural oils as sustainable biolubricants*. Tribology International, 2015. **90**: p. 123-134.

131. Fox, N., B. Tyrer, and G. Stachowiak, *Boundary lubrication performance of free fatty acids in sunflower oil*. Tribology Letters, 2004. **16**(4): p. 275-281.
132. Lundgren, S.M., et al., *Unsaturated fatty acids in alkane solution: adsorption to steel surfaces*. Langmuir, 2007. **23**(21): p. 10598-10602.
133. Tomoaia-Cotișel, M., et al., *Insoluble mixed monolayers: III. The ionization characteristics of some fatty acids at the air/water interface*. Journal of colloid and interface science, 1987. **117**(2): p. 464-476.
134. Lundgren, S.M., et al., *Effects of unsaturation on film structure and friction of fatty acids in a model base oil*. Journal of colloid and interface science, 2008. **326**(2): p. 530-536.
135. *Global consumption of vegetable oils from 1995/1996 to 2014/2015, by oil type (in million metric tons)*. [cited 09/02/2016; Available from: <http://www.statista.com/statistics/263937/vegetable-oils-global-consumption/>, cited on 09/02/2016.
136. Gharby, S., et al., *The Stability of Vegetable Oils (Sunflower, Rapeseed And Palm) Sold on the Moroccan Market at High Temperature*. Int. J. Chem. Biochem. Sci. IJCBS, 2014. **5**: p. 47-54.
137. Erhan, S.Z. and S. Asadauskas, *Lubricant basestocks from vegetable oils*. Industrial Crops and Products, 2000. **11**(2-3): p. 277-282.
138. Erhan, S.Z., B.K. Sharma, and J.M. Perez, *Oxidation and low temperature stability of vegetable oil-based lubricants*. Industrial Crops and Products, 2006. **24**(3): p. 292-299.
139. Yunus, R., et al., *Lubrication properties of trimethylolpropane esters based on palm oil and palm kernel oils*. European Journal of Lipid Science and Technology, 2004. **106**(1): p. 52-60.
140. Naghshineh, M., et al., *Effect of saturated/unsaturated fatty acid ratio on physicochemical properties of palm olein–olive oil blend*. Journal of the American Oil Chemists' Society, 2010. **87**(3): p. 255-262.
141. Farhanah, A., et al., *Modification of RBD Palm Kernel and RBD Palm Stearin Oil with ZDDP additive addition*. Jurnal Teknologi, 2015. **74**(10): p. 121-126.

142. Azhari, M.A., M.F. Tamar, and N.R. Mat Nuri, *Physical property modification of vegetable oil as bio-lubricant using ZDDP*. ARPN Journal of Engineering and Applied Sciences, 2015. **10**(15): p. 6525-6528.
143. Pawlak, Z., *Tribochemistry of lubricating oils*. 1st ed. Vol. 45. 2003, Amsterdam, Netherlands: Elsevier.
144. Baş, H. and Y.E. Karabacak, *Investigation of the effects of boron additives on the performance of engine oil*. Tribology Transactions, 2014. **57**(4): p. 740-748.
145. Wan, Q., et al., *Tribological Behaviour of a Lubricant Oil Containing Boron Nitride Nanoparticles*. Procedia Engineering, 2015. **102**: p. 1038-1045.
146. Çelik, O., N. Ay, and Y. Göncü, *Effect of nano hexagonal boron nitride lubricant additives on the friction and wear properties of AISI 4140 steel*. Particulate Science and Technology, 2013. **31**(5): p. 501-506.
147. Talib, N., R.M. Nasir, and E. Rahim. *Tribology characteristic of hBN particle as an additive in modified jatropha oil as a sustainable metalworking fluids*. in *Proceedings of Malaysian International Tribology Conference 2015*. 2015. Malaysian Tribology Society, Kuala Lumpur, Malaysia.
148. Taylor, B.J. and T.S. Eyre, *A review of piston ring and cylinder liner materials*. Tribology International, 1979. **12**(2): p. 79-89.
149. Glaeser, W.A., *Materials for Tribology*. 1992, Amsterdam, Netherlands: Elsevier.
150. Sugishita, J. and S. Fujiyoshi, *The effect of cast iron graphites on friction and wear performance I: Graphite film formation on grey cast iron surfaces*. Wear, 1981. **66**(2): p. 209-221.
151. Buckley, D.H., *Effect of carbon content on friction and wear of cast irons*. 1977.
152. Leach, P.W. and D.W. Borland, *The unlubricated wear of flake graphite cast iron*. Wear, 1983. **85**(2): p. 257-266.
153. Prasad, B., *Sliding wear response of a grey cast iron: Effects of some experimental parameters*. Tribology International, 2011. **44**(5): p. 660-667.

154. Prasad, B.K., *Sliding wear response of a cast iron under varying test environments and traversal speed and pressure conditions*. *Wear*, 2006. **260**(11–12): p. 1333-1341.
155. Bian, S., S. Maj, and D.W. Borland, *The unlubricated sliding wear of steels: The role of the hardness of the friction pair*. *Wear*, 1993. **166**(1): p. 1-5.
156. Khruschov, M.M., *Principles of abrasive wear*. *Wear*, 1974. **28**(1): p. 69-88.
157. Moore, M.A., *The relationship between the abrasive wear resistance, hardness and microstructure of ferritic materials*. *Wear*, 1974. **28**(1): p. 59-68.
158. Mokhtar, M.O.A., M. Zaki, and G.S.A. Shawki, *Effect of mechanical properties on frictional behaviour of metals*. *Tribology International*, 1979. **12**(6): p. 265-268.
159. Bowden, F.P., D. Tabor, and F. Palmer, *The Friction and Lubrication of Solids*. *American Journal of Physics*, 1951. **19**(7): p. 428-429.
160. Mokhtar, M.O.A., *The effect of hardness on the frictional behaviour of metals*. *Wear*, 1982. **78**(3): p. 297-304.
161. Standard, B., *BS EN 1561:2011 Founding Grey Cast Iron*. 2011.
162. A.J. Shturmakov, C.R.L., Jr., *Predictive Analysis of Mechanical Properties in Commercial Gray Iron*. *American Foundry Society*, 2002. **99**(94): p. 609-615.
163. Terheci, M., R.R. Manory, and J.H. Hensler, *The friction and wear of automotive grey cast iron under dry sliding conditions Part 1-relationships between wear loss and testing parameters*. *Wear*, 1995. **180**(1–2): p. 73-78.
164. Rac, A., *Influence of load and speed on wear characteristics of grey cast iron in dry sliding — selection for minimum wear*. *Tribology International*, 1985. **18**(1): p. 29-33.
165. Liu, Y.C., J.M. Schissler, and T.G. Mathia, *The influence of surface oxidation on the wear resistance of cast iron*. *Tribology International*, 1995. **28**(7): p. 433-438.
166. Angus, H.T., *Cast iron: physical and engineering properties*. 2013: Elsevier.

167. Adedayo, A.V., *Relationship between graphite flake sizes and the mechanical properties of grey iron*. International Journal of Materials Science and Applications, 2013. **2**(3): p. 94-98.
168. Sugishita, J. and S. Fujiyoshi, *The effect of cast iron graphites on friction and wear performance*. Wear, 1981. **68**(1): p. 7-20.
169. Castro, W., et al., *A study of the oxidation and wear properties of vegetable oils: Soybean oil without additives*. JAOCS, Journal of the American Oil Chemists' Society, 2006. **83**(1): p. 47-52.
170. Adhvaryu, A. and S.Z. Erhan, *Epoxidized soybean oil as a potential source of high-temperature lubricants*. Industrial Crops and Products, 2002. **15**(3): p. 247-254.
171. Yamagata, H., *The science and technology of materials in automotive engines*. 2005: Elsevier.
172. MAHLE, F., *Cylinder components: properties, applications, materials*. 2010.
173. Glaeser, W., *Materials for tribology*. Vol. 20. 1992: Elsevier.
174. Goetze. *Piston Rings and Piston Ring Elements- Cast Iron Materials*. [cited 2017 May]; Available from: http://korihandbook.federalmogul.com/en/pdf/section_64_en.pdf.
175. Hirasata, K., K. Hayashi, and Y. Inamoto, *Friction and wear of several kinds of cast irons under severe sliding conditions*. Wear, 2007. **263**(1): p. 790-800.
176. Souza, T.N.F., et al., *Mechanical and microstructural characterization of nodular cast iron (nci) with niobium additions*. Materials Research, 2014. **17**(5): p. 1167-1172.
177. Kostylev, A., et al., *Advanced chromium carbide coatings on piston rings by CVD: A highly adaptable new method with relative low cost*. Advanced Materials & Processes, 2012. **170**(7): p. 22-26.
178. Demarchi, V. and E. Tomanik, *Nitrided Piston Ring Pack for Diesel Engines*. 1995, SAE Technical Paper.
179. Morkhov, M. and K. Egorova, *Chrome-plating of piston rings*. Chemical and Petroleum Engineering, 1965. **1**(2): p. 144-145.

180. Hepworth, J., *Chrome plating of piston rings*. Industrial Lubrication and Tribology, 1950. **2**(12): p. 13-15.
181. Kamo, L., et al. *Ceramic coated piston rings for internal combustion engines*. in *World Tribology Congress III*. 2005. American Society of Mechanical Engineers.
182. Ahn, J., B. Hwang, and S. Lee, *Improvement of wear resistance of plasma-sprayed molybdenum blend coatings*. Journal of thermal spray technology, 2005. **14**(2): p. 251-257.
183. Smith, T.J. and S.J. Sytsma, *Piston ring coating*. 2006, U.S Patent No. 7121192.
184. Kim, Y., et al., *Development of Nano Diamond Polymer Coating on Piston Skirt for Fuel Efficiency*. SAE Int. J. Engines, 2011. **4**(1): p. 2080-2086.
185. Zabala, B., et al., *Friction and wear of a piston ring/cylinder liner at the top dead centre: Experimental study and modelling*. Tribology International, 2017. **106**: p. 23-33.
186. Ye, Z.A. and H.S. Cheng, *Tribological behavior of advanced material pairs of piston-ring/cylinder-liner*. 1996, SAE Technical Paper.
187. Woś, P. and J. Michalski, *Effect of initial cylinder liner honing surface roughness on aircraft piston engine performances*. Tribology letters, 2011. **41**(3): p. 555-567.
188. Jocsak, J.J.A., *The effect of surface finish on piston ring-pack performance in advanced reciprocating engine systems*. 2005, Massachusetts Institute of Technology.
189. Andersson, P., J. Tamminen, and C.-E. Sandström, *Piston ring tribology. A literature survey*. VTT Tiedotteita-Research Notes. Vol. 2178. 2002, Espoo, Finland: VTT Technical Research Centre of Finland.
190. Tanaka, M., et al., *Ceramic metal composite coated piston ring and cylinder liner of marine low speed diesel engine*. J MESJ, 1993. **12**: p. 77-88.
191. Gérard, B., *Application of thermal spraying in the automobile industry*. Surface and Coatings Technology, 2006. **201**(5): p. 2028-2031.

192. Moreau, C., et al., *On-line control of the plasma spraying process by monitoring the temperature, velocity, and trajectory of in-flight particles*. 1994, ASM International, Materials Park, OH (United States).
193. Edrisy, A., et al., *Wear of thermal spray deposited low carbon steel coatings on aluminum alloys*. *Wear*, 2001. **251**(1): p. 1023-1033.
194. Tiruvenkadam, N., et al., *Synthesis of new aluminum nano hybrid composite liner for energy saving in diesel engines*. *Energy Conversion and Management*, 2015. **98**: p. 440-448.
195. Skopp, A., et al., *Thermally sprayed titanium suboxide coatings for piston ring/cylinder liners under mixed lubrication and dry-running conditions*. *Wear*, 2007. **262**(9): p. 1061-1070.
196. Mobarak, H., et al., *Effect of DLC coating on tribological behavior of cylinder liner-piston ring material combination when lubricated with Jatropha oil*. *Procedia Engineering*, 2014. **90**: p. 733-739.
197. Jayakumar, N., S. Mohanamurugan, and R. Rajavel, *Study Of Wear In Chrome Plated Cylinder Liner In Two Stroke Marine Diesel Engine Lubricated By Hans Jensen Swirl Injection Principle*. *Materials Today: Proceedings*, 2017. **4**(2): p. 1535-1541.
198. Hollinghurst, R., *High Temperature Lubrication Requirements of European Gasoline and Diesel Engines for Cars*. SAE International, 1974. **740973**: p. 3057-3076.
199. Mogul, F. *Piston Rings and Piston Ring Elements*. [cited 2017 6 June]; Available from: http://korihandbook.federalmogul.com/en/pdf/section_66_en.pdf.
200. *Mean Piston Speed*. [cited 2017 6 June]; Available from: <http://hpwizard.com/mean-piston-speed.html>.
201. Obert, P., et al., *The influence of oil supply and cylinder liner temperature on friction, wear and scuffing behavior of piston ring cylinder liner contacts—A new model test*. *Tribology International*, 2016. **94**: p. 306-314.
202. *Stroke Ratio*. [cited 2017 6 June]; Available from: https://en.wikipedia.org/wiki/Stroke_ratio.

203. Hollinghurst, R., *High Temperature Lubrication Requirements of European Gasoline and Diesel Engines for Cars*. SAE Technical Paper, 1974. **740973**: p. 3057-3076.
204. Roberts, A., R. Brooks, and P. Shipway, *Internal combustion engine cold-start efficiency: A review of the problem, causes and potential solutions*. Energy Conversion and Management, 2014. **82**: p. 327-350.
205. Blau, P.J., *A review of sub-scale test methods to evaluate the friction and wear of ring and liner materials for spark-and compression ignition engines*. 2002, ORNL Oak Ridge National Laboratory (US).
206. Bhushan, B., *Modern tribology handbook, two volume set*. 2000: CRC press.
207. *Consumption of vegetable oils worldwide from 1995/1996 to 2015/2016, by oil type (in million metric tons)*. [cited 13/6/2016; Available from: <http://www.statista.com/statistics/263937/vegetable-oils-global-consumption/>].
208. Jung, M., S. Yoon, and D. Min, *Effects of processing steps on the contents of minor compounds and oxidation of soybean oil*. Journal of the American Oil Chemists Society, 1989. **66**(1): p. 118-120.
209. Kanegsberg, B. and E. Kanegsberg, *Troubleshooting your ultrasonic process*. Metal Finishing, 2009. **107**(9): p. 31-33.
210. *Formtracepack, Surface Texture Parameter, User's Manual*. Vol. 99MBB384A1. 2009: Mitutoyo Corporation.
211. Bernard, J.H., R.S. Steven, and O.J. Bo, *Fundamentals of fluid film lubrication*. 2nd ed. ed. 2004, New York, USA: Marcel Dekker Inc.
212. Ian, M.H. and I.M. Hutchings, *Tribology : friction and wear of engineering materials*. 1992, London: Butterworth-Heinemann.
213. Brown, J.R., *Foseco Foundryman's Handbook*. 2000, Oxford: Butterworth-Heinemann.
214. Rigney, D.A. and J.P. Hirth, *Plastic deformation and sliding friction of metals*. Wear, 1979. **53**(2): p. 345-370.

215. Moore, A.J.W. and W.J.M. Tegar, *Relation between Friction and Hardness*. Proceedings of the Royal Society of London. Series A, Mathematical and Physical Sciences, 1952. **212**(1111): p. 452-458.
216. Rigney, D.A., *The roles of hardness in the sliding behavior of materials*. Wear, 1994. **175**(1): p. 63-69.
217. Plint, G. *The Sliding Hertzian Point Contact in Tribotesting: Understanding its Limitations as a Model of Real Systems*. in *70th Annual Meeting & Exhibition, 17 May -21 May 2015*. Texas: STLE.
218. Ponter, A.R.S., A.D. Hearle, and K.L. Johnson, *Application of the kinematical shakedown theorem to rolling and sliding point contacts*. Journal of the Mechanics and Physics of Solids, 1985. **33**(4): p. 339-362.
219. Williams, J.A., *The influence of repeated loading, residual stresses and shakedown on the behaviour of tribological contacts*. Tribology International, 2005. **38**(9): p. 786-797.
220. *BS EN ISO 945-1: 2008*, in *Microstructure of cast irons. Part 1: Graphite classification by visual analysis*.
221. Stott, F.H. and G.C. Wood, *The influence of oxides on the friction and wear of alloys*. Tribology International, 1978. **11**(4): p. 211-218.
222. Campanella, A., et al., *Lubricants from chemically modified vegetable oils*. Bioresource Technology, 2010. **101**(1): p. 245-254.
223. Bowden, F., J. Gregory, and D. Tabor, *Lubrication of metal surfaces by fatty acids*. Nature, 1945. **156**(3952): p. 97-101.
224. Stachowiak, G. and A.W. Batchelor, *Engineering tribology*. 2013: Butterworth-Heinemann.
225. Arabyan, S., et al., *Improvement of antifriction properties of motor oils*. Chemistry and Technology of Fuels and Oils, 1986. **22**(11): p. 595-597.
226. Chiong Ing, T., et al., *Tribological behaviour of refined bleached and deodorized palm olein in different loads using a four-ball tribotester*. Scientia Iranica, 2012. **19**(6): p. 1487-1492.

227. *Tempering (metallurgy)*. [cited 22/6/2016; Available from: [https://en.wikipedia.org/wiki/Tempering_\(metallurgy\)](https://en.wikipedia.org/wiki/Tempering_(metallurgy))).
228. Svahn, F., Å. Kassman-Rudolphi, and E. Wallen, *The influence of surface roughness on friction and wear of machine element coatings*. *Wear*, 2003. **254**(11): p. 1092-1098.
229. Qu, J., J. Truhan, and P. Blau, *Detecting the onset of localized scuffing in a pin-on-twin fuel-lubricated test for heavy-duty diesel fuel injectors*. *International Journal of Engine Research*, 2005. **6**(1): p. 1-9.
230. UFA, *Lubricant Handbook*. 2008, UFA Petroleum Agency.
231. Somayaji, A., *A study of the antiwear behavior and oxidation stability of fluorinated zinc dialkyl dithio phosphate in the presence of antioxidants*. 2008: ProQuest.
232. De Barros Bouchet, M.I., et al., *Mechanisms of MoS₂ formation by MoDTC in presence of ZnDTP: effect of oxidative degradation*. *Wear*, 2005. **258**(11–12): p. 1643-1650.
233. Carden, P., et al., *The Effect of Low Viscosity Oil on the Wear, Friction and Fuel Consumption of a Heavy Duty Truck Engine*. *SAE International Journal of Fuels and Lubricants*, 2013. **6**(2): p. 311-319.
234. Chu, Y.-H. and Y.-L. Kung, *A study on vegetable oil blends*. *Food Chemistry*, 1998. **62**(2): p. 191-195.
235. Anand, M., et al., *Ionic liquids as tribological performance improving additive for in-service and used fully-formulated diesel engine lubricants*. *Wear*, 2015. **334**: p. 67-74.
236. Kirk, R.E., D.F. Othmer, and A. Seidel, *Kirk-Othmer Food and Feed Technology*. 2008: Wiley.
237. Shahbazi, K., et al., *The effect of oxidation on viscosity of oil-based drilling fluids*. *Journal of Canadian Petroleum Technology*, 2006. **45**(06).
238. Salih, N., et al., *Biolubricant basestocks from chemically modified plant oils: ricinoleic acid based-tetraesters*. *Chemistry Central Journal*, 2013. **7**(1): p. 128.

239. Reeves, C.J., et al. *Evaluating the tribological performance of green liquid lubricants and powder additive based green liquid lubricants*. in *Proceedings of 2012 STLE Annual Meeting & Exhibition, STLE*. 2012.
240. Farhanah, A., et al., *MODIFICATION OF RBD PALM KERNEL AND RBD PALM STEARIN OIL WITH ZDDP ADDITIVE ADDITION*. *Jurnal Teknologi*, 2015. **74**(10).
241. bin Azhari, M.A., M.F. bin Tamar, and N.R. bin Mat Nuri, *PHYSICAL PROPERTY MODIFICATION OF VEGETABLE OIL AS BIO-LUBRICANT USING ZDDP*. 2006.
242. Singer, I.L. and H. Pollock, *Fundamentals of friction: macroscopic and microscopic processes*. Vol. 220. 2012: Springer Science & Business Media.
243. PerkinElmer. *Phosphorus, calcium and magnesium analysis of soybean oil-feedstock for biodiesel production using the optima inductively coupled plasma-optical emission spectrometer (ICP-OES)*. ICP-Optical Emis. Spectrom 2007 [cited 2016 20 November]; 1-4]. Available from: http://www.perkinelmer.com/pdfs/downloads/FAR_AnalysisOfSoybeanOilUsingICP-OES.pdf.
244. Taylor, L. and H. Spikes, *Friction-enhancing properties of ZDDP antiwear additive: part I—friction and morphology of ZDDP reaction films*. *Tribology transactions*, 2003. **46**(3): p. 303-309.
245. Taylor, L., A. Dratva, and H. Spikes, *Friction and wear behavior of zinc dialkyldithiophosphate additive*. *Tribology transactions*, 2000. **43**(3): p. 469-479.
246. High Temperature Corrosion Centre (HTC) Chalmers University of Technology. *SEM/EDX Analysys of Boron, A case Study*. 2011 [cited 2016 20 November]; Available from: http://fy.chalmers.se/~f10mh/Halvarsson/EM_intro_course_files/SEM_EDX%20Boron.pdf.
247. Morina, A., et al., *ZDDP and MoDTC interactions and their effect on tribological performance—tribofilm characteristics and its evolution*. *Tribology Letters*, 2006. **24**(3): p. 243-256.
248. Canning, G., et al., *Spectromicroscopy of tribological films from engine oil additives. Part I. Films from ZDDP's*. *Tribology letters*, 1999. **6**(3-4): p. 159-169.

249. Minfray, C., et al., *A multi-technique approach of tribofilm characterisation*. Thin Solid Films, 2004. **447**: p. 272-277.
250. CC Jensen A/S. *Oxidation in lubricant base oils*. [cited 2016 20 November]; Available from: http://www.cjc.dk/fileadmin/user_upload/pdf/News_Press/Press_Info/Oxidation_in_lubricant_base_oils_The_Filter_2006.pdf
251. Kirk, R.E., D.F. Othmer, and A. Seidel, *Food and Feed Technology*. 1st ed. Vol. 1. 2008: John Wiley & Sons.
252. Somayaji, A., *A study of the antiwear behavior and oxidation stability of fluorinated zinc dialkyl dithio phosphate in the presence of antioxidants*. 2008, The University of Texas at Arlington, USA.
253. Willermet, P., L. Mahoney, and C. Haas, *The effects of antioxidant reactions on the wear behavior of a zinc dialkyldithiophosphate*. ASLE Transactions, 1979. **22**(4): p. 301-306.
254. Behnam, M.J., P. Davami, and N. Varahram, *Effect of cooling rate on microstructure and mechanical properties of gray cast iron*. Materials Science and Engineering: A, 2010. **528**(2): p. 583-588.
255. Shashidhara, Y. and S. Jayaram, *Tribological studies on AISI 1040 with raw and modified versions of Pongam and Jatropha vegetable oils as lubricants*. Advances in Tribology, 2012. **2012**: p. 1-6.
256. Lou, A.T.H. and R. Erwin, *Biobased lubricants and greases*. 2011, Chichester, UK: John Wiley and Sons.
257. Jones Jr, W.R., *Boundary lubrication: Revisited*. 1982.
258. Vižintin, J., A. Arnšek, and T. Ploj, *Lubricating properties of rapeseed oils compared to mineral oils under a high load oscillating movement*. Lubrication Science, 2000. **17**(3): p. 201-217.
259. Plint, G., *The Sliding Hertzian Point Contact in Tribotesting: Understanding its Limitations as a Model of Real Systems*, in *STLE 70th Annual Meeting & Exhibition*, STLE, Editor. 2015: Dallas, Texas, USA.

260. Studt, P., *Boundary lubrication: adsorption of oil additives on steel and ceramic surfaces and its influence on friction and wear*. Tribology international, 1989. **22**(2): p. 111-119.
261. Azhari, M.A., M.F. Saroji, and M.F. Abdul Latif, *Comparison of Tribological Properties Between Canola Oil+ZDDP and SAE 40 Lubricants*. Journal of Engineering and Applied Sciences, 2016. **11**(10): p. 2126-2129.
262. Suarez, A.N., et al., *The influence of base oil polarity on the tribological performance of zinc dialkyl dithiophosphate additives*. Tribology International, 2010. **43**(12): p. 2268-2278.
263. Fischer, A. and K. Bobzin, *Friction, wear and wear protection*. Vol. 10. 2009: John Wiley & Sons.

Appendices

Appendix 1

Measurement datasheet for hardness on intended wear scar of GCI specimens

# Measurement	Scar #	Point 1	Point 2	Point 3	Average						
1	1	212	208	209	209.7	41	2	208	202	228	212.7
2	2	210	196	202	202.7	42	3	198	203	206	202.3
3	3	202	205	208	205.0	43	1	205	207	198	203.3
4	1	253	232	235	240.0	44	2	199	202	205	202.0
5	2	237	229	234	233.3	45	3	202	208	205	205.0
6	3	233	246	240	239.7	46	1	222	241	235	232.7
7	1	193	205	222	206.7	47	2	240	238	244	240.7
8	2	235	241	233	236.3	48	3	235	233	233	233.7
9	3	231	241	237	236.3	49	1	198	199	193	196.7
10	1	213	216	216	215.0	50	2	192	192	188	190.7
11	2	221	241	233	231.7	51	3	192	188	191	190.3
12	3	257	226	235	239.3	52	1	200	177	182	186.3
13	1	234	221	218	224.3	53	2	252	229	243	241.3
14	2	203	203	218	208.0	54	3	229	222	222	224.3
15	3	201	200	215	205.3	55	1	170	196	175	180.3
16	1	227	209	213	216.3	56	2	217	225	223	221.7
17	2	233	238	235	235.3	57	3	243	229	260	244.0
18	3	244	238	238	240.0	58	1	187	197	198	194.0
19	1	196	197	194	195.7	59	2	200	190	206	198.7
20	2	198	197	194	196.3	60	3	198	183	210	197.0
21	3	192	197	198	195.7	61	1	223	226	212	220.3
22	1	208	198	212	206.0	62	2	227	226	223	225.3
23	2	212	239	255	235.3	63	3	222	222	227	223.7
24	3	223	240	243	235.3	64	1	240	249	257	248.7
25	1	206	202	217	208.3	65	2	231	235	220	228.7
26	2	199	209	205	204.3	66	3	243	260	240	247.7
27	3	199	207	199	201.7	67	1	241	231	225	232.3
28	1	220	212	198	210.0	68	2	224	225	224	224.3
29	2	245	232	260	245.7	69	3	246	223	226	231.7
30	3	248	238	245	243.7	70	1	202	232	229	221.0
31	1	210	204	202	205.3	71	2	215	238	227	226.7
32	2	194	204	192	196.7	72	3	210	206	231	215.7
33	3	195	194	193	196.0	73	1	202	211	192	201.7
34	1	197	193	185	191.7	74	2	179	187	186	184.0
35	2	216	207	217	213.3	75	3	189	182	193	188.0
36	3	193	198	180	190.3	76	1	207	235	202	214.7
37	1	204	212	201	205.7	77	2	238	223	220	227.0
38	2	191	201	198	196.7	78	3	207	235	217	219.7
39	3	199	200	210	203.0	79	1	187	203	227	205.7
40	1	197	209	198	201.3	80	2	216	207	204	209.0
						81	3	198	173	189	186.7
						82	1	207	212	198	205.7
						83	2	206	199	205	203.3
						84	3	192	205	194	197.0
						85	1	228	196	211	211.7
						86	2	217	225	194	212.0
						87	3	214	205	201	206.7
						88	1	234	257	228	239.7
						89	2	226	222	239	229.0
						90	3	245	255	227	242.3
						91	1	207	176	196	193.0
						92	2	177	204	183	188.0
						93	3	189	179	208	192.0
						94	1	220	225	224	223.0
						95	2	224	212	233	223.0
						96	3	210	216	218	214.7
						97	1	222	211	209	214.0
						98	2	226	244	252	240.7
						99	3	229	240	229	232.7
						100	1	193	208	203	201.3
						101	2	209	194	199	200.7
						102	3	202	204	205	203.7
						103	1	232	228	245	235.0
						104	2	213	213	218	214.7
						105	3	223	235	220	226.0
						106	1	205	215	201	207.0
						107	2	204	220	203	209.0
						108	3	241	221	206	222.7
						109	1	204	208	211	207.7
						110	2	244	217	220	227.0
						111	3	221	232	232	228.3
						112	1	198	210	204	204.0
						113	2	195	215	209	206.3
						114	3	218	206	206	210.0
						115	1	203	196	202	200.3
						116	2	190	199	192	193.7
						117	3	175	185	190	183.3
						118	1	190	182	193	188.3
						119	2	215	239	213	222.3
						120	3	216	218	229	221.0
						121	1	205	204	217	208.7
						122	2	203	226	204	211.0
						123	3	193	205	221	206.3
						124	1	232	245	224	233.7
						125	2	221	209	225	218.3
						126	3	246	218	244	236.0
						127	1	199	201	214	204.7
						128	2	192	204	203	199.7
						129	3	205	202	220	209.0
						130	1	190	187	192	189.7
						131	2	215	209	213	212.3
						132	3	229	227	205	220.3
						133	1	212	214	217	214.3
						134	2	201	190	196	195.7
						135	3	210	207	210	209.0
						136	1	197	210	197	201.3
						137	2	221	201	191	204.3
						138	3	205	220	196	207.0
						139	1	202	204	212	206.0
						140	2	206	202	202	203.3

Continue on next page...

Appendix I (continue)

140	2	206	202	202	203.3
141	3	220	201	206	209.0
142	1	194	204	201	199.7
143	2	203	199	203	201.7
144	3	204	202	205	203.7
145	1	198	197	194	196.3
146	2	193	198	192	194.3
147	3	191	199	208	199.3
148	1	215	204	204	207.7
149	2	207	218	197	207.3
150	3	204	208	208	206.7
151	1	197	196	198	197.0
152	2	197	191	196	194.7
153	3	212	211	202	208.3
154	1	191	192	180	187.7
155	2	193	199	202	198.0
156	3	214	224	215	217.7
157	1	188	186	194	189.3
158	2	194	189	198	193.7
159	3	192	183	193	189.3
160	1	204	213	210	209.0
161	2	204	200	202	202.0
162	3	202	204	210	205.3
163	1	204	199	205	202.7
164	2	216	215	216	215.7
165	3	225	223	223	223.7
166	1	181	196	190	189.0
167	2	192	192	187	190.3
168	3	187	184	192	187.7
169	1	205	207	206	206.0
170	2	207	206	206	206.3
171	3	215	205	203	207.7
172	1	197	203	208	202.7
173	2	194	177	182	184.3
174	3	196	197	205	199.3
175	1	195	200	201	198.7
176	2	213	207	192	204.0
177	3	216	205	200	207.0
178	1	203	209	209	207.0
179	2	190	196	198	194.7
180	3	191	210	196	199.0
181	1	207	200	201	202.7
182	2	206	198	178	194.0
183	3	206	203	211	206.7
184	1	196	191	197	194.7
185	2	183	207	185	191.7
186	3	207	217	224	216.0
187	1	201	210	216	209.0
188	2	208	204	194	202.0
189	3	204	214	213	210.3
190	1	193	204	192	196.3
191	2	225	213	213	217.0
192	3	221	218	227	222.0
193	1	194	195	187	192.0
194	2	223	216	232	223.7
195	3	233	232	229	231.3
196	1	209	207	209	208.3
197	2	202	209	203	204.7
198	3	212	244	216	224.0
199	1	202	214	221	212.3
200	2	218	220	223	220.3
201	3	196	198	198	197.3
202	1	250	255	223	242.7
203	2	209	203	203	205.0
204	3	210	207	203	206.7
205	1	184	194	193	190.3
206	2	240	223	229	230.7
207	3	229	235	243	235.7
208	1	216	220	209	215.0
209	2	210	210	202	207.3
210	3	212	212	204	209.3
211	1	228	215	229	224.0
212	2	198	203	220	207.0
213	3	208	208	220	212.0
214	1	194	190	185	189.7
215	2	203	206	200	203.0
216	3	186	197	192	191.7
217	1	200	204	208	204.0
218	2	197	202	210	203.0
219	3	195	205	202	200.7
220	1	199	191	186	192.0
221	2	201	208	202	203.7
222	3	228	218	229	225.0
223	1	198	199	201	199.3
224	2	244	237	229	236.7
225	3	225	234	231	230.0
226	1	203	207	214	208.0
227	2	206	205	206	205.7
228	3	213	214	211	212.7
229	1	185	182	186	184.3
230	2	220	211	216	215.7
231	3	218	216	215	216.3
232	1	208	209	207	208.0
233	2	196	215	205	205.3
234	3	210	226	217	217.7
235	1	204	217	208	209.7
236	2	205	206	205	205.3
237	3	211	208	204	207.7
238	1	202	209	197	202.7
239	2	204	192	195	197.0
240	3	194	207	194	198.3
241	1	184	186	185	185.0
242	2	199	197	208	201.3
243	3	182	182	187	183.7
244	1	222	240	227	229.7
245	2	197	198	204	199.7
246	3	211	187	205	201.0
247	1	206	201	210	205.7
248	2	197	202	210	203.0
249	3	215	210	220	215.0
250	1	197	195	202	198.0
251	2	202	193	228	207.7
252	3	186	208	209	201.0
253	1	221	200	206	209.0
254	2	202	200	194	198.7
255	3	202	212	206	206.7
256	1	199	196	196	197.0
257	2	199	188	193	193.3
258	3	206	182	186	191.3
259	1	220	201	227	216.0
260	2	202	229	203	211.3
261	3	197	189	201	195.7
262	1	193	182	190	188.3
263	2	207	206	202	205.0
264	3	191	192	196	193.0
265	1	217	220	223	220.0
266	2	210	216	212	212.7
267	3	207	206	201	204.7
268	1	228	234	234	232.0
269	2	243	245	226	238.0
270	3	195	222	200	205.7
271	1	240	237	224	233.7
272	2	214	224	200	212.7
273	3	217	213	202	210.7
274	1	188	190	191	189.7
275	2	182	200	189	190.3
276	3	197	194	190	193.7
277	1	232	257	245	244.7
278	2	218	212	220	216.7
279	3	208	231	202	213.7
280	1	191	197	182	190.0
281	2	183	190	194	189.0
282	3	198	197	188	194.3
283	1	205	202	201	202.7
284	2	173	188	193	184.7
285	3	203	202	217	207.3
286	1	180	191	184	185.0
287	2	187	207	201	198.3
288	3	202	225	215	214.0
289	1	206	224	209	213.0
290	2	206	204	205	205.0
291	3	226	207	204	212.3
292	1	196	196	192	194.7
293	2	231	238	238	235.7
294	3	225	240	228	231.0
295	1	210	207	210	209.0
296	2	198	209	216	207.7
297	3	203	208	198	203.0
298	1	193	207	199	199.7
299	2	240	238	229	235.7
300	3	241	234	237	237.3
301	1	205	211	195	203.7
302	2	207	210	198	205.0
303	3	224	208	222	218.0
304	1	191	201	192	194.7
305	2	207	188	186	193.7
306	3	207	207	198	204.0
307	1	196	202	201	199.7
308	2	206	196	209	203.7
309	3	193	221	190	201.3

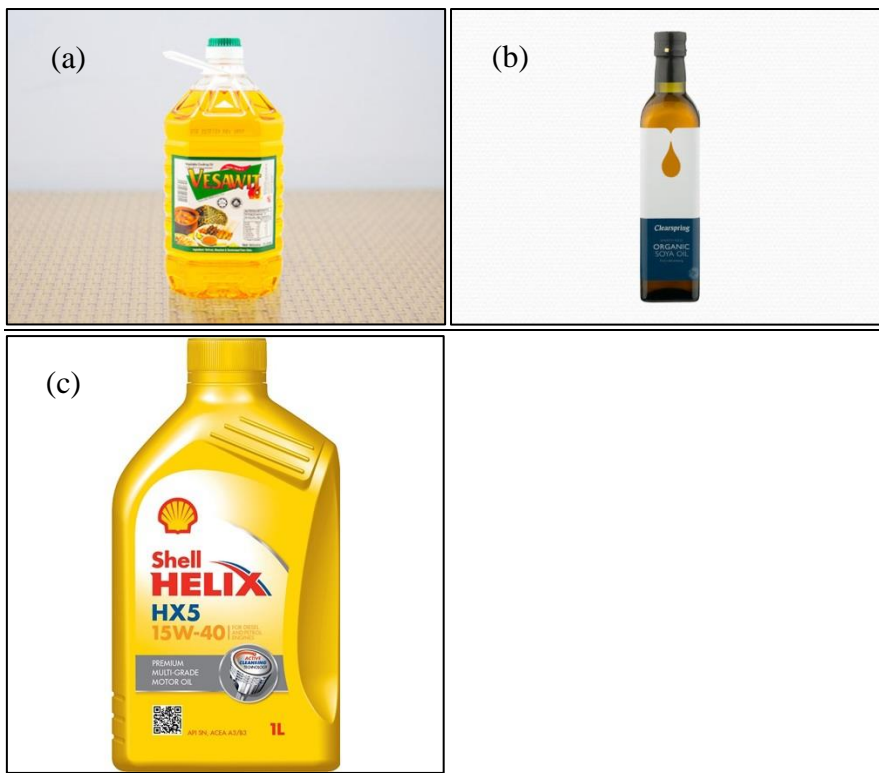
Continue on next page...

Appendix I (continue)

310	1	202	223	201	208.7	367	1	202	200	207	203.0
311	2	209	223	212	214.7	368	2	187	209	190	195.3
312	3	208	216	220	214.7	369	3	192	186	192	190.0
313	1	228	228	222	226.0	370	1	198	204	197	199.7
314	2	220	212	208	213.3	371	2	202	212	205	206.3
315	3	213	209	216	212.7	372	3	231	227	211	223.0
316	1	192	192	207	197.0	373	1	191	198	192	193.7
317	2	200	223	215	212.7	374	2	227	227	224	226.0
318	3	211	198	198	202.3	375	3	222	196	221	213.0
319	1	211	232	213	218.7	376	1	197	221	225	214.3
320	2	201	203	204	202.7	377	2	207	193	201	200.3
321	3	213	218	217	216.0	378	3	215	212	204	210.3
322	1	202	201	199	200.7	379	1	210	205	200	205.0
323	2	194	197	186	192.3	380	2	217	194	187	199.3
324	3	187	186	174	182.3	381	3	213	216	188	205.7
325	1	209	215	222	215.3	382	1	188	195	186	189.7
326	2	215	208	207	210.0	383	2	193	202	222	205.7
327	3	214	210	211	211.7	384	3	206	205	210	207.0
328	1	210	202	198	203.3	385	1	222	221	211	218.0
329	2	192	190	204	195.3	386	2	201	208	199	202.7
330	3	194	220	208	207.3	387	3	202	204	213	206.3
331	1	218	202	204	208.0	388	1	191	199	195	195.0
332	2	202	208	202	204.0	389	2	194	208	206	202.7
333	3	213	199	200	204.0	390	3	194	205	202	200.3
334	1	188	195	196	193.0	391	1	226	227	216	223.0
335	2	192	202	193	195.7	392	2	195	207	206	202.7
336	3	186	205	205	198.7	393	3	196	192	215	201.0
337	1	193	178	194	188.3	394	1	192	201	180	191.0
338	2	218	202	199	206.3	395	2	187	186	194	189.0
339	3	201	206	204	203.7	396	3	195	186	197	192.7
340	1	200	246	235	227.0	397	1	199	213	207	206.3
341	2	211	194	205	203.3	398	2	221	234	222	225.7
342	3	203	206	199	202.7	399	3	199	203	203	201.7
343	1	228	229	212	223.0	400	1	225	220	229	224.7
344	2	221	226	224	223.7	401	2	212	197	197	202.0
345	3	211	208	206	208.3	402	3	205	204	199	202.7
346	1	212	210	211	211.0	403	1	218	212	201	210.3
347	2	218	200	200	206.0	404	2	199	199	196	198.0
348	3	202	206	206	204.7	405	3	213	215	200	209.3
349	1	182	196	186	188.0	406	1	185	202	197	194.7
350	2	238	223	223	228.0	407	2	221	218	220	219.7
351	3	214	229	215	219.3	408	3	225	226	229	226.7
352	1	197	200	210	202.3	409	1	241	235	215	230.3
353	2	199	207	210	205.3	410	2	201	204	197	200.7
354	3	205	215	208	209.3	411	3	208	199	196	201.0
355	1	193	195	194	194.0	412	1	191	182	186	186.3
356	2	220	223	225	222.7	413	2	188	194	194	192.0
357	3	231	233	217	227.0	414	3	190	186	193	189.7
358	1	215	208	202	208.3	415	1	246	239	257	247.3
359	2	196	209	200	201.7	416	2	203	189	212	201.3
360	3	209	217	198	208.0	417	3	203	215	208	208.7
361	1	204	214	228	215.3	418	1	228	217	209	218.0
362	2	218	233	224	225.0	419	2	229	213	218	220.0
363	3	202	191	201	198.0	420	3	201	208	190	199.7
364	1	253	202	200	218.3	421	1	197	202	196	198.3
365	2	207	206	207	206.7	422	2	186	198	223	202.3
366	3	196	203	208	202.3	423	3	199	200	200	199.7
						424	1	205	210	226	213.7
						425	2	194	201	203	199.3
						426	3	206	217	210	211.0

Appendix 2

Main lubricants used in this study: (a) Palm oil (b) Soybean oil (c) Mineral oil



Appendix 3

Product information sheet for ZDDP

ZDDPlus
Restores ZDDP
Saves Engines

REAL ZDDP

After 70+ years of trouble-free, metal-to-metal engine protection, the E.P.A. is forcing ZDDP (Zinc Dialkyl Dithio Phosphate = zinc and phosphorus) from domestic motor oil. If your engine was designed prior to the 1990s, the non-roller lifters require ZDDP in the motor oil to avoid premature deterioration. Don't let the lifters run metal-to-metal. Keep ZDDP, via ZDDPlus™, in your motor oil. Add a 4 oz bottle of ZDDPlus™ to every 4- to 5-quart oil change. One bottle of ZDDPlus™ contains more ZDDP than two bottles of GM's EOS.


ZDDPlus
Restores ZDDP
Saves Engines

THIS PRODUCT IS INTENDED FOR USE ON PRE-OBDII OFF-ROAD, INDUSTRIAL, AGRICULTURAL AND RACING VEHICLES ONLY.

Net Wt. 4 oz / 113.4 g

Appendix 4

Product information sheet for hBN

Product information		PI 17/09/09/2016	LIQUI MOLY																								
Cera Tec																											
<p>Description</p> <p>Micro ceramic solid lubricant suspension based on hexagonal boron nitride (BN) in mineral oil. The laminar graphite-similar structure reduces friction and wear and prevents direct metal-to-metal contact. The < 0.5 µm particle size guarantees optimal filter flow properties and protects against depositing of solid lubricant particles.</p>																											
<p>Properties</p> <ul style="list-style-type: none"> - reduces frictional losses - suitable for diesel particulate filters - mixable with all commercially available motor oils - increases smooth operation - highest thermal stability - excellent high and low temperature behavior - tested for catalytic converters - stable under extreme pressures - compatible with fine filters - no deposits - long engine service life - chemically inert - reduces fuel consumption 		<p>Application</p> <p>300 ml is sufficient for up to 5 liters of motor oil. Long-term effect up to 50,000 km. Shake container before use.</p>																									
		<p>Comment</p> <p>Not suitable for use with wet clutches!</p>																									
<p>Technical data</p> <table border="0"> <tr> <td>Base</td> <td>BN Mikrokeramik / BN micro ceramic</td> </tr> <tr> <td>Color / appearance</td> <td>orange</td> </tr> <tr> <td>Particle size</td> <td>Mehrheit < 0,5 / Majority < 0.5 µm</td> </tr> <tr> <td>Temperature stability of the ceramic particles</td> <td>bis + 1200 / up to 1200 °C</td> </tr> <tr> <td>Density at 20 °C</td> <td>0,893 g/cm³ DIN 51757</td> </tr> <tr> <td>Viscosity at 20 °C</td> <td>~250 mPas DIN 51398</td> </tr> <tr> <td>Flash point</td> <td>> 100 °C DIN ISO 2592</td> </tr> <tr> <td>Pour point</td> <td>-20 °C DIN ISO 3016</td> </tr> <tr> <td>Form</td> <td>flüssig / liquid</td> </tr> <tr> <td>Odor</td> <td>charakteristisch / characteristic</td> </tr> </table>		Base	BN Mikrokeramik / BN micro ceramic	Color / appearance	orange	Particle size	Mehrheit < 0,5 / Majority < 0.5 µm	Temperature stability of the ceramic particles	bis + 1200 / up to 1200 °C	Density at 20 °C	0,893 g/cm ³ DIN 51757	Viscosity at 20 °C	~250 mPas DIN 51398	Flash point	> 100 °C DIN ISO 2592	Pour point	-20 °C DIN ISO 3016	Form	flüssig / liquid	Odor	charakteristisch / characteristic	<p>Available pack sizes</p> <table border="0"> <tr> <td>300 ml Bottle aluminum</td> <td>3721 D-GB-I-E-P-NL-F-ARAB-RUS</td> </tr> <tr> <td>300 ml Bottle aluminum</td> <td>7181 D-GR-PL-TR-CZ-RO-H-BG</td> </tr> </table>		300 ml Bottle aluminum	3721 D-GB-I-E-P-NL-F-ARAB-RUS	300 ml Bottle aluminum	7181 D-GR-PL-TR-CZ-RO-H-BG
Base	BN Mikrokeramik / BN micro ceramic																										
Color / appearance	orange																										
Particle size	Mehrheit < 0,5 / Majority < 0.5 µm																										
Temperature stability of the ceramic particles	bis + 1200 / up to 1200 °C																										
Density at 20 °C	0,893 g/cm ³ DIN 51757																										
Viscosity at 20 °C	~250 mPas DIN 51398																										
Flash point	> 100 °C DIN ISO 2592																										
Pour point	-20 °C DIN ISO 3016																										
Form	flüssig / liquid																										
Odor	charakteristisch / characteristic																										
300 ml Bottle aluminum	3721 D-GB-I-E-P-NL-F-ARAB-RUS																										
300 ml Bottle aluminum	7181 D-GR-PL-TR-CZ-RO-H-BG																										
		<p>Our information is based on thorough research and may be considered reliable, although not legally binding.</p>																									
<p>Areas of application</p> <p>Added to the lubricating oil of engines, compressors, pumps and transmissions. Excellent for use in passenger car and commercial vehicle engines (gasoline and diesel). Mixable with all commercially available motor oils.</p>																											
LIQUI MOLY GmbH Jerg-Wieland-Str. 4 89081 Ulm-Lehr	Postfach 2829 89018 Ulm Germany	Phone: +49 (0)73 1/1420-13 Fax: +49 (0)73 1/1420-82 e-mail: info@liqui-moly.de	Service-hotline: 0900/8223230 Technical hotline: +49 (0)731/1420-871 www.liqui-moly.de																								

Appendix 5

Example of calculation sheet for estimating the film thickness (Mineral Oil)

1				
2	EHL Pressure-Viscosity Coefficient, α EHL			
3				
4	$Z = [7.81(H_{40} - H_{100})]^{1.5}(F_{40})$			
5				
6	$H_{40} = \log(\log(\mu_{40}) + 1.200)$			
7	$H_{100} = \log(\log(\mu_{100}) + 1.200)$			
8	$F_{40} = (0.885 - 0.864 H_{40})$			
9				
10	$\rho_t = \rho_{15.6}[1 - 0.00063(T - 15.6)]$			
11				
12	$\alpha_{EHL} = Z[5.1 \times 10^{-9}(\ln \mu_0 + 9.67)]$			
13				
14	Viscosity data from Measurement (New Oil)			
15				
16	Dynamic viscosity at 40°C, μ_{40}	92.45	cP (mPa.s)	
17	Dynamic viscosity at 100°C, μ_{100}	12.32	cP (mPa.s)	
18	Dynamic viscosity at temperature T (atm pressure)	12.32	cP	0.0123 Pa.s
19	H40	0.50049814		
20	H100	0.35995129		
21	F40	0.45256961		
22	Z	0.52046752		
23	α_{EHL}	1.3998E-08	Pa ⁻¹	
24	α_{EHL}	14.00	GPa ⁻¹	
25				
26				
27	Calculation of Film Thickness			
28				
29	$\hat{H}_{e,min} = 3.63U^{0.68}G^{0.49}W^{-0.073}(1 - e^{-0.68k})$			
30				
31				
32	Load, w	40	N	
33	Ball Radius	3	mm	
34	Sliding speed	0.13	m/s	
35	Modulus of elasticity of Ball Specimen	215	Gpa	
36	Modulus of elasticity of Flat Specimen	103	GPa	
37	Poisson ration of Ball Specimen	0.3		
38	Poisson ration of Flat Specimen	0.26		
39	Effective Radius in x direction, R _x	0.0015	m	
40				
41	Mean surface velocity, u	0.065	m/s	
42	Effective Modulus of Elasticity, E'	1.5055E+11	Pa	
43	Dimensionless Material Parameter, G	2107.31324		
44	Dimensionless Load Parameter, W	0.00011809		
45	Dimensionless Speed Parameter, U	3.5462E-12		
46	Ellipticity Parameter, k	1		
47	Dimensionless Minimum Film Thickness, H _{min}	2.4115E-06		
48	Minimum Film Thickness, h _{min}	3.6E-09	m	
49		0.003617	μm	
50		3.617242	nm	
51				

Appendix 7

Calculation sheet for ANOVA analysis of COF for Mineral Oil, Palm Oil, Soybean

Oil lubricated specimens

	A	B	C	D	E	F	G
1	ANOVA analysis						
2							
3		MO	PO	SBO			
4	1	0.100154829	0.10428	0.11371			
5	2	0.091407109	0.10433	0.10782			
6	3	0.088436448	0.10511	0.11398			
7							
8	Anova: Single Factor						
9							
10	SUMMARY						
11	<i>Groups</i>	<i>Count</i>	<i>Sum</i>	<i>Average</i>	<i>Variance</i>		
12	MO	3	0.28	0.09333	3.7E-05		
13	PO	3	0.31373	0.10458	2.2E-07		
14	SBO	3	0.33551	0.11184	1.2E-05		
15	ANOVA						
16	<i>Source of Variation</i>	<i>SS</i>	<i>df</i>	<i>MS</i>	<i>F</i>	<i>P-value</i>	<i>F crit</i>
17	Between Groups	0.000521494	2	0.00026	15.8148	0.004053806	5.14325285
18	Within Groups	9.8925E-05	6	1.6E-05			
19	Total	0.000620419	8				
20							

Appendix 8

Elements spectrum of low, medium and high hardness specimens

Hardness	EDAX graph
Low	
Medium	
High	
Low (unlubricated)	

Appendix 9

Surface temperature calculation sheet

Total Surface Temperature

$$T_c = T_b + \Delta T_{nom} + \Delta T_f$$

Circular contact radius (initial Hertzian)	a	0.106 mm 0.000106 m
Contact Pressure	P	170000000 N/m ²
Bulk Temperature	T _b	100 °C

Thermal Diffusivity

where $\kappa = \frac{k}{\rho C} =$ thermal diffusivity.

Geometry of the circular, square and linear contacts.

GCI (A)	Thermal conductivity	k	48.5 W/mK
	Density	ρ	7200 kg/m ³
	Specific heat	C	460 J/kgK
	Thermal diffusivity	K	1.46437E-05 m ² /s

Steel Ball (B)	Thermal conductivity	k	42.4 W/mK
	Density	ρ	7800 kg/m ³
	Specific heat	C	464 J/kgK
	Thermal diffusivity	K	1.172E-05 m ² /s

Peclet number is defined as:

$$Pe = \frac{Va}{2\kappa}$$

L < 0.1 one surface moves very slowly with respect to the other. There is enough time for the temperature distribution of the contact to be established in the stationary body. In this case, the situation closely approximates to steady state conduction [4+].
 0.1 < L < 5 intermediate region. One surface moves faster with respect to the other and a slowly moving heat source model is assumed.
 L > 5 one surface moves fast with respect to the other and is modelled by a fast moving heat source. There is insufficient time for the temperature distribution of the contact to be established in the stationary body and the equations of linear heat diffusion normal to the surface apply [4+]. The depth to which the heat penetrates into the stationary body is very small compared to the contact dimensions.

Shape of Heat Source	Heat Flux Distribution	Figure No.	Maximum Flash Temperature Rise (Steady State)		
			Stationary or Low Speed Pe < 0.1	High Speed Pe > 10	Approximate Expression for All Velocities
Band	Uniform	6.7	$\frac{2qb}{k\sqrt{\pi}}$	$\frac{2qb}{k\sqrt{\pi Pe}}$	$\frac{2qb}{k\sqrt{\pi(1+Pe)}}$
Square	Uniform	6.10a	$\frac{1.122qb}{k}$	$\frac{2qb}{k\sqrt{\pi Pe}}$	$\frac{2qb}{k\sqrt{\pi(1.011+Pe)}}$
Circular	Uniform	6.5	$\frac{qa}{k}$	$\frac{2qa}{k\sqrt{\pi Pe}}$	$\frac{2qa}{k\sqrt{\pi(1.273+Pe)}}$
Circular	Parabolic	6.10b	$\frac{3\pi qa}{8k}$	$\frac{2.32qa}{k\sqrt{\pi Pe}}$	$\frac{2.32qa}{k\sqrt{\pi(1.234+Pe)}}$
Elliptical	Uniform	6.10c	$\frac{qa}{k\sqrt{Se}}$	$\frac{2qa}{k\sqrt{\pi Pe}}$	$\frac{2qa}{k\sqrt{\pi(1.273Se+Pe)}}$
Elliptical	Semi-ellipsoidal	6.10d	$\frac{3\pi qa}{8k\sqrt{Se}}$	$\frac{2.32qa}{k\sqrt{\pi Pe}}$	$\frac{2.32qa}{k\sqrt{\pi(1.234Se+Pe)}}$

GCI (A)	Surface velocity of GCI	U ₁	0 m/s
	Peclet Number	Pe	0
	Pe < 0.1		

Steel Ball (B)	Surface velocity of Steel Ball	U ₂	0.13 m/s
	Peclet Number	Pe	0.4705089
	0.1 < Pe < 5		

For Circular Contact

For the entire range of Peclet number, the maximum steady-state flash temperature rise can be approximated as (Greenwood, 1991):

$$\Delta T_{max} = \frac{2qa}{k\sqrt{\pi(1.273+Pe)}} \quad (6.27)$$

$$l_{b2} = \frac{a}{\pi^{1/2}} \tan^{-1} \left[\frac{2\pi\kappa_2}{aV} \right]^{1/2}$$

	SBO	PO	MO	
Friction Coefficient	u	0.11	0.11	0.09
Heat per unit area	q (W/m ²)	24752000.00	23205000.00	20553000.00
Max Flash Temp Rise	Tmax (°C)	46.23	43.34	38.39
Eff. Diff. length	lb2 (m)	0.00	0.00	0.00
Nominal Temp	Tnom (°C)	36.40	34.12	30.22
Total contact Temp.	Tc (°C)	182.63	177.46	168.61

$$T_c = T_b + \Delta T_{nom} + \Delta T_f$$